Intensité du champ magnétique terrestre en périodes stables et de transition, enregistrée par des séquences de coulées volcaniques du quaternaire

Annick Chauvin

A. CHAUVIN

ISSN 0755-978X
ISBN 2-905532-22-X

intensité du champ magnétique terrestre en périodes stables et de transition, enregistrée par des séquences de coulées volcaniques du quaternaire

MEMOIRES ET DOCUMENTS
du Centre Armoricain d'Etude Structurale des Socles
n° 23
Rennes 1989

MEMOIRES ET DOCUMENTS
DU
CENTRE ARMORICAIN D'ETUDE STRUCTURALE DES SOCLES

N°23

A. CHAUVIN

Intensité du champ magnétique terrestre en périodes stables et de transition, enregistrée par des séquences de coulées volcaniques du quaternaire.

Thèse de Doctorat de l'Université de Rennes I
soutenue le 10 Janvier 1989.

Centre Armoricain d'Etude Structurale des Socles
LP CNRS n°4661
Université de Rennes I
Campus de Beaulieu
F-35042 - RENNES Cédex
(France)

1989

ISSN : 0755-978 X

ISBN : 2-905532-22-X

Centre Armoricain d'Etude Structurale des Socles
LP CNRS n°4661
Université de Rennes I - Campus de Beaulieu
F-35042 - RENNES Cédex (France)

A. CHAUVIN (1989)

Intensité du champ magnétique terrestre en périodes stables et de transition, enregistrée par des séquences de coulées volcaniques du quaternaire.

Mém. Docum. Centre Arm. Et. Struct. Socles, Rennes, 23 ; 217.

Je tiens à remercier monsieur Bonhommet, pour m'avoir accueillie dans le laboratoire de Géophysique Interne de Rennes, où j'ai eu l'occasion d'effectuer un DEA en sismologie avant de m'orienter vers le paléomagnétisme.

Ma reconnaissance va également à messieurs Hoffman, Laj, Perroud, et Prévot, et pour avoir accepté de faire parti de mon jury mais aussi pour avoir eu la gentillesse de m'accorder un peu de leur temps afin de discuter de mes résultats.

Je souhaite remercier également l'ORSTOM, et plus particulièrement messieurs Aubrat et Recy, pour avoir financé en grande partie les travaux sur la Polynésie.

J'exprime toute ma reconnaissance à Pierrick Roperch dont l'efficacité et la disponibilité m'ont été d'un grand secours tout au long de ces quatre dernières années.

La gentillesse des 'dames' du laboratoire (madame Calza et madame LeSolliec) a été grandement appréciée tout au long de mon travail.

Enfin je dis un grand et chaleureux merci à tous les amis côtoyés à l'institut de geologie, qu'ils y soient ou non encore présents, pour leur soutien et leurs encouragements.

AVANT PROPOS

Le travail présenté dans ce mémoire a pour principal objectif l'étude du comportement du Champ Magnétique Terrestre (CMT) en direction et en intensité, au cours de périodes dites "normales" ou de transition (excursion ou renversement de polarité). Pour atteindre ce but, des études paléomagnétiques ont été effectuées sur des coulées volcaniques, d'âges s'échelonnant de 5.000 ans à 1.1 millions d'années, échantillonnées à l'île de la Réunion (Océan Indien), à Tahiti (Polynésie Française), en Islande et dans la Chaîne des Puys.

Une étude de la variation séculaire du CMT (déclinaison, inclinaison, intensité) a porté sur deux empilements volcaniques du Piton de la Fournaise (île de la Réunion), représentant un total de 30 coulées. Les âges obtenus sur ces deux sites les situent tous les deux dans la période de Brunhes (5000 à plus de 11.000 ans, 82 à 98.000 ans). La localisation des sites (21°S) est originale, du fait de l'asymétrie évidente dans la localisation des études antérieures du même type, concentrées principalement dans l'hémisphère Nord. Les résultats de paléointensité acquis sur le plus jeune site sont en bon accord avec les données concernant les variations du moment dipolaire sur la période 0-12000 ans, de même que les intensités obtenues sur le site le plus ancien. De plus une étude détaillée des propriétés magnétiques des échantillons a été effectuée. La première partie du mémoire est consacrée à cette étude.

La deuxième partie est consacrée à l'acquisition de nouvelles données paléomagnétiques venant confirmer l'existence d'une excursion du CMT dans la période de Brunhes (excursion dite du Laschamp). Des paléointensités obtenues sur une coulée de la Chaîne des Puys (coulée de Louchadière) et sur les coulées d'Islande, contemporaines du Laschamp montrent clairement que le champ magnétique était dans un état anormal, dit de transition à cette période. Le texte concernant les résultats obtenus en Islande a été placé dans l'annexe 1.

Enfin la troisième partie du mémoire présente et décrit l'étude des 3 renversements de polarité les plus récents : Matuyama-Brunhes, Jaramillo Supérieur et Inférieur, ainsi qu'un événement nommé Cobb Mountain, enregistrés par une séquence de 123 coulées volcaniques de l'île de Tahiti. Les enregistrements du Jaramillo supérieur et du Cobb constituent les premières données détaillées, acquises sur roches volcaniques, durant ces 2 périodes. Les directions paléomagnétiques et donc la géométrie du champ de transition ainsi que son intensité absolue ont été étudiées et discutées.

Chacune de ces trois parties constituant à elle seule des travaux complets, elles ont été rédigées en anglais sous forme d'articles.

INTRODUCTION GENERALE.

Les variations du champ magnétique terrestre (CMT) s'étalent dans le temps depuis le millième de seconde jusqu'à sans doute plus de la centaine de millions d'années (Courtillot et Le Mouel, 1988). Les variations de période inférieure à une année sont attribuées au champ dit externe, dont les sources se situent dans la ionosphère et la magnétosphère alors que celles de périodes plus longues sont d'origine interne. Toutefois les spectres des variations du champ externe et interne se recoupent, comme le montre la variation de période 11 ans, qui est liée au cycle de l'activité solaire.

Dans ce mémoire, seules les variations du champ interne sont étudiées. La solution actuellement acceptée quant à l'origine du champ géomagnétique est un effet dynamo dans le noyau. Son évolution dans le temps serait due au mouvement du liquide hautement conducteur constituant le noyau externe.

Les données concernant les variations de courtes périodes du CMT nous proviennent essentiellement des quelques 180 observatoires magnétiques répartis à travers le monde. Soixante-dix d'entre eux devraient être bientôt regroupés au sein d'un réseau relié par satellite (EOS, 69, 1564, 1988). Ceux-ci nous fournissent des enregistrements historiques ne permettant pas de remonter dans le temps au-delà des deux derniers siècles.

Pour obtenir des informations sur les variations de plus longues périodes, il est nécessaire d'étudier, l'aimantation fossile portée soit par les roches (sédiments, intrusions ou coulées volcaniques): c'est le domaine du paléomagnétisme, soit par des d'objets anciens: c'est l'archéomagnétisme.

Le champ magnétique terrestre, tel qu'il est mesuré à la surface du globe peut être associé à celui développé par un dipôle, placé au centre de la Terre et faisant un angle d'environ 11°5 avec l'axe de rotation. Cette représentation rend compte d'environ 90% du CMT ; le reste est appelé champ non-dipôle.

Un développement en harmonique sphérique du champ fait apparaitre une série de coefficients g_m^n h_m^n interprétés de la manière suivante. Le terme g_1^0 représente l'intensité du dipôle axial centré, alors que les termes, g_1^1 et h_1^1 représentent la composante dipolaire du champ dans le plan équatorial. Les termes de degrés supérieurs correspondent au champ non-dipolaire (par exemple les termes pour lesquels n = 2 représentent la composante quadripolaire, et ceux pour lesquels n = 3 la

composante octopolaire. Le champ dipôle et le champ non-dipôle varient tous les deux dans le temps. La variation séculaire du champ est définie comme la dérivée par rapport au temps du champ principal.

Un des résultats les plus inattendus de l'étude des fluctuations du CMT enregistré au cours du 20ème siècle, est la mise en évidence d'une secousse dans la variation séculaire en 1969 (Courtillot et Le Mouel, 1976 ; Courtillot et al., 1978). Un tel événement correspond à un saut de la dérivée seconde temporelle du CMT. Un saut de variation séculaire semblable a été plus récemment détecté aux environs de 1913 (Gire, 1985).

D'autre part, l'étude du champ récent, a permis moyennant certaines approximations, le calcul du mouvement du fluide à la surface noyau-manteau, responsable de la variation séculaire et notamment de la dérive vers l'ouest des composantes non-dipolaires du CMT (Gire et al., 1985 ; Le Mouel et al., 1985).

En dehors des données de la variation séculaire récente, les données archéomagnétiques et paléomagnétiques constituent les meilleurs contraintes pour les théoriciens cherchant à établir un modèle de géodynamo.

Ainsi il est clairement établi qu'une des propriétés les plus remarquables du CMT est le changement de polarité suivant un processus non régulier, contrairement par exemple au champ magnétique du soleil, dont l'inversion a lieu tous les onze ans.

D'autres faits semblent également bien établis pour certaines périodes (Merrill et Mc Elhinny, 1983) :

- Le champ est essentiellement dipolaire (vérifié sur les 5 derniers millions d'années)
- Le changement de polarité (ou transition) s'effectue sur un temps très court, à l'échelle des temps géologiques de l'ordre du millier à la dizaine de milliers d'années (vérifié pour les derniers 100 millions d'années).
- Le champ magnétique existe depuis au moins 3 milliards d'années.
- L'intensité du champ dipolaire a varié de l'ordre de 50% durant les dix derniers milliers d'années.

La plupart des données paléomagnétiques se rapportent uniquement à la direction passée du vecteur champ, mais peu de travaux concernent son intensité. La raison majeure en est que l'aimantation naturelle des roches, si elle correspond bien à la direction du paléochamp n'est pas toujours reliée à son intensité.

PREMIERE PARTIE

VARIATION SÉCULAIRE DU CHAMP MAGNÉTIQUE, EN DIRECTION ET EN INTENSITÉ

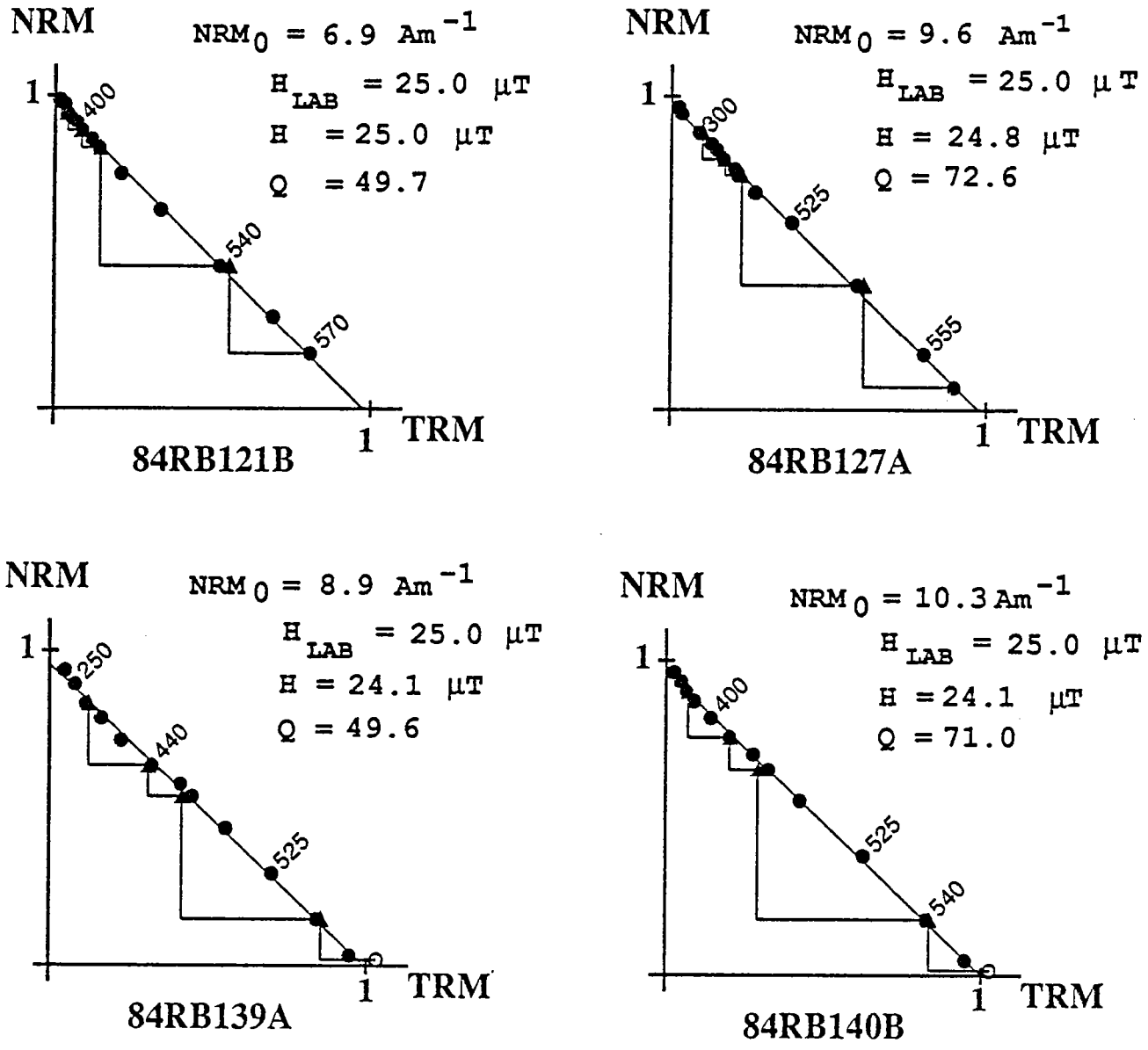

Figure I.1. Diagrammes ARN-ATR (NRM-TRM en anglais), pour quatre échantillons préalablement réaimantés dans un champ artificiel de 25 μT. Les étapes de température sont indiquées en degrés Celsius. NRM_0: intensité de l'ARN, H_{lab}: champ de laboratoire, H: 'paléointensité' calculée, Q: facteur de qualité (Coe et al., 1978).

INTRODUCTION

La variation séculaire du champ magnétique n'est souvent décrite qu'en terme de directions du paléochamp. En effet seuls certains objets archéologiques et les roches volcaniques ont une aimantation naturelle qui est une aimantation thermorémanente permettant de retrouver l'intensité absolue du champ. De plus l'obtention de données fiables de paléointensité demeure une expérience délicate dans bon nombre de cas.

La première partie de ce mémoire est consacrée à l'étude des variations de l'intensité du champ, enregistrées par deux séquences de coulées volcaniques du Quaternaire récent de l'île de La Réunion. Avant de présenter le but et les résultats de cette étude (cf. l'article qui suit), il parait intéressant de préciser quelques points concernant la méthode de détermination de la paléointensité qui a été utilisée, c'est à dire la méthode de Thellier (Thellier et Thellier, 1959).

L'appareillage utilisé pour les déterminations de paléointensité est strictement identique à celui décrit par J.S. Salis (1987). La version originale de la méthode de Thellier a été appliquée. Ainsi, entre les deux chauffes à une même température, le sens du champ était inversé, alors que les échantillons gardaient la même orientation dans le four. Les chauffes ont eu lieu sous vide, le champ étant appliqué durant les chauffes et les refroidissements.

1) Test

Afin de me faire une idée de l'erreur expérimentale, lors d'une expérience faite dans ces conditions, j'ai effectué le test suivant.

-Quatre échantillons de basaltes de l'île de la Réunion, déjà traités par la méthode de Thellier ont été chauffés à nouveau à l'air à 650°C, durant 1h30mn, dans un champ de laboratoire de 25 μT.

-Ensuite, j'ai effectué sur ces échantillons une détermination de paléointensité en utilisant un champ artificiel de 25 μT et en travaillant sous vide.

Les résultats de ce test sont présentés sur la Figure I.1. Les champs calculés s'étendent de 24.1 à 25 μT. La qualité de ces diagrammes démontre la fiabilité du processus expérimental, en particulier la bonne répétition de la température.

Deux remarques peuvent être faite sur cette expérience:

a) l'effet de la chauffe à l'air libre, se rapproche de celui d'une oxydation haute température avec notamment une augmentation des températures de blocage. Si les échantillons RB121 et 127 avaient déjà des températures de blocage élevées avant la chauffe à l'air libre, ce n'était pas le cas pour les spécimens RB139 et 140 (voir

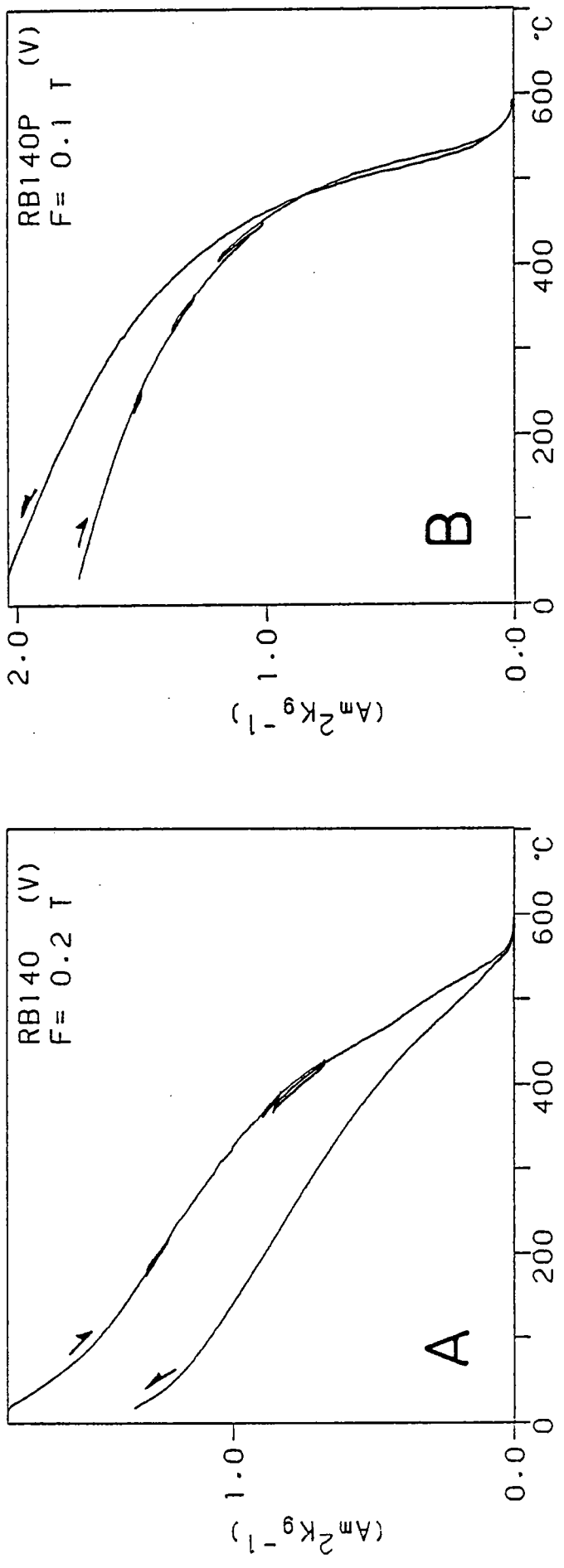

Figure I.2 Balance de Curie effectuée sur un échantillon avant (A) et après (B) une chauffe à l'air libre à 650°C durant 1h30mn. La chauffe à l'air a eu pour effet d'augmenter la température de Curie. L'expérience a été faite sous vide, dans un champ F de 0.1 et 0.2 Tesla.

Annexe 2). L'effet de la chauffe à l'air est très clair si l'on compare les balances de Curie effectuées sur la carotte RB140 avant tout traitement thermique et après la chauffe à l'air (Figure I.2). Les meilleurs résultats ont été obtenus sur les 2 échantillons (RB121 et 127) ayant déjà naturellement subi une oxydation haute température au moment de la mise en place de la coulée.

b) Cette simple expérience permet de vérifier la loi d'addition et d'indépendance des ATR partielles (ATRP).

Cependant deux publications récentes ont remis en cause, d'une part les fondements de la méthode de Thellier (Wörm et al., 1988) et d'autre part l'interprétation 'classique' des diagrammes ARN-ATR (Walton, 1988).

2) Discussion des résultats de Wörm et al.

Wörm et ses collaborateurs, ont étudié, sur des échantillons synthétiques composés de grains mono (ou pseudo-mono) domaines et multidomaines de magnétite, le comportement au cours de désaimantations thermiques, d'ATRP acquises entre 350 et 400°C dans des champs de 0.5 à 5 Oe appliqués de 10 mn à 5 jours. Leur conclusion est que la température de désaimantation de l'ATRP est supérieure à la température d'aimantation; autrement dit l'ATRP acquise entre 350-400°C ne se désaimanterait totalement qu'au-dessus de 400°C. Ce phénomène serait plus important dans le cas des multidomaines que dans le cas de grains plus fins. De ce fait, les ATRP ne seraient pas indépendantes.

Sans vouloir mettre en cause totalement les résulats de cette étude, il faut toutefois noter, que l'ATRP dans l'intervalle de température utilisé (350-400°C) ne représente qu'un très faible pourcentage de l'ATR totale (cf Figure 2 de Wörm et al., 1988), tout particulièrement dans le cas des monodomaines. De plus ils n'ont pas montré clairement que les chauffes n'entrainaient pas d'altération de leurs échantillons. Compte-tenu de ces remarques et des résultats présentés sur la Figure I.1., je pense que les phénomènes décrits par Wörm et al. peuvent être considérés, dans le cas des monodomaines tout au moins, comme des phénomènes de second ordre, qui ne remettent pas en cause les résultats de Thellier.

3) Discussion à propos de la méthode de Walton

Il est bien connu que les chauffes successives pratiquées pour la détermination de la paléointensité entraînent très fréquemment des modifications physico-chimiques des minéraux magnétiques qui sont d'autant plus importantes que la température est élevée. Le principal problème est de pouvoir détecter ces modifications. L'absence

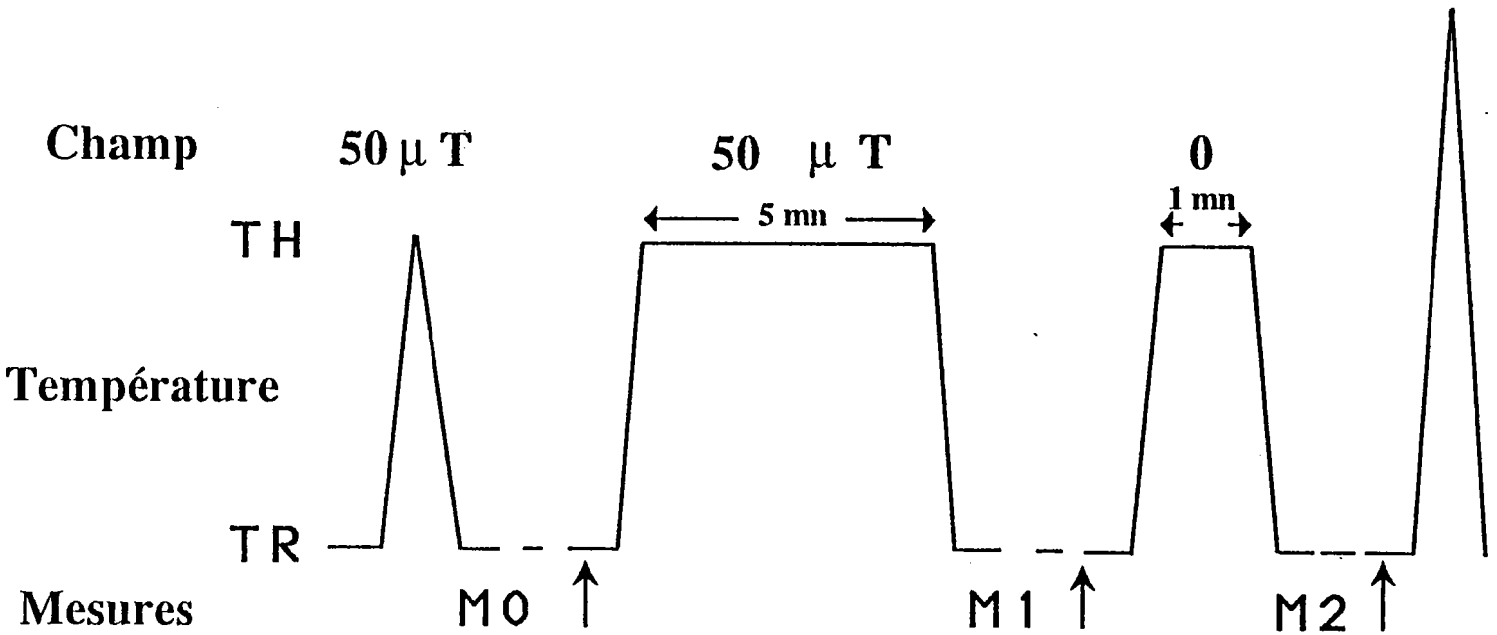

Figure I.3 Descriptions des trois chauffes successives proposées par Walton (1988). Pour des températures inférieures à T_R, le champ de laboratoire est coupé. M_0, M_1 et M_2 sont les trois moments mesurés après chacune des chauffes à la température T_H

d'altération de l'échantillon dans un intervalle de température est attesté par un alignement des points du diagramme ARN-ATR le long d'une droite. D'autre part des tests de stabilité de la capacité d'acquisition d'ATR sont couramment pratiqués dans le but de mettre en évidence d'éventuelles altérations de l' échantillon.

Récemment, ces deux critères de stabilité ont été mis en doute par Walton (1988), qui propose une méthode pour d'une part détecter l'altération des minéraux magnétiques durant les chauffes et d'autre part pour corriger les points du diagramme ARN-ATR de l'effet de l'altération.

La technique de Walton comprend trois chauffes successives par étape de température (Figure I.3.). La première chauffe est très rapide et est effectuée sous champ. l'échantillon acquiert alors une ATR entre les températures T_H et T_R (T_R étant la température de référence, pour des températures inférieures à T_R le champ est coupé). A la fin de cette première chauffe la rémanence mesurée est notée M_0. La seconde chauffe, effectuée sous le même champ que précédemment, est plus longue puisque l'échantillon est maintenu à la température T_H durant 5 mn. Le moment M_1 est ensuite mesuré. Enfin la troisième chauffe est faite en champ nul, l'échantillon étant maintenu à la température T_H durant 1 mn. Le moment M_2 est alors mesuré.

L'altération de l'échantillon est mesurée par la différence entre les moments M_1 et M_0. De plus, la différence (M_1-M_0) est multipliée par un facteur f constant qui tient compte du fait qu'une partie de l'altération peut se produire avant la première mesure M_0. L'ARN est déduite de la mesure M_2 et est également corrigée de l'effet de l'altération. Donc en résumé, à chaque étape de température T_i, l'ATR_i est corrigée par un facteur qui peut s'écrire: $f * \sum_{j=1}^{i} (M_{1j}-M_{0j})$, et qui cumule les effets d'altération sur les étapes de chauffe précédentes; l'ARN_i est également corrigée par un facteur équivalent.

Le mode opératoire suivi par Walton est très différent de celui que j'ai utilisé. Il est adapté au matériel étudié en archéomagnétisme, c'est à dire de très petits spécimens chauffés individuellement dans un mini-four et mesurés au cryogénique.

Le facteur f utilisé par Walton a deux particularités. Premièrement il est indépendant de la température, or comme le font remarquer Aitken et al. (1988), on peut plutôt penser que l'altération lors de la première chauffe est fonction de la température. D'autre part, ce facteur f a été déterminé à partir d'expériences de Thellier faites sur des briques récentes pour lesquelles l'intensité du champ au moment de leur fabrication était bien connu. Ce même facteur est ensuite utilisé quelque soit l'âge et la composition des matériaux étudiés. Ceci est un facteur limitatif de la méthode car, du moins en ce qui concerne les roches volcaniques, il parait peu

raisonnable d'appliquer un même facteur correctif pour tous les spécimens quelque soient leurs caractéristiques magnétiques (température de blocage, coercivité etc...).

Compte-tenu des résultats présentés sur la Figure I.1., contrairement à ce que suggère Walton, il parait difficile de considérer qu'une erreur systématique importante puisse être faite en calculant la paléointensité sur un segment linéaire du diagramme ARN-ATR, contenant une large fraction de l'ARN ainsi que des tests d'ATRP positifs. L'altération de l'échantillon est mise en évidence facilement si les étapes de température sont suffisamment nombreuses.

Le problème le plus important est le choix de l'intervalle de température retenu pour calculer la paléointensité, lorsque les points du diagramme ARN-ATR sont distribués sur une large courbe, du fait de l'évolution de l'échantillon aux cours des chauffes. Cet aspect est développé dans l'article qui constitue la première partie de mémoire. La méthode de correction proposée par Walton du fait de son caractère empirique ne me parait pas d'une grande utilité.

4) Effet de la vitesse de refroidissement sur l'intensité de l'ATR;

Des études théoriques ont montré que les températures de blocage d'un ensemble de grains de magnétite sont dépendantes de la vitesse de refroidissement. Une vitesse de refroidissement lente aurait tendance à diminuer les températures de blocage (Dodson et McClelland Brown, 1980; Halgedahl et al., 1980). De ce fait l'intensité de l'ATR mesurée à la température ambiante augmenterait lorsque le taux de refroidissement diminuerait (McClelland Brown, 1984).

Dodson et McClelland ont prédit, pour un assemblage de grains monodomaines de magnétite, une augmentation de 5% de l'intensité d'ATR lorsque le taux de refroidissement diminue d'un facteur 10, alors que Halgedahl et al., ont suggéré une variation deux fois plus importante.

La dépendance de l'intensité de l'ATR en fonction de la vitesse de refroidissement a été vérifiée expérimentalement par Fox et Aitken (1980). Toutefois, d'autres tests effectués sur des échantillons synthétiques ont montré que pour les grains pseudo-monodomaines ou multidomaines de titanomagnétites, un effet inverse à celui décrit précédemment se produit. L'intensité de l'ATR produite lors d'un refroidissement rapide est plus forte que celle obtenue après un refroidissement plus lent (McClelland Brown, 1984).

Au vue de ces données et compte-tenu de leur importance dans la détermination de la paléointensité, j'ai effectué quelques expériences à ce sujet.

Notre équipement a permis de refroidir les échantillons de trois façons différentes:
1- Un refroidissement rapide (noté R) pour lequel la température passe de 500 à 400°C en un peu plus de 2 mn et de 400 à 300°C en 4 mn, alors que la température ambiante

est atteinte en 1h15mn. 2- Un refroidissement plus lent (noté L) qui est obtenu en laissant le four autour des échantillons après avoir arrêté la régulation thermique. Dans ce cas, on passe de 500 à 400°C en 30 mn, de 400 à 300°C en 1h. La température ambiante est atteinte en 8h environ. 3- Un refroisissement encore plus lent (noté L+) a été effectué pour lequel entre 650 et 400°C, la décroissance en température est de 1°C/mn alors que après 400°C, la décroissance en température est la même que dans le cas précédent.

Six échantillons de basaltes de la Réunion ont été utilisés. Ces échantillons ont comme caractéristiques magnétiques, des points de Curie élevés, une forte résistance au champ alternatif et ils peuvent être être considérés comme proche des monodomaines.

Ces 6 spécimens ont été chauffés à 650°C (sous vide) dans un champ de 50 μT, le premier refroidissement étant rapide. Le moment mesuré à la température ambiante a alors servi de référence.

Puis ces échantillons ont été chauffés 4 fois à 650°C, sous vide, et refroidit de la manière suivante: 1- refroidissement lent (L), 2- taux de refroidissement rapide (R), 3- refroidissement plus lent (L+) et enfin 4- refroidissement rapide (R).

Les étapes 2 et 4 m'ont permis de mesurer l'effet de l'altération des échantillons après les différentes chauffes. Les résultats (en pourcentage du moment initial) sont reportés sur la figure I.4.

On peut constater que dans tous les cas, l'intensité de L'ATR augmente quand la vitesse de refroidissement diminue. Quelques évolutions des échantillons sont visibles. L'augmentation maximale de l'ATR est proche de 14%. Les échantillons avec les températures de blocage les plus élevés (représentés par les carrés noirs sur la Fig I.4a et les cercles creux sur la Fig. I.4b) sont ceux pour lesquels l'écart est le moins important (6 à 8% respectivement).

Ces résultats peuvent laisser penser que l'intensité de l'ATR est inversement proportionnelle au taux de refroidissement, ce qui n'est vraisemblablement pas le cas, comme le témoigne les résultats de Fox et Aitken (1980). Une valeur maximale est sans doute rapidement atteinte.

Au vue de ces données. on peut donc soupçonner un effet du taux de refroidissement sur l'intensité de l'ATR, mais qui est variable d'un échantillon à l'autre.

Peu de données existent dans la littérature à ce sujet. Une étude extensive de coulées historiques, pour lesquelles l'intensité du champ serait connue lors de leur mise en place, pourrait être très utile pour quantifier cet effet. Lorsque de telles comparaisons ont été faites, il semble que les écart entre la valeur obtenue et la valeur réelle ne dépassent pas 10% (Khodair données non-publiées, communication personnelle de Coe, 1987).

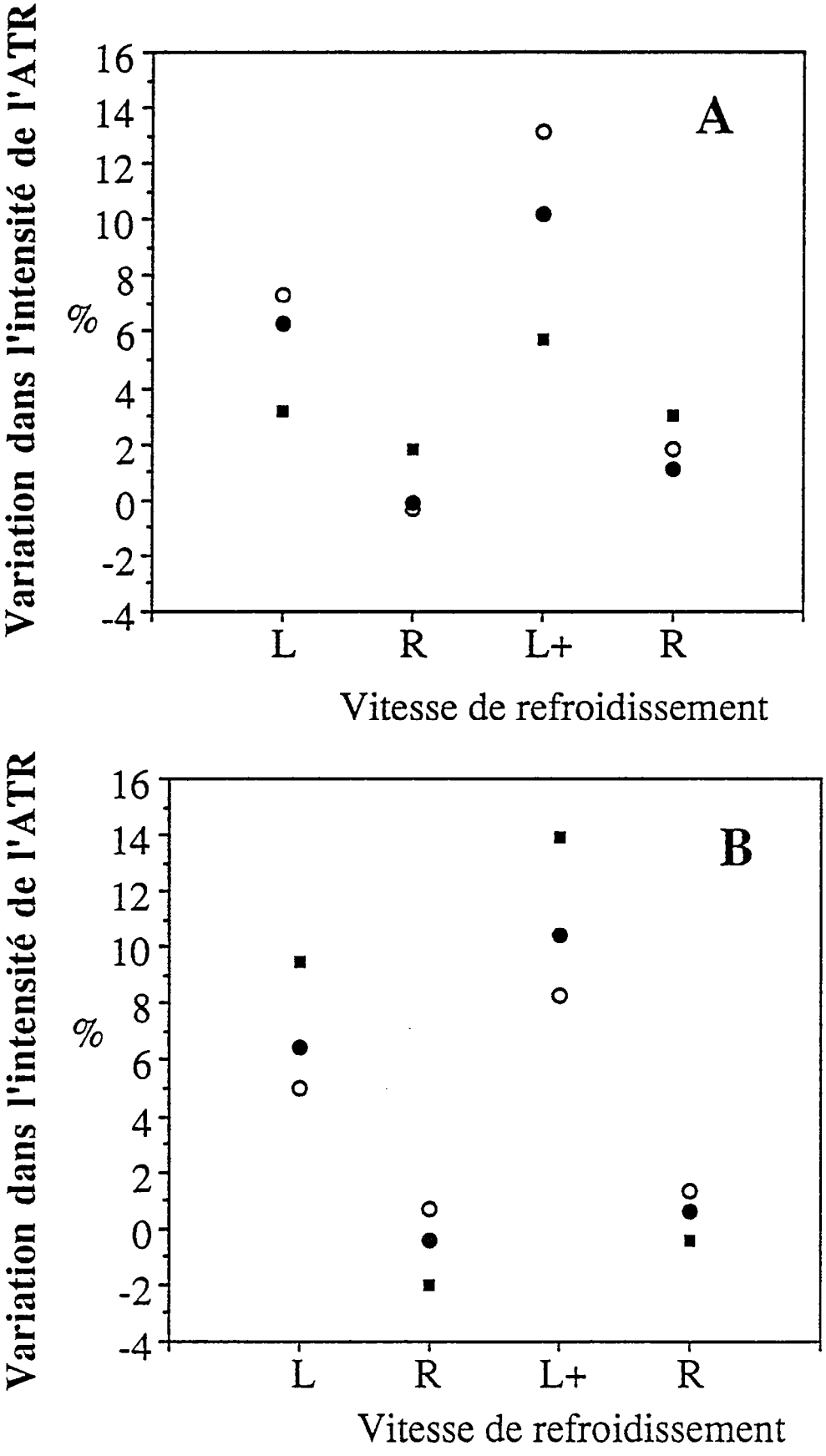

Figure I.4 Variations de l'intensité de l'ATR en fonction de la vitesse de refroidissement, exprimées en pourcentage de l'intensité de l'ATR initiale produite dans un champ de 50 μT et acquise lors d'un refroidissement rapide. R: indique les refroidissements rapides d'une heure et demi; L indique un refroidissement de 8h; L+ un refroidissement encore plus lent.

Compte-tenu de cette dernière remarque et du fait que les résultats de mon expérience ne sont que très partiels, j'ai décidé de ne pas prendre en compte cet effet lors de la présentation des résultats de paléointensité.

5) Effet de l'anisotropie

Une forte anisotropie dans les échantillons (telle que celle souvent observée dans les tuiles ou briques) peut entraîner des erreurs non-négligeables dans la détermination de la paléointensité. Pour les coulées volcaniques l'anisotropie attendue est assez faible. Sur la Figure I.5. est présentée l'inclinaison moyenne de l'ATR, observée lors des 2 dernières étapes de température, pour les 66 échantillons de La Réunion ayant donné des résultats. Le champ de laboratoire étant appliqué suivant l'axe Z des échantillons, une inclinaison proche de 90° est attendue.

On constate que pour la majorité des échantillons, l'inclinaison de l'ATR totale est supérieure à 88°, ce qui compte-tenu des erreurs expérimentales (notamment le positionnement des échantillons dans le four) est négligeable. Cependant, pour 5 d'entre eux, des déviations de l'ATR de 4 à 6° sont observées. Ceci suggère une légère anisotropie de ces échantillons, entraînant sans doute une faible erreur sur la paléointensité calculée.

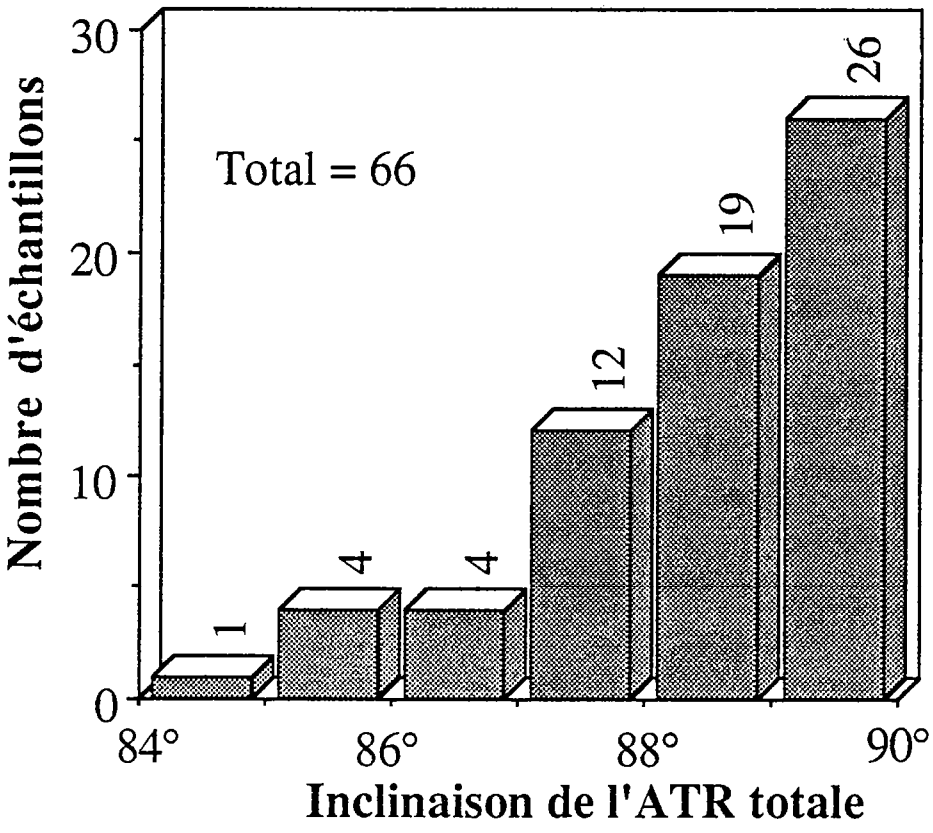

Figure I.5 Inclinaison moyenne de l'ATR mesurée lors des deux dernières étapes de température dans l'expérience de Thellier, pour 66 échantillons de La Réunion.

PALEOINTENSITY OF THE EARTH'S MAGNETIC FIELD RECORDED BY TWO LATE QUATERNARY VOLCANIC SEQUENCES, AT THE ISLAND OF LA RÉUNION (INDIAN OCEAN).

Annick Chauvin[1], Pierre-Yves Gillot[2] and Norbert Bonhommet[1]

Laboratoire de Géophysique Interne, CAESS, Universite de Rennes I, 35042 Rennes Cedex, France.

Centre des Faibles Radioactivités, CEA-CNRS, Avenue de la Terrasse, 91190 Gif/Yvette, France

submitted to Journal of Geophysical Research

ABSTRACT

Up to now, most of the paleointensity data come from sites grouped in the Northern hemisphere. In order to improve our knowledge of the past variations of the geomagnetic field intensity, data from the South hemisphere are still necessary. For this reason, a paleomagnetic study has been undertaken on two dated volcanic sequences from the Piton de la Fournaise volcano (island of La Réunion, Indian Ocean). The analysis of the paleomagnetic directions clearly indicates that the extrusion rate of the lava flows was not constant with time. A detailed study of the magnetic properties of the samples was carried out. Paleointensity experiments were performed following the original version of the Thellier method. Values of the paleofield strength have been obtained on 23 flows among the 30 which were sampled. Virtual dipole moments (VDMs) determined on the younger site, which belongs mostly to the Holocene period, follow quite well the global dipole moment curve known for the last 12,000 years. On the other hand, data from the older site are the first paleointensity values obtained in the time period 82,000-98,000 years and suggest that the field did not depart from its average behavior.

INTRODUCTION

Late Quaternary secular variations of the earth's magnetic field are recorded by different materials, archaeological artefacts, dated lava flows and lake or marine sediments.

The direction of the past geomagnetic field is generally easily determined because it is almost equal to the direction of the magnetic remanence. In contrast, the intensity of the magnetic remanence is not only dependent on the intensity of the field but is strongly related to the material, thus making the determination of the paleointensity of the geomagnetic field more difficult to establish than its paleodirection. Although the knowledge of the variations of intensity of the geomagnetic field is as important as its directional behavior, very few studies describe the paleomagnetic field as a complete vector.

Volcanic rocks as well as archaeological materials provide spot-readings of the geomagnetic field while sediments provide the only means of obtaining continuous records of the secular variation at one site. Moreover, sedimentary records from lake or marine cores are numerous enough to allow a better geographic coverage. However, the magnetization process is complex and supposed to smooth the original magnetic signal. An other major drawback to sediments is the difficulty to recover the paleointensity from the paleomagnetic record. In the best cases, only relative paleointensity changes can be obtained (Levi and Banerjee, 1976; King et al., 1983).

Thermoremanent magnetizations (TRM) of volcanic deposits and archaeological materials allow the determinations of both direction and absolute intensity of the geomagnetic field, because TRM is proportional to the weak inducing field and can be reproduced in the laboratory.

Paleointensity data for the late Quaternary have been mostly obtained from the northern hemisphere, Europe (Schweitzer and Soffel, 1980 ; Kovacheva, 1980, 1983 ; Thellier, 1959 ; Salis, 1987, Burlatskaya, 1983 ; Walton, 1979, 1984 ; Aitken et al., 1984), Egypt (Games, 1980, 1983; Aitken et al., 1983), India (Ramaswamy et al., 1985), Japan (Tanaka, 1980 ; Hirooka, 1983), Hawaii (Coe, 1967a

; Coe et al., 1978), China (Wei, et al., 1987) and North America (Sternberg and Butler, 1978 ; Sternberg, 1983 ; Champion, 1980).

Only a few data from Australia (Barbetti, 1983) and Peru (Kono et al., 1986; Games, 1983) compose the data base for the southern hemisphere. Moreover, most of these data correspond to the last 2,000 years.

Paleointensity data indicate that the strength of the paleofield at any locality can change by a factor of two over a period of time as short as a few hundreds years (Kovacheva, 1982; Barbetti, 1983). Such variations in intensity associated to uncertainties in the age determinations and the geographic distribution of the sites makes difficult the analysis of global intensity data (Merrill and McElhinny, 1983).

Compilations of worldwide paleointensity data have been performed for three periods of time, the last 12,000 years, and 50,000 years and the last 5 Ma. (Barton et al., 1979, Senanayake and McEhlinny, 1982 and McFadden and McEhlinny, 1982). By averaging the field over short periods of a few hundreds years (500 or 1000 years) and for several localities, the non dipole contribution is assumed to be averaged out. The curve of the variations of the mean VDMs versus time is fairly well established for the last 10,000 years. In the time interval 15,000 to 50,000 there is some strong evidences that the field was lower than in more recent time (McElhinny and Senanayake, 1982; Salis, 1987), as well as compared with the average field for the last 5 Ma. Also, a detailed statistical analysis of the VDMs for the last 5 Ma indicates that non dipole fields are almost proportional to the strength of the dipole field (McFadden and McElhinny, 1982). Such positive correlation between the magnitude of the dipole and non dipole fields are not observed during polarity transitions.

Recently, it has been suggested that perturbations at the core mantle boundary, some fixed and some other drifting, may provide specific features with some geographic dependency (Gubbins, 1988). To test this hypothesis, paleomagnetic data from the southern hemisphere are needed.

In this paper, we will report a detailed paleomagnetic study of two young volcanic sequences from the island of La Réunion (Indian ocean, -21°S). Several paleointensity determinations have been attempted using the Thellier and Thellier (1959) stepwise double heating method which has been considered as the most reliable (Coe and Gromme, 1973; Prévot et al., 1985; Aitken et al., 1988).

GEOLOGY GEOCHRONOLOGY AND SAMPLING

The island of La Réunion lies in the western Indian Ocean (21°S, 55.5°E°) and is constituted of two volcanic cones (Fig. 1) which define the present location of an intra-oceanic hot-spot volcanism. The

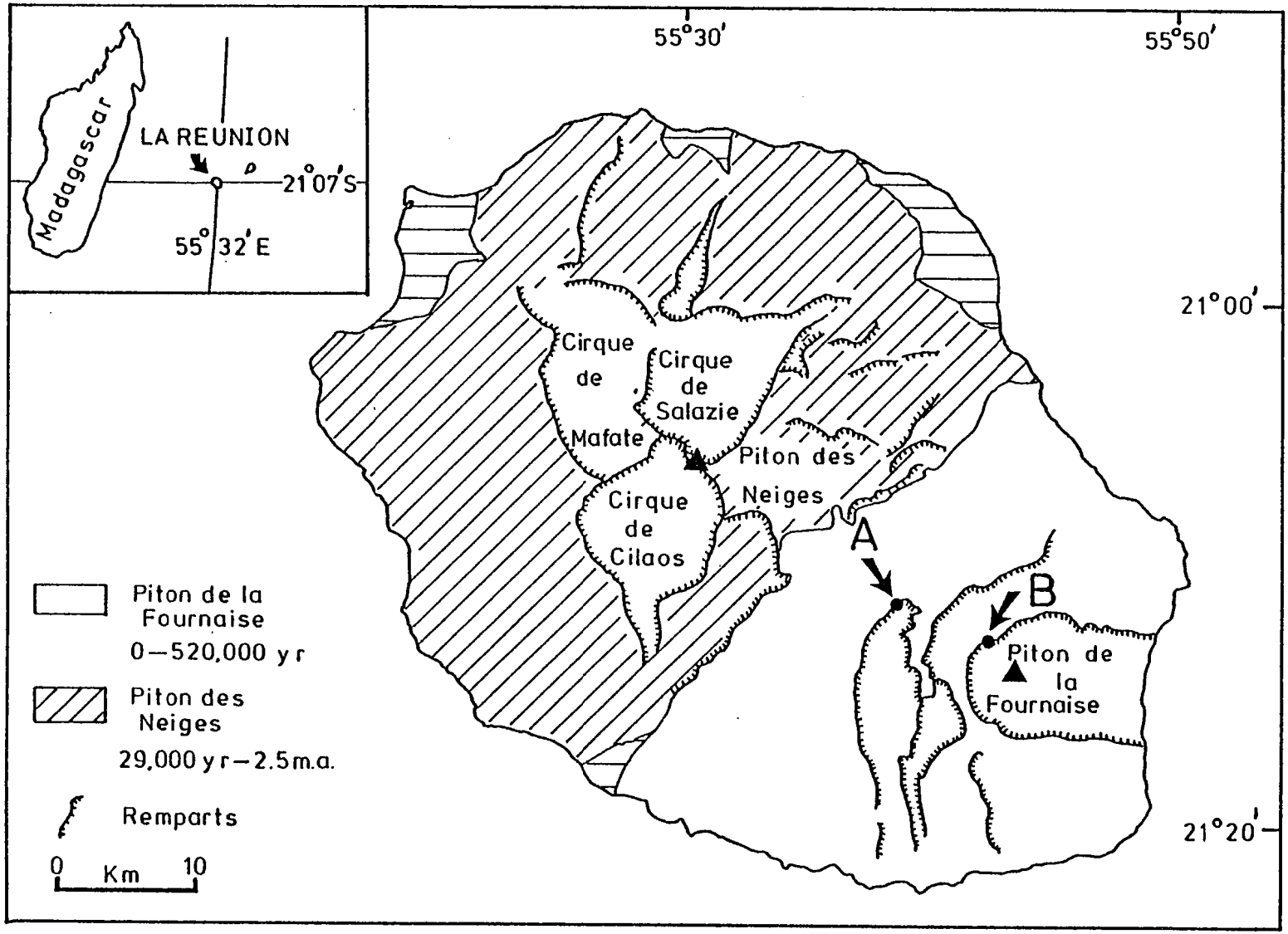

Fig.1: Sampling map of the island of La Réunion showing the two volcanos (Piton des Neiges and Piton de la Fournaise). The sampling corresponds to two vertical sections at site A and B.

larger one,the Piton des Neiges which occupies the northwestern part of the island, is now extinct, while the youngest, the Piton de la Fournaise is still active.

The first stratigraphy and chronology of the volcanics, based on K-Ar radiometric datings was established by McDougall (1971). The addition of recent studies (Gillot and Nativel, 1982, Gillot, 1984) contributes to well define the geological evolution of the island. The Piton des Neiges is composed of two different series of lava flows: an oceanite and a differentiated serie. The oceanite formation extends from 2 Ma. to 0.4 Ma. The activity of the Piton de la Fournaise started at the time of the last extrusions of the oceanite formation at the Piton des Neiges (between 0.52 and 0.43 Ma.).

Four volcanic phases are recognized at the Piton de la Fournaise; the first one finished with the collapse of the caldera named Rivière de Remparts, around 0.28 Ma. The second cycle extends from 0.2 to around 0.06 Ma. and is marked by the collapse of the second caldera, the Plaine des Remparts. The third phase is contemporaneous with the last activity recorded at the Piton des Neiges dated around 30 Ka. (1Ka.=1 thousand years). The fourth phase which started about 10 Ka. ago, shows the built up of the new caldera named Enclos du Fouqué where is located the present volcanic activity.

The age determination of very young volcanic rocks by K-Ar method is difficult because of the small decay constant of ^{40}K. Argon is also a major component of the atmosphere and equilibrates with the lavas as they cool. Thus, attention must be paid to the principal correction in age calculation, that for argon contamination. Several factors may limit the precise measurement of small amounts of radiogenic ^{40}Ar within a total Ar signal, which is composed principally of atmospheric argon trapped by the sample and the extraction system. The distinctive feature of the method of Cassignol and Gillot (1982) is regular and repeated argon isotopic measurements of pipetted aliquots from a reservoir of atmosphere, to determine precisely the atmospheric ratio of $^{40}Ar/^{36}Ar$, recorded by the spectrometer. Other significant aspect of this technique are the omission of spike frequently included to determine the absolute concentration of ^{40}Ar and adjustment of the air argon and sample argon volumes to a common argon pressure. Samples dated by the Centre des faibles radioactivités, were collected during the same field trip than those used for paleomagnetic study. K-Ar ages are given at $\pm 2\sigma$.

Two volcanic sections from the Piton de la Fournaise were sampled (see Fig 1). The first section called Remparts de Bellecombe (site B) consists of thirteen lava flows and represents a stratigraphic height of one hundred meters. The top of this section has been dated by ^{14}C performed on carbonized wood (Bachelery 1981) at 4754 years and the 8th flow gives a K-Ar age of 11 Ka. ± 2.6.

Seventeen lava flows constitute the second section called Rivière des Remparts (site A). Radiometric age determinations by K-Ar have given ages of 82 Ka. ± 6. for the first lava, 85.5 Ka. ± 3.0 for the 6th and 98 Ka. ± 4.0 for the last lava flow sampled, at the bottom of the section. This section represents an elevation of 185 m.

One hundred seventy seven cores were collected, using a gasoline-powered portable core drill; this gives an average of 5 to 6 cores per flow.

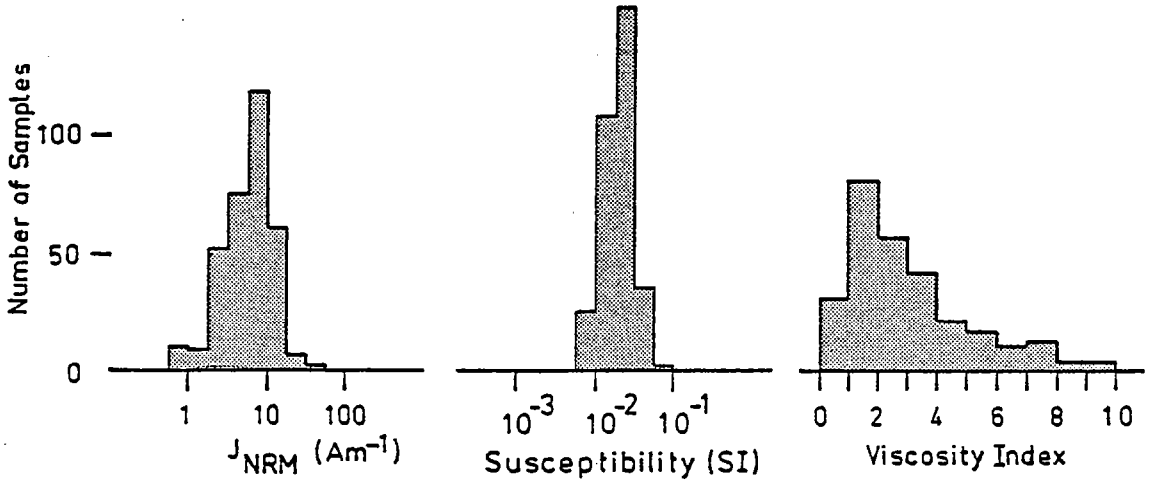

Fig.2: Distribution of the intensity of remanent magnetization (J_{NRM}), weak-field susceptibility (χ) and viscosity index for all specimens.

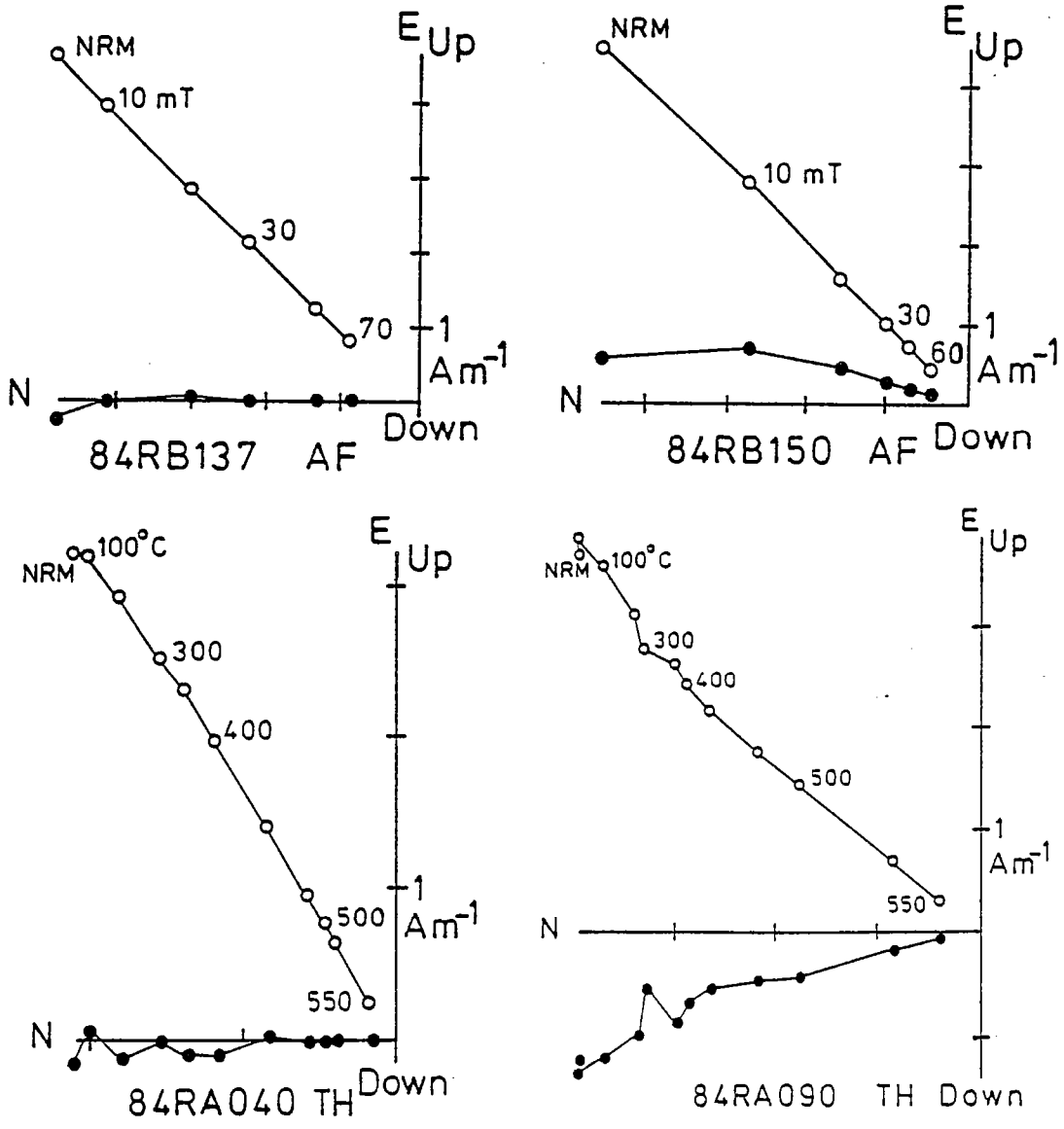

Fig.3: Examples of thermal (TH) and alternating field (AF) demagnetizations; open circles represent the projection in the vertical plane, filled circles correspond to the horizontal plane.

REMANENT DIRECTIONS

Measurements and demagnetizations were carried out using the Schonstedt equipment. Natural remanent magnetization (NRM) intensity ranges from 1 to 40 Am^{-1}, with a maximum in the distribution around 7 to 10 Am^{-1} (Fig. 2).

Stepwise thermal or alternating field (af) demagnetizations were performed on one sample from each core. Characteristic directions were obtained according to the best fitting line on orthogonal vector plots. In computing the mean directions per flow, a few samples were omitted if field notes suggested possible orientation mistakes or if complete cleaning of the secondary magnetization was not obtained, especially in the case of the strong magnetic overprint due to lightning strike recorded by some flows of the site A (flows RA10 and RA12).

Well defined primary remanent directions have generally been obtained (Fig. 3). The shape of the af demagnetization curves are variable as well as between flows and within samples from a same flow. About 30 % of samples from the site A have a medium demagnetizing field (MDF) higher or equal to 30 mT, while almost three-quarter of samples from the site B have this high stability against the alternating field. The various spectrum of unbloking temperatures indicates that titanomagnetites are the magnetic carriers of the remanence.

A) Results from the site B: Rempart de Bellecombe (Tab 1)

The mean directions per flow are listed in table 1 and plotted on a stereographic projection (Fig. 4). The corresponding virtual geomagnetic poles (VGP) are displayed in Fig. 5. According to the radiometric age determinations, this section represents a time interval of few thousands years but less than 10 Ka..

From figure 4, two groups of directions can easily be identified. On an other hand, the first group from RB1 to RB9 has an elongated pattern which can be subdivided into 3 small groups of successive flows having recorded very close directions (RB9 to RB5, RB4 RB3 and RB2 RB1) (see also table 1). The relatively low number of samples (5 to 6) per flow, does not enable statistical distinction using the α_{95}. The precision parameter of Fisher statistics associated to the mean direction (0°.0,-43°.2) calculated from the 13 units is relatively high (k=105) and confirms that a small part of secular variation was recorded at this site.

B) Results from the site A: Rivière des Remparts (Table 1, Fig 4 and 5))

The distribution of the paleomagnetic directions shows greater variations than those observed in the previous sequence. Although the low number of samples per flow makes statistical tests inconclusive, several groups of successive flows having recorded similar directions may be identified on the stereographic projection (Fig. 4). For example, the 3 first flows RA1 to RA3 have close directions with an inclination about -45°, while the underlying flows (RA4 to RA9) have steep inclinations about -60°. Flows RA10 and RA11 have similar directions than the first group, on the top of the section. The

Table 1: Paleomagnetic data

Rivière des Remparts: **site A**

Lava Flows	n/N	D	I	k	α_{95}	R	Lat	long	J_{NRM}	χ
RA1	3/5	7.8	-45.2	68.3	15.0	2.9707	81.0	184.8	15.5	2.3
RA2	3/5	1.5	-48.5	249.2	7.8	2.9920	81.6	226.5	6.7	2.2
RA3	3/8	1.3	-43.4	116.0	11.5	2.9828	85.7	219.5	8.4	1.6
RA4	4/5	352.0	-64.8	135.6	7.9	3.9878	63.6	247.9	2.4	1.3
RA5	3/5	353.1	-63.9	25.0	25.2	2.9220	65.0	247.0	3.5	1.3
RA6	3/6	343.7	-61.0	220.3	8.3	2.9909	65.1	265.1	3.7	1.3
RA7	6/6	350.9	-57.8	202.8	4.7	5.9753	71.1	257.9	2.6	2.0
RA8	6/6	346.4	-58.8	97.5	6.8	5.9487	68.3	264.8	2.1	3.3
RA9	5/6	348.8	-58.1	358.2	4.0	4.9988	70.0	261.7	2.4	3.0
RA10	4/6	5.6	-47.9	17.5	22.6	3.8286	80.7	203.5	13.0	2.2
RA11	6/8	3.4	-52.6	161.1	5.3	5.9690	77.6	222.1	2.7	1.1
RA12	2/6	332.9	-39.0	-	-	-	64.8	318.5	5.8	1.1
RA13	5/5	335.9	-43.9	549.2	3.3	4.9927	67.5	309.3	4.7	2.9
RA14	6/6	334.3	-50.5	139.9	5.7	5.9643	64.9	296.6	1.0	2.4
RA15	6/6	335.1	-38.4	158.9	5.3	5.9685	66.8	319.9	5.2	2.2
RA16	6/7	359.1	-36.7	112.3	6.3	5.9555	88.9	7.4	5.6	3.0
RA17	6/7	351.9	-44.0	194.2	4.8	5.9742	81.3	292.3	3.2	3.5
MEAN	17	350.7	-50.9	46.7	5.3	16.657	76.2	269.8		

Remparts de Bellecombe: **site B**

Lava Flows	n/N	D	I	k	α_{95}	R	Lat	long	J_{NRM}	χ
RB1	6/6	1.1	-40.9	208.6	4.6	5.9760	87.6	211.1	9.8	1.3
RB2	5/6	0.8	-41.4	150.5	6.3	4.9734	87.3	219.7	8.6	1.5
RB3	5/5	358.7	-33.2	139.8	6.5	4.9714	86.7	33.6	8.9	1.5
RB3bis	5/5	357.9	-38.4	918.7	2.5	4.9956	88.0	313.0	9.7	1.5
RB4	6/6	356.0	-34.8	406.6	3.3	5.9877	85.7	353.3	6.7	1.6
RB5	5/5	3.8	-41.0	461.2	3.6	4.9913	86.3	184.7	7.7	1.4
RB6	6/6	5.4	-43.8	129.5	5.9	5.9614	83.4	188.3	5.4	1.6
RB7	5/7	10.6	-41.8	579.0	3.2	4.9931	79.8	163.9	5.3	2.2
RB8	5/5	6.7	-43.8	87.8	8.2	4.9544	82.4	182.5	8.0	1.8
RB9	5/5	4.7	-42.5	73.0	9.0	4.9452	84.5	184.7	7.5	0.9
RB10	5/5	350.0	-50.0	117.8	5.8	4.9775	76.9	276.5	9.6	2.4
RB11	5/5	352.6	-53.5	262.7	4.7	4.9848	75.6	260.9	8.5	1.6
RB12	5/5	347.7	-54.3	140.6	6.5	4.9715	72.6	271.3	9.2	3.5
MEAN	13	0.0	-43.2	104.7	4.1	12.885	85.7	237.9		

Table 1 RA (Réunion site A); RB (Réunion site B). n/N: number of samples used in the analysis/total number of samples collected; D, I: mean declination and inclination; k: precision parameter of Fisher; α_{95}: 95% confidence cone about mean direction; R: vector sum of the N unit vectors; Lat, Long: latitude and longitude respectively of VGP position; J_{NRM}: geometric mean NRM intensity; χ: geometric mean susceptibility (SI units).

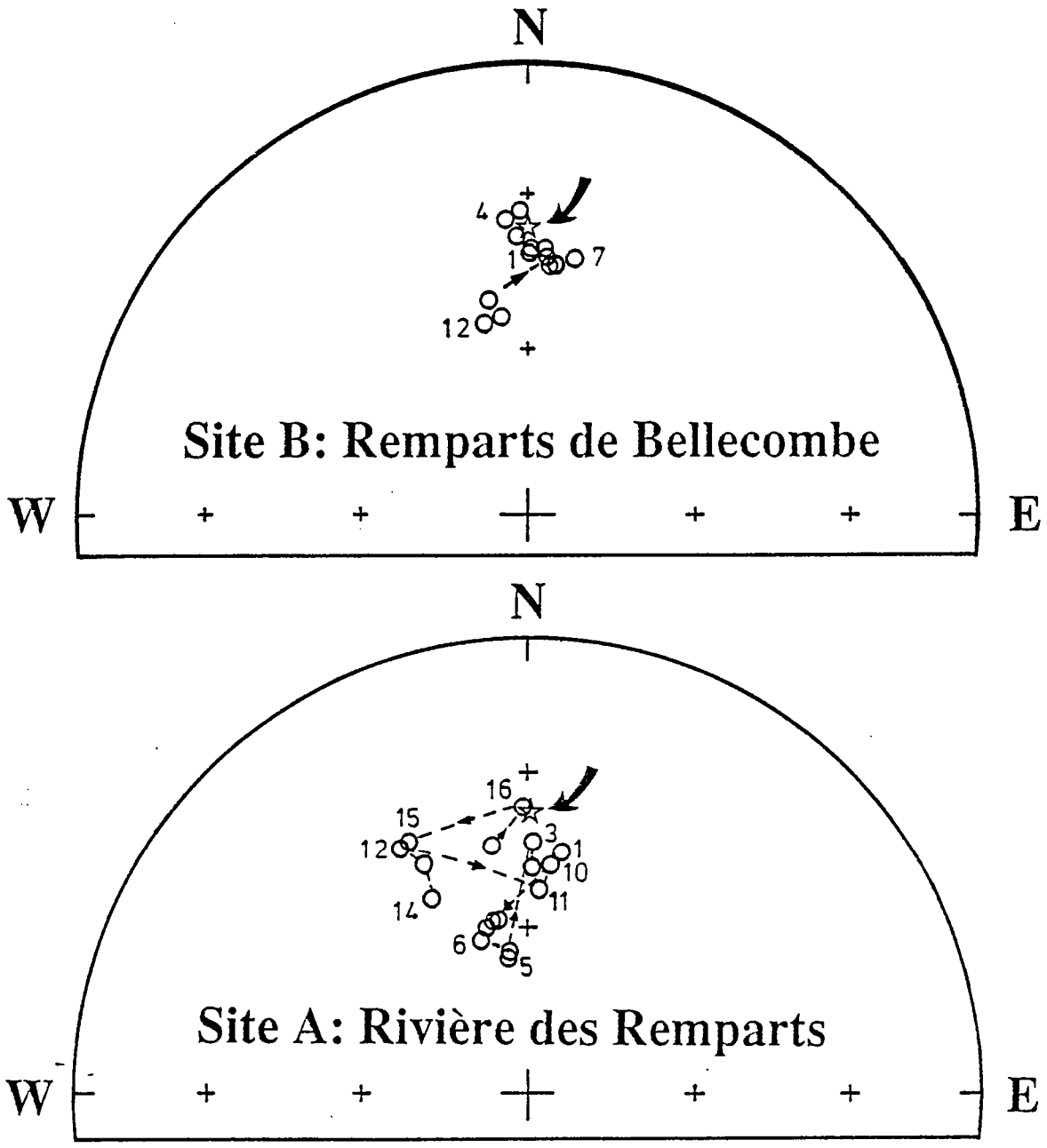

Fig.4: Stereographic projection of mean paleomagnetic directions per flow for both sequences B and A. Open circles are projection on the upper hemisphere. The sequences of flows are numbered from top to bottom; the stars pointed out by the arrows correspond to the geocentric axial dipole direction.

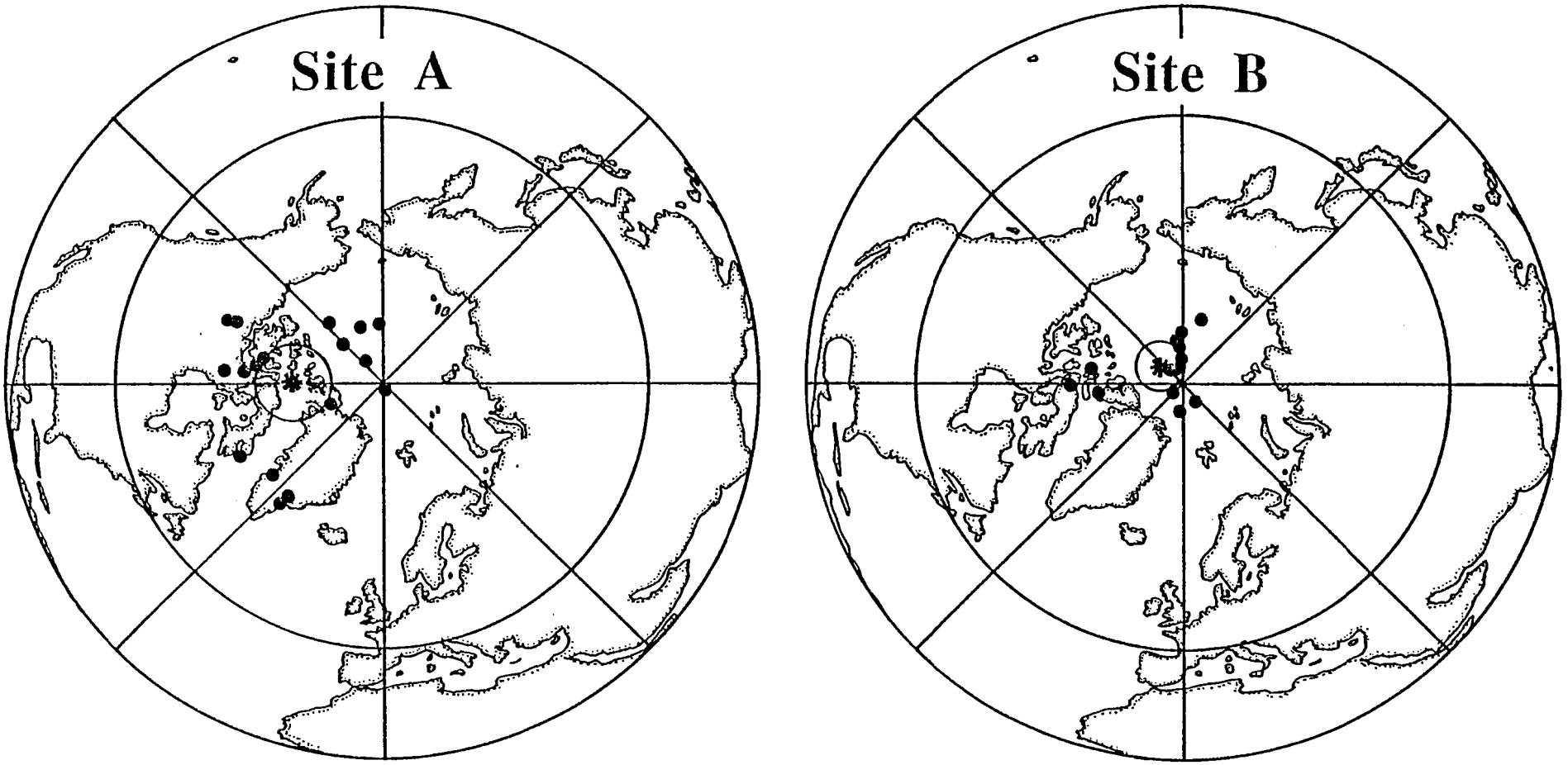

Fig.5: Virtual geomagnetic pole associated to mean directions of Fig.4; the stars are the mean VGPs for each sequence.

underlying group of flows (RA15 to 12) have a north-west declinations. At the bottom of the section, two flows RA17 and RA16 have recorded directions close to the axial dipole expected at this site.

Almost all the individual directions have steeper inclinations than the one expected from an axial dipole, thus the mean direction for the section (350.7, -50.9) is at more than 10° from the expected one. The dipersion parameter (k=46.7) suggests that a full secular variation pattern has not been averaged for this site. The total angular dispersion of VGPs (ST), if we discard flow RA12 for which only two samples were used in computing the mean direction, has a value of 12.5. The angular dispersion of the field (SF= 11.7) has lower and upper limits (Cox, 1969) at 95% of 9.3 and 15.6 (with $SF^2=ST^2-SW^2/n$, SW is the average angular dispersion within flows, here SW=9.6 and n is the average number of samples per flows, here n=4.7).

The value of SF is lower than that given by recent models of secular variation (see for examples models F and G of McFadden and Merrill, 1984 ; McFadden et al., 1988) but is well within the statistical confidence limits.

Comparison with previous studies, based on dispersed sampling, at La Réunion (Watkins, 1973, Chamalaun, 1968), or at other islands in the Indian Ocean (Watkins and Nougier, 1973) indicates clearly that our sampling did not record a similar amount of variation of the magnetic field.

PALEOMAGNETISM AND CHRONOLOGY OF THE VOLCANISM

According to the radiometric datings, both sections A and B cover a time interval of a few thousands years. A question arises: have the flows been extruded regularly over these time intervals?

Radiometric methods are unable to resolve such fine scale variations. In contrast, the pattern of paleosecular variation may be used to constrain the chronology of past volcanic activity.

A) Comparison with Archeomagnetic secular variation

Because the present day geomagnetic field is not atypical (McFadden et al., 1988), we can speculate that the type of archaeomagnetic secular variation curves provide good examples of what we should observe in a record of paleosecular variation. Curves of variations of the earth's magnetic field for the last 2 Ka. have been defined for specific geographical areas as Bulgaria (Kovecheva 1982), Paris (Thellier, 1981), China (Wei et al, 1981) London (Aitken, 1970) from archaeomagnetic material, or from known age lava flows from Hawaii (Holcomb et al., 1986) or Sicily (Tanguy et al., 1985). All these curves clearly exhibit much higher variations than the record from Rempart de Bellecombe. On the other hand, secular variation of the earth's magnetic field may be divided in two parts, one due to variation of the non-dipole field and the second corresponding to the dipole wobble. Averaging several data of the same age, well distributed around the world, provides a mean field that corresponds to the dipole value. Champion (1980) compiled VGPs from archaeomagnetic data which then were averaged by 100 years intervals. In order to not overweight data from Europe, 8 different regions were defined and a mean VGP was calculated within each region. The mean field was calculated from these eight different mean values. Merrill and McElhinny, (1983) completed the analysis made by Champion. This process averages out the non-dipole field and enables to recognize the successive motions of the dipole (dipole

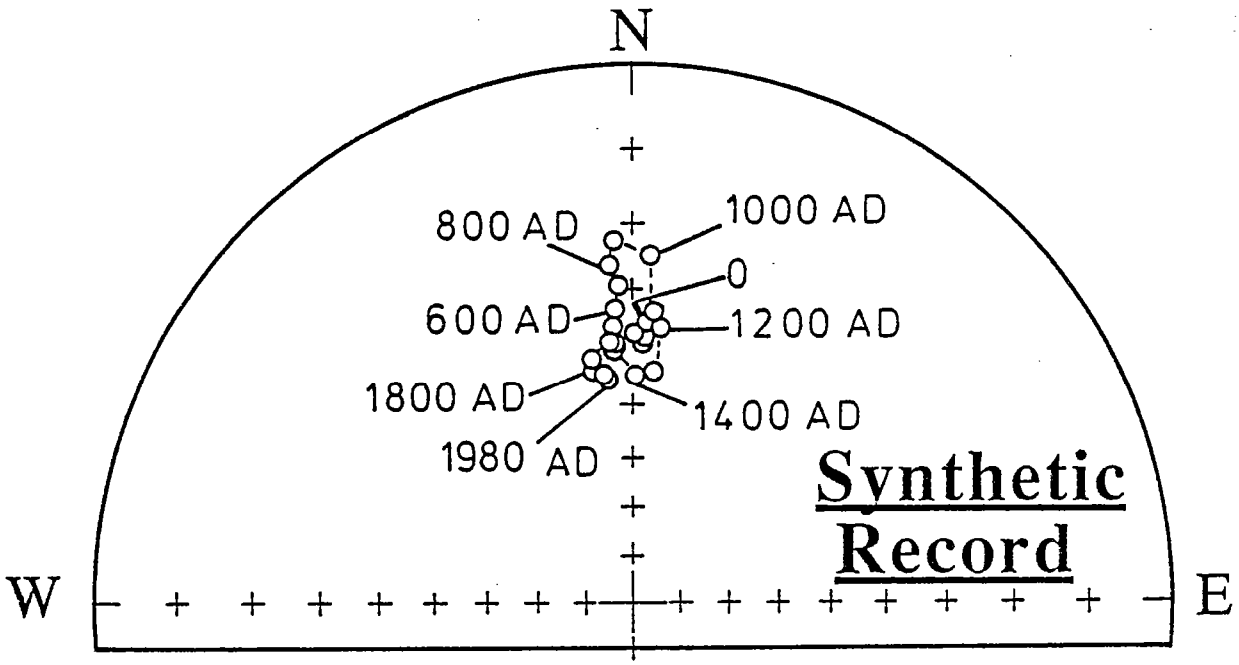

Fig.6: Synthetic record of directions calculated from the mean global dipole wobble for the last 2,000 years, from Merrill and McElhinny (1983) at the site of La Réunion.

wobble). Figure 6 shows the field directions calculated from these mean dipoles at 100 years intervals, at the site of La Reunion. This synthetic record shows that significant non-dipole fields have been recorded at the site Rivière des Remparts.

It is very likely that jumps in the secular variation record would correspond to hiatus in the volcanic activity. Of course, paleomagnetism enables to identify these gaps but does not put any constraint on their length.

Several jumps are observed at the site Rivière des Remparts (RA3-RA4; RA9-RA10; RA11-RA12; RA15-RA16) (see Figure 4 and Table 1). On the contrary, only one discontinuity (RB9-RB10) is apparent at Remparts de Bellecombe. We will see later that variations in paleointensities fit quite well the directional behavior.

B) The statistical test of Watson and Beran

Watson and Beran (1967) have proposed a statistical test to detect serial correlations of directions. Their statistical method compares the sum of the cosines of the angles between observed successive directions to sums calculated from a great number of randomly generated sequences computed from the same data set. The degree to which the observed data are serially correlated is then deduced from the amount that the first sum exceeds the mean of the second group of sums. The result of this test for site B shows that the directions are strongly correlated at the 99% level of confidence.

The test of Watson and Beran performed on data from the site A suggests that the directions are also serially correlated. However this test does not recognize groups of flows and it seems that the sampling of the geomagnetic directions by the lava flows at site A has not been very regular in time. For example, we can expect a very short time separating the extrusion of the flows RA6 to RA9.

The test of Watson and Beran in fact cannot give a definite answer to the question, because a sequence of flows may have recorded directions regularly separated in time and that are serially correlated because when long-period change in secular variation occur (McElhinny and Merrill, 1975).

MAGNETIC PROPERTIES

The investigation of the magnetic properties of our samples has been conducted for a better understanding of the behavior of the samples during paleointensity experiments.

Measurements of weak field susceptibility, at room temperature, of viscosity index, strong field thermomagnetic experiments and records of variations of the weak field susceptibility from the liquid nitrogen to room temperature were performed for almost all cores. Saturation magnetization Js and saturation remanence Jrs were determined for about 40 samples from the two sampled sites. Lowrie-Fuller tests (Lowrie and Fuller, 1971), which consist in comparing the shape of the af demagnetization curves of the NRM and of the isothermal remanent magnetization (IRM) are also available for these samples.

A) Weak field susceptibility at room temperature

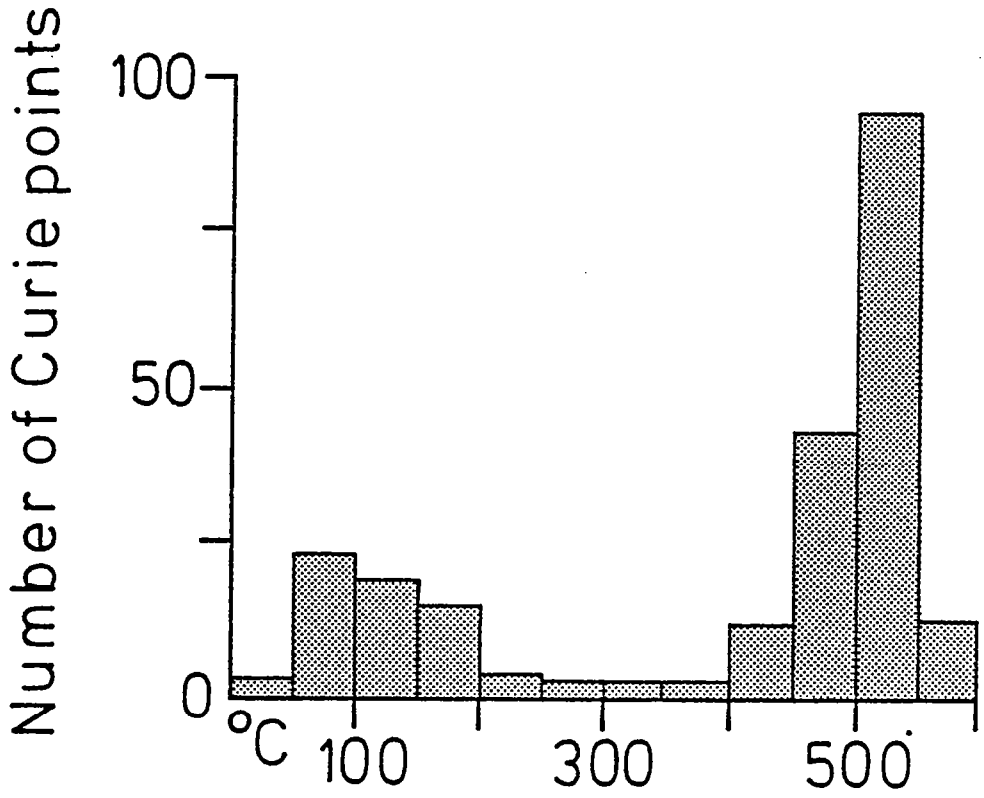

Fig.7: Distribution of the Curie temperatures for all studied samples.

Weak field susceptibility, at room temperature, was determined using a Bartington susceptibility-meter.

Susceptibility values typically range from 10^{-2} to 7.5 10^{-2} SI units (see Fig 2); samples which show a strong high temperature oxidation have a susceptibility less than 10^{-2} SI units.

B) Magnetic viscosity

The distribution of viscosity index, which are the ratio of the intensity of the viscous remanent magnetization (VRM) acquired within 10 days of storage in the laboratory field to that of the NRM (Thellier and Thellier, 1944), is shown in Figure 2. This test was performed on all specimens (299). Most of the samples (80%) have a viscosity index lower than 5%.

C) Thermomagnetic behavior

Strong field thermomagnetic (Js-T) curves were obtained using an automated Curie balance, with heating and cooling rate of 8°C/mn. The experiments performed in vacuum, in order to minimize oxidation during heating, enable to determine the Curie points (i.e. the sample magnetic phases and its oxidation state) and recognize magnetochemical changes during heating. In order to better define temperatures at which such magnetochemical changes occurred, the heating runs were commonly interrupted three times, allowing the sample to cool about 50°C after which the heating resumed.

Amongst the three methods generally used in determining the Curie temperatures of rocks (Grommé et al., 1969, Moskowitz, 1981, Prévot et al., 1983), the one corresponding to the temperature of the inflection point of the thermomagnetic curve was chosen because it provides a better estimate of the broad distribution of Curie points within such rocks (Prévot et al., 1983).

Thermomagnetic experiments were performed on 164 samples. Curie temperatures are distributed between room temperature to 570° C close to the Curie point of pure magnetite (see Fig 7). Also, two Curie points were often determined for one individual sample. Such variations in magnetic mineralogy occur between different samples of a same lava flow as well as between flows. Only samples from flows RA4, RA5 and RA6 have predominant low Curie temperatures.

The reversibility of the heating and cooling curves shows evidence of stochiometry; indeed low temperature oxidation produces cation-deficient titanomagnetites for which thermomagnetic curves are not reversible.

Thermomagnetic experiments provide quantitative values such as Curie points but the information associated to mineralogical changes between heating and cooling is much more difficult to quantify. For this reason, the various J_S-T curves have been grouped into 4 different categories (Fig 8) which will be described in details.

However, we must say that such classifications are not always clearly delimited because there is a continuous spectrum of variations between samples rather than sharp distinctions.

Type 1 curves show a single Curie point, which ranges from 480 to 560°C and were the most common encountered type (87 samples). They can be subdivided into 5 categories, according to the shape of the cooling curves, changes in Curie temperature and Js intensity after heating at about 600 °C.

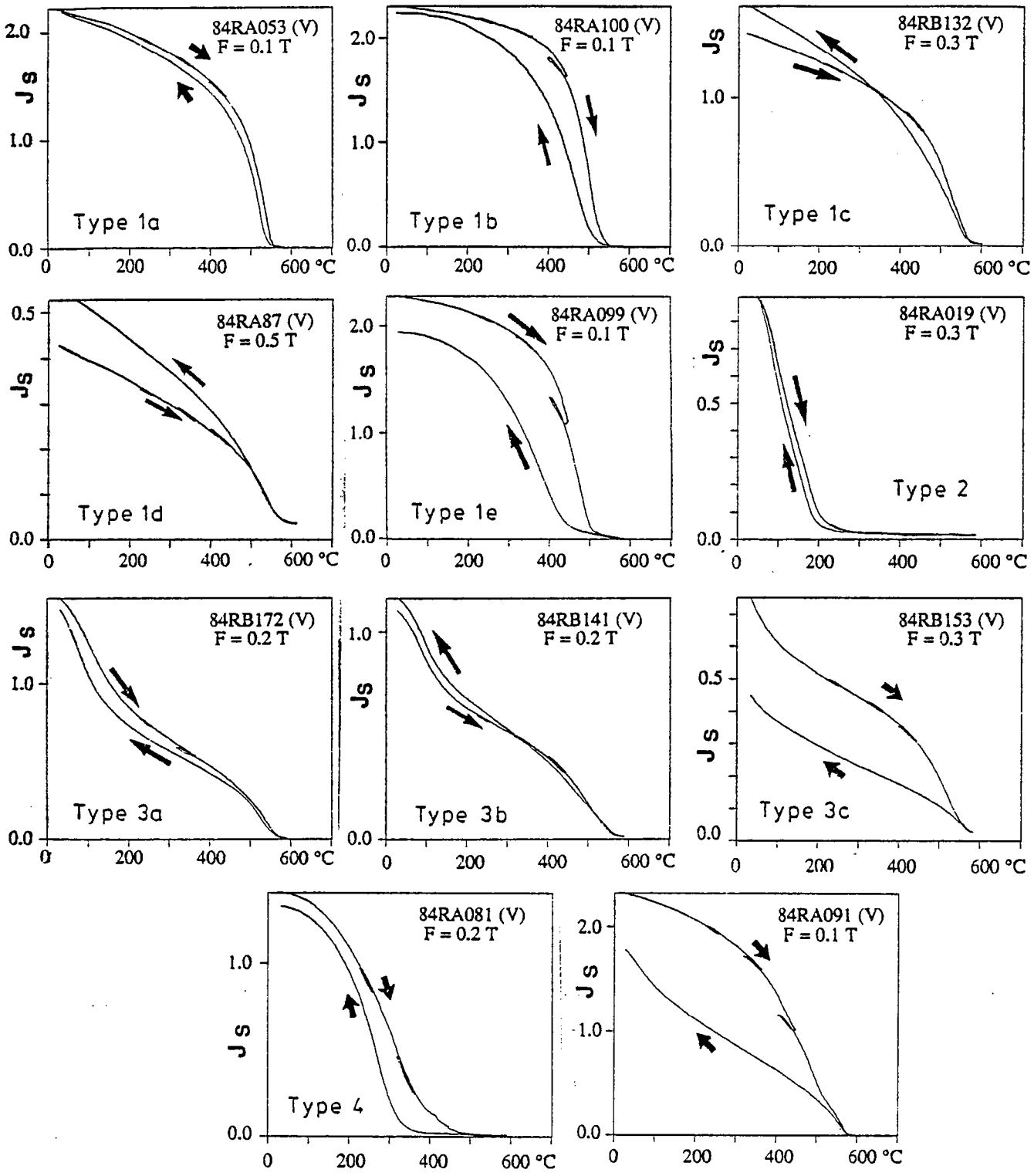

Fig.8: Examples of Curie experiments performed in vacuum (V) showing the different types of behavior. The value of the applied field (F, in tesla) is indicated for each experiment. Heating and cooling curves are shown by arrows. The unit of the magnetic moment (J_S) is given in Am^2Kg^{-1}

Curves of type 1a (20 samples) show a single well defined Curie point and little or no change between heating and cooling curves, with a decrease in Js, after heating being less than 4%.

The change in Js for type 1b (28 samples) curves is less than 10% at room temperatures, but heating and cooling curves differ in shape for temperatures above 200°C, and the Curie point during the cooling is always lower by a few degrees than during heating.

Type 1c curves correspond to 16 samples for which the cooling curves crosses the heating curves at temperature between 150 to 300°C. For this group, the value of Js, at room temperature, after heating is greater than the initial value (from 5 to 12%). Also Curie temperatures decrease by a few degrees after heating.

Type 1d curves (7 samples) exhibit a large increase in Js (up to 28%) at temperatures between 400-500°C, while no change in Curie temperatures is observed after cooling. Finally, type 1e curves (11 samples) correspond to irreversible heating and cooling curves. A decrease in Js of more than 10% and a reduction of the Curie temperature by a few tens of degrees is also observed.

The magnetic phases which produce type 1 curves could be either an original Ti-poor titanomagnetite or more probably result from high temperature oxidation of a primary Ti-rich titanomagnetite to a Ti-poor titanomagnetite containing ilmenite lamellae, in agreement with some optical microscope observations. Small differences observed between the five subcategories can be explained by some minor variations in magnetic grains, their oxidation state or in bulk rock (Mankinen et al., 1985).

Type 2 curves (9 samples) also show a single ferrimagnetic phase but with Curie temperature below 140°C, and a good reversibility of the heating and cooling curves. According to the reversibility of the curves during the experiment, we can expect that these Ti-rich titanomagnetites were not oxidized at low-temperature, that is the oxidation index z is very small (about 0). Using contour diagram given by Readman and O'Reilly (1972), Curie points lower than 140°C would indicate a titanium content parameter x around 0.7 to 0.6. Titanomagnetites with such x values are often observed on mid ocean ridge basalts (Prévot et al., 1983, Gromme et al., 1979).

Type 3 curves are characterized by the presence of two ferrimagnetic phases. The first one has Curie temperatures between room temperature and 300°C, the second has higher Curie points commonly ranging from 480 to 550°C. This type of curves were produced by 66 samples. Depending on whether the cooling follows or not the heating cycle, 3 categories can be defined in this group.

Type 3a curves (36 samples) show few changes in Js after cooling, while the two Curie points are not altered

The cooling and heating curves for the 13 samples which compose the type 3b, crosses at temperatures about 200-300 °C.

Type 3c curves show an irreversible change in the magnetic phase after heating and Js is greatly reduced (15 to 50%)

These bimodal curves are often observed on samples where high temperature deuteric oxidation has not been completed, converting only one part of a primary high Ti titanomagnetite to a Ti poor

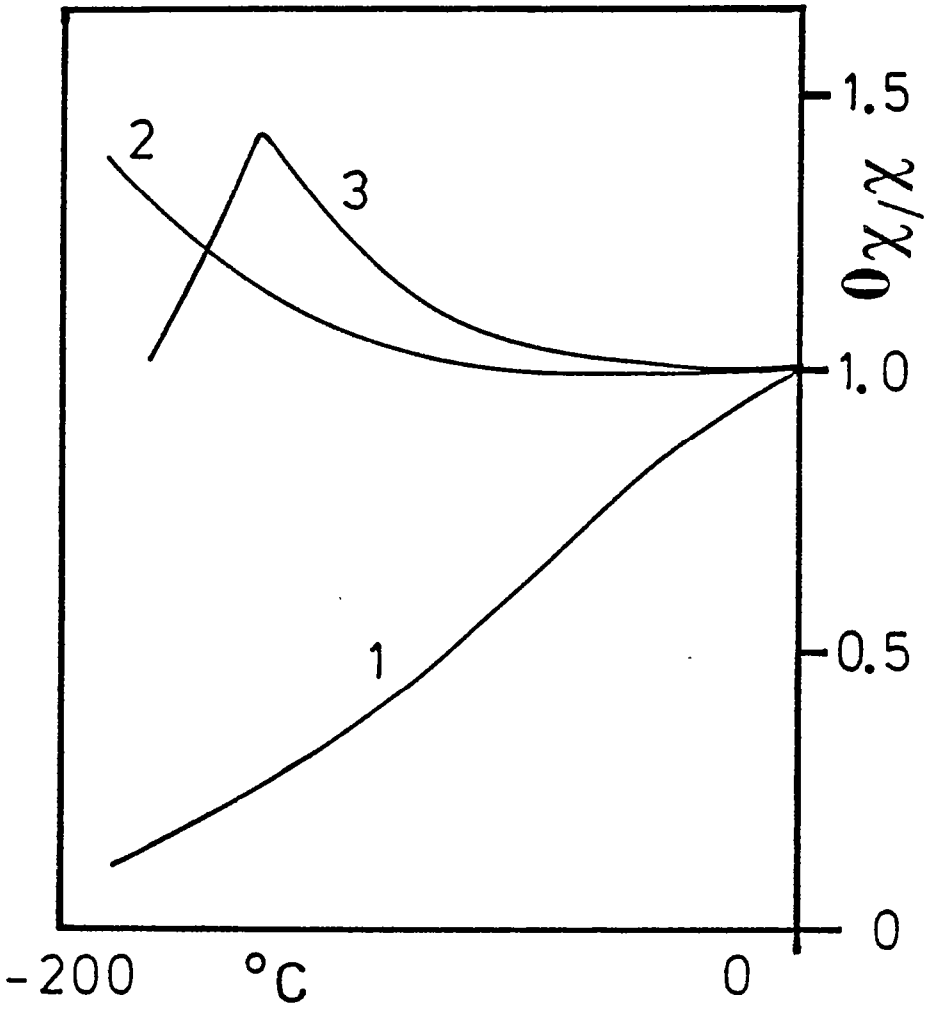

Fig.9: Behavior of the weak-field susceptibility from nitrogen temperature to room temperature (χ-T curves). Following Senanayake and McElhinny (1982), type 1 curves may correspond to Ti-rich titanomagnetites predominantly MD, type 2 curves to Ti poor titanomagnetites with many ilmenite lamellae and type 3 to multidomain magnetites.

titanomagnetite (Ade-hall et al., 1971). Irreversibility of the heating and cooling curves is interpreted as reflecting some low-temperature oxidation of one (or both) magnetic phase.

Type 4 thermomagnetic curves are represented only by 3 samples from the same flow, showing an unusual single Curie point between 300 and 430°C.

Irregularities in the common uniform decrease in Js, at the end of the heating cycles have been noted on some curves of type 3 and 1 (sample RA091, Fig. 8). They seem similar to those pointed out by Mankinen et al. (1985). According to these authors we attribute these features to the presence of two different Ti-poor titanomagnetites.

On 2 samples, no Curie point was determined. In view of the shape of the Js-T curves, it seems that the magnetic phases present in these samples have Curie point below room temperature (see sample RB135, Fig 11)

D) Low temperature behavior of weak field susceptibility (χ)

Several workers (Radhakrishnamurty and Deutsch, 1974, Radhakrishnamurty et al., 1979 ; Senanayake and McElhinny, 1981, 1982) have studied the variation in magnetic susceptibility of basalts from liquid nitrogen temperature (78° K) to room temperature.

Senanayake and McElhinny (1981) have shown that according to their low temperature characteristics, more than 95% of their basalts could be classified into three groups (Fig.9).

Group 1 samples show a decay in susceptibility to an average value of 0.28 of the room temperature value, at 78°K.

Group 2 samples exhibit an increase in susceptibility to an average value of 1.26 of the room temperature value at 78°K.

Group 3 samples describe a peak in susceptibility on cooling, averaging 1.24 of the room temperature value, returning to close to the initial value again at 78°K.

By comparing these behaviors obtained on natural rock with variation in weak field susceptibility observed on synthetic samples, they concluded that group 1 basalts are dominated by unoxidized titanomagnetites ($x > 0.3$), predominantly multidomain (MD), group 2 samples are mainly titanomagnetite grains with exsolved ilmenite lamellae, while group 3 basalts consists predominantly of multidomain magnetite or Ti-poor titanomagnetite. Because in large grains of Ti-poor titanomagnetite, the susceptibility is controlled by magnetocristalline anisotropy, the susceptibility peak observed in group 3 samples is attributed to the isotropic point, when the sign of the magnetocristalline constant K_1 changes from negative to positive, around 130°K (i.e. -143°C). Characteristics of group 2 samples were explained by stress effects from the ilmenite lamellae (Senanayake and McElhinny, 1981). These interpretations were supported by further experiments including optical microscope observations of polished surfaces, Curie temperature measurements, af demagnetizations, electron microprobe and X ray analyses.

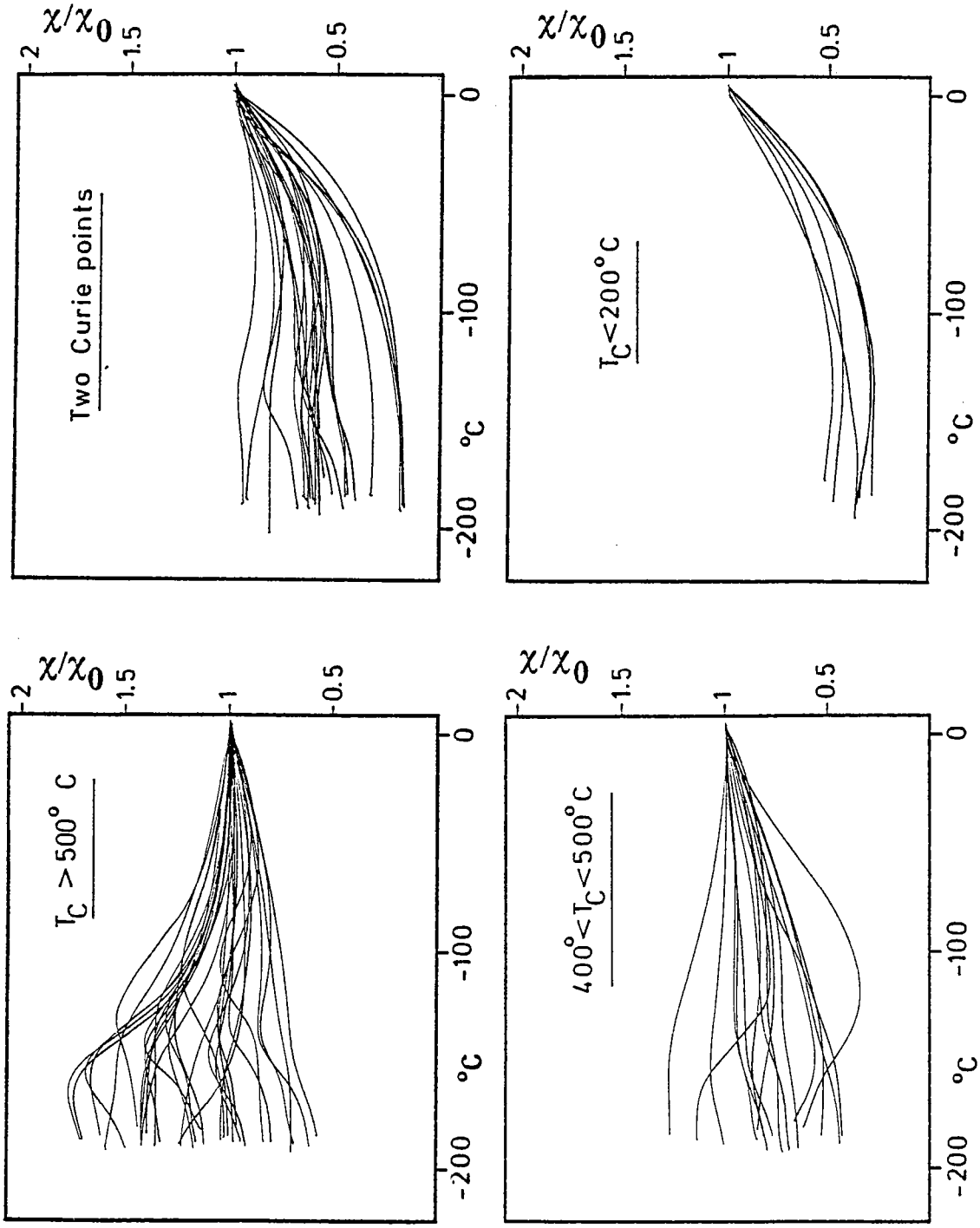

Fig.10: Correlation between χ-T curves and 4 groups of Curie points.

Senanayake and McElhinny (1982) have then examined the effect of successive heatings on the low temperature susceptibility of samples from each group. They have found, after repeating heatings, that group 1 basalts gradually oxidize above 300°C to produce the characteristics of group 2 basalts. This oxidation takes the form of producing exsolved ilmenite lamellae (Kono, 1987). In the opposite, both group 2 and 3 basalts appear stable to oxidation, until at least 500°C.

Because chemical changes of the magnetic mineralogy are the most limiting factors in paleointensity experiments, they concluded that group 2 and 3 samples are the most suitable material for paleointensity.

Given that Senanayake et al. (1982) did obtain reliable paleointensity data, using samples selected following this criteria, susceptibility characteristics down to liquid nitrogen temperature have been investigated for most of the Réunion samples.

Low temperature susceptibility measurements are made in the following way. Sample and the thermocouple (Copper-Constantan) are moulded using plasticine and cooled by immersion in liquid nitrogen. Record of the magnetic susceptibility is performed by a Bartington sensor protected from temperature changes by a water jacket. This prevents drift of the Bartington susceptibility meter with temperature. Measurement of the susceptibility and temperature during warming up of samples are recorded by computer for further numerical analysis and graphical display.

We will now compare the results of these weak field susceptibility-low temperature experiments (i.e. χ-T curves) with some other magnetic parameters in order to differentiate composition and grain size effects.

Comparison with high field thermomagnetic experiments

Some examples of these experiments (Fig 10) are presented in 4 different groups according to their Curie points.

Samples with Curie temperature below 200 °C all belong to group 1 defined by Senanayake and McElhinny, (1981) the value of the susceptibility at liquid nitrogen temperature being one half of that at room temperature.

Samples having Curie points higher than 500 °C can be classified in groups 2 or 3 and most of them exhibit the susceptibility peak characteristic of the magnetite magnetocristalline transition. A few of them show a progressive increase of their susceptibility from liquid nitrogen temperature to room temperature but the ratio of the low temperature susceptibility to one at room temperature is greater than 0.65. In fact, such samples have a behavior in between group 1 and 2 because low temperature susceptibility behavior is strongly dependent upon the composition of the titanomagnetite, that is its titanium content.

This intermediate behavior between group 1 and 2 is clearly observed for samples having two Curie points or those with a single Curie point between 400 and 500°C.

A few samples exhibit χ-T curves which cannot be classified in any of the three previous categories and require alternative explanations.

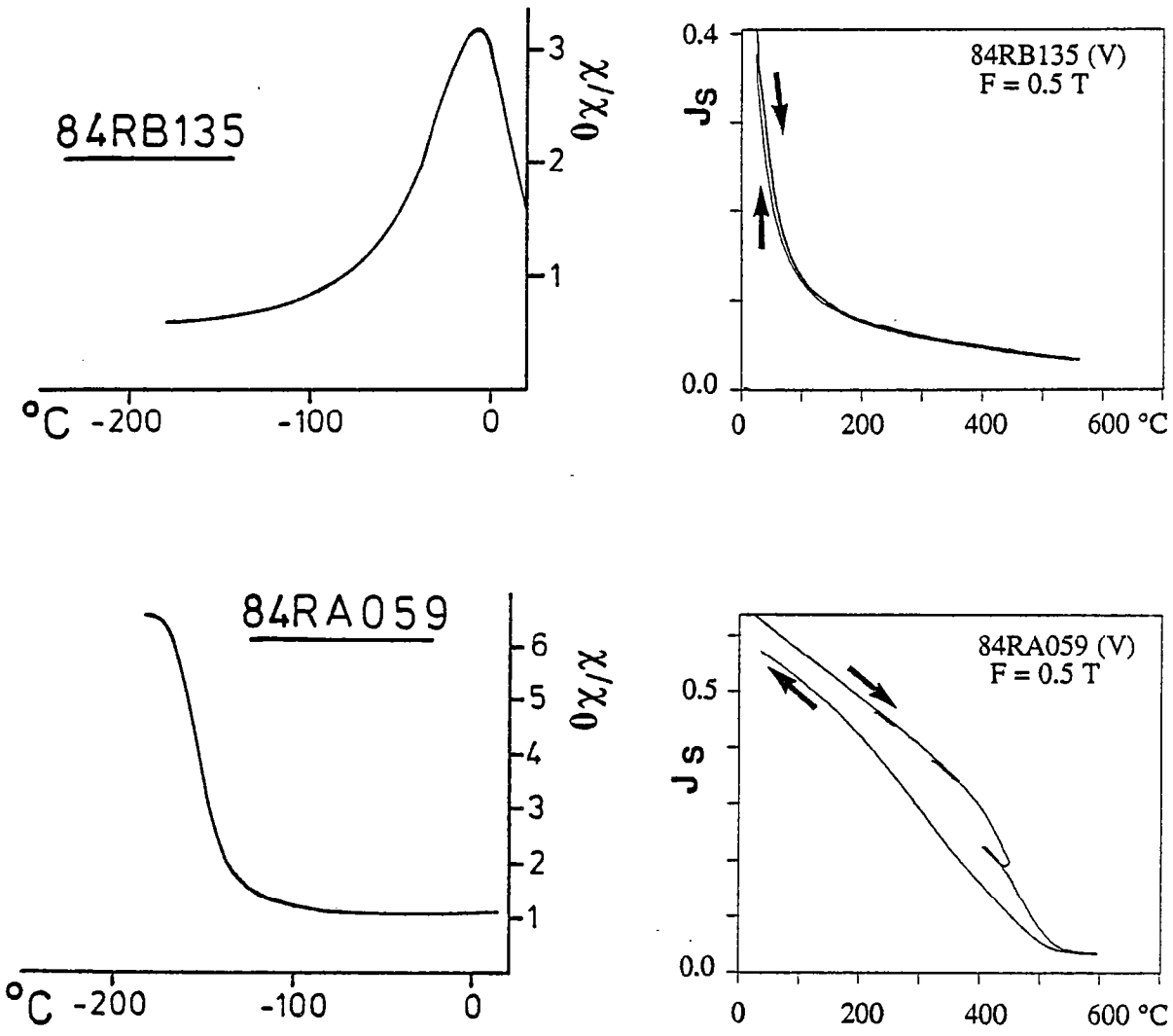

Fig.11: Comparison between χ-T curves (left) and Js-T experiments (right) for two atypical samples. Sample RA059 shows a large increase in susceptibility at liquid nitrogen temperature (up to 6 times the one at room temperature). Sample RB135 exhibits a large peak at temperature below room temperature.

Sample RB135 (Fig.11) shows a large susceptibility peak around -10°C, with value of χ higher than 3 times the one at room temperature. Thermomagnetic curve performed in high field (0.5 T) seems to indicate a Curie point lower than room temperature. Since the large susceptibility peak could be interpreted as a Curie point.

Two other samples, from the same flow RA11, give similar χ-T curves than the sample RA059 (Fig.11). At temperature lower than -150°C, a large susceptibility peak, up to 6 times the value at room temperature is observed. High field experiment, on the other hand, shows a Curie temperature above 500°C. The large value of χ at low temperature could be interpreted as a Curie point of a magnetic phase. Similar low temperature Curie points have already been observed on basalts from Hawaii (Gromme et al., 1969). However, very large enhancement of low field susceptibility at blocking temperature could be observed (Dunlop, 1974). Clark and Schmidt (1982) suggest that this type of χ peak could also be due to hyperfine particles which have blocking temperature close to 78°K.

Comparison with Jrs/Js ratios and remanence coercivities

We have shown a strong correlation between χ-T type curves and Curie points of samples.

In order to see if a clear relation exists between χ-T type curves and the domain structure of grains, we have determined the ratio of saturation remanence (J_{rS}) upon the saturation magnetization (J_S) for 36 selected samples, showing no or very small overprints and which have typical low temperature susceptibility behavior. This ratio is a good grain size parameter, even if it is compositional dependent. For a given grain size, the J_{rS}/J_S ratio increases with increasing titanium content (Day et al., 1977, Cisowski, 1980).

The behavior of the NRM and the IRM versus alternating field has also been checked (Lowrie, Fuller, 1971 ; Dunlop, 1983).

J_S was estimated from curves of the ratio J/H versus the applied field H, with a maximum field strength of 7.5 KGauss. In most cases, the paramagnetic contribution of other Fe-rich minerals, like olivine, produces a linear increase of the total moment at high fields. To account for this fact, we have extrapolated a straight line through the high field points on the J/H - H curves, back to zero field H.

Values of J_{rS} were determined by progressive IRM acquisition, up to maximum applied fields of 500-600 mT. In all cases, saturation was obtained for fields lower than 250-300 mT.

The observed values of J_{rS}/J_S extend from 0.07 to 0.32, with an arithmetic mean value of 0.2 ± 0.06.

A value of J_{rS}/J_S of 0.5 is predicted for uniaxial SD grains of magnetite, however in basalt containing titanomagnetite, realistic SD or PSD (pseudo-single domain) values are $0.17 \leq Jrs/Js \leq 0.27$, while for MD grains a ratio $J_{rS}/J_S < 0.1$-0.13 is expected (Dunlop, 1983, 1981). The distribution of Jrs/Js ratios indicates that most of the selected samples contains SD or PSD grains, but a few have large magnetic particles.

Dunlop (1983) did study the behavior of a large collection of continental igneous rocks during a.f. demagnetizations of remanences acquired in weak, intermediate and strong fields (some kind of Lowrie-Fuller test). Remanences were either a TRM, ARM or IRM.

Four general categories of behavior have been recognized :

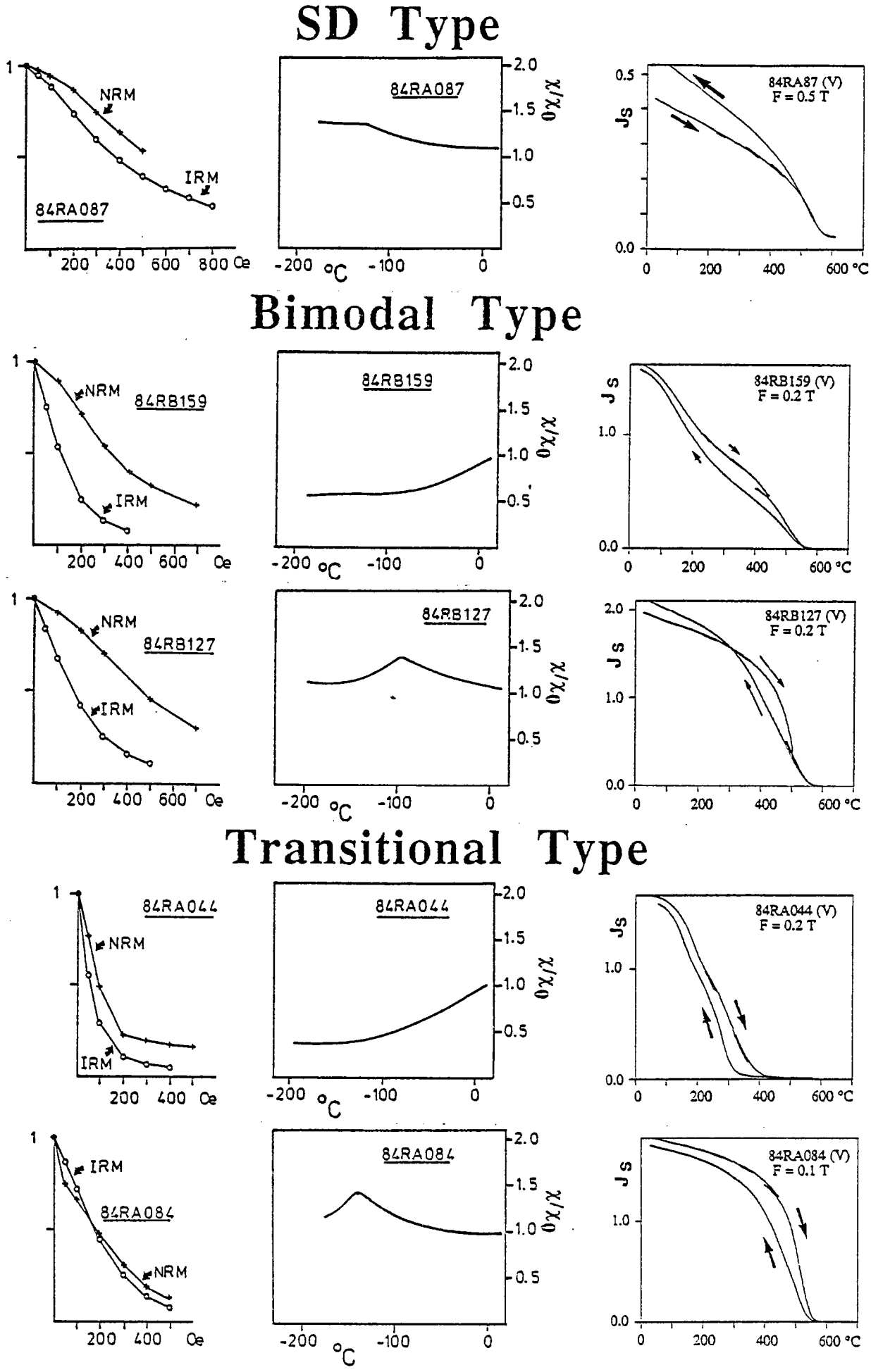

Fig.12: Comparison of the AF demagnetization spectrum of NRM and IRM (left) with low temperature susceptibility (center) and Js-T experiments (right). Three classifications, SD type, Bimodal type and Transitional type are made according to the proposition of Dunlop (1983).

MD-type: soft and rapidly decaying curves, with the IRM curves being hardest, which corresponds to MD grains above PSD threshold size.

SD-type: harder, initially slowly decaying curves, the IRM curve being softest. This behavior is produced by SD and PSD grains.

Transitional type: which produces closely-spaced curves with or without crossovers. These curves correspond either to a single magnetic phase whose size spectrum peaks between SD (or PSD) and MD grains, or to two phases with overlapping size spectra.

Bimodal type: characterized by widely separated curves with SD-type relative hardnesses for weak field remanence, combining MD-type IRM curves. This behavior results of two phases, one MD, the other PSD or SD, with widely separated size spectra. The fine grains dominate weak-field remanence while the coarse grains dominate strong-field remanence. (Dunlop, 1983).

Three of these four kinds of behavior were recognized in our 36 selected samples, for which decays of the NRM (which is assumed to be the primary TRM) and the IRM have been compared. Examples of each sample type are given in Fig. 12.

It appears that SD-type samples have Jrs/Js > 0.23, a medium demagnetizing field (MDF) for the NRM: MDF_{NRM} >340 Oe and for IRM: MDF_{IRM} > 225 Oe. Their low-temperature susceptibility behavior follows group 2 of Senanayake et Mc Elhinny (1981). Curie temperatures for these samples are higher than 537°C. Four samples belong to this category.

Transitional type samples show a Jrs/Js ratio between 0.07 to 0.16 with two exceptions for which the value is higher and close to 0.21-0.25. Their MDF_{NRM} and MDF_{IRM} are between 60 to 220 Oe and their χ-T curves correspond to group 1 or 2 of Senanayake and McElhinny (1981). Strong field thermomagnetic curves indicate either a single Curie point either higher than 530°C or lower than 120°C or two Curie temperatures (i.e. two magnetic phases). Fourteen samples are in this category, including the particular sample RA059 (Fig. 11). In the case of samples with low Curie points, it is easy to understand that these unoxidized titanomagnetites are larger magnetic particles.

Bimodal type samples are the most common (18 samples). They exhibit Jrs/Js ratio from 0.11 up to 0.31; 217< MDF_{NRM}< 500 Oe and 88< MDF_{IRM}<206 Oe. The low-temperature susceptibility behavior of these samples follows either group 1 or 3 of Senanayake and McElhinny (1981). It appears, according to the thermomagnetic curves that these samples have either two Curie points (one lower than 200°, the other above 450°C) or only one Curie temperature.

We have not observed large MD type behavior characterized by the IRM demagnetization curve above that of the NRM.

In conclusion, it appears first that χ-T curve are compositional and grain size dependent ; this result is in good agreement with those obtained in previous studies (Senanayake and Mc Elhinny, 1981, 1982). Thermomagnetic curves performed on almost each sample demonstrate the great variety in the composition and the oxidation state of our samples. Hysteresis properties have shown domain structure

of either SD or PSD or a mixture of domain types. We will see in the next section, how magnetic properties could or could not explain some non-ideal behavior during the Thellier experiment.

PALEOINTENSITY DETERMINATION

A) Experimental procedure

The original method of paleointensity proposed by Thellier and Thellier (1959) is based upon the law of additivity of partial thermoremanent magnetizations (PTRM). At each temperature step, the specimens are heated twice at the same temperature T_i and cooled in the ambient geomagnetic field. Between these two heatings, the sample position is reversed 180° with respect to the direction of field. The total magnetization (residual NRM + PTRM) is measured after each heating. Because of the additivity of PTRMs, the two PTRMs acquired between T_i and room temperature are of the same magnitude but in opposite sense. This procedure enables to recover the NRM left in the sample and the PTRM acquired. Coe (1967b) suggested performing the first heating in zero field in order to determine directly the NRM left. The second heating, performed in a field, enables to measure the PTRM acquired. This procedure has been widely used. Kono (1977) has proposed a modified version of the Thellier's technique. It consists in only one heating at each temperature step with a laboratory field applied orthogonal to the NRM directions of the samples. However, even if this method is less time consuming, it requires a complex sample holder for a very precise orientation of the samples with respect to the applied field.

Errors analysis performed on both coordinates (NRM and TRM components) of the results of the Thellier experiments have shown that among the three previous versions, the original procedure is the most superior (Kono and Tanaka, 1984). Moreover, experiments performed to test the additivity of PTRMs have indicated that deviations from additivity should have no effect on paleointensity determinations by the original procedure of Thellier, because identical blocking relationships are associated with both heatings at each temperature steps. On the other hand, departures from additivity could have some (even very small) effects in the Coe's version because the two heatings are not perfectly symmetrical (Levi, 1979).

For these reasons, we have chosen to use the original Thellier's technique and the laboratory field was reversed between the two heatings at each temperature step while the samples are let in the same position. This procedure allows a better repetition in the temperature reached by the sample when a low thermal gradient exists in the furnace. This repetition in temperature was about 1°. The laboratory field was applied both during heating and cooling as suggested by Levi (1975). The samples were heated in a quartz tube evacuated to pressures less than 10^{-2} Torrs in order to prevent oxidation during heating (Khodair and Coe, 1975). Each heating and cooling cycle lasted about 3 hours.

Generally, eleven to twenty temperature steps have been distributed in the range 100°C through the higher Curie point of the samples and according to their unblocking temperature spectrum. One of the major advantage of the Thellier's technique is that it allows to check the stability of PTRM acquisition

capacity as the temperature is progressively increased. Numerous PTRM checks were performed during each experiments, but in two different ways: (1) by periodic measurements of the PTRM acquired at a given low temperature interval, after a previous heating at higher temperature or (2) by successive PTRM checks spanning higher temperature intervals as the temperature step increases (Prévot et al., 1985).

B) Sample selection

The most straightforward selection criterion is that the natural magnetization of the sample should have a direction close to the characteristic direction determined on several samples from the same flow.

Samples with high Curie points and a good reversibility of the heating and cooling curves are generally assumed to be the most suitable samples for paleointensity determinations. It has also been suggested that large particles (MD grains) can produce non ideal behavior during Thellier experiments (Levi, 1977; Worm et al., 1988). Because MD grains are well known to have coercivities lower than 200 Oe. (Soffel, 1971; Levi and Merrill, 1977), samples having MDF equal or above 300 Oe generally provide the most accurate paleointensity results.

No strict selection criteria have been used in order to perform experiments for most of the lava flows . On the contrary, we will try to compare our extensive paleointensity experiments with the other available magnetic parameters in order to provide some additional constraints on sample selection for paleointensity.

Paleointensity experiments were attempted on 96 specimens and 66 provided results. This corresponds to a success rate of about 70%. Very few samples provided linear paleointensity over the whole temperature spectrum. Those which did not show any linear segment have been rejected.

C) Paleointensity analysis

Choice of the points on the NRM-TRM diagram

Results of paleointensity experiments were reported in the classical NRM-TRM diagram. The interpretation of the NRM-TRM curves was conducted in the following way.

Points must be distributed on a straight line in the temperature interval (Tmin-Tmax) chosen for paleointensity calculation. The minimum number of points used in calculating the paleointensity should be five with a corresponding fraction of NRM used being at least 15% of the initial NRM intensity (Coe, 1967b, Prévot et al, 1985).

The minimum temperature (Tmin) should be the one at which the secondary magnetization such a small VRM is completely removed. The highest temperature (Tmax) is defined as the temperature at which modifications of the magnetic mineralogy occur. Such magnetochemical changes can be detected by non linearity in the NRM-TRM curve, changes in the PTRM checks or by chemical remanent magnetization (CRM) acquisition. CRM buildup during heating is recognized if the applied field is not colinear with the existing NRM (Coe et al, 1978; Coe et al, 1984). Indeed, CRM is generally parallel

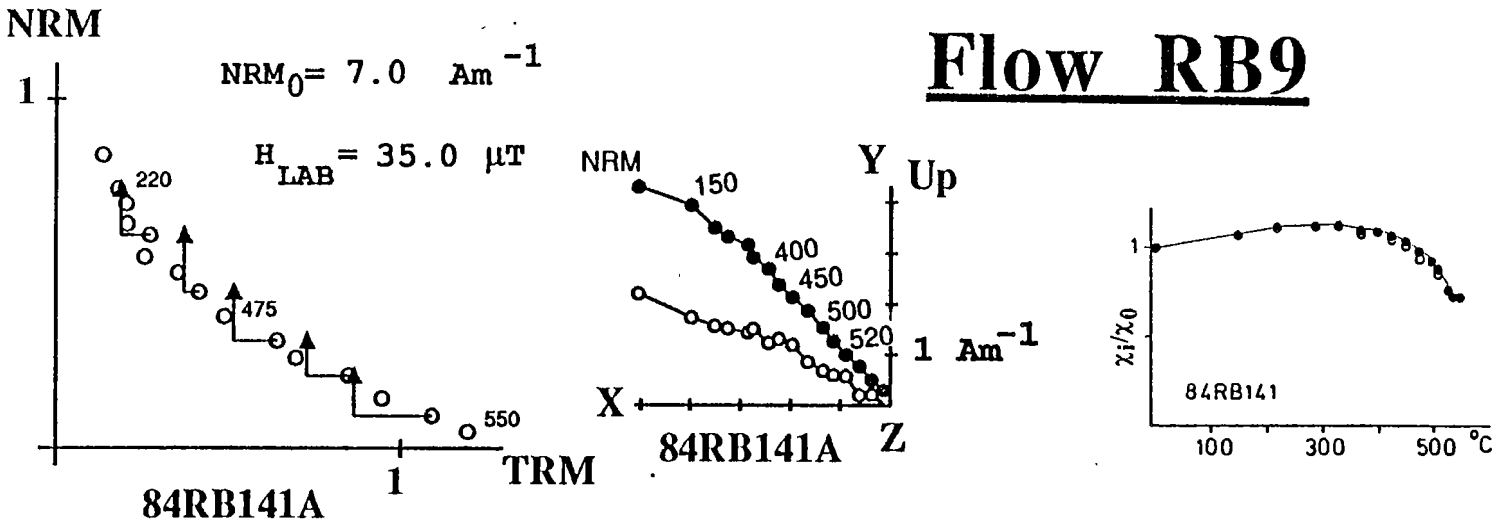

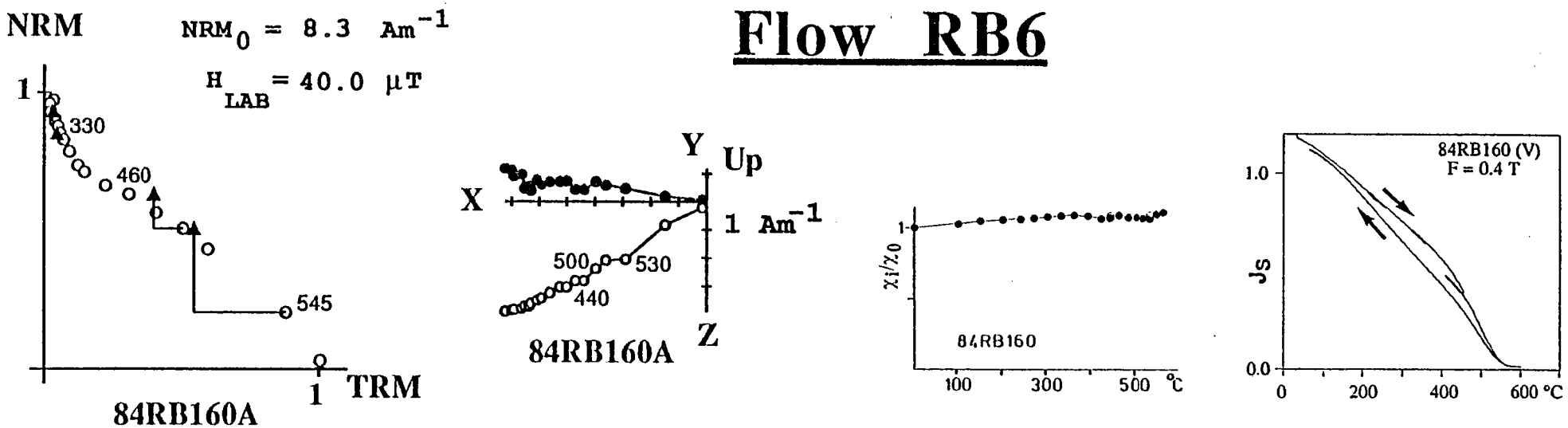

Fig.13: Examples of increase in PTRM capacity during the Thellier experiments and comparison with the stability of the NRM direction, measurements of the room temperature susceptibility and Js-T experiments. The NRM-TRM diagram is normalized with the initial NRM_0 and the triangles are the PTRM checks. H_L refers to the laboratory field. Temperature steps are in °Celsius. The filled symbols on the susceptibility diagrams correspond to the measurement after the first heating while the open symbols indicate measurements after the second heating. These diagrams are normalized with the initial susceptibility (χ_0) measured before the first heating. Orthogonal plots of the NRM evolution are reported in samples coordinates.

to the applied field and has higher unblocking temperature than the one at which it was created. Thus the apparent residual NRM is the sum of the true residual NRM and the CRM vector. An other tool to recognize magnetochemical changes is the measurement of the weak field susceptibility at room temperature after each heating.

Numerical analysis

The reliability of a paleointensity determination was estimated from the NRM fraction (f) used in the calculation of the paleofield strength (Fe), the gap factor (g) and the scattering of the points about a linear segment (Coe et al, 1978). The quality factor (q) defined by Coe et al., (1978) is a function of these parameters ($q=b*f*g/\sigma_b$) with b being the slope of the straight line and σ_b the standard error of the slope. The weighted average paleointensities (<Fe>) within a single volcanic unit were computed using the weighting factor w defined by Prévot et al. (1985) ($w=q/\sqrt{(N-2)}$, where N is the number of points in the straight segment.

An estimate of the potential for error caused by CRM acquisition is given for each sample by the factor R defined by Coe (1984) $R=(CRM_{max}/\Delta TRM)*100$ (where ΔTRM is the portion of the TRM which defines the straight segment). It represents, in percent of the applied field, the maximum error that CRM would cause to the paleointensity determination.

D) Non ideal behavior during Thellier experiments

In this paragraph, we will describe briefly the various examples of non-ideal behavior and compare the Thellier experiments with other available magnetic parameters. Some of them were determined on different specimens of a same core and thus we make the assumption that the magnetic properties are homogeneous over the core.

Effect of viscosity

Three samples which have a viscosity index above 5 % (i.e. between 7 and 12%) did not provide any linear NRM-TRM curves. Also, these samples have Curie points below 400°C (type 4 J_S-T curves) and they exhibited low temperature susceptibility behavior of Type 1. These parameters as well as low Jrs/Js ratio determined on one sample suggest that they have rich Ti-titanomagnetite with relatively large magnetic particles.

These examples strengthen previous analysis (Prévot et al., 1985) suggesting that viscous samples must be avoided from paleointensity experiments.

Long-term viscosity acquired during the last thousands years may not be easily recognized because it is almost colinear with the primary normal direction. Demagnetization of such a viscous led generally to concave up curvature of the NRM-TRM diagram (Coe, 1967b).

Susceptibility modifications

Generally, the susceptibility increased during the first temperature steps up to 10% of its initial value. This increase seems to be a "stress" effect rather than reflecting mineralogical changes.

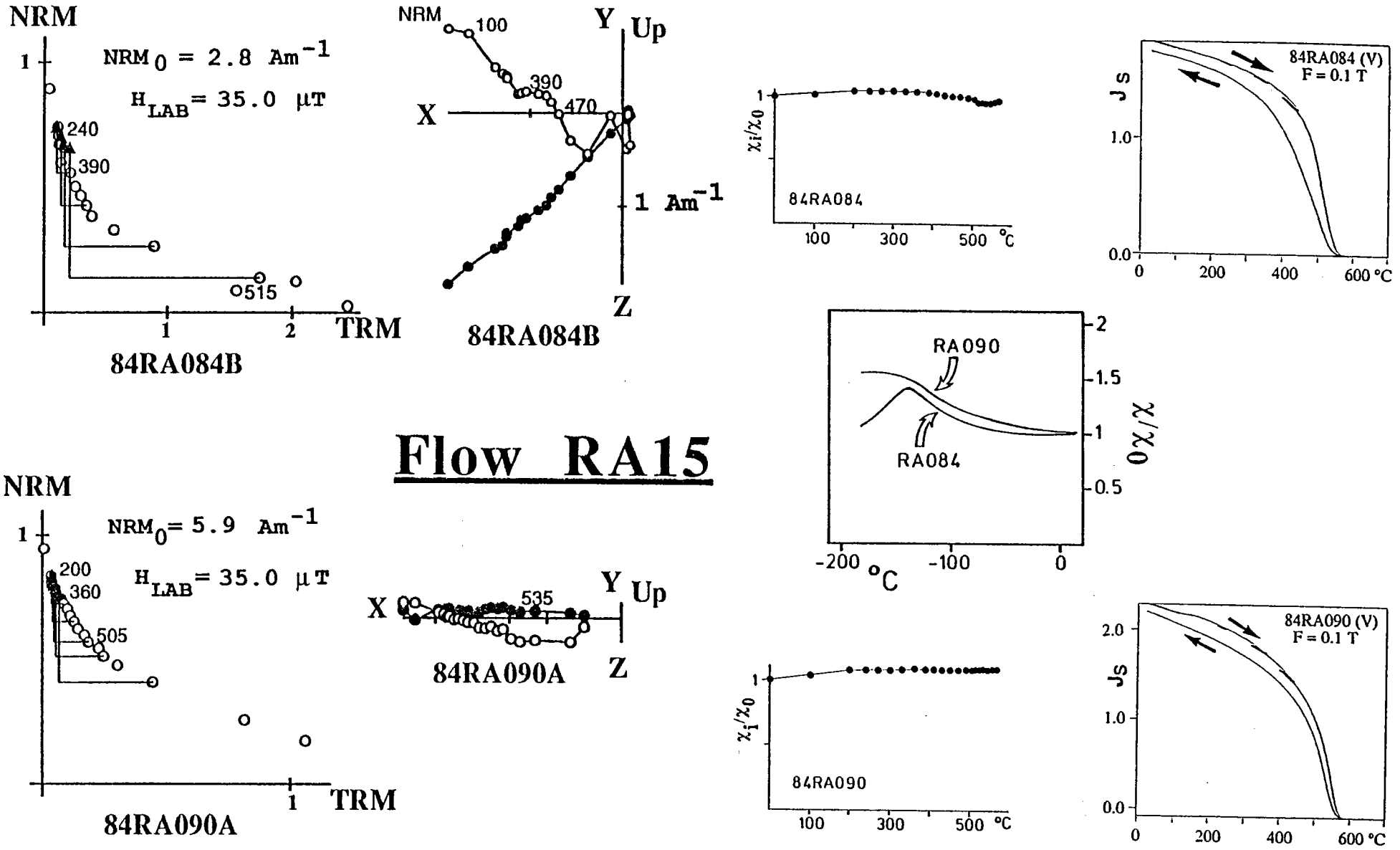

Fig.14: Same conventions than on figure 13. The NRM direction does not decay through the origin but rather is deviated toward the direction of the applied field which was vertical down in sample coordinate. The variation of the susceptibility at low temperature is also given.

Variations in the range ± 20% are not easily correlated to remanence changes as already reported by Coe (1967b) and Prévot (1975). Nevertheless, the largest susceptibility variations are generally associated to non ideal behavior during Thellier experiments.

Also mineralogical changes appear to be more strongly related to temperature than to experimental time durations. Changes of the weak field susceptibility always occur after the first heating at each temperature. The successive second heating at the same temperature step has very little effect and the susceptibility was almost the same as after the first heating. On the contrary, an increase in temperature of a few tens of degrees at the next Thellier step is generally sufficient to make further susceptibility changes.

The systematic measurements of susceptibility during paleointensity indicate that no change in susceptibility is not always associated with good reliability of the paleointensity (Fig. 13, sample RB 160). But, important changes in susceptibility always reflect a low thermal stability of the sample (Fig. 13 sample RB141).

Increases in PTRM acquisition

The most common behavior is an increase in PTRM acquisition. Two examples are given in Fig. 13. This behavior is probably due to the formation of titanomagnetite richer in iron and then more magnetic than the original one.

CRM acquisition

Some samples have clearly shown deviations of the NRM direction toward the one of the field applied during the first heating which is vertical down (Fig. 14). This is interpreted as the acquisition of a CRM during the experiment. Our experiments clearly show that CRM was parallel and in the sense of the field applied during the first heating at each temperature step. As it was already pointed out for samples which show large variations of the susceptibility at room temperature, the first heating is the most important. There is no clear correlation between CRM and the other magnetic data. The best examples (Fig. 14) show no important variation of the susceptibility at room temperature and their Js-T curves indicate à single high temperature Curie point. However, informations provided by low temperature susceptibility and the Lowrie-Fuller test, suggest large PSD grains.

Non-ideal behavior characterized by a 'kink'

Kinks in the paleointensity diagram have been observed for 11 samples. They are defined as a large drop in the NRM intensity without any acquisition of laboratory TRM, in an intermediate temperature interval, 200-400 °C (Fig. 15). This kind of behavior was already reported by Bogue and Coe (1984). PTRM checks indicated first a decrease followed at higher temperatures by an increase in PTRM capacity. Such a 'kink' was found on samples with one or two Curie points. The reversibility of the heating and cooling thermomagnetic curves was variable. These samples have c-T curves following group 1 or 3 of Senanayake and Mc Elhinny (1981), and the shape of the demagnetization of the NRM and IRM suggest that they are bimodal or transitional-type samples. The largest changes of room

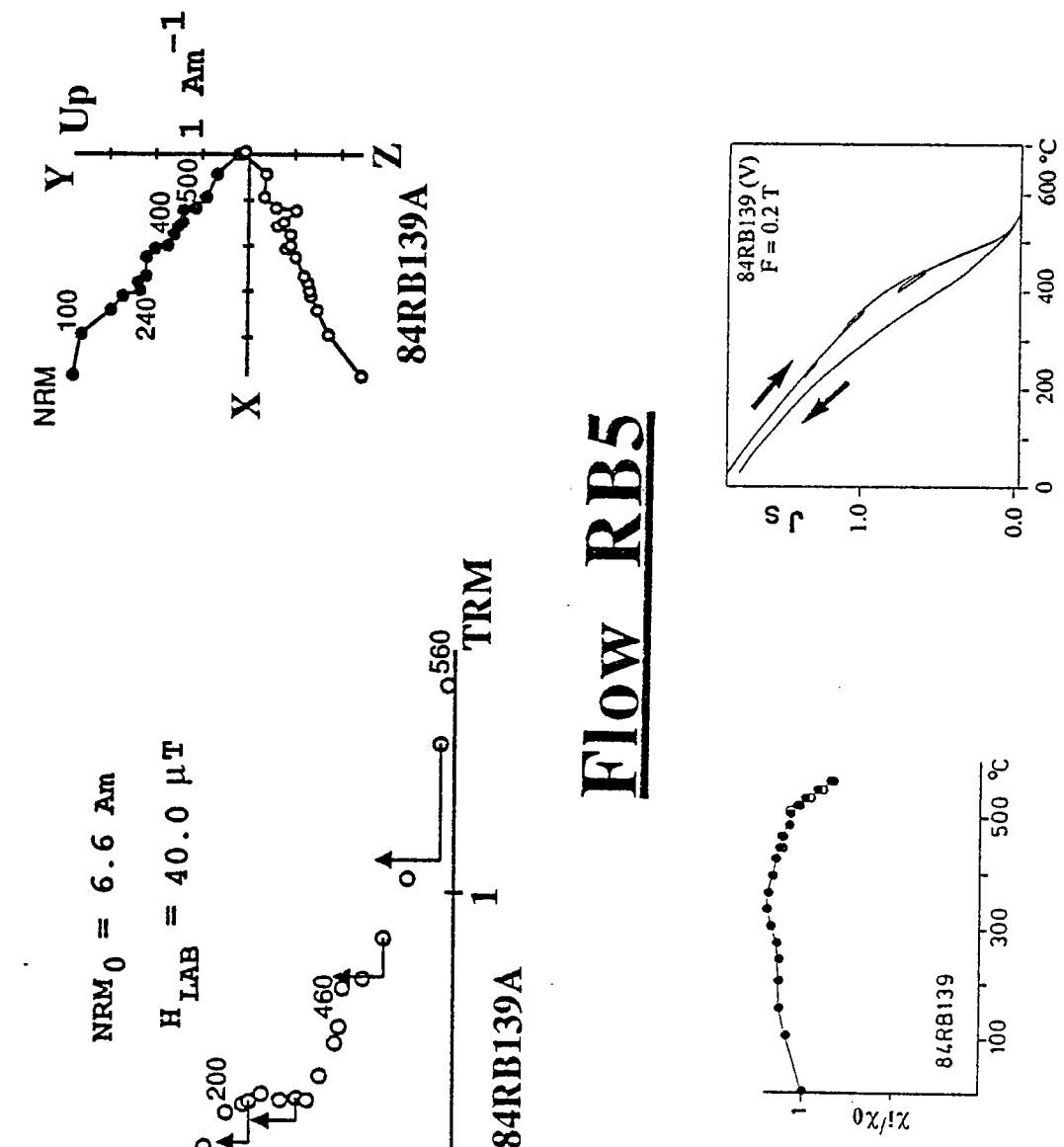

Fig.15: The NRM-TRM diagram is characterized by a 'kink' with a large decrease in NRM without any TRM acquisition in the temperature range 200-400°C.

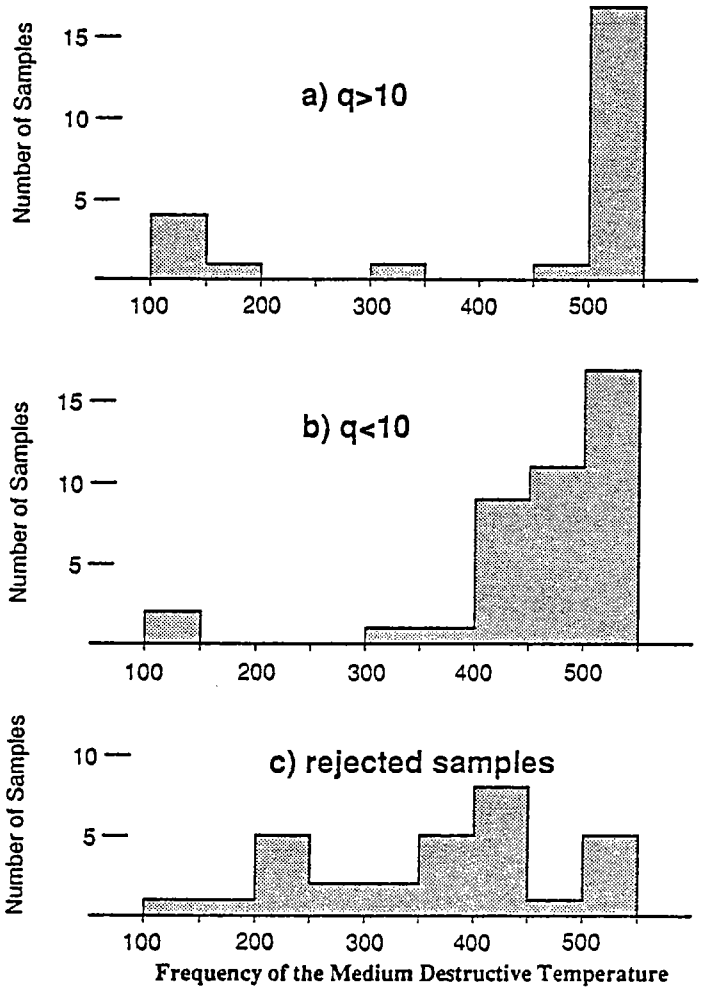

Fig.16: Distribution of the MDT (medium destructive temperature) for 2 classes of samples according to the value of the quality factor (q) in paleointensity experiments and for samples for which the paleointensity diagrams were rejected.

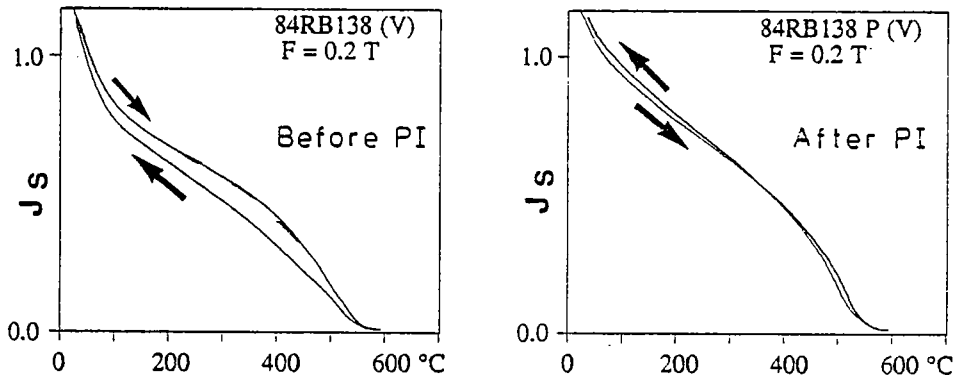

Fig.17: Comparison of thermomagnetic experiments performed before and after a paleointensity experiment. The low Curie point shown by the first experiment is much less clear after the paleointensity.

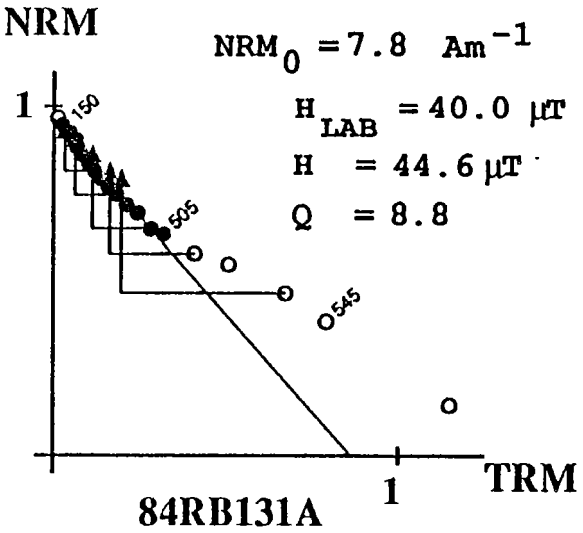

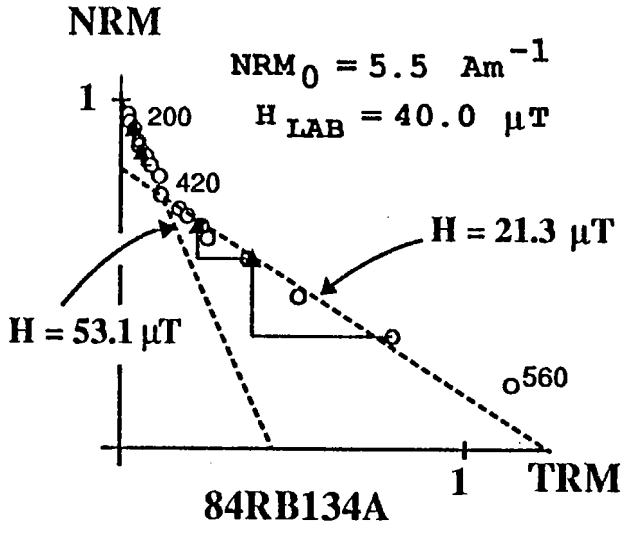

Flow RB4

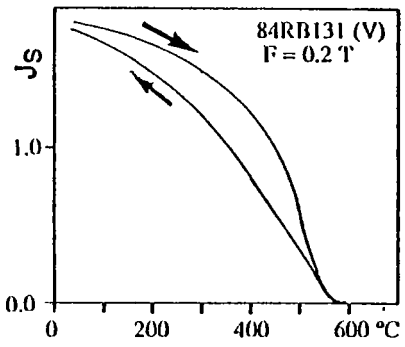

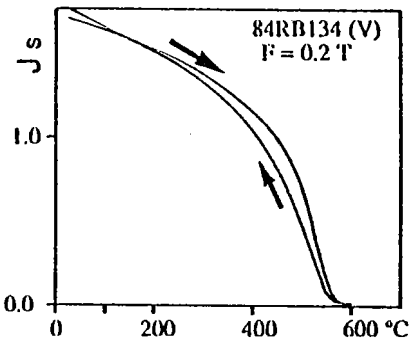

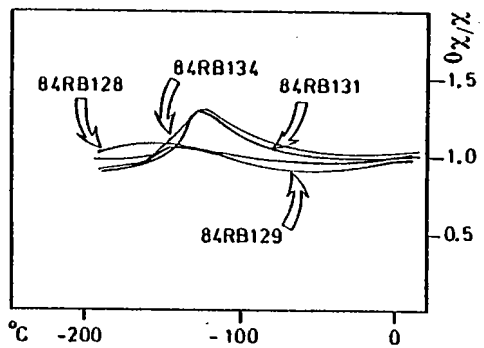

Fig.18: Examples of concave-up behavior for two samples of a same flow (RB4). The dashed lines (sample RB134) correspond to two different interpretations of the NRM-TRM diagram. For sample RB131, the filled circles correspond to the points used for the paleointensity calculation. Js-T curves indicate a single magnetic phase close to pure magnetite. These samples RB131 and RB134 exhibit the peak at low temperature of the magnetite magnetocrystalline transition which is not observed on two other samples from the same flow (samples RB128 and 129).

temperature susceptibility, measured after each heating, are observed within this group of samples (Fig. 15).

Non ideal behavior and Js-T curves

Samples which have two magnetic phases have often shown poor reliability in paleointensity experiments. Sample RB141 (Fig. 13) is one of these. It is not easy to correlate quantitatively Js-T curves with paleointensity quality. Instead, we have compared the temperature at which half of the natural remanence is demagnetized (MDT) with the quality factor q of the paleointensity experiment. These MDT reflect grossly the thermal stability of the samples. Three classes have been done (Fig. 16). It is clear from this figure that samples which have the best behavior in paleointensity (q>10) have either high and narrow unblocking temperatures while low quality samples and rejected samples have MDTs which indicates lower unblocking temperatures.

On the other hand, a few samples from flows with only one low Curie point have also provided successful paleointensity results.

Magnetic changes observed during Js-T experiments are not always occurring the same way during paleointensity experiments. An example is given by sample RB138 (Fig. 17) for which Js-T experiments were performed before and after a paleointensity experiment. While during the initial Js-T experiment, mineralogical changes did correspond to a small reduction, with a decrease of a few degrees in both low and high Curie points, on the contrary, the Js-T experiment after paleointensity shows that numerous paleointensity heatings resulted in a slight oxidation of the sample. However this is not a general case and some opposite behaviors have also been found. Thus it is uneasy to interpret non ideal behavior during paleointensity in light of the kind of reversibility of Js-T curves, possibly because the experimental heating conditions are not identical in both experiments.

We can conclude that the best candidates for paleointensity are the high temperature oxidized samples with high unblocking temperatures but we will see later that samples with a single well defined low temperature Curie phase should not be systematically rejected.

Concave up behavior

In some cases, the points are distributed on a curve where two line segments can be defined (sample RB134, Fig. 18) and without any strong indication of mineralogical alteration. It has been suggested that multidomain grains contribute to this curvature (Levi, 1977). χ-T curves provide some indication of grain size. An example is given by 4 experiments conducted on flow RB4. Samples RB128 and RB129 which do not show the magnetite peak transition have provided very convincing paleointensity results (see table 2), while samples RB131 and 134 show some evidence of larger grain size and they provided concave up curvature. Selecting the lower temperature interval is one of the basis of the Thellier method because it is well known that alteration increases with increasing temperature. However, because of multidomain grain effects, it is also tempting to fit the line through the intermediate temperature interval. This will provide a paleointensity value half of the determination using the low temperature spectrum (Fig. 18). The curvature was less pronounced for sample RB131 which we did not reject. As a result it provides a slightly higher paleointensity value. Because of its

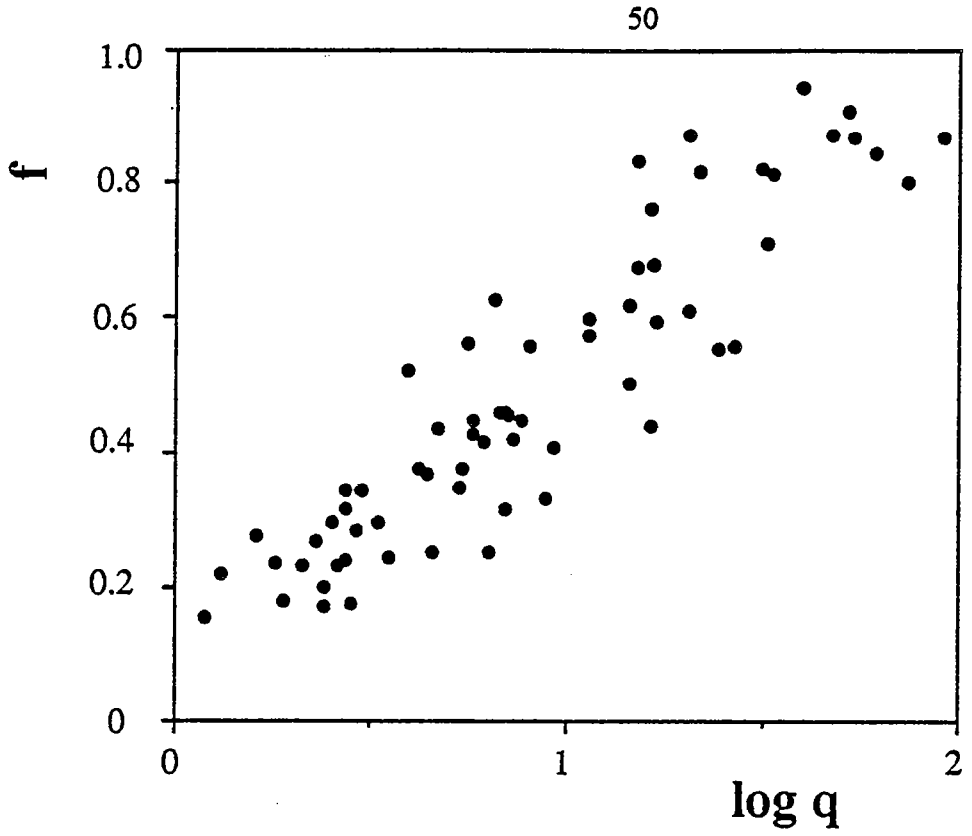

Fig.19: Plot of the NRM fraction (f) used in the paleointensity determination versus the logarithm of the quality factor (q). A strong correlation is observed.

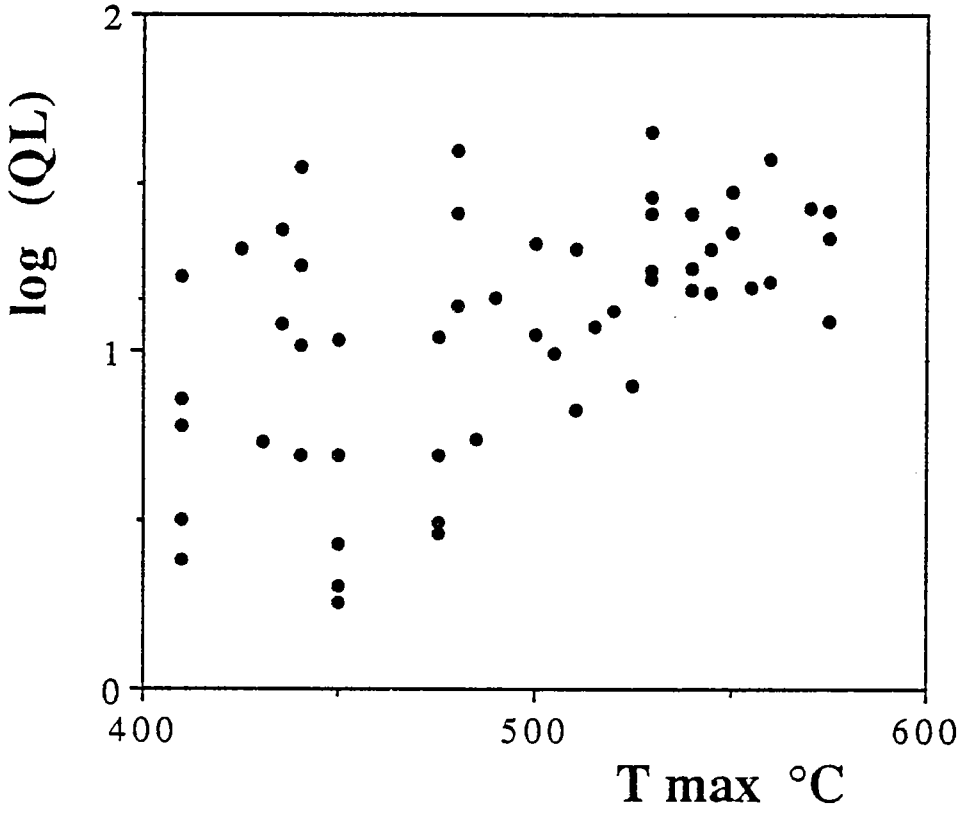

Fig.20: Plot of the logarithm of the laboratory Koenigsberger (Q_L) versus the maximum temperature of the interval for paleointensity calculation (Tmax).

lower quality value, it does not have much weight in the flow average. The grain size difference suggested by the low temperature susceptibility curves was not observed with the AF demagnetization which provided MDF greater than 30 mT.

In the analysis of the Réunion data, in the case of ambiguous samples, we choose the first approach (i.e. fitting the line through the lower temperature interval like with sample RB131) which is certainly the more rigorous. However, it should be remenbered that for such samples, the curve is fitted using a small NRM fraction and thus the quality factor is also low. As a consequence, discussion about paleointensity variations should be done in keeping in mind the importance of the quality factor.

Also, we shall emphasize that paleointensity experiments should be performed up to an almost complete demagnetization of the NRM. Indeed, this allows a better assessment of the true behavior of the sample.

E) Paleointensity Results (Table 2)

Reliability of the results

Typically, the NRM fractions f reported in Table 2 varies from 0.15 to 0.9 and the quality factor q ranges from 1.2 to 91.2. The average number of points N which define the straight line of the paleointensity data is close to 10.

A strong correlation is observed between f and q (Fig. 19) and it is obvious that f is the main factor in the calculation of $\tilde{q}$. Thus care must be taken to not increase artificially the factor q by increasing f in keeping points which may be off the line.

Differences in grain size between samples can be estimated from the laboratory Koenisberger ratio Q_L, defined by Prévot et al. (1985). Data from the Steen Mountain have shown a clear correlation between Q_L and the maximum temperature (T_{max}) usable for paleointensity determination, before the beginning of magnetochemical changes. T_{max} reflects in fact the thermal stability of samples. For values of T_{max} between 400 and 600°C, no such clear correlation is observed in our results between Q_L, and T_{max}. However, the lowest values correspond to T_{max} below 500°C (Fig.20).

Description of the results

The variation between samples for a single unit is often larger than each individual error thus demonstrating the need of several determination per flow.

We present successively the data for the site B and site A.

Forty six samples from the site B (Remparts de Bellecombe) were studied. Paleointensity results have been obtained for 10 flows among 13, with at least 2 determinations per flow. The exception is flow RB8 for which three experiments were attempted and only one was successful. Very accurate data have been obtained on some flows, 13 samples have a quality factor greater than 10. An example is given with sample RB129 (Fig.21). Some others samples provided results with intermediate quality, like samples RB164 (Fig.21). Paleointensities with low quality factors ($q \leq 3$) have been obtained for 3 flows RB1, 11, 12 and these paleointensities are certainly less reliable. The scatter of the points on the

Table 2:Paleointensity results

Lava Flow	Sample	D	I	T_C °C	J_S-T Type	JNRM Am^{-1}	H_L µT	N	∂T	f	g	q	r	%R	Q_L	Fe±σFe µT	Fe±s.d. µT	<Fe> µT	VDM
SITE B Remparts de Bellecombe																			
RB1	RB108	6.0	-37.0	505	3c	5.2	35	7	200-440	0.274	0.797	1.6	0.953	13.7	35.4	36.6±5.5			
	RB109	5.0	-40.0	514	1b	16.3	40	9	330-480	0.174	0.866	2.8	0.990	2.1	39.3	37.5±1.7			
	RB110	1.2	-35.8	526	1b	9.3	35	5	250-410	0.178	0.738	1.9	0.993	20.5	17.0	37.2±2.5	37.1±0.5	37.2	7.9
RB2	RB113	12.0	-35.8	523	1e	8.8	40	13	200-480	0.295	0.901	3.3	0.964	15.8	13.7	54.7±8.3			
	RB114	0.3	-35.7	516	1a	8.5	35	11	200-530	0.575	0.858	11.4	0.992	12.6	16.5	50.8±2.2			
	RB115			531	1a	8.0	35	13	300-540	0.503	0.880	14.4	0.995	18.6	15.3	55.2±1.7			
	RB116	2.0	-34.0	465	1c	5.8	35	6	200-410	0.234	0.783	1.8	0.979	11.9	7.2	48.7±5.0			
	RB117	354.0	-34.0	547	1b	13.4	35	8	370-520	0.610	0.818	20.5	0.998	9.2	13.4	38.7±0.9	49.6+6.7	46.4	9.8
RB3	RB119	0.9	-37.5	506	1b	7.7	40	15	240-560	0.819	0.846	31.2	0.997	5.0	16.2	26.9±0.6			
	RB120			531	1a	16.6	35	15	200-540	0.552	0.841	24.5	0.998	11.4	25.9	37.6±0.7			
	RB121	355	-31.0	536	1d	11.0	40	14	270-560	0.870	0.857	53.6	0.999	4.0	37.3	36.7±0.5	33.7±5.9	34.2	7.8
RB3'	RB124	4.0	-36.0	540	1c	6.5	40	14	240-545	0.708	0.861	32.4	0.998	4.7	15.2	34.0±0.6			
	RB125	0.0	-34.5	542	1c	10.7	35	9	370-530	0.439	0.826	16.3	0.998	6.5	44.4	37.4±0.8			
	RB127	357.6	-38.3	530	1c	12.8	40	14	240-545	0.814	0.841	33.2	0.997	4.1	20.2	33.2±0.7	34.9±2.2	34.5	7.5
RB4	RB128	5.0	-35.3	514	1a	10.6	35	13	290-550	0.844	0.894	61.0	0.999	2.9	22.7	32.4±0.4			
	RB129	2.4	-30.	510	1b	9.3	35	11	330-540	0.868	0.871	91.2	0.999	2.6	17.7	33.9±0.3			
	RB131	354.0	-28.5	519	1b	7.8	40	16	150-505	0.331	0.921	8.8	0.992	9.9	9.9	44.6±1.5	37.0±6.7	33.9	7.6
RB8	RB154	6.0	-50.	533	1d	10.3	40	20	200-555	0.802	0.924	74.3	0.999	4.3	15.6	42.6±0.4	42.6±0.4		
RB9	RB158	2.0	-35.5	545	3a	8.4	40	10	240-480	0.420	0.875	7.3	0.990	4.9	25.8	34.6±1.7			
	RB159	10.0	-40.0	511	3a	6.4	40	11	150-435	0.416	0.888	6.1	0.983	9.4	12.2	48.1±2.9			
	RB161	355.0	-43.5	509	3a	8.8	35	13	290-550	0.910	0.882	52.1	0.999	3.0	29.9	36.5±0.6	39.7±7.3	37.4	7.8
RB10	RB164	340.0	-50.0	507	1b	11.1	40	11	240-500	0.374	0.858	5.4	0.984	8.3	11.3	47.1±2.8			
	RB165	355.0	-50.0	513	1a	9.8	40	11	240-500	0.348	0.868	5.3	0.985	9.6	11.3	45.7±2.6			
	RB166	9.0	-46.5	510	1c	11.5	40	14	150-480	0.252	0.894	6.3	0.992	3.8	13.7	40.6±1.4	44.5±3.4	44.4	8.6
RB11	RB169	351.0	-55.0	501	1c	8.2	35	7	100-410	0.344	0.710	3.0	0.984	7.9	6.0	48.4±3.9			
	RB170	355.0	-57.0	546	3a	6.2	40	9	240-435	0.283	0.831	2.9	0.978	9.7	23.1	33.1±2.6			
	RB161	354.0	-45.0	541	3a	10.4	35	7	200-440	0.233	0.813	2.1	0.980	7.3	18.1	40.3±3.6	40.6±7.7	41.2	7.6
RB12	RB173	330.0	-52.5	463	1a	7.7	35	6	250-440	0.220	0.699	1.3	0.972	19.3	4.9	55.4±6.5			
	RB175	353.0	-53.0	477	1a	11.2	35	7	290-475	0.266	0.769	2.3	0.980	15.7	11.1	35.1±3.1			
	RB176	350.0	-50.0	497	1a	10.6	40	10	240-450	0.170	0.852	2.4	0.986	10.5	10.8	47.2±2.8			
	RB177	353.0	-54.0	497	1a	9.5	35	6	250-440	0.155	0.703	1.2	0.986	16.7	10.5	37.8±3.2	43.1±9.3	43.1	7.9

Lava Flow	Sample	D	I	T_C °C	Js-T Type	JNRM Am^{-1}	H_L µT	N	∂T	f	g	q	r	%R	Q_L	Fe±σFe µT	Fe±s.d. µT	<Fe> µT	VDM
SITE	**A Rivière des Remparts**																		
RA1	RA002	1.3	-47.8	538	1a	16.4	35	17	300-575	0.873	0.892	20.4	0.990	1.6	21.7	34.7±1.3			
	RA005	358.0	-44.5	519	1c	7.7	35	10	300-510	0.425	0.858	5.7	0.983	17.6	6.8	41.0±2.6	37.9±4.5	36.4	7.4
RA2	RA009	8.5	-47.0	552	1c	13.8	35	18	270-575	0.816	0.881	21.8	0.991	4.6	26.3	32.8±1.1	32.8±1.1		
RA3	RA011	4.5	-38.5	499	1e	10.7	35	14	200-515	0.593	0.905	16.8	0.994	5.9	12.0	33.1±1			
	RA013		-41.0	513	1a	13.1	35	11	200-490	0.445	0.856	7.6	0.989	5.8	14.7	26.2±1.3			
	RA014		-27.5	491	1b	12.0	35	9	220-500	0.250	0.851	4.5	0.992	11.1	20.9	27.7±1.3			
	RA015		-49.0	506	1b	8.2	35	11	340-530	0.460	0.861	6.7	0.984	5.3	17.5	33.5±2.0			
	RA017			527	1b	5.6	35	6	220-425	0.198	0.782	2.4	0.992	13.2	20.1	42.2±2.7	32.5±6.3	31.9	6.6
RA4	RA020	20.0	-55.0	117	2	3.2	35	6	70-135	0.618	0.750	14.5	0.998	6.1	5.9	58.6±1.9			
	RA021	6.2	-63.0	115	2	2.9	35	5	55-115	0.559	0.641	8.0	0.997	6.0	5.9	49.3±2.2	54.0±6.6	55.0	8.8
RA5	RA024	1.0	-56.0	131	2	4.6	35	12	70-215	0.679	0.895	16.6	0.993	14.1	8.9	53.9±2.0			
	RA026	358.5	-55.0	346	1c	3.9	35	7	150-425	0.459	0.825	6.9	0.992	9.1	5.2	59.2±3.3			
	RA027	357.0	-57.5	166	3a	4.9	35	14	70-240	0.244	0.897	3.5	0.976	19.1	12.5	40.7±2.5	51.3±9.5	54.2	8.8
RA6	RA030	355.0	-56.0	146	2	5.4	35	12	70-215	0.761	0.865	16.4	0.992	8.8	12.2	43.1±1.7			
	RA031	1.0	-53.5	n.d.	n.d.	3.8	35	10	70-175	0.596	0.833	11.3	0.992	8.3	6.9	47.4±2.1			
	RA032	352.0	-53.5	142	2	3.7	35	14	70-290	0.675	0.879	15.0	0.991	8.4	9.6	44.9±1.8			
	RA033	358.0	-55.0	138	2	3.1	35	5	70-145	0.624	0.795	6.5	0.985	10.8	4.2	58.4±4.4	48.5±6.9	47.9	8.1
RA7	RA038	16.0	-49.0	550	1c	2.2	35	7	200-410	0.433	0.811	4.7	0.986	14.6	2.4	47.3±3.5			
	RA039	355.0	-56.0	543	1c	3.7	35	9	200-430	0.454	0.844	7.0	0.989	7.3	5.4	41.8±2.3			
	RA040	8.9	-55.0	536	1a	4.4	35	8	220-475	0.561	0.850	5.6	0.978	12.8	4.9	47.4±4.1	45.5±3.2	45.3	8.0
RA9	RA047	350.0	-50.	534	1a	2.6	35	9	240-450	0.316	0.845	2.7	0.965	14.3	1.8	48.3±4.8			
	RA048	348.0	-54.0	536	1a	2.6	35	9	200-450	0.376	0.861	4.2	0.979	20?5	2?0	48.1±3.7			
	RA049	10.0	-59.0	527	1b	2.9	35	8	220-475	0.520	0.820	3.9	0.965	17.0	2.9	37.5±4.0			
	RA051	358.0	-50.0	531	1b	2.8	35	9	200-450	0.343	0.840	2.7	0.961	22.5	2.7	43.3±4.6	44.3±5.1	44.0	7.7
RA10	RA053	2.0	-46.0	555	1a	14.3	35	8	400-530	0.314	0.805	6.9	0.996	11.3	28.7	33.1±1.2			
	RA057	8.0	-49.0	546	1a	14.2	35	7	370-510	0.241	0.811	2.7	0.987	16.8	20.4	43.2±3.1	38.2±7.1	36.1	7.2
RA11	RA064	4.6	-54.0	557	1c	12.1	35	17	200-570	0.946	0.793	39.8	0.997	7.2	26.8	30.0±0.6			
	RA066	6.0	-47.5	499	1a	5.1	35	20	200-575	0.873	0.924	47.1	0.997	2.1	12.3	28.8±0.5	29.4±0.8	29.4	5.5
RA13	RA073	340.0	-39.0	534	1d	2.5	35	7	300-450	0.293	0.825	2.5	0.977	14.6	4.9	29.6±2.8			
	RA077	327.0	-38.0	536	1a	3.3	35	7	240-410	0.445	0.825	5.7	0.990	14.1	3.2	31.1±1.6	30.4±1.1	30.6	6.3
RA15	RA086	336.5	-38.0	551	1d	3.5	35	15	200-525	0.406	0.881	9.2	0.990	14.9	8.0	26.0±1.0			
	RA087	344.0	-38.0	564	1d	1.1	35	14	200-530	0.559	0.895	26.9	0.998	9.6	25.7	16.7±0.3	21.4±6.6	19.0	4.1
RA17	RA099	16.5	-22.0	484	1e	5.3	35	8	220-475	0.231	0.837	2.6	0.983	13.7	3.1	43.8±3.3			
	RA100	353.0	-37.0	517	1b	3.8	35	9	200-450	0.368	0.863	4.4	0.982	14.0	2.0	37.0±2.6			
	RA105	5.0	-37.0	551	3a	5.0	35	17	85-485	0.832	0.872	15.3	0.983	8.8	5.5	53.4±2.5	44.7±8.2	47.8	9.9

Table 2 D, I are the magnetic declination and inclination of the NRM left in the ∂T interval; Tc is the Curie temperature of the sample; Js-T is the type of the thermomagnetic curve; J_{NRM} is the intensity of the natural remanence in Am^{-1}; H_L is the intensity of the laboratory field in µT; N is the number of points in the ∂T interval; ∂T is the interval of temperature used the determine the paleointensity; f, g, q, are NRM fraction, gap factor, and quality factor respectively (Coe et al., 1978); r is the linear correlation coefficient; R% is the maximum percentage of CRM (Coe et al., 1984); Q_L is the laboratory Koenigsberger; Fe is the paleointensity estimate for individual specimen in µT, σ(Fe) is its standard error, F_e±s.d. is the unweighted average paleointensity of individual lava flow in µT, plus or minus its standard deviation; <F_e> is the weighted mean in µT.; VDM is the virtual dipole moment in 10^{22} Am^2.

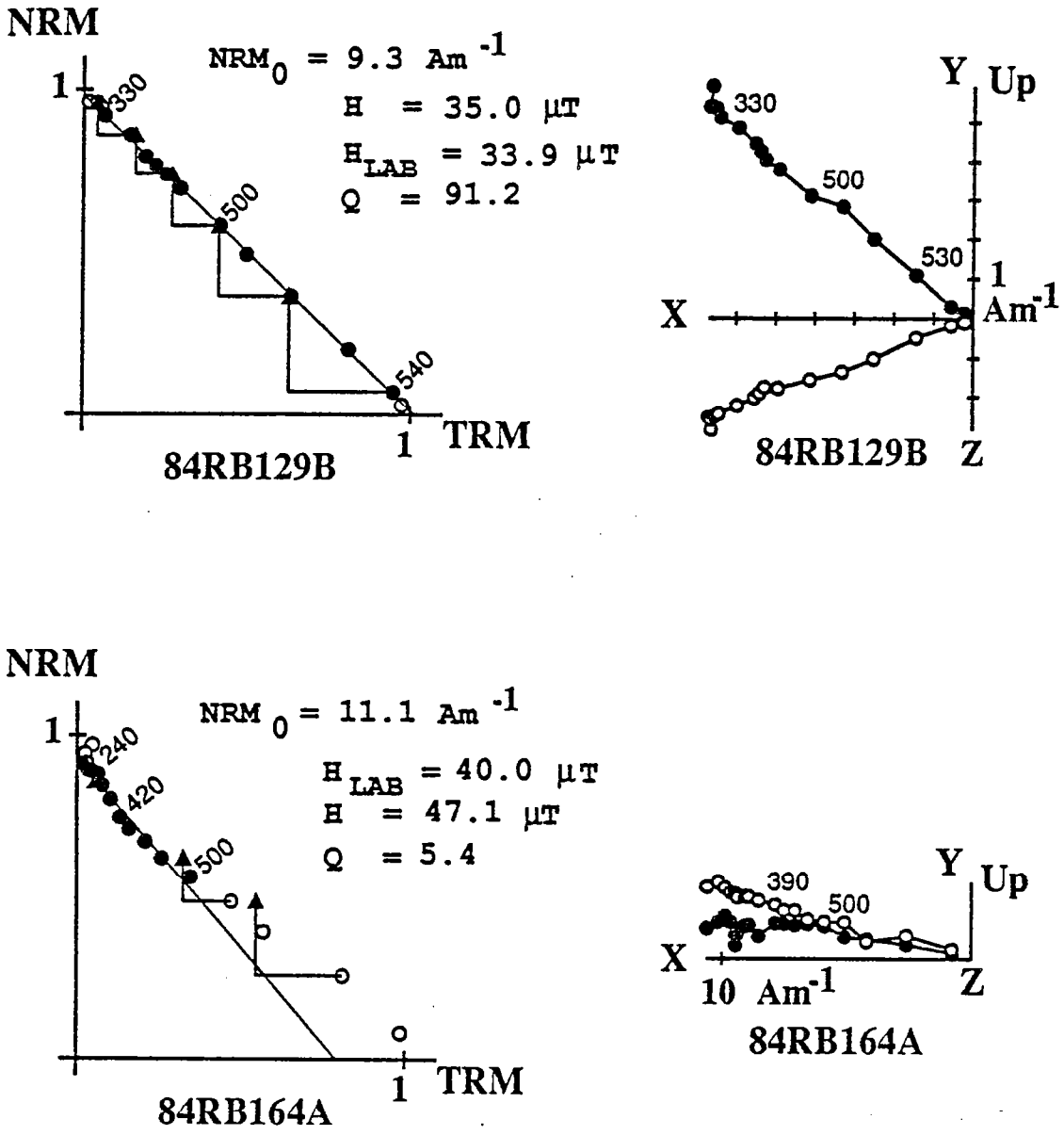

Fig.21: Examples of successful paleointensity experiments for two samples from site B. NRM_0 is the initial intensity of magnetization, H_L is the laboratory field and q the quality factor. The NRM demagnetization is shown in sample coordinate.

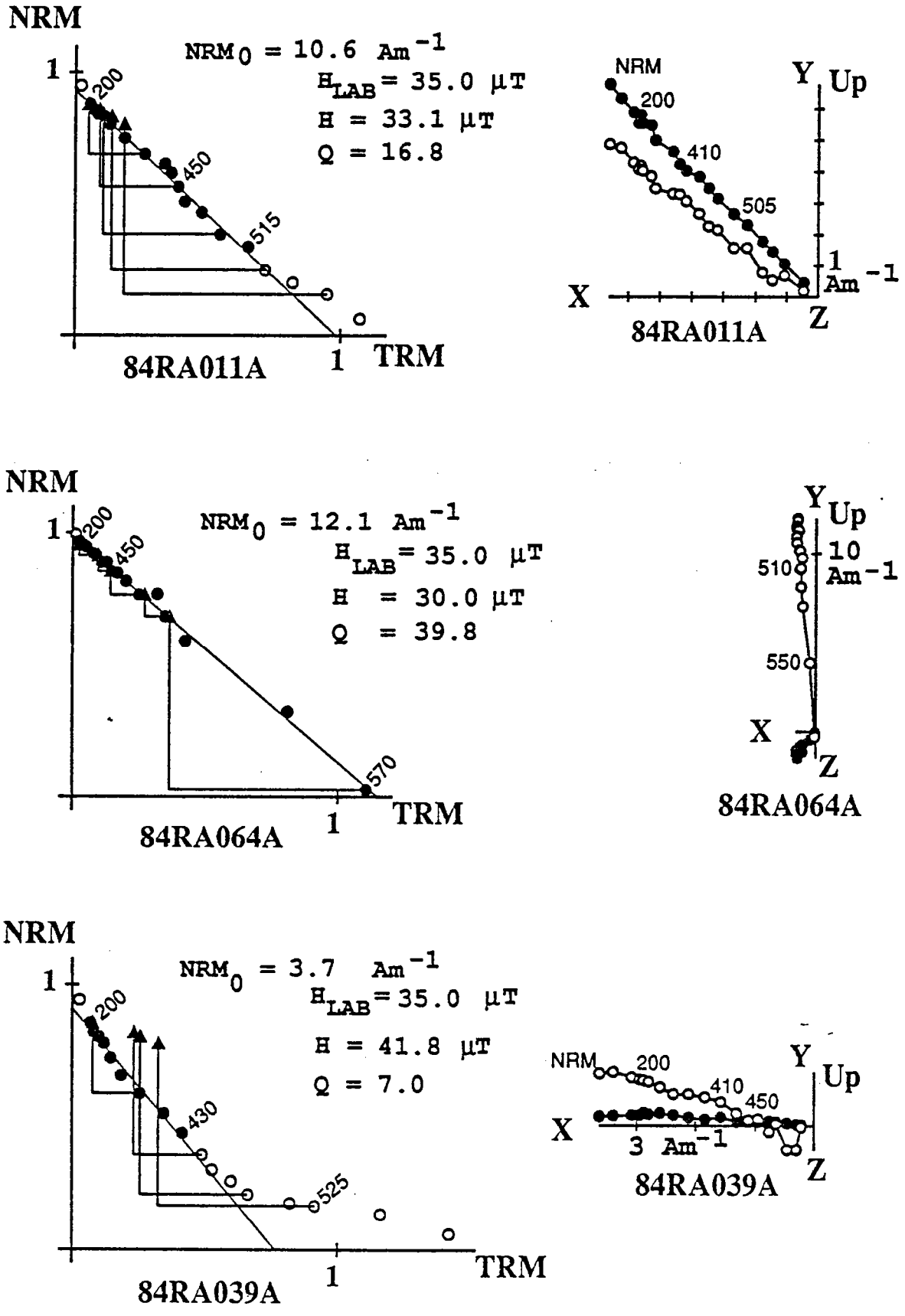

Fig.22: Examples of reliable paleointensities for 3 samples from Site A.

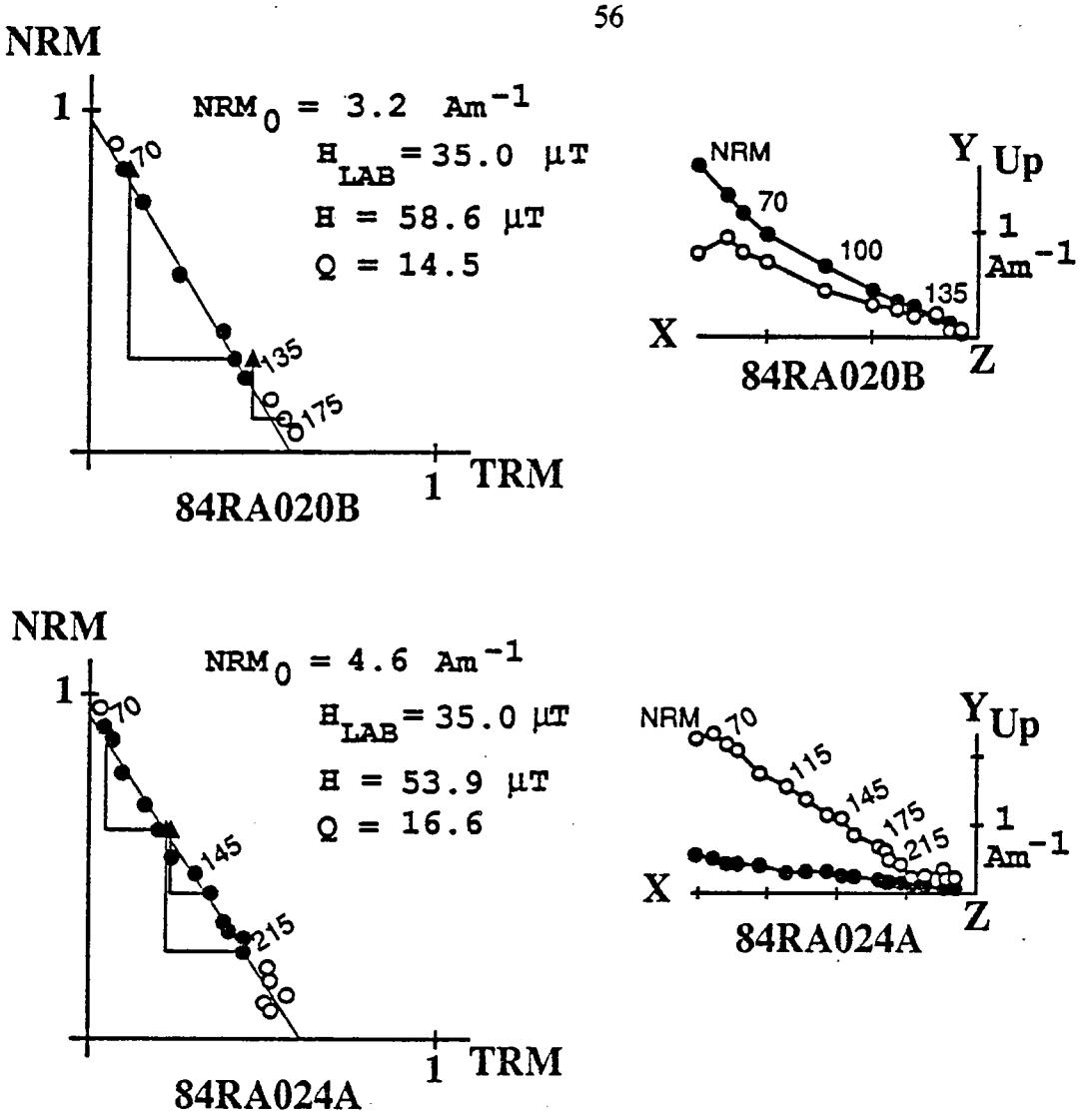

Fig.23: Examples of reliable paleointensities for 2 samples with low unblocking temperatures due to Ti-rich titanomagnetites.

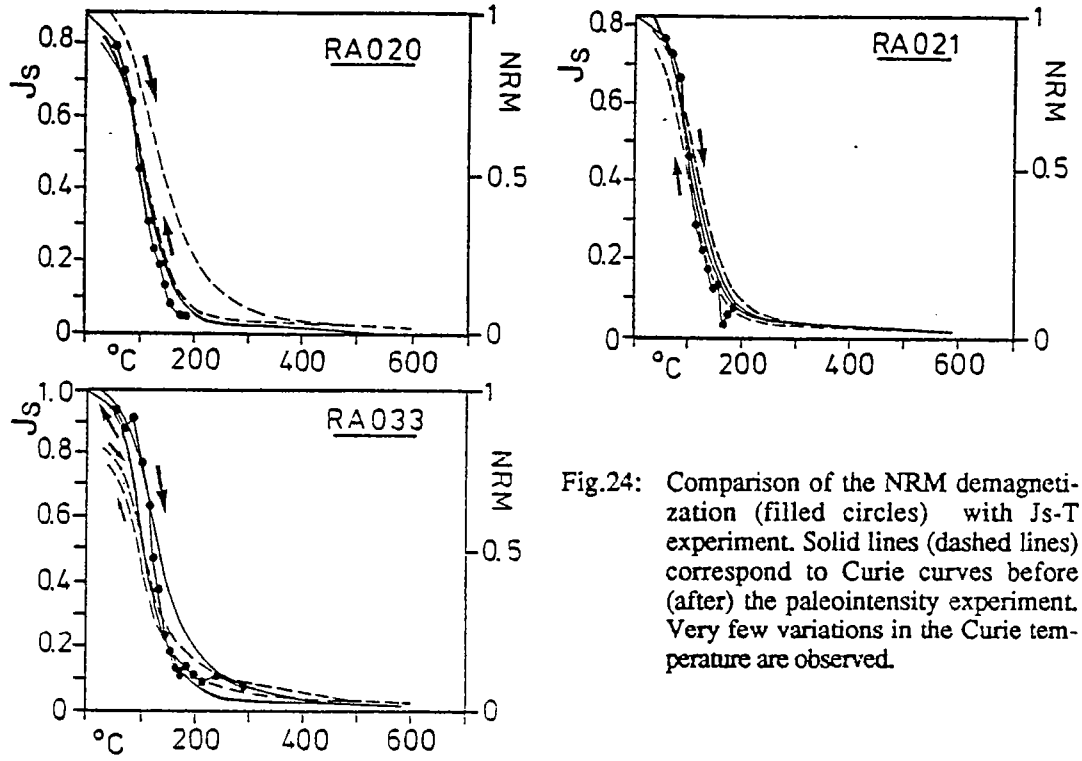

Fig.24: Comparison of the NRM demagnetization (filled circles) with Js-T experiment. Solid lines (dashed lines) correspond to Curie curves before (after) the paleointensity experiment. Very few variations in the Curie temperature are observed.

straight line which defines the paleointensity slope is commonly low (see the coefficient of linear correlation r in Table 2).The paleointensities range from 34 to 46 μT.

Fifty samples from the site A (Rivière des Remparts) were studied and 35 have given reliable results. Average paleointensities were obtained on 12 flows, among the 17 which compose the site. Only one result was acquired on the flow RA2. It was not so easy to find suitable samples for paleointensity determinations at this site, because of the existence of secondary component of magnetization Some examples of paleointensity diagrams are given on Fig.22.

Samples composed of non-oxidized titanomagnetites type 2 Js-T curves, were found on lava flows RA4, 5 and 6. As they did not carry important VRM or other overprints, Thellier experiment were performed on 7 samples. Such unoxidized Ti-rich titanomagnetite are often observed on mid ocean ridge basalts. Measurements of geomagnetic paleointensity using the Thellier's method have given good results on such fresh material, that is on specimens which have not been subjected to low temperature oxidation (Gromme et al., 1979). On our subaerial basalts, convincing results were obtained (Fig. 23, Table 2). Usually more than 50% of the initial NRM intensity was used for the paleointensity determination, before any magnetochemical change was observed. However, it has been shown that linearity of NRM against TRM as well as no change in PTRM capacity are not sufficient to prove the absence of physical or chemical changes in the temperature range used to calculate the strength of the paleofield (Prévot et al., 1983). In order to check that no important alteration of the sample magnetic mineralogy has occurred during Thellier experiments, we have compared, the Js-T curves performed before and after paleointensity measurements. Differences in Curie point are not important (Fig. 24). No change is observed for sample RA021, while an increase of 14°C and a decrease of 13°C were determined for samples RA020 and RA033 respectively. During Thellier experiments, samples were heated at temperatures higher than the maximum temperature used to define the linear segment and then the little mineralogical changes observed, may have started at the end of the determination only, as shown by PTRM checks (Fig. 23). So we think that the temperature intervals used for the calculation are free of any magnetochemical changes. This check was important, because the maximum paleointensity values for the site A were obtained on samples with low Curie temperatures, from these lava flows RA4,5 and 6. At this site, average paleointensities range from 19 to 55 μT.

In conclusion, our extensive experiments are in large agreement with previous studies concerning the sample selection criteria which should be absence of viscosity, samples with a single magnetic phase and constituted mostly of single domain grains. However, even selected samples may not always give reliable results.

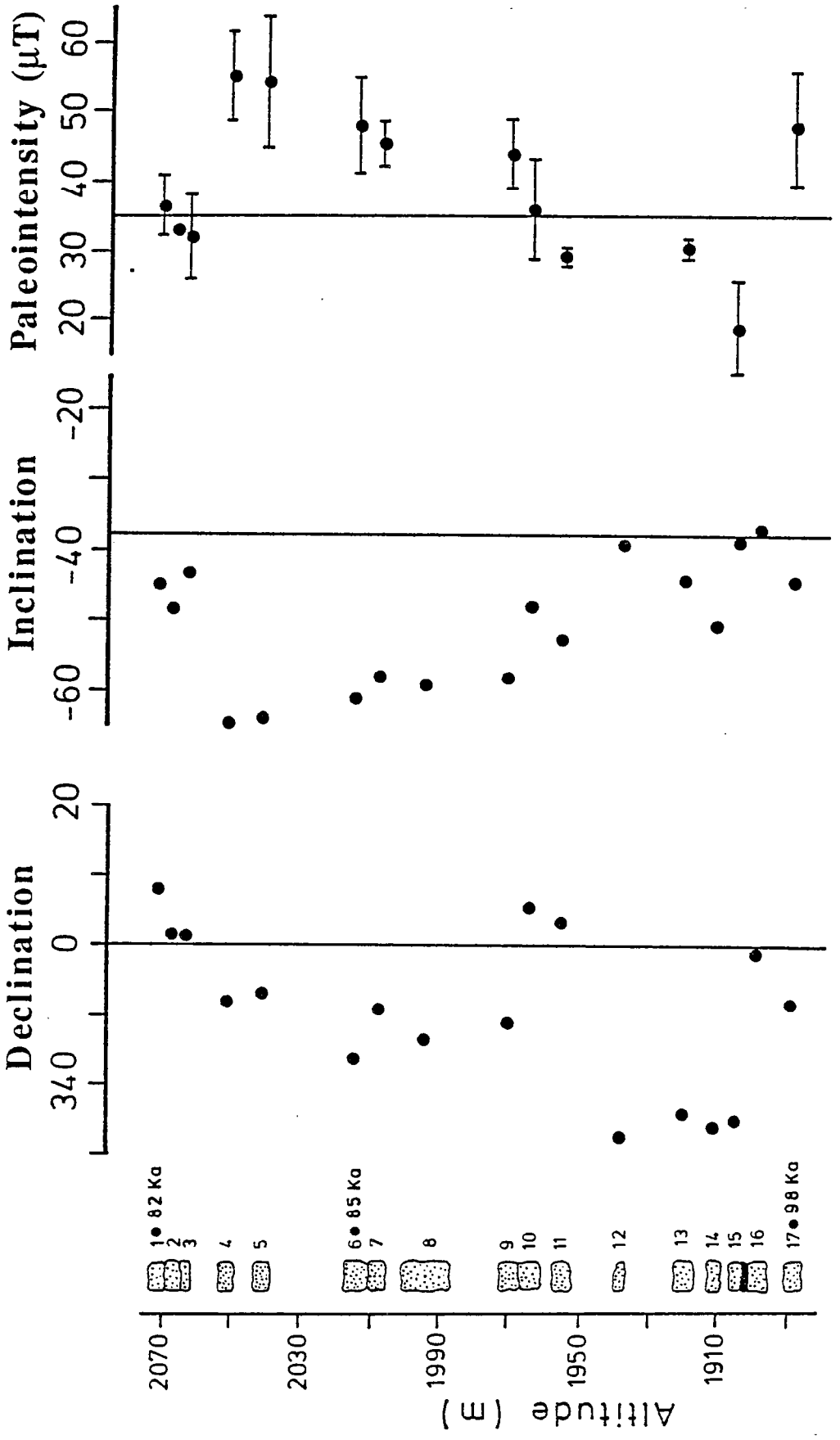
Site A Rivière des Remparts
Declination
340
0
20
Inclination
-60
-40
-20
Paleointensity (μT)
20
30
40
50
60
Altitude (m)
2070
2030
1990
1950
1910
1• 82 Ka
2
3
4
5
6• 85 Ka
7
8
9
10
11
12
13
14
15
16
17• 98 Ka

Figure 25a

DISCUSSION

Geomagnetic field variations in direction and intensity recorded at site A and B have been plotted on Figure 25a and b as a function of the volcanic stratigraphy. We can recognize that the site B has recorded less variations in direction as well as in intensity than flows from site A. Also, groups of flows which have recorded very little variation in direction have provided similar paleointensity values within each group. For example, this is particularly clear for flows RB3, 3bis, RB4 at section B and flows RA1, 2, 3 from section A. The major exceptions to this good relationship come from flows RB1-RB2 and RA13-RA15. Flow RB2 provides a mean paleointensity higher than the overlying flow RB1 which has the same paleomagnetic direction. This difference possibly does not correspond to true field variations but rather reflects problems in paleointensity because of the low quality factors of the paleointensities from flow RB1 and the large scattering in the determinations available for flow RB2. The difference between flows RA13 and RA15 is also uncertain.

A) Comparison with the present day field

Contrary to previous claims it has recently been suggested that the secular variation of the present day field is typical of that for the past 5 Ma (McFadden et al., 1988). This result gives us confidence in the comparison between the present day field at La Réunion and our paleomagnetic records.

A sampling of the present day field on a parallel at about the latitude of La Réunion, indicates variation in intensity from 24 to 53 μT. Assuming a westward drift of the non-dipole sources of 0.2° per year, these intensities would be equivalent to a set of paleomagnetic data covering a period of 1,800 years. The range of intensity variations of the present day field on this parallel is more important than that observed at site B, but of the same order as the one recorded at site A.

When significant directional changes occur between flows, paleointensities also vary as for example between lava flows RA3 and RA4 (Fig. 25a). On the contrary, there are no strong evidences that the field intensity vary without any change in direction. This is simply because the growth and decay of the regional nondipole features do not generally match variations of the main dipole. For example looking at the present day field, the probability that, at one site, the 3 components of the field change in the same sense and rate of variation is very low.

In our record a close examination of the relationships between directions and intensity of the field reveals that steepenings in inclination correspond to increases in intensity. This behavior is particularly clear on flows RA4-RA9. Such variations of both inclination and intensity , in the same way, could be explained by dipole wobble and non-dipole sources. The present day field shows also these features in the southern hemisphere with for example low intensity and low inclination over South America and high inclination and high intensity over the Indian ocean.

Recent analysis of the magnetic field at the core mantle boundary (CMB) derived from observations since the beginning of the eighteen century has suggested that some features in the field have been stationary, while others appear at some fixed parts of the CMB before they drift westward (Bloxham and Gubbins, 1985). Drifting features have been confined to the Atlantic hemisphere for the entire period,

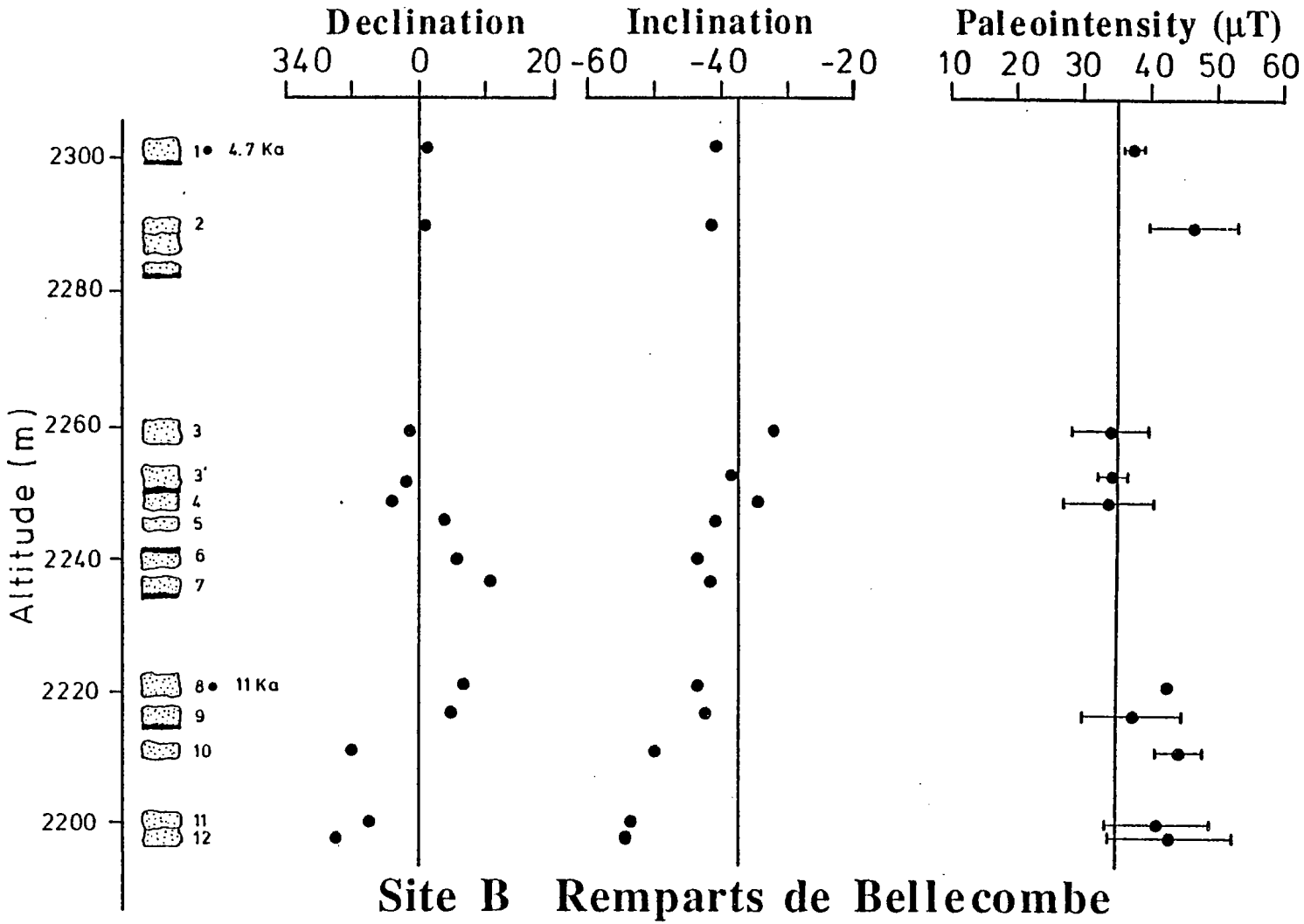

Fig.25b ; For each sequence A and B, mean paleomagnetic directions and paleointensity results in μT (with standard error) versus the stratigraphic height of each flow. Small black dots close to flow numbers indicate those flows which were dated. Vertical lines refer to the inclination expected at this site for an axial dipole (-38°) and to the present day field intensity (35μT).

while low secular variation was observed in Pacific hemisphere. Particularly, intenses patches of reverse flux have been observed in the southern hemisphere around 90° east (South Africa) and are drifting westward toward South America. Both stationary and drifting features are interpreted to be associated to temperature anomalies in the lower mantle which are supposed to occur over the long time scale of mantle convection (Gubbins, 1988). The localization of these features at the CMB led Gubbins to predict some anomalies in the time averaged magnetic field. For example, positive inclination anomalies (defined as the difference between the observed inclination and the one expected from a geocentric axial dipole) should exist for sites south of 45°S while negative anomalies may be found at sites north of 30°S in the Atlantic hemisphere. The island of La Réunion is geographically well situated to test this model. Even though we may suspect that both flow sequences A and B did not average completely the secular variation, they both have negative inclination anomalies in support of Gubbin's predictions.

B) Comparison with other data from the same site

Paleointensity determinations, using both the Thellier and Shaw methods, were carried out by Senanayake et al. (1982), on volcanic rocks from the island of La Réunion. These lava flows which are significantly older (i.e. from 0.6 to 2 Ma.) provided field strengths from 19.4 to 40.2 μT. It indicates a similar range of variation than the one recorded on our late Quaternary sites.

C) Comparison with worldwide data

For the purpose of comparing our intensity data with those from sampling sites at different latitudes, it is convenient to calculate their equivalent virtual dipole moments (VDM) which are reported in Table 2.

-In interpreting the results, we must keep in mind that individual VDM values are composed by three factors: 1) the true dipole moment, 2) a portion due to non-dipole components of the field which is unknown, 3) and errors in paleointensity determinations.

Global archaeomagnetic intensity data were analyzed by Barton et al. (1979), Champion (1980) and by McElhinny and Senanayake (1982) using a largest data set. In order to average out non-dipole field variations, results over 500 or 1000 year intervals have been averaged. The analysis of McElhinny and Senanayake shows that the mean dipole moment for the last 10,000 year interval is 8.75 10^{22} Am^2, a value very close to that obtained for the last 5 Ma. (i.e. 8.7 10^{22} Am^2, McFadden et McElhinny, 1982).

The average VDMs for the site B is 8.1 ±0.7 10^{22} Am^2; a value in good agreement with the mean dipole moment for the last 10 Ka.

The VDMs associated to the two dated lava flows from the site B (RB1 and RB8) are respectively 7.9 and 8.8 10^{22} Am^2. These two values lie relatively close to the global curve established by McElhinny and Senanayake (1982) (Fig. 26) while VDMs obtained on ^{14}C dated lava flows between 2.6–4.6 Ka BP, from Hawaii by Coe et al. (1978) are above the mean curve. These discrepancies are easily interpreted as non-dipole fields effects which statistically produce a scattering with a standard deviation of almost 20% of the dipole moment.

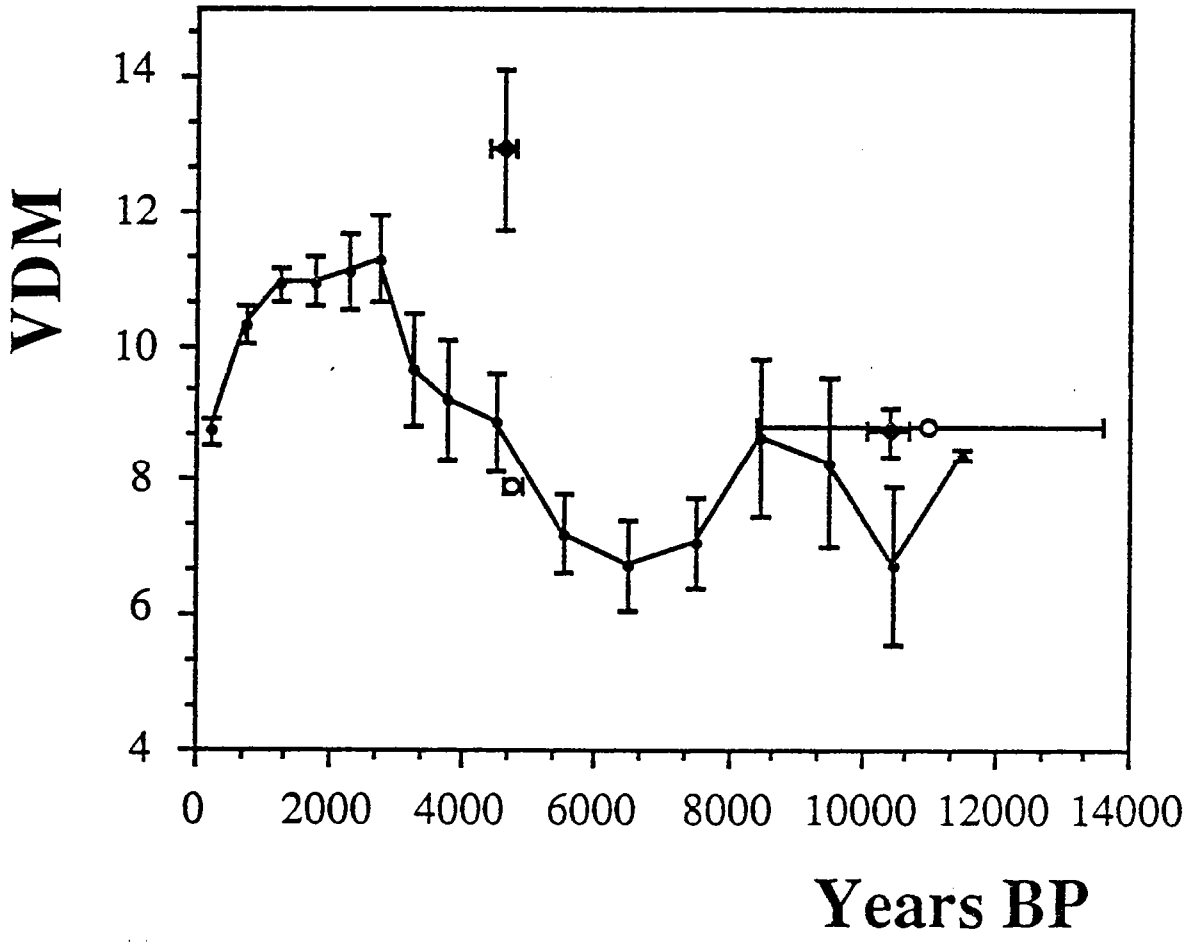

Fig.26: Variation of the VDMs versus time. The connected dots denote the variation of the global mean dipole moment. Open circles are the VDMs for the two dated flows from sequence B (flows RB1 and RB8) at La Réunion while diamonds correspond to Hawaiian data of almost the same age (after Coe et al., 1978). The dipole moment unit is in 10^{22} Am^2.

Most of the data corresponding to the time period 15-50 Ka (Barbetti and Flude,1979; McElhinny and Senanayake, 1982; Salis, 1987) tend to show that the geomagnetic field intensity was lower than the average value for the Holocene period. Several excursions of the field have also been reported in this period around 40–50 Ka. and low paleointensity values have been reported for the Laschamp excursion (Roperch et al., 1988; Marshall et al, 1988, Chauvin et al., 1989). There are no available data prior 50Ka and we may question whether the intensity low observed after the Laschamp excursion did also occur in the preceding period.

VDMs obtained from the site A extend from 4.1 to 9.9 10^{22} Am^2 with a mean value around 7.3 ± 1.5 10^{22} Am^2, in good agreement with the mean value for the last 5 My. Because section A span a time interval from 100 Ka. to 80 Ka., the paleointensity results suggest that any dipole intensity low (if there is any) would not have last longer than 30Ka prior to the Laschamp excursion and 20 Ka. after the Blake excursion which did occur 120 Ka. ago.

SUMMARY AND CONCLUSIONS

A detailed paleomagnetic study has been undertaken on two young volcanic sequences from the island of La Réunion; one was built 100 to 80 Ka ago while the youngest belongs to the Holocene period with age determinations from 11 to 5 Ka.

The analysis of the geomagnetic secular variation recorded by these sections indicates that the extrusion of the lava flows occurred by pulses separated by long periods of quiescence. As a result of the extrusion process, the sampling of the paleomagnetic field was not complete enough to enable a statistically accurate determination of the mean field direction.

A detailed investigation of the magnetic properties of the samples was carried out in parallel with numerous attempts of determination of the paleointensity of the magnetic field. A comparison of the low field susceptibility variations from liquid nitrogen temperature to room temperature with strong field thermomagnetic experiments confirms a previous study by Senanayake and McElhinny (1981) and indicates that low temperature experiments provide a first order approach of the magnetic composition of these basaltic rocks. This study emphasizes the need of selecting samples for paleointensity experiments. Samples without viscosity, with single domain grains and with one single well defined magnetic phase are the best candidates for paleointensity experiments even though these conditions may not be sufficient for an ideal behavior.

Paleointensity estimates were obtained on 23 lava flows among the 30 which were sampled. For the youngest sequence, the VDMs do not depart much from the global mean dipole moment curve corresponding to the last 12 Ka. This is interpreted as evidence of low non-dipole sources at this site during that time.

For the other sequence, the VDMs variations are typical of non dipole field contributions superimposed on a mean VDM of possibly the same strength than the mean VDM of the last 10 Ka. This interpretation is supported by the paleomagnetic directions which also show some non dipole contributions.

REFERENCES

AITKEN M.J., Dating by archaeomagnetic and thermoluminescent methods, *Phil. Trans. R. Soc. London*, A269, 77-88, 1970.

AITKEN M.J., P.A. AKOCK, G.D. BUSSEL and C.J. SHAW, Paleointensity studies on archaeological material from the near east, in *Geomagnetism of baked clays and recent sediments*. Creer K.M., Tucholka P. and C.E. Barton, Elsevier, 1983.

AITKEN M.J., A.L. ALLSOP, G.D. BUSSEL and M.B. WINTER, Greek archeomagnitudes, *Nature*, 314, 753, 1984.

AITKEN M.J., A.L. ALLSOP, G.D. BUSSELL and M.B. WINTER, Determination of the intensity of the Earth's magnetic field during archaeological times : reliability of the Thellier technique, *Rev. Geophys.and Space Phys.*, 26, 1, 3-12, 1988.

BACHELERY P., Le Piton de la Fournaise (Ile de la Réunion) Etude volcanique, structurale et pétrologique - *Thèse de spécialité, Clermont-Ferrand*, 215 p, 1981.

BARBETTI M.F., Archaeomagnetic results from Australia, in *Geomagnetism of baked clays and recent sediments*. Creer K.M., Tucholka P. and C.E. Barton, Elsevier, 1983.

BARBETTI M.F. and M.W. McELHINNY, The lake Mungo geomagnetic excurion, *Phil. Trans. R. Soc. Lond.*, A281, 515-542, 1976.

BARBETTI M.F. AND K. FLUDE, Geomagnetic variation during the late Pleistocene period and changes in the radiocarbon time scale, *Nature*, 279, 202-205, 1979.

BARTON C.E., R.T. MERILL and M.F. BARBETTI, Intensity of the earth's magnetic field over the last 10 000 years, *Phys. Earth Planet. Int.*, 20, 96-110, 1979.

BLOXHAM J. and D. GUBBINS, The secular variation of the Earth's magnetic field, *Nature*, 317, 777-781, 1985.

BOGUE S.W. and R.S. COE, Transitional paleointensities from Kawaï, Hawaï and geomagnetic reversal models, *J. Geophys. Res.*, 89, 10341-10354, 1984.

BURLATSKAYA S.P., Archaeomagnetic investigations in the USSR, in *Geomagnetism of baked clays and recent sediments*, Creer K.M., Tucholka P. and C.E. Barton, Elsevier, 1983.

CASSIGNOL P. and P.Y. GILLOT, Range and affictiveness of uns iked potassium-argon dating : experimental groundwork and applications, in : *Numerical Dating in Stratigraphy, edited by GS Odin, John Wiley & Sons*, 1982.

CHAMALAUN F.H., Paleomagnetism of Réunion island and its bearing on secular variation, *J. Geophys. Res.*, 73, 14, 4647-4659, 1968.

CHAMPION D.E., Holocene geomagnetic secular variation in the Western United States : Implications for the global Geomagnetic Field, *Ph.D Thesis, California*, 1980.

CHAUVIN A., R.A. DUNCAN, N. BONHOMMET AND S. LEVI, Paleointensity of the Earth's magnetic field and K-Ar dating of the Louchadière volcanic flow (Central France). New evidence for the Laschamp excursion, in préparation, 1988.

CISOWSKI S.M., The relationship between the magnetic properties of terrestrial igneous rocks and the compostion and internal structure of their components Fe oxyde grains, *Geophys. J. R. Astr. Soc.*, 60,107-122, 1980.

CLARK D.A. and P.W. SCHMIDT, Theretical analysis of thermomagnetic properties, low-temperature hysteresis and domain structure of titanomagnetite, *Phys. Earth & Planet. Int.*, 30, 300-316, 1982.

COE R.S., Poles-intensities of the Earth's magnetic field determined from Tertiary and Quaternary rocks,*J. Geophys. Res.*, 72, 3247-3262, 1967a.

COE R.S., Determination of paleo-intensities of the Earth's magnetic field with emphasis on mechanisms which could cause non-ideal behavior in Thellier's method, *J. Geomag. Geoelect.*, 19, 157-179, 1967b.

COE R.S. and .S. GROMME, A comparison of three methods of determining geomagnetic paleointensities, *J. Geomag.Geoelec.*, 25, 415-435, 1973.

COE R.S., .S., Gromme and E.A., Mankinen, Geomagnetic paleointensities from radiocarbon dated lava flows on Hawai and the question of the Pacific non-dipole low, *J. Geophys. Res.*, 83, 1740-1756, 1978.

COE R.S., S. GROMME AND E.A. MANKINEN, Geomagnetic paleointensities from excursion sequences in lavas on Oahy, Hawai, *J. Geophys. Res.*, 89, 1059-1069, 1984.

COX A., Research note : Confidence limits for the precision parameter k, *Geophys. J. R. Astr. Soc.*, 18, 545-549, 1969.

DAY R., M. FULLER and V.A. SCHMIDT, Hysteresis properties of titanomagnétites : grain size and compositional dependance, *Phys. Earth Planet. Int.*, 13, 260-267, 1977.

DUNLOP D.J., Thermal enhancement of magnetic susceptibility, *J. Geophys.*, 40, 439-451, 1974

DUNLOP D.J., The rock magnetism of fine particles, *Phys. Earth Planet. Int.*, 26, 1-26, 1981.

DUNLOP D.J., Determination of domain structure in igneous rocks by alternating field and other methods, *Earth Planet. Sci. Let.* 63, 353-367, 1983.

GAMES K.P., The magnitude of the archaeomagnetic field in Egypt between 3000 and 0 BC, *Geophys. J. R. Astr. Soc.*, 63, 45-56, 1980.

GAMES K.P., Archaeomagnitude results from Egypt, in *Geomagnetism of baked clays and recent sediments*. Creer K.M., Tucholka P. and C.E. Barton. Elsevier, 1983.

GAMES K.P., Results from Peru, in *Geomagnetism of baked clays and recent sediments*. Creer K.M., Tucholka P. and C.E. Barton, Elsevier, 1983.

GILLOT P.Y., Datation par la méthode du Potassium-Argon des roches volcaniques récentes (Pleistocène et Holocène). Contribution à l'étude chronostratigraphique et magnétique des provinces volcaniques de Camyanie, des Iles Eoliennes, de Pantelleria (Italie du Sud) et de la Réunion (Océan Indien), *Thèse, Paris*, 225 p, 1984.

GILLOT P.Y. and P. NATIVEL, K-Ar chronology of the ultimate activity of Piton des Neiges volcano, Réunion Iceland, Indian Ocean, *Journal of Volcanology and Geothermal Research*, 13, 131-146, 1982.

GROMME C.S., T.L. WRIGHT and D.L. PECK, Magnetic properties and oxidation of iron-titanium oxide minerals in Alae and Makaopuhi lava lakes, Hawai, *J. Geophys. Res.*, 74, 5277-5293, 1969.

GROMME, S., E.A. MANKINEN, M. MARSHALL AND R.S. COE, Geomagnetic paleointensities by the Thellier's method submarine pillow basalts, effects of seafloor weathering, *J. Geophys. Res.*, 84, 3553-3575, 1979.

GUBBINS D., Thermal core-mantle interaction and time-averaged paleomagnetic field, *J. Geophys. Res.*, 93, 3413-3420, 1988.

HIROOKA K., Results from Japan, in *Geomagnetism of baked clays and recent sediments* Creer K.M., Tucholka P. and C.E. Barton, Elsevier, 1983.

HOLCOMB R., D. CHAMPION and M. McWILLIAMS, Dating recent Hawaian lava flows using paleomagnetic secular variation, *Bull. Soc. Geol. Amer.*, 97, 829-839, 1986.

KHODAIR A.A. and R.S. COE, Determination of geomagnetic paleointensities in vacuum, *Geophys. J. R. Astr. Soc.*, 42, 107-115, 1975.

KING J.W., S.K., BANERJEE and J. MARVIN, A new rock-magnetic approach to selecting sediments for geomagnetic paleointensity studies: application to paleointensity for the last 40 000 years, *J. Geophys. Res.*, 88, 5911-591, 1983.

KONO M., Changes in TRM and ARM in a basalt due to laboratory heating, *Phys. Earth & Planet. Int.*, 46, 1-19, 1987.

KONO M. and N. UENO, Paleointensity determination by a modified Thellier method, *Phys. Earth and Planet. Int.*, 13, 305-314, 1977.

KONO M. and H.TANAKA, Analysis of the Thellier's method of paleointensity determination 1 : Estimation of statistical errors, *J. Geomag. Geoelectr.*, 36, 267-284, 1984.

KONO M, N. UENO and Y. ONUKI, Paleointensities of the geomagnetic field obtained form Pre-Inca potsherds, near Cajamarca. Northern Peru, *J. Geomag. Geoelectr.*, 38, 1339-1348, 1986.

KOVACHEVA M., Summarized results of the archaeomagnetic investigation of the geomagnetic field variation for the last 8 000 yr in South-Eastern Europe, *Geophys. J. R. Astr. Soc.*, 61, 57-64, 1980.

KOVACHEVA M., Archaeomagnetic investigations of geomagnetic secular variations, *Phil. Trans. R. Soc. Lond.*,.A 306, 79-86, 1982.

KOVACHEVA M., Existing archeointensity data from Bulgarra and South Eastern Yougoslavia. in *Geomagnetism of baked clays and recent sediments*, Creer K.M., Tucholka P. and C.E. Barton. Elsevier, 1983.

LEVI S., Comparison of two methods of performing the Thellier experiment (or, how the Thellier method should not be done), *J. Geomag. Geoelectr., 27*, 245-255, 1975.

LEVI S., The effect of magnetite particle size on paleointensity determinations of the geomagnetic field, *Phys. Earth Planet. Int.*, 13, 245-259, 1977.

LEVI S., The additivity of partial thermal remanent magnetization in magnetite, *Geophys. J. R. Astr. Soc.*, 59, 205-218, 1979.

LEVI S. and S.K. BANERJEE, On the possibility of obtaining relative paleointensities from Lake sediments, *Earth. Planet. Sci. Lett.*, 29, 219-2226, 1976.

LEVI S. and R.T. MERILL, Properties of single-domain, pseudo-single-domain and multidomain magnetite, *J. Geophys. Res.*, 83, 245-259, 1977.

LOWRIE W. and M. FULLER, On the alternating field demagnetization characteristics of multidomain thermoremanent magnetization in magnetite, *J. Geophys. Res.*, 76, 6339-6349, 1971.

MANKINEN E.A, M. PREVOT, G.S. GROMME and R.S. COE, The Steen's Mountain (Oregon) geomagnetic polarity transition. 1. Directional history, duration of episodes and rocks magnetism, *J. Geophys. Res.*, 90, 10393-10416, 1985.

MARSHALL M., A. CHAUVIN AND N. BONHOMMET, Preliminary paleointensity measurements and detailed magnetic analysis of basalts from the Skalamaelifell excursion, southwest Iceland, *J. Geophys. Res.*, 93, 11681-11698, 1988.

McDOUGALL I., The geochronology and evolution of the young volcanic island of Réunion, Indian Ocean, *Geochim. Cosmochim. Acta*, 35, 2b1-288, 1971.

McELHINNY M.W. and R.T. MERRILL, Geomagnetic secular variation over the past 5 m.y, *Reviews Geophys. Space Phys.*,13, 687-708, 1975.

McELHINNY M.W. and W.E. SENANAYAKE, Variations in the geomagnetic dipole 1 the past 50,000 years, *J. Geomag. Geoelect.*, 34, 39-51, 1982.

McFADDEN P.L. and M.W. McELHINNY, Variations in the geomagnetic dipole 2 statistical analysis of VD Ms for the past 5 millions years, *J. Geomg. Geoelect.*, 34, 163-189, 1982.

McFADDEN, P.L. and R.T. MERILL, A physical model for palaeosecular variation, *Geophys. J. R. Astr. Soc.*, 78, 809-830, 1984.

McFADDEN P.L., R.T. MERRILL and M.W. McELHINNY, Dipole/quadrupole family of paleosecular variation, *J. Geophys.Res.*, 93, 11583-11588, 1988.

MERRILL R.T. and M.W. McELHINNY, The Earth's magnetic field, its history, origin and planetary perspective, in *International Geophysics Series*, 32, *Academic Press*, 1983.

MOSKOWITZ B.M., Methods for estimating Curie temperature of titanomagnétites from experimental Js-T data, *Earth and Planet. Sci. Let.*, 53, 84-88, 1981.

PREVOT M., Magnetisme et minéralogie magnétique de roches néogènes et quaternaires, contribution au paleomagnetisme et à la géologie du Velay, *Thèse, Université P. et M. Curie*, Paris, 1975.

PREVOT M., E.A. MANKINEN and S. GROMME, High paleointensities of the Geomagnetic field from thermomagnetic studies on rift valley pillow basalts from the Mid-Atlantic ridge, *J. Geophys. Res.*, 88, 2316-2326, 1983.

PREVOT, M., E.A. MANKINEN, R.S. COE AND C.S. GROMME, The steens Mountain geomagnetic polarity transition 2. Field intensity variation and discussion of reversal models, *J. Geophys. Res.*, 90, 10417-10448, 1985.

RADHAKRISHNAMURTY C. and E.R. DEUTSCH, Magnetic techniques for as certaining the nature of iron oxide grains in basalts, *J. Geophys.*, 453-465, 1974.

RADHAKRISNAMURTY C., E.R. DEUTSCH and G.S. MURTHY, On the presence of titanomagnetite in basalts, *J. Geophys.*, 45, 433-446, 1979.

RAMASWAMY K., M. DHEENATHAYALU and S. BHARATHAN, Archaeomagnetic determination of the ancient intensity of the geomagnetid field in Tamilnadu, India, *Phys. Earth Plan. Int.*, 40, 61-64, 1985.

READMAN P.L. and W. O'REILLY, Magnetic properties of oxidized (cation-deficient) titanomagnetite (Fe, Ti)$_3$ O$_4$, *J. Geomag. Geoelect.*, 24, 69-90, 1972.

ROPERCH P., N. BONHOMMET and S. LEVI, Paleointensity of the earth's magnetic field during the Laschamp excursion and geomagnetic implications, *Earth Planet. Sci. Let.*, 88, 209-219, 1988.

SALIS J.S., Variation séculaire du champ magnétique terrestre. Directions et paleointensités - sur la période 7000-70 000 ans BP, dans la Chaîne des Puys, *Thèse, Mémoires et documents du CAESS*, Rennes, 1987.

SCHWEITZER C., and H.C. SOFFEL, Paleointensity measurements on post glacial lavas from Iceland. *J. Geophys.*, 47,57-60, 1980.

SENANAYAKE W.E. and M.W. McELHINNY, Hysteresis and susceptibility characteristics of magnetite and titanomagnetites : interpretation of results from basaltic rocks, *Phys. Earth Planet. Int.*, 26, 47-55, 1981.

SENANAYAKE W.E. and M.W. McELHINNY, The efects of heating on low temperature susceptibility and hysteresis properties of basalts, *Phys. Earth. Planet. Int.*, 30, 317-321, 1982.

SENANAYAKE W.E., M.W. McELHINNY and P.L. Mc FADDEN, Comparison between the Thellier's and Shaw's paleointensity methods using basalts less than 5 million years old, *J. Geomag. Geoelect.*, 34, 141-161, 1982.

SOFFEL H., The single domain-multidomain transition in natural intermediate titanomagnetites, *J. Geophys.*, 37, 451-470, 1971.

STERNBERG R.S., Archaeomagnetism in the Southwest of North America, in *Geomagnetism of baked clays and recent sediments*. Creer K.M., Tucholka P. and C.E. Barton, Elsevier, 1983.

STERNBERG R.S. and R.F. BUTLER, An archaeomagnetic paleointensity study of some Hohokan potsherds from Snaketown, Arizona, *Geophys. Res. Lett.*, 5, 101-104, 1978.

TANAKA H., Intensity variation of the geomagnetic field in Japan during the last 30,000 years, determined from volcanic rocks and potteries. *Ph.D These, Tokyo Institute of Technology*, 1980.

TANGUY J.C., I. BUCUR and J.F.C. THOMPSON, Geomagnetic secular variation in Sicily and revised ages of historic lava from Mount Etna, *Nature*, 318, 453-455, 1985.

THELLIER E., Sur la direction du Champ Magnétique Terrestre, en France, durant les deux derniers millénaires, *Phys. Earth and Planet. Int.*, 24, 89-132, 1981.

THELLIER E. and O. THELLIER, Recherches géomagnétiques sur des coulées volcaniques d'Auvergne, *Ann. Geophys.*, 1; 37-42, 1944.

THELLIER E. AND O. THELLIER, Sur l'intensité du champ magnétique terrestre dans le passé historique et géologique, *Ann. Geophys., 15*, 285-376, 1959.

WALTON D., Geomagnetic intensity in Atheens between 2,000 BC and AD 400, *Nature*, 277, 643-644, 1979.

WALTON D., Re-evalution of Greek archaeomagnitudes, *Nature*, 310, 740-743, 1984.

WATKINS N.D., Brunhes epoch geomagnetic secular variation on Réunion Island, *J. Geophys, Res.*, Vol 78, n°2, 7763-7768, 1973.

WATKINS N.D. and J. NOUGIER, Excursions and secular variation of the Brunhes Epoch. Geomagnetic field in the Indian Ocean region, *J. Geophys. Res.*, 78, 26, 6060-6068, 1973.

WATSON G.S., BERAN R.J., Testing a sequence of unit vectors for senal correlation, *J. Geophys. Res.*, V 72, 5655-5659, 1967.

WEI Q.L., T.C. LI, G.Y. CHAO, W.S. CHANG and S.P. WANG, Secular variation of the direction of the ancient geomagnetic field for Lo yang region Chine, *Phys. Earth and Planet. Int.*, 25, 107-112, 1981.

WEI Q.Y., WEI-XI Z., DONG-JIE L., M.J. AITKEN, G.D. BUSSELL and M. WINTER, Geomagnetic intensities as evaluated from ancien Chinese pottery, *Nature*, 328, 330-333, 1987.

WORM H.L., M.JACKSON, P. KELSO and S.K. BANERJEE, Thermal demagnetization of partial thermoremanent magnetization, *J. Geophys. Res.*, 93, 12196-12204, 1988.

DEUXIEME PARTIE

NOUVELLES DONNÉES CONFIRMANT L'ORIGINE GÉOMAGNÉTIQUE DE L'EXCURSION DU LASCHAMP

INTRODUCTION

On regroupe sous le terme d'excursion du CMT, toute déviation importante par rapport aux états dipolaires, suivie par un retour à la polarité de départ. Elles peuvent dont être mises en évidence par exemple par une série de pôles géomagnétiques virtuels (PGVs) atteignant de faibles latitudes (inférieures à 45°), en dehors des nuages de variation séculaire.

La détection d'excursions dans les enregistrements paléomagnétiques n'est pas facile, du fait de leur courte durée. Le caractère épisodique et irrégulier des éruptions volcaniques explique facilement qu'un événement bref, de l'ordre du millier d'années, ne soit pas toujours détecté par une séquence de coulées.

Dans le cas des enregistrements sédimentaires l'origine géomagnétique des excursions détectées n'est pas toujours facile à démontrer, les directions intermédiaires observées dans un sédiment pouvant également résulter d'une mauvaise séparation des composantes d'aimantation ou de perturbations dans l'acquisition de la rémanence détritique ou post-détritique, ou d'altération chimique (Verosub et Banerjee, 1977).

La meilleure preuve de l'existence des excursions du CMT provient de l'étude d'une séquence d'environ mille coulées volcaniques d'Islande d'âge couvrant les 13 derniers millions d'années (Harrisson, 1980). Environ 40% des coulées ayant un PGV de faible latitude ne se sont pas mises en place durant un renversement de polarité connu. Ceci signifie soit, qu'un grand nombre de renversements de polarités n'ont pas encore été détectés, ou plus probablement que les excursions du champ sont des phénomènes fréquents. Des résultats similaires, à partir d'un plus grand nombre de coulées ont été obtenus plus récemment (Kristjansson, 1985 ; Kristjansson, Mc Dougall, 1982).

1) Excursions dans la période de Brunhes.

Un intérêt tout particulier a été porté sur les possibles excursions survenues dans la période de Brunhes. Celles-ci méritent une attention particulière pour plusieurs raisons :

1). Elles peuvent servir d'excellents marqueurs stratigraphiques.

2). Elles devraient être plus faciles à découvrir.

3). L'intervalle de confiance des datations radiométriques (K-Ar, ^{14}C, $^{40}Ar/^{39}Ar$) est suffisamment faible pour permettre de démontrer clairement, d'une part que ces excursions sont indépendantes des renversements connus et d'autre part pour espérer pouvoir corréler entre elles des excursions mises en évidence sur des sites géographiquement séparés.

L'excursion du Laschamp (Bonhommet et Babkine, 1967) fut la première proposée dans la période de Brunhes. Du fait du caractère inverse des directions primaires observées sur les coulées de Laschamp et d'Olby (Chaîne des Puys), l'hypothèse d'un renversement complet du champ a d'abord été avancée. L'origine géomagnétique de l'excursion du Laschamp a été longtemps contestée, certains auteurs n'y voyant qu'un effet d'auto-inversion des porteurs magnétiques (Heller, 1980; Heller et Petersen, 1982). Récemment cette interprétation a été rejetée (Roperch et al., 1988).

De plus une étude détaillée de paléointensité a montré que l'intensité du CMT était très faible durant l'excursion du Laschamp, de l'ordre de 8 μT (Roperch et al., 1988). Cette faible intensité suggère qu'une polarité inverse stable n'a pas été atteinte et que le champ était dans un état intermédiaire (ou de transition) durant l'événement du Laschamp.

J'ai pour ma part effectué une étude détaillée de l'intensité du champ lors de la mise en place de la coulée de Louchadière (Chaîne des Puys). Cette étude est présentée dans l'article qui suit cette introduction. Les données radiométriques de thermoluminescence (Guérin, 1983) ainsi que les nouvelles datations par K-Ar (effectuées à l'université d'Oregon et présentées dans l'article qui suit cette introduction), montrent clairement que cette coulée est contemporaine de celles d'Olby et de Laschamp. La coulée de Louchadière a enregistré une direction purement intermédiaire du CMT à laquelle est associée un paléochamp de 13 μT. Ces données sont en excellent accord avec celles obtenues par Roperch et al. (1988).

D'autre part, dans l'article sur Louchadière de nouvelles datations par K-Ar sur Olby et Laschamp sont présentées. Elles suggèrent un âge légèrement plus jeune pour la coulée d'Olby que pour celle du Laschamp. Jusqu'ici les données radiométriques (Gillot, 1979 ; Guérin, 1983) suggéraient toutes l'inverse, à savoir un âge plus ancien pour la coulée d'Olby que pour la coulée de Laschamp. Au vu des résultats paléomagnétiques obtenus sur ces deux unités volcaniques qui montrent qu'elles ont toutes deux enregistré la même direction de champ et la même paléointensité, j'interprète ces nouvelles datations comme étant la démonstration que ces deux coulées sont contemporaines et que l'incertitude sur les âges obtenus ne permettent pas de séparer l'excursion du Laschamp en deux épisodes distincts (Guérin, 1983).

La meilleure confirmation de l'origine géomagnétique de l'excursion du Laschamp, acquise à ce jour, est présentée dans ce mémoire. J'ai eu l'occasion de participer aux déterminations de paléointensités que M. Marshall a effectuées au laboratoire, sur des coulées Pleistocène d'Islande, ayant enregistré une direction purement intermédiaire du champ (Kristjansson, Gudmunsson, 1980). Les résultats obtenus sont présentés dans un article situé en annexe 1, ils indiquent une paléointensité proche de 4 μT, confirmée par le travail mené sur les mêmes coulées par l'équipe de Corvallis (Levi.et al., 1987). Des datations par K-Ar, effectuées par R.A. Duncan (Corvallis) et P.Y. Gillot

(CFR) indiquent un âge proche de 40-50 000 ans pour ces coulées islandaises, montrant quelles sont contemporaines de celles d'Olby-Laschamp et Louchadière.

L'excursion du Laschamp est donc maintenant bien décrite du point de vue direction et intensité du champ sur deux sites distincts et son âge le plus probable est compris entre 45 et 50 000 ans. Son caractère global ou local (Europe ou Atlantique Nord) reste toutefois à définir.

Plusieurs autres excursions ont été proposées dans la période de Brunhes. Leur distinction avec un renversement complet de polarité, de très courte durée, n'est pas toujours aisée, particulièrement lorsque aucune donnée d'intensité n'est disponible. Ainsi récemment Champion et al. (1988) ont suggéré l'existence de 8 subchrons dans la période de Brunhes (Figure II. 1.), et deux dans le Matuyama supérieur. Si pour certains d'entre eux, comme le Blake, les enregistrements disponibles sont suffisamment détaillés pour les associer à des renversements complets (Verosub, 1982 ; Creer et al., 1980 ; Tucholka et al., 1987), il me parait clair que les données obtenues sur d'autres (notamment le Laschamp ou le Cobb Mountain (Voir 3e partie)) suggèrent plutôt qu'il s'agit uniquement d'excursions.

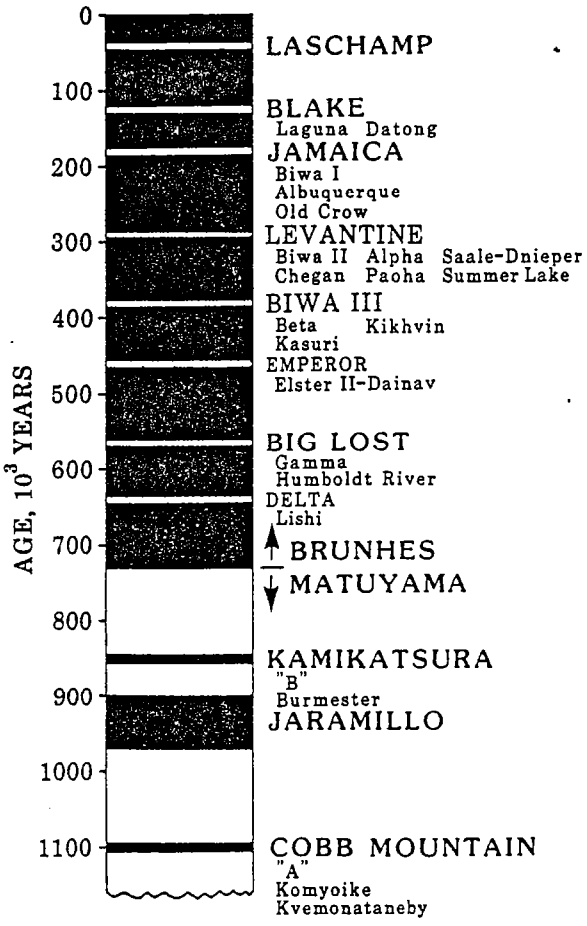

Figure II.1. Position des renversements de polarité proposés dans la période de Brunhes et du Matuyama supérieur (d'après Champion et al., 1988)

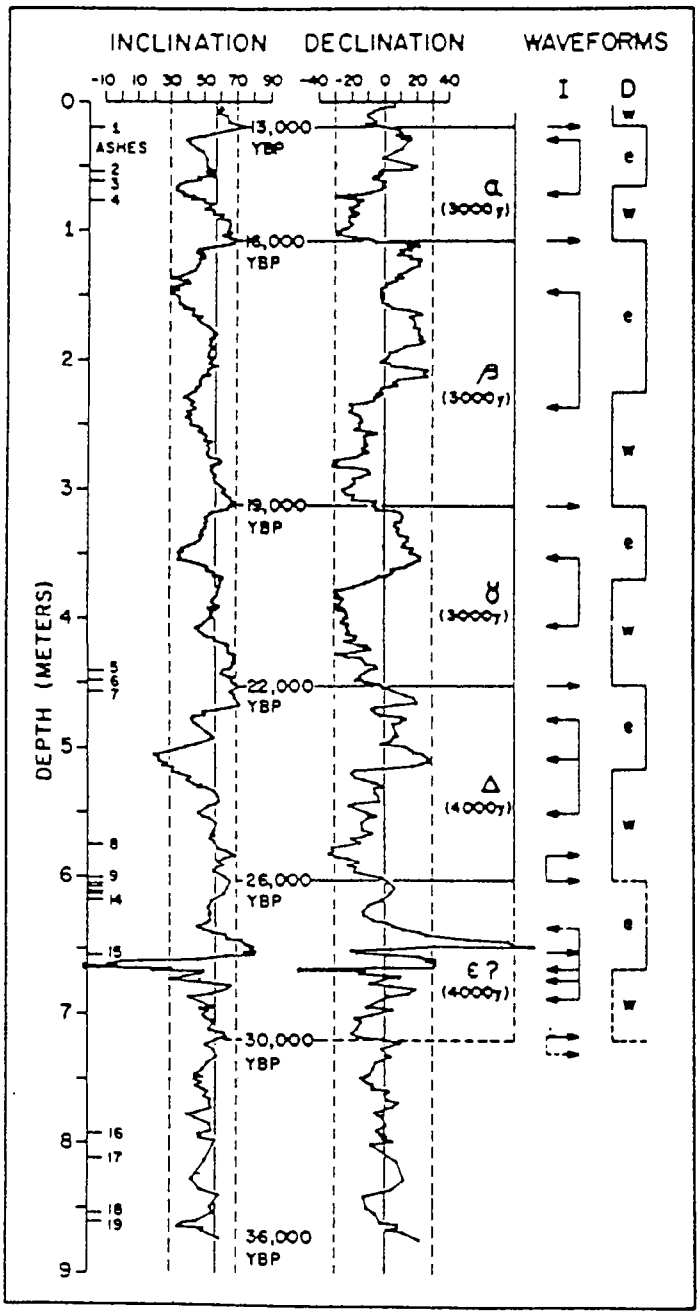

Figure II.2. Variation séculaire enregistrée au Mono Lake, avant et après l'excursion proprement dite, notée ε (d'après Lund et al., 1988).

2) Interprétation des excursions du champ magnétique.

Trois hypothèses sont généralement avancées pour expliquer les excursions du champ (Merrill et Mc Elhinny, 1983, Coe et al., 1984).

1- Une variation importante de la direction dipolaire

2- Une croissance de l'intensité des sources non-dipolaires

3- Une décroissance de l'intensité du champ dipôle, conduisant à une domination des termes non-dipolaires sur une large partie du globe (ou sur tout le globe).

Dans le cas où l'hypothèse 1 ou 2 serait vérifiée, les excursions seraient fortement liées à la variation séculaire du champ. Par contre la 3e hypothèse implique un comportement similaire du champ durant une excursion et la première phase d'un renversement de polarité, caractérisée par une diminution de l'intensité du dipôle. Dans ce cas les excursions pourraient être interprétées comme des renversements ayant échoué (Cox et al., 1975 ; Harrison, 1980 ; Hoffman, 1981 ; Roperch et Chauvin, 1987)

L'hypothèse 1 est sans doute la moins probable. Aucune évidence n'existe dans la littérature en faveur de large écarts du dipôle par rapport à l'axe de rotation, ce qui serait bien sur un phénomène global et donc devrait être largement observé.

Une augmentation d'intensité des sources non-dipolaires, sans diminution significative de l'intensité du dipôle impliquerait que les excursions soient caractérisées aussi bien par des faibles et des fortes intensités. Or, à ma connaissance, la totalité des données de paleointensité acquises sur des laves ayant enregistré une excursion du champ, indique une baisse très importante de l'intensité (cf Roperch et al., 1988, Marshall et al., 1988, Coe, 1978). La seule exception semble être les données du lake Mungo (Barbetti et McElhinny, 1976). Cependant il apparait peu probable que ces résultats correspondent au réel comportement du champ géomagnétique (Roperch et al.,1988). De plus Harrisson (1980), a indiqué que les PGVs de faible latitude, observés sur des coulées d' Islande, qu'ils soient ou non associés à des renversements connus, ont été obtenus sur des coulées dont l'intensité d'aimantation est significativement plus faible que celle des coulées à PGVs de haute latitude. Ceci suggère également un champ de plus faible intensité durant les excursions. Une conclusion similaire est obtenue si l'on examine les enregistrements sédimentaire les plus détaillés, comme par exemple l'excursion du Mono Lake (Denham et Cox, 1971, Liddicoat et Coe, 1979). Il ne semble donc pas y avoir beaucoup d'arguments en faveur de la seconde hypothèse.

On doit cependant noter, que de nouvelles données, acquises récemment suggèrent un lien étroit entre la variation séculaire et les excursions

En effet, une étude des sédiments du Mono Lake (Lund et al., 1988) portant sur les strates situées au-dessus et sous l'excursion proprement dite, semble indiquer, d'une

part un comportement différent du champ avant et après l'excursion, d'autre part, après l'excursion proprement dite, on observe la répétition à quatre reprises (sur une période de 15 000 ans) de mouvements particuliers en déclinaison et inclinaison, analogues à ceux caractéristiques de l'excursion, dont l'amplitude diminue dans le temps (Figure II. 2)

L'élément le plus significatif en faveur de l'interprétation des excursions comme une tentative de renversement qui a échouée est celle de la baisse apparante de l'intensité du moment dipolaire dans la période 15 000-50 000 ans (Merrill et McElhinny, 1983, Salis, 1987). Or c'est dans cette même tranche d'âge que quelques unes des excursions les plus détaillées (Mono Lake, Summer lake, Laschamp) sont décrites. De plus des intensités aussi faibles que 8 et 4 μT (obtenues pour le Laschamp) militent en faveur d'une baisse de l'intensité du champ dipolaire.

Les analyses les plus récentes de l'échelle des polarités ont montré qu'il n'y a pas d'arguments pour rejeter l'hypothèse selon laquelle la fréquence des inversions suivrait une loi de Poisson (McFadden et Merrill, 1984), ce qui signifie que les renversements de courte durée devraient être nombreux (Cox, 1968)(voir troisième partie). La fréquence des inversions dans le signal paléomagnétique (cf Harrisson, 1980, Kristjansson et McDougall, 1984, Kristjansson, 1985) serait alors aussi un argument en faveur de leur interprétation comme des tentatives de renversements ayant échouée.

PALEOINTENSITY OF THE EARTH'S MAGNETIC FIELD AND K-AR DATING OF THE LOUCHADIERE VOLCANIC FLOW (CENTRAL FRANCE). NEW EVIDENCE FOR THE LASCHAMP EXCURSION.

A. Chauvin[1], R.A. Duncan[2], N. Bonhommet[1] and S. Levi[2]

1) Laboratoire de Géophysique Interne, CAESS-CNRS, Université de Rennes I, 35042 Rennes, France.

2) College of Oceanography, Oregon State University, Corvallis, Oregon 97331, USA.

submitted to Geophysical Research Letter

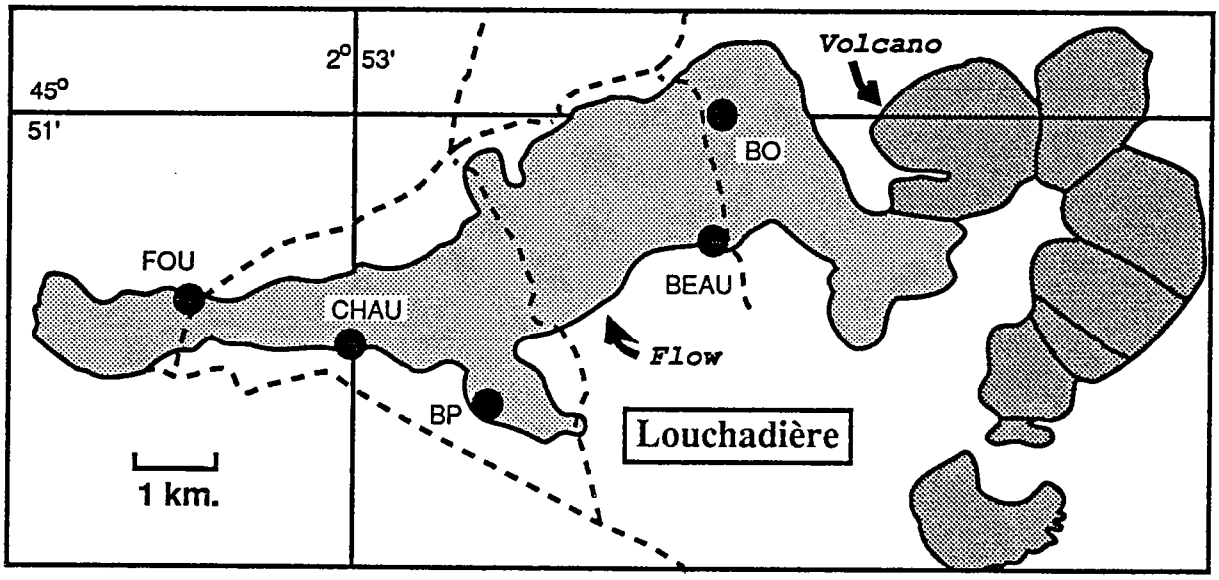

Fig. 1. Location map and sampling sites (BO, BEAU, FOU, BP and CHAU) of the Louchadière flow, Chaîne des Puys, France.

Abstract: We report paleointensity results of the Earth's magnetic field from an upper Pleistocene lava flow (Louchadière, Central France), which recorded an intermediate paleomagnetic direction. New K-Ar datings confirm that this flow is contemporaneous with the Laschamp and Olby flows, and that this excursion occured around 45 Ka. ago. Using the Thellier double heating method, reliable paleointensities have been obtained for ten samples from three different sites, providing an average field strength of 13 μT. This low value and previous results of the Laschamp excursion from France and Iceland confirm that the Earth's magnetic field was in an intermediate state during the Laschamp excursion.

Introduction

Analyses of the magnetic polarity time scale indicate that reversals are essentially Poisson distributed [McFadden and Merrill, 1984] as first suggested by Cox [1968]. This implies that many additional short-lived polarity subchrons (or excursions) might exist in the geological record. The Bruhnes chron is an apparent long period of normal polarity in which several excursions or short reversals have been reported [Champion et al., 1988].

Interest in upper Pleistocene excursions lies in the fact that they should be more easily identified at different sites around the world, providing an opportunity for studying the global morphology of the geomagnetic field during such magnetic disturbances. In addition, geomagnetic excursions can be valuable for stratigraphic correlations.

The Laschamp excursion was the first event identified in the Bruhnes period [Bonhommet and Babkine, 1967], and it was originally discovered in two volcanic flows of Laschamp and Olby (Chaîne des Puys, Central France). Because these two lava flows recorded an almost reversed direction, a full polarity reversal was considered and detailed paleomagnetic and radiometric studies were conducted on these two volcanic units. Recently, a paleointensity study has shown that the strength of the Earth's magnetic field was about 8μT during the Laschamp event [Roperch et al., 1988]. This result indicates that the field was in an intermediate state and that the Laschamp should be more properly classified as a geomagnetic excursion.

Some other transitional directions were also found in the same volcanic province, notably the one recorded at several sites of the Louchadière flow [Bonhommet, 1972]. Previous thermoluminescence dating of this flow are in the same range than those from the Laschamp flow [Guerin, 1983].

In this paper, we report a detailed paleomagnetic investigation and paleointensity determinations from the Louchadière flow. New K-Ar ($^{40}Ar/^{39}Ar$ *are being attempted*) datings show that this volcanic unit is contemporaneous with the Laschamp event.

Sampling and Paleomagnetic method

A total of 41 cores were drilled at five sites of the Louchadière Flow (BP: Beauloup, BO: le Bouchet, FOU: Fougères, BEAU: Beauregard and CHAU: Chausselles), separated by at least several kilometers from one another (Fig 1). Two sites (BP and CHAU) were situated in non-oxidized part of the

Table 1 : n/N: number of samples used in the mean calculation/ total number of collected samples; D, I: mean declination and inclination per site; k: precision paramater of Fisher, α95: 95% confidence cone about the mean direction; Lat, Long: latitude and longitude of the Virtual Geomagnetic Pole; Mean: average values for all 5 sites.

Sites	n/N	D°	I°	k	α95	Lat	Long
Fou	6/10	119.0	62.8	130	5.9	15.0	43.4
Beau	8/11	123.1	59.3	84	6.1	9.9	43.5
Chau	5/6	102.3	62.3	107	7.4	22.8	53.0
BP	6/8	109.8	48.6	75	7.8	8.5	58.8
BO	6/6	117.0	57.2	237	4.4	10.9	48.7
Mean	5	114.1	58.2	130	6.7	13.2	49.8

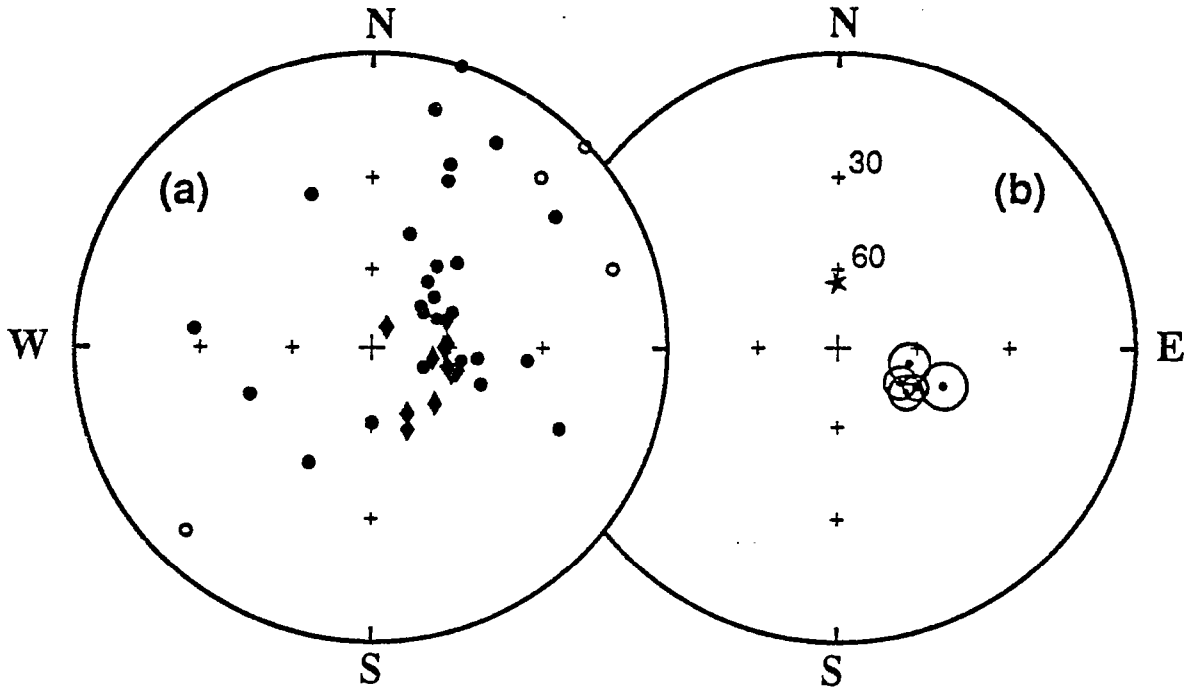

Fig. 2. a) Stereographic projections of NRM directions of all samples collected on the Louchadière flow. Solid symbols (open symbols) are on the lower (upper) hemisphere.
The star represents the direction of the axial dipole field. Diamonds are the directions of the samples selected for the paleointensity determinations.
b) Mean direction per sites and α95 confidence cones, after af and thermal cleanings.

flow, while the other three comprised more oxidized rock and scoria. Small areas at two sites (FOU and BEAU) were clearly affected by lightning showing significant deviations of the magnetic compass.

Paleomagnetic measurements and progressive demagnetizations by alternating fields (AF) were performed with Schonstedt equipment. Thermomagnetic experiments were done, in vacuum and in air, using a continuously recording Curie balance, in fields between 0.1 and 0.3 T. Paleointensity determinations were done by the original version of the Thellier and Thellier [1959] stepwise double heating method. During each heating and cooling cycle performed in vacuum (10^{-2} Torrs), the laboratory field was applied, and its direction was reversed between the two heatings at each temperature step.

Paleomagnetic results

Directions

Progressive AF demagnetization of the Natural Remanent Magnetizations (NRM) indicated two kinds of overprints: (1) a viscous component (VRM) in the direction of the present day field and (2) a secondary component with shallow inclinations and scattered declinations for samples at the edges of the areas affected by lightning. However, several samples have NRM directions close to the characteristic direction (Fig.2).

Samples carrying a viscous component have NRM intensities typically between 1 to 5 Am^{-1} and are mostly from sites CHAU and BP. Samples affected by lightning have much higher NRM intensities (up to $30Am^{-1}$). Samples for which the strong magnetic overprint was not completely removed during AF demagnetization were omitted in calculating the characteristic mean directions per site.

No classical thermal demagnetization was done, but characteristic directions were determined in the course of the paleointensity experiments. Samples for which a possible orientation error was noted during sampling, were also rejected for the computation of the mean direction. Average direction of the characteristic magnetization per site are reported in Table 1 and Figure 2b. The mean direction of the flow (D= 114°.1, I= 58°.2, VGP Latitude= 13°.2) shows a large departure (42°) from the axial dipole field. This is clearly an intermediate direction, out of the range of the normal secular variation.

Paleointensity

Eleven samples from three sites (FOU, BEAU and BO) were used, for paleointensity experiments by the Thellier method. They were selected on the basis of having minimum overprint (Fig.2a), high Curie points, and good reversibility between heating and cooling thermomagnetic behavior. Strong field thermomagnetic experiments on samples from sites BP and CHAU indicated low Curie temperatures due to the relatively low oxidation state of the Ti-rich titanomagnetites. Because this type of mineralogy often led to mineralogical changes during heating, no samples from these two sites were selected. During the Thellier experiment, the samples were treated in various applied fields: 10, 15 and 20 μT. Numerous PTRM checks were performed in order to test the stability of TRM acquisition during the heating [Prévot et al., 1985].

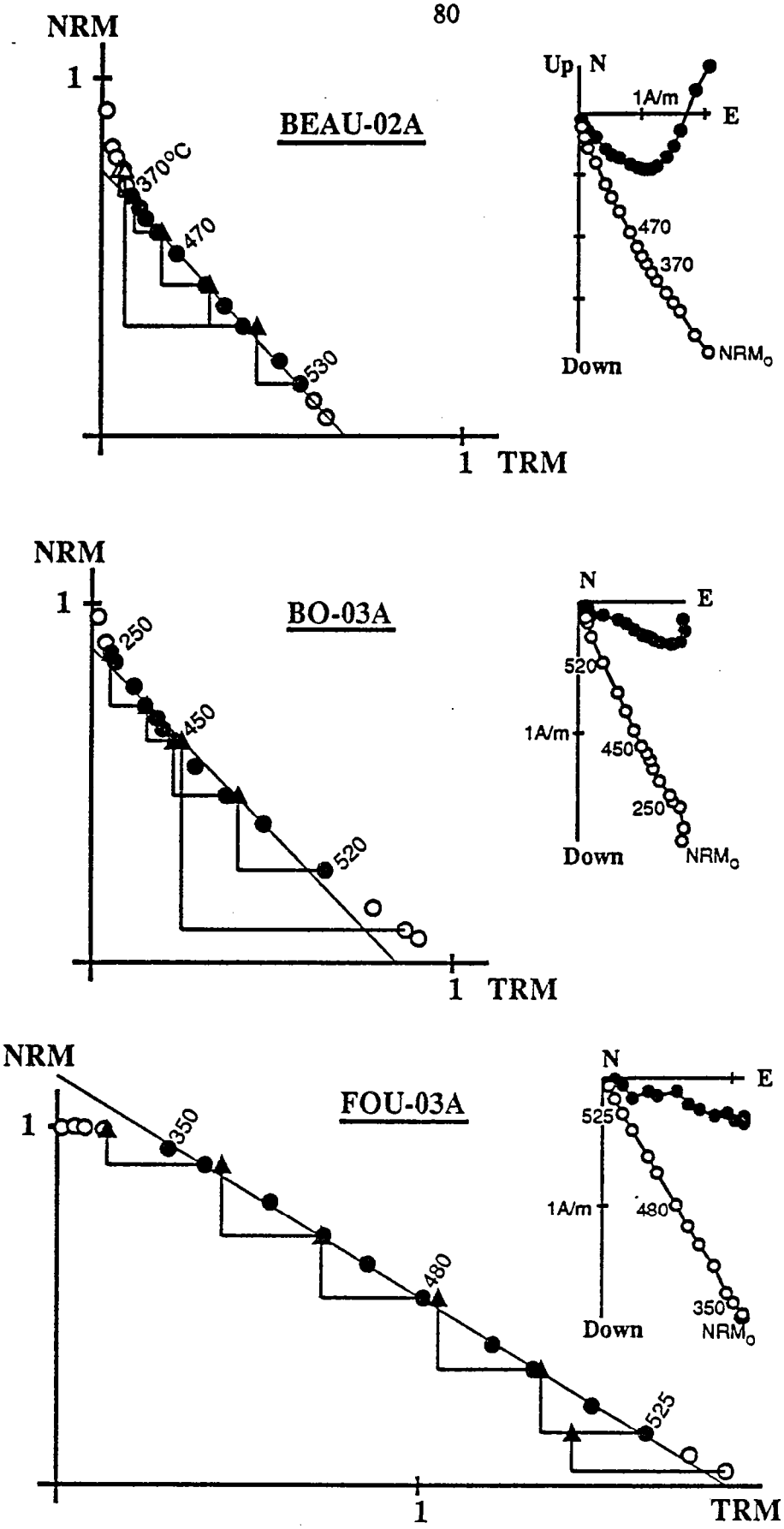

Fig. 3. Examples of reliable paleointensity determinations (NRM-TRM diagrams), for 3 samples from the sites BEAU, BO, and FOU. Black dots are used to calculate the slope; triangles represent PTRM checks.
The associated orthogonal vector plots of the thermal demagnetization of the NRM are shown in geographical (in situ) coordinates on the right of each NRM-TRM plot.
Temperature steps are indicated in C.

Among the eleven selected samples, only one did not provide a paleointensity result because a drastic decrease in the capacity of TRM acquisition at temperatures above 410°C. Table 2 summarizes the paleointensity results. From each site, one example of NRM-TRM diagram and evolution of the NRM vector during the heating are shown in Figure 3. Although cores with large overprints were avoided, the samples selected for paleointensity measurements were not completely free from small secondary VRM components. However, these secondary magnetizations were commonly removed at temperature between 200 and 350°C.

Except of one sample (Beau06), the NRM directions in the temperature interval used for paleointensity determinations, are close to the characteristic direction of the flow. The exception is due to inaccurate orientation of a broken core; we decided to use this core because it had fairly good magnetic characteristics for paleointensity; however, the direction was not used in computing the mean direction of the site.

At least 9 to 10 steps, and a large fraction of the NRM were used to determine the paleointensity. The quality factor q and the standard error of single determination were calculated following the statistical method developed by Coe et al. [1978]. The weighted average paleointensity of the flow was obtained using the weighting factor proposed by Prévot et al. [1985]. The maximum error that CRM acquisition might have caused, in percent of the laboratory field is indicated by the index R (Table 2), as defined by Coe et al. [1984]. Over our data set, this index takes low value, typically lower or around 10%. This is further support for the high stability of the samples.

The paleointensity results range from 11 to 15 μT, with only one determination, (sample BO 01), out of this range (22 μT). The quality factor of this determination is not high, so its contribution to the weighted mean is not very important. The unweighted mean intensity of the flow is 13.9 μT, and the weighted mean, that is considered to be the best estimate of the paleointensity of the flow [Prévot et al., 1985] is 12.9 μT. This result is one third to one quarter the strength of the present day field. The virtual dipole moment (VDM) associated to this flow is 2.2 10^{22} Am^2, which is considerably lower value than the average VDM obtained for the last 10 Ka. [McElhinny and Senanayake, 1982] or the last 5 m.y.[McFadden and McElhinny, 1982], which is about 8.7 10^{22} Am^2.

Dating

Thermoluminescence dating (TL) on plagioclases performed by Guerin [1983], on samples from sites BO and BP provided similar ages (33.8 ± 2.7 and 36.4 ± 3.1 Ka.) to those obtained by the same method on samples from the Laschamp flow: (35 ± 3.0 and 33.5 ± 5.0 Ka.) [Gillot et al., 1979].

K-Ar radiometric datings made at the Oregon State University, on samples from the site BP, suggest that the flow could be a little older, around 41.7 ± 4 Ka. This age is also very similar to those obtained on the Laschamp and Olby flows (Table3). A good consistency between these new results on Laschamp and Olby and those obtained by other authors [Gillot et al., 1979; Hall and York, 1978] is observed. Thus, significant age differences seem to occur between TL and K-Ar methods rather than between the three different volcanic units.

Table 2 : D, I: magnetic declination and inclination of the NRM left in the ∂T temperature interval; N: number of temperature steps in the ∂T interval; H_{lab}: laboratory field (in μT); J_{NRM}: initial intensity of magnetization in Am^{-1}; ∂T: interval of temperature used to calculate the paleointensity; f, g, q: NRM fraction used, gap factor and quality factor respectively [Coe et al., 1978]; r: linear correlation coefficient; R%: maximun percentage of CRM; Fe: paleointensity estimate for individual specimen in μT; sFe: standart error; Fe±s.d.: unweigted average paleointensity of the Louchadière lava flow plus or minus its standart deviation; <Fe> : weighted mean in μT. VDM: virtual dipole moment associated.

Samples	D°	I°	N	H_{lab}	J_{NRM}	∂T	f	g	q	r	R%	Fe±sFe
Beau 02a	145.0	60.0	10	10	4.4	370-530	0.700	0.868	36.4	0.998	18.6	11.0±0.2
Beau 06a	104.0	86.0	10	15	3.8	200-500	0.672	0.854	8.4	0.981	3.4	13.5±0.9
Bo 01a	110.5	57.5	9	20	1.4	350-515	0.419	0.860	7.7	0.992	11.5	22.4±1.0
Bo 02a	111.5	54.5	15	10	1.5	250-550	0.891	0.908	30.3	0.995	1.9	15.1±0.4
Bo 03a	117.0	64.0	11	15	2.0	250-520	0.697	0.860	12.1	0.989	2.6	15.5±0.8
Bo250a	123.0	53.0	11	10	2.2	350-540	0.701	0.879	28.9	0.998	10.3	11.2±0.3
Bo252a	126.5	58.0	10	10	1.2	300-510	0.533	0.860	14.9	0.996	7.9	12.1±0.4
Fou 03a	108.0	59.5	10	20	2.2	350-525	0.704	0.883	61.8	0.999	3.2	12.3±0.1
Fou 04a	113.0	63.0	10	10	1.9	300-510	0.724	0.873	36.0	0.998	3.6	12.7±0.2
Fou 05a	110.0	60.5	10	10	4.2	200-500	0.914	0.863	19.0	0.993	3.5	13.3±0.5

Mean: Fe ± s.d.= 13.9 μT± 3.3 <Fe> = 12.9 μT VDM = 2.2 10^{22} Am^2

Discussion

An other volcanic unit, in the Chaine des Puys, the Royat lava,may also be related to this excursion. The remanence direction of this flow deviates significantly beyond normal secular variation (Table 3) and paleointensity determinations performed also by the Thellier method on sediments baked by the Royat flow [Barbetti and Flude, 1979], also suggest a low field close to 15 μT. The Royat flow has been dated by TL around 40-46 Ka. [Guerin, 1983].

The global or regional extent of the Laschamp excursion is up to now not very well constrained. The only excursion recorded in lavas to be correlated to Laschamp is the one found in Iceland [Kristjansson and Gudmundsson, 1980]. Paleointensity determinations by the Thellier method have been performed by two teams and provided paleofield as low as 4.3 [Marshall et al., 1988] and 4.2 μT [Levi et al., 1988]. Radiometric datings show that these flows were erupted around 40-50 Ka., and are contemporaneous with the Laschamp excursion [Levi et al., 1988, Gillot, 1984].

A reversed direction recorded in welded tuffs in Japan [Tanaka and Tachibana, 1981], was first reported to be around 30 Ka. old, and then was correlated to the Laschamp excursion. New dating provided an age around 0.7 m.y., showing that in fact, the reversed direction was acquired during the Matuyama period (Tanaka 1988, personnal communication).

A very well defined intermediate direction (D= 101°.1, I= -36°.1) has been recently found on 63 sites in 8 distinct lava flows of the Albuquerque volcanos (New Mexico)[Geissman et al, 1988]. Preliminary K-Ar datings suggest latest Pleistocene (i.e. 20 to 100 Ka.) as the time of the extrusion. More accurate age determinations are needed in order to correlate this excursion with one of the others proposed in the Late Pleistocene.

Three situations can be visualized to explain geomagnetic excursions: (1) a dramatic change in direction of the dipole field; (2) a large increase in strength of the non-dipole sources; (3) a decrease in strength of the main dipole field inducing non-dipole domination over a large portion of the globe. The last hypothesis was recently used in order to interpret directions and paleointensities obtained on the Laschamp and Olby flows [Roperch et al., 1988]. For example, a dipole of only one fourth its present value, with non-dipole fields of the same order as the present day non dipole field can produce regional intermediate directions. We may speculate that such a decrease in the dipole field might have been a first step in a polarity attempt which then aborted. This interpretation is supported by the fact that all reliable paleointensities obtained, for the moment, during the period 20-50 Ka., in the Chaîne des Puys [Salis, 1987] and other sites around the world [McElhinny and Senanayake, 1982] are systematically lower that the average archeomagnetic field strength.

Thus, intermediate directions may not be expected necessarily everywhere, but the decrease in the intensity of the dipole would have been a worldwide phenomenon. The absence of the Laschamp excursion from sedimentary sections spanning the appropriate time interval, such as Lac du Bouchet in Central France [Creer, 1988] might indicate that the sedimentation process is discontinuous or that this sediment was not suitable in recording short geomagnetic event associated to low field intensity, showing that it cannot provide a detailed and accurate record of the past geomagnetic field behavior.

Table 3 : D,I : average declinations and inclinations per site; Lat VGP: latitude of the VGP associated to the mean direction; <Fe> weighted average paleointensity of the site. Ages are indicated in thousands years. Error estimates from Gillot (1984, 1979) are 2 s.d., while those from Hall and York are 1 s.d..

Flows	D°	I°	Lat VGP	<Fe> µT	Dating Method: TL	error	K-Ar	error	$^{40}Ar/^{39}Ar$	error
Laschamp	241.0	-66.0	-49.0	7.7#	35.0+	3.0	43.0+	5.0		
					33.5+	5.0	49.0	-		
Olby	231.0	-68.0	-56.0	7.7#	38.0+	6.0	50.0+	7.5		
					44.1+	6.5	38.0	-		
Laschamp + Olby							45.4§	2.5	47.4§	1.9
Royat	284.7	68.2	42.1	15.0◊	40.6•	3.1				
					43.5•	4.1				
Louchadière	114.1	58.2	13.2	12.9	33.8•	2.7	41.7	4.0		
					36.4•	3.1		-		
Skalamaelifell	265.0	-22.0	-12.0	4.3Δ			41.0*	5.0		
							50.0	13.0		

Δ: Marshall et al., 1988; #: Roperch et al., 1988; +: Gillot et al.1979;•: Guerin, 1983; ◊: Barbetti and Flude, 1979; §: Hall and York, 1978;*: Gillot, 1984

References

Barbetti, M. and K. Flude, Palaeomagnetic field strengths from sediments baked by lava flows of the Chaîne des Puys, France, Nature, 278, 153-156, 1979.

Bonhommet, N., Sur la direction d'aimantation des laves de la Chaîne des Puys, et le comportement du champ terrestre en France au cours de l'évènement du Laschamp. Thèse, Université Louis Pasteur de Strasbourg, 1972.

Bonhommet, N. and J; Babkine, Sur la présence de directions inversées dans la Chaîne des Puys, C. R. Acad. Sci. Paris, 264, 92-94, 1967.

Champion, D.E., M.A., Lanphere and M.A., Kuntz, Evidence for a new geomagnetic reversal from Lava flows in Indaho: Discussion of short polarity reversals in the Brunhes and late Matuyama polarity chrons, J. Geophys. Res., 93, 11667-11680, 1988.

Coe, R.S., S. Gromme and E.A. Mankinen, Geomagnetic paleointensities from radiocarbon dated lava flows on Hawaii and the question of the pacific non-dipole low, J. Geophys. Res., 83, 1740-1756, 1978.

Coe, R.S., S. Gromme and E.A. Mankinen, Geomagnetic paleointensities from excursion sequences in lavas on Oahu, Hawaii, J. Geophys. Res., 89, 1059-1069, 1984.

Cox, A., Lenghts of geomagnetic polarity intervals, J. Geophys. Res., 73, 3247, 1968.

Creer, KM Communication Nato Meeting Adv. Study. Inst. on Geomag. and Paleomag., Newcastle, 1988

Gillot, P.Y., Datation par la méthode du Potassium-Argon des roches volcaniques récentes (Pleistocène et Holocène). Contribution à l'étude chronostratigraphique et magnétique des provinces volcaniques de Camyanie, des Iles Eoliennes, de Pantelleria (Italie du Sud) et de la Réunion (Océan Indien), Thèse, Paris-Orsay, 225p, 1984..

Gillot, P.Y., J. Labeyrie, C. Laj, G. Valladas, G. Guerin, G. Poupeau and G. Delibrias, Age of the Laschamp paleomagnetic excursion revisited, Earth Planet. Sci. Lett., 42, 444-450, 1979.

Geissman, J.W., S.S. Harlan, B. Turrin and L.D. McFadden, Bruhnes chron geomagnetic excursion recorded during the latest Pleistocene, Albuquerque volcanos, Albuquerque Basin, New Mexico, USA, NATO, Adv. Study. Inst. on Geomag. and Paleomag., New Castle, 1988.

Guerin, G., La thermoluminescence des plagioclases. Méthode de datation du volcanisme. Applications au domaine volcanique français: Chaîne des Puys, Mont Dore et Cezallier, Bas Vivarais, Thèse, Paris, 1983.

Hall, C.M. and D. York, K-Ar and 40Ar/39Ar age of the Laschamp geomagnetic polarity reversal, Nature, 274, 462-464, 1978.

Kristjansson, L. and A. Gudmundsson, Geomagnetic excursion in late-glacial basalts outcrops in south-western Iceland, Geophys. Res. Lett., 7, 337-340, 1980.

Levi, S., H. Audusson, R.A. Duncan and L. Kristjansson, The geomagnetic excursion of Skalamaelifell Iceland: additional evidence for unstable geomagnetic behavior circa 40 Ka ago, EOS, Trans. Amer. Geophys. Union, 68, 1249, 1987.

Marshall, M., A. Chauvin and N. Bonhommet, Preliminary paleointensity measurements and detailed magnetic analysis of basalts from the Skalamaelifell excursion, southwest Iceland, J. Geophys. Res., 93, 11681-11698, 1988

McElhinny, M.W. and W.E. Senanayake, Variations in the geomagnetic dipole 1: The past 50,000 years, J. Geomag. Geoelectr., 34, 39-51, 1982.

McFadden, P.L. and M.W. McElhinny, Variations of the geomagnetic dipole 2: statistical analysis of VDMs for the past 5 millions years, J. Geomag. Geoelectr., 34, 163-189, 1982.

McFadden, P.L. and R.T. Merrill, Lower mantle convection and geomagnetism, J. Geophys. Res., 89, 3354-3362, 1984.

Prévot, M., E.A. Mankinen, R.S. Coe and C.S. Gromme, The Steens Moutain (Oregon) geomagnetic polarity transition. 2 Field intensity variations and discussion of reversal models, J. Geophys. Res., 90, 10417-10448, 1985.

Roperch, P., N. Bonhommet and S. Levi, Paleointensity of the earth's magnetic field during the Laschamp excursion, and its geomagnetic implications, Earth Planet. Sci. Lett., 88, 209-219, 1988.

Salis, J.S., variation seculaire de champ magnetique terrestre- Directions et paléointensité- sur la période 7000-70000 ans BP, dans la Chaîne de Puys, Thèse, Mémoires et Documents du CAESS, Rennes, 1987.

Tanaka, H. and K. Tachibana, A geomagnetic reversal in the latest Bruhnes epoch discovered at Shibutami, Japon, J. Geomag. Geoelectr., 33, 287-292, 1981.

Thellier, E. and O. Thellier, Sur l'intensité du champ magnétique terrestre dans le passé historique et géologique, Ann. Geophys., 15, 285-376, 1959

TROISIEME PARTIE

RENVERSEMENTS DE POLARITÉ

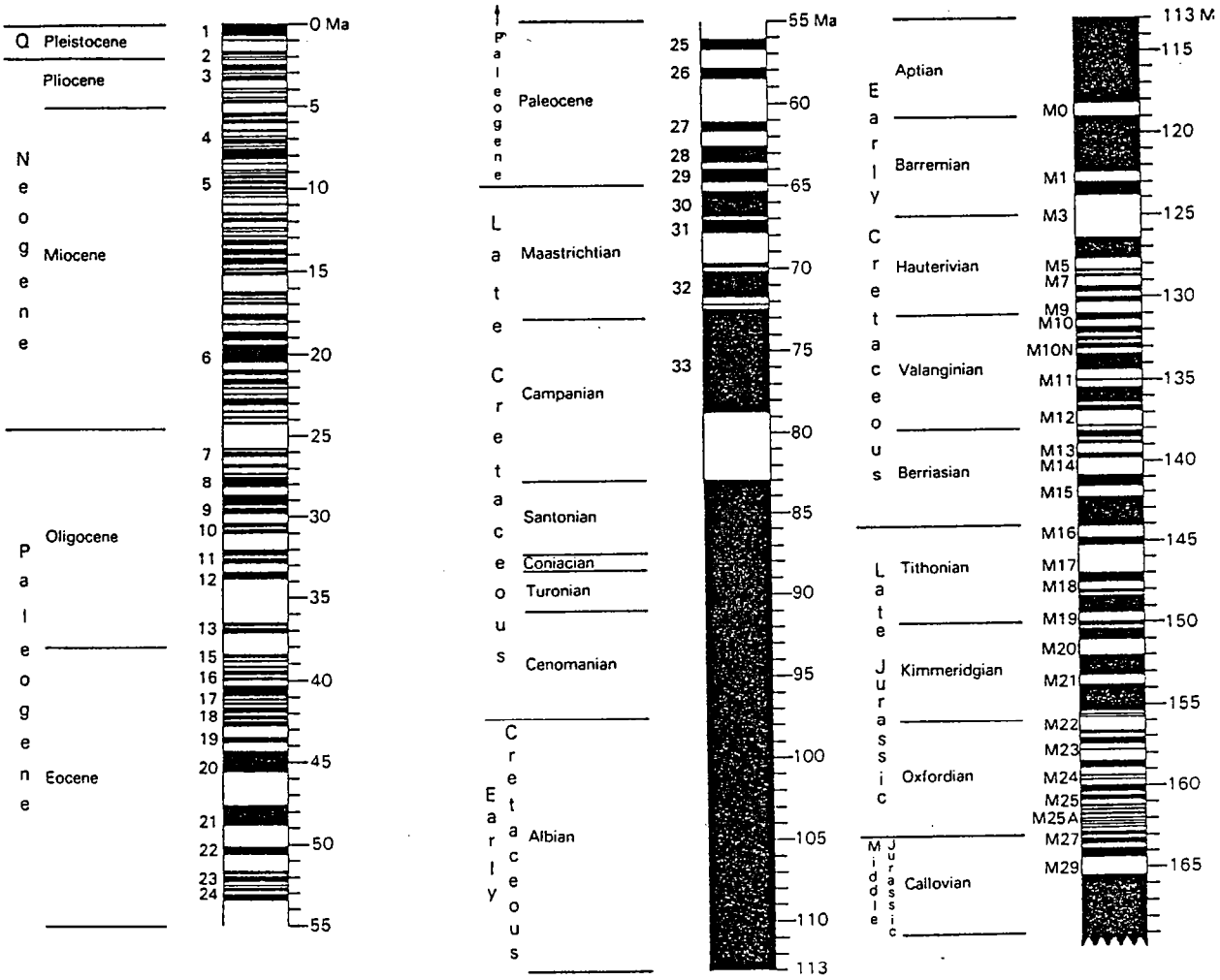

Figure III.1. Echelle de référence des inversions géomagnétiques sur les derniers 170 millions d'années (d'après Cox , Harland, 1982)

INTRODUCTION

L'analyse des inversions du champ magnétique terrestre peut se faire suivant deux approches différentes mais complémentaires.

La première approche consiste à étudier la distribution des renversements en fonction du temps.

L'établissement des premières échelles de polarité a été entrepris aux début des années 60 et a été favorisé par le développement de la méthode de datation isotopique par K-Ar qui permis pour la première fois de dater avec une bonne précision des roches volcaniques plus jeunes que 5 à 7 millions d'années.

Ainsi, en combinant des études paléomagnétiques de séquences volcaniques sur différents sites à travers le monde, avec des datations par K-Ar, une échelle des polarités sur les derniers 5 millions d'années (Ma.) a pu être rapidement proposée (Cox, 1963, 1969). Une synthèse complète des données sur la chronologie des renversements au cours des 5 derniers Ma a été établie par McDougall (1979) et Mankinen et Darlymple (1979).

L'étude des anomalies magnétiques liées à l'aimantation rémanente de la croûte océanique, à l'origine de la théorie de la tectonique des plaques a permis d'étendre l'échelle des renversements jusqu'à environ 170 Ma. Sur cet intervalle de temps, diverses échelles de polarités ont été proposées (Heirtzler et al., 1968, LaBrecque et al., 1977, Ness et al., 1980, Lowrie et Alvarez, 1981, Cox et al., 1982, Berggren, 1985). L'échelle de Cox est présentée sur la Figure III.1. Le terme de Chron est utilisé pour désigner un intervalle de temps dominé par une polarité (exemple Bruhnes, Matuyama, Gilbert), alors que les éléments de polarité opposée qui recoupent un Chron sont appelés Sub-Chron.

Au-delà de 170 Ma., l'histoire des polarités du champ magnétique reste assez mal connue (McDougall, 1985). Dans le Paléozoique supérieur, une longue période de polarité inverse nommée Kiaman, semble bien établie, entre 313 et 227 Ma. (Permo-Carbonifère) (Irving et Pullaiah, 1976). D'autre part, de nombreux renversements ont été reconnus dans le Jurassique (Cox, 1982).

1) Analyse de l'échelle des polarités

Trois aspects ont été généralement développés:

1- Existe-t'il une tendance générale dans la distribution des renversements?

2- Quelle loi statistique gouverne le processus de renversement?

3- Y a t-il une périodicité dans la fréquence des renversements?

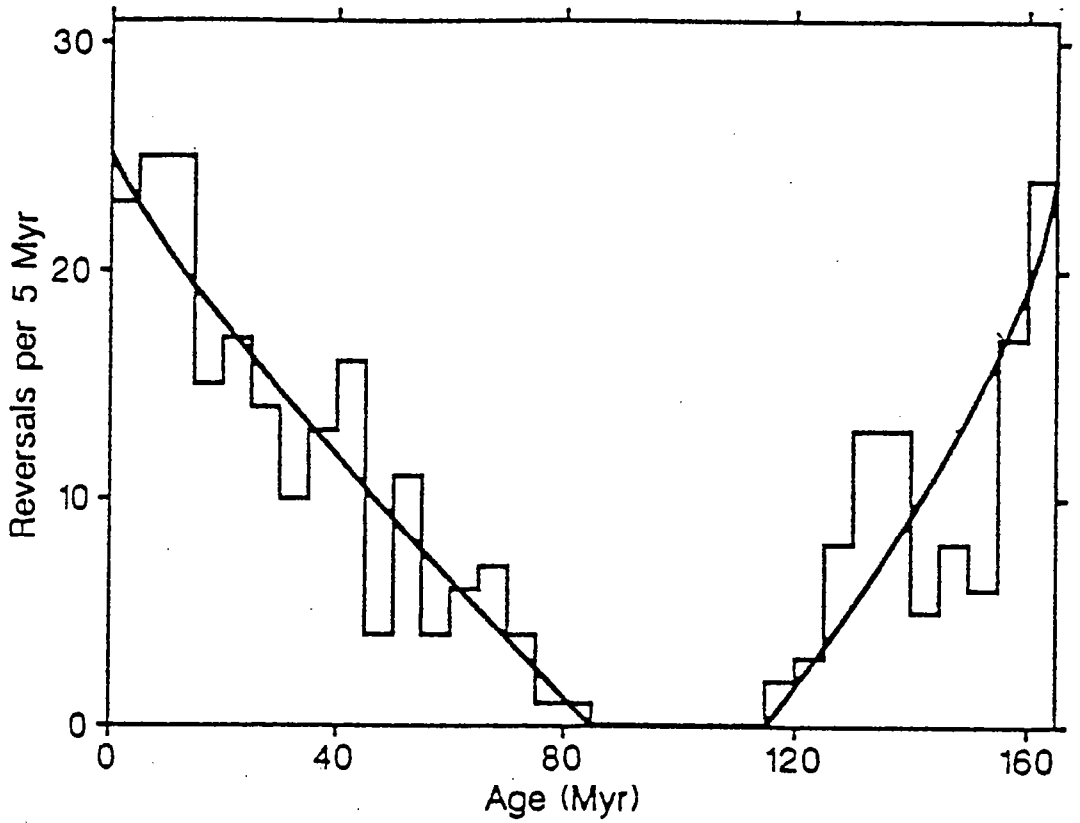

Figure III.2. Variations de longue période dans la fréquence des renversements sur les derniers 160 millions d'années, établies à partir de l'échelle de Cox, 1982 (d'après Lutz et Watson, 1988).

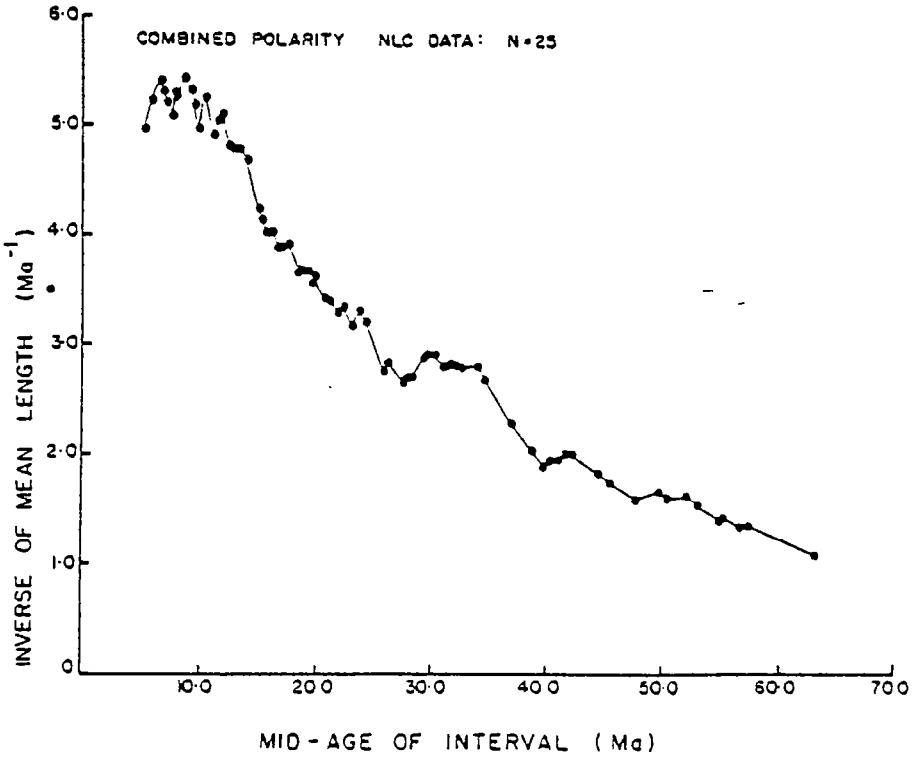

Figure III.3. Analyse de la fréquence des renversements entre le Crétacé supérieur et l'actuel par une fenêtre glissante formée de 25 intervalles de polarité (d'après McFadden et Merrill, 1984).

1- L' échelle des polarités sur les derniers 170 Ma. fait apparaître une très longue période de polarité normale au Crétacé. Du fait de son exceptionnelle durée (36 Ma.), cette longue période de polarité normale est désignée par le terme de Super-chron. De part et d'autre de ce superchron, on constate une diminution (entre 165 et 119 Ma.) et une augmentation (sur les derniers 83 Ma.) quasi monotone de la fréquence des renversements (Figures III.2. et III.3.). Cette tendance de longue période semble difficile à expliquer. McFadden et Merrill (1984) ont proposé que des différences de température à la frontière noyau-manteau, pouvant être liées à de la convection dans le manteau inférieur, pourraient expliquer cette tendance générale, et particulièrement le superchron observé au Crétacé. Ces auteurs ont également proposé une augmentation régulière dans la fréquence des renversements depuis le superchron de polarité inverse du Kiaman. Récemment une nouvelle analyse de la dérive vraie du pôle (définie comme le mouvement du manteau part rapport à l'axe de rotation de la terre) sur les derniers 200 Ma., a montré que celle-ci a été relativement rapide (5 cm par an) sauf durant la période 170-110 Ma. (Courtillot et Besse, 1987). Cette période de stabilité semble correspondre avec la diminution de la fréquence des inversions. Inversement, la dérive vraie du pôle parait plus importante lorsque la fréquence des renversements augmente (Figure III.4.).

2- Quelle loi statistique gouverne le processus de renversement?

La première analyse statistique de l'échelle des renversements fut menée par Cox (1969). Il observa que la répartition des intervalles en fonction de leur durée décrit une courbe exponentielle. Il supposa alors que les renversements sont engendrés par des instabilités distribuées de façon aléatoire dans le temps, et donc que la probabilité qu' une inversion se produise dans un quelconque intervalle de temps t+dt est une constante. Les inversions seraient donc distribuées dans le temps suivant une loi de Poisson (Cox, 1968, 1969) ce qui suggère l'existence de nombreux événements de courte durée (subchron).

L'autre alternative serait que la durée des intervalles de polarité obéisse à une loi de distribution Gamma (le paramètre de distribution k est égal à 1, dans le cas d'une loi de Poisson, et est supérieur à 1 dans le cas d'une distribution Gamma). Dans ce cas les renversements ne seraient pas indépendants, la géodynamo ayant une sorte de 'mémoire' des événements passés.

Le résultat de Cox a suscité de nombreuses controverses. Naidu (1971) a abouti à une conclusion inverse, du fait d'une apparente discontinuité dans la valeur de k aux alentours de 48 Ma. Phillips (1977) pour sa part, a constaté que le paramètre k serait égal à 1 dans le cas des polarités inverses et supérieur à 1 dans le cas des périodes de polarité normale, ceci pour les derniers 86 Ma.. En d'autre termes, les périodes de polarité normale seraient plus stables que les périodes de polarité inverse. Ce qui

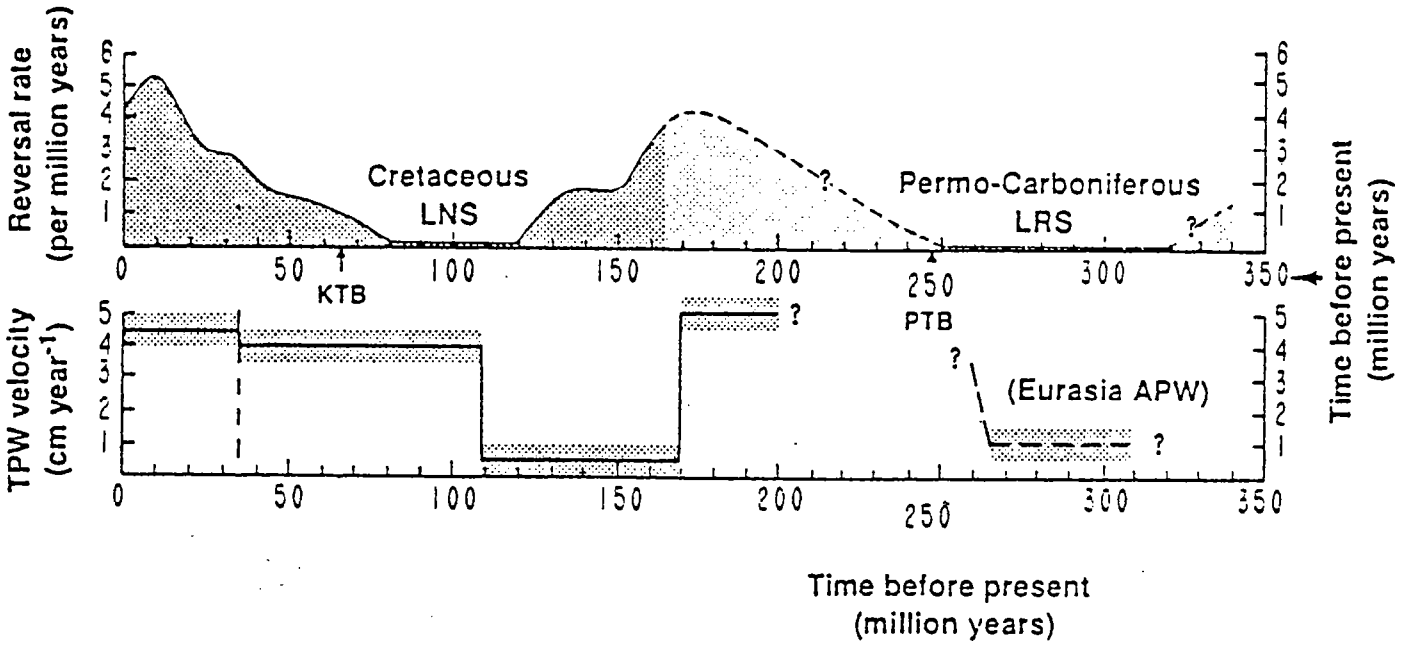

Figure III.4. Variation de la fréquence des renversements au cours des derniers 350 millions d'années, la portion de la courbe hypothétique est marquée en pointillée; dérive vraie du pôle sur la même période (en cm par an) (d'après Courtillot et Besse, 1988).

parait surprenant étant donné que la durée moyenne des intervalles de polarité est la même pour les périodes normales et inverses.

Les analyses précédentes ont été effectuées à partir de l'échelle de polarité de Heirtzler (1968). Les échelles plus récentes (LaBrecque, 1977 et Ness et al., 1980) comprennent un plus grand nombre d'intervalles de polarité courts (subchrons) que la précédente. et ont suscité de nouvelles études. En particulier, l'échelle de LaBrecque comprend 57 anomalies océaniques supplémentaires, de faible intensité. Lowrie et Kent dans leur analyse de cette échelle ont conclu que si ces anomalies correspondent bien à des renversements, alors les inversions suivent un processus de Poisson. Par contre, ils ont abouti à une conclusion inverse de celle de Phillips; à savoir qu'une forte dissymétrie entre les deux états de polarité existerait bien, mais en faveur de la polarité inverse.

McFadden et Merrill, (1984), dans une étude détaillée, utilisant l'échelle de Ness et al. (1980) ont montré que la valeur de k est très sensible au nombre d'événements de courte durée inclus dans le jeu de données. Pour eux, la dissymétrie entre les deux polarités du champ ne serait qu'un artefact. Du fait que les valeurs moyennes (μ) de la durée des intervalles de polarité sont identiques pour les périodes normales et inverse, ils conclurent à l'absence de dissymétrie entre les deux états stables du champ. L'addition des 57 intervalles courts présents dans l'échelle de LaBrecque et al., ne modifient pas cette conclusion (McFadden et Merrill, 1987). De plus McFadden et Merrill (1984) ont indiqué l'absence d'arguments permettant de rejeter l'interprétation de la distribution des renversements comme étant un processus de Poisson.

De telles analyses apportent quelques contraintes sur les différents modèles de géodynamo proposés. En particulier, McFadden et Merrill (1986) considèrent que les instabilités qui provoquent les renversements sont indépendantes du processus engendrant le champ principal. Ils ont suggéré que les inversions se produiraient durant une réorganisation du régime thermique du noyau. Ils ont ainsi proposé un modèle, spéculatif, respectant cette condition, qui suggère l'émission de panaches chauds ou froids suivant leur origine (limite noyau externe-noyau interne ou noyau externe-manteau) qui déstabiliseraient le régime thermique du noyau. Ces même auteurs ont proposé un nouveau modèle moins restrictif que le précédent, qui repose sur le couplage entre une famille de champs dipolaires et et une autre de champs quadripolaires (Merrill et McFadden; 1988).

3- Y a t-il une périodicité dans la fréquence des renversements?

Superposés à la régulière augmentation de la fréquence des renversements depuis le Crétacé, des oscillations sinusoïdales sont observées (Figure III.5.). En éliminant la tendance générale, et par méthode d'analyse du signal, différents auteurs ont proposé une périodicité dans les variations de la fréquence des de renversements. Ainsi,

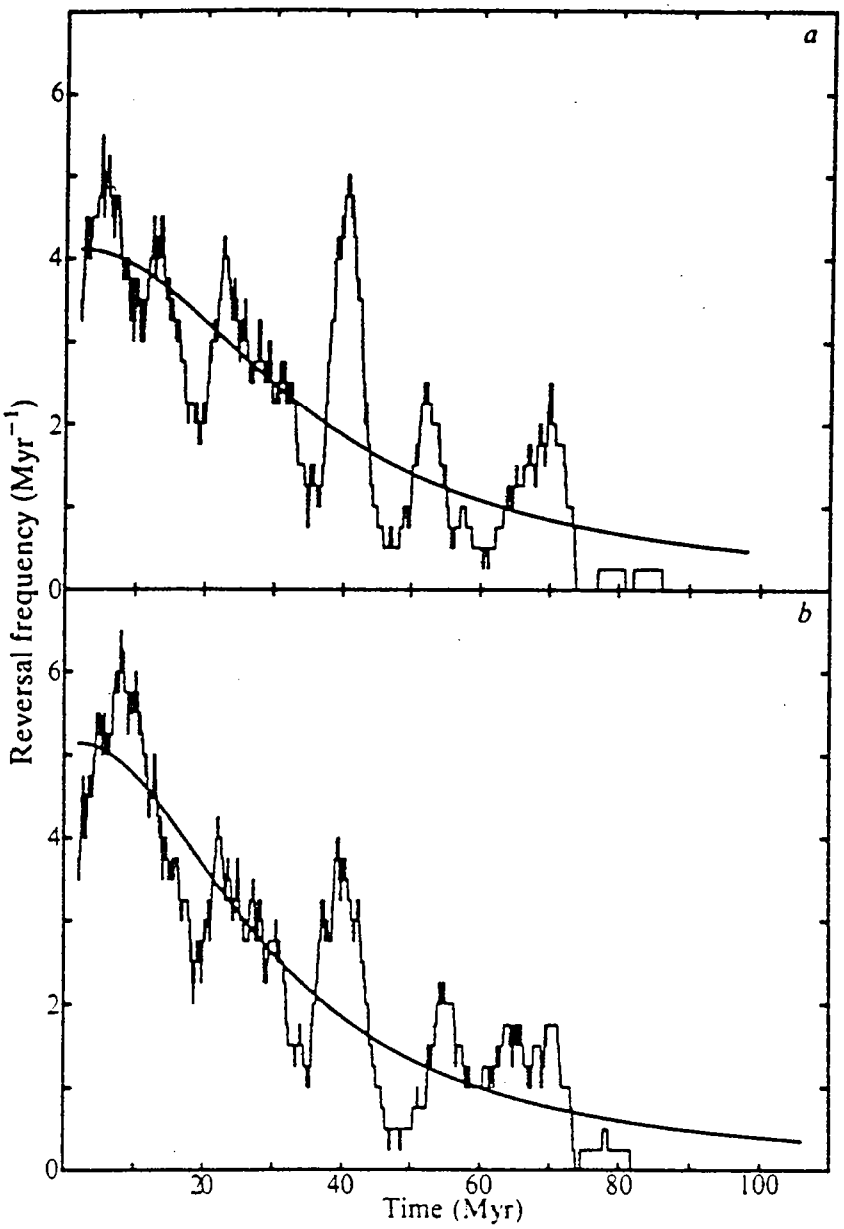

Figure III.5. Variation de la fréquences des inversions vue à travers une fenêtre glissante de 4 millions d'années à partir de 2 échelles: a) échelle de Lowrie et Alvarez, 1981, b) échelle de LaBrecque et al., 1977 (d'après Mazaud et al., 1983).

Mazaud et al. (1983), proposent une période de 15 Ma., Stothers (1986) observe des pics dans l'analyse spectrale à 132, 37 et 30 Ma.. Ces résultats sont fortement contestés par divers auteurs qui n'y voient que le résultat de l'utilisation de techniques d'analyse inadéquats (Lutz, 1985; Lutz et Watson, 1988).

2) Causes externes des renversements?

Récemment, l'hypothèse du déclenchement des inversions par des causes externes a été développée. Un lien hypothétique entre inversions, extinctions d'espèces et collisions avec des objets extraterrestres a été suggéré à partir de l'apparente périodicité de 30 Ma des renversements du champ déduite de certaines des études précédentes (Pal et Creer, 1986, Stothers, 1986). Ainsi la périodicité dans la fréquence des renversements, serait associée avec une périodicité supposée des extinctions d'espèces, qui pour certains résulteraient d'impact d'objets extraterrestres (Rampino et Stothers, 1984, Muller et Morris, 1986). Cependant, il semble que très peu d'arguments soient en faveur de cette hypothèse (Merrill et McFadden, 1988).

3) Enregistrements paléomagnétique des transitions

Une étude détaillée de l'enregistrement paléomagnétique des transitions, est une seconde approche dans l'analyse des inversions géomagnétiques.

De telles études s'appuient sur des enregistrements paléomagnétiques détaillés, provenant de roches sédimentaires, intrusives ou volcaniques qui sont difficiles à acquérir compte tenu de la brièveté des transitions de polarité .

Certaines caractéristiques du champ de transition semblent maintenant bien établie: la durée d'une inversion serait de 1000 à 10000 ans (Clement et Kent, 1984, Mankinen et al., 1985), l'intensité du champ serait réduite jusqu'à 90%, le champ serait principalement non-dipolaire. Néanmoins, d'autres propriétés du champ de transition restent spéculatives

L'article qui constitue la troisième partie de ce mémoire est consacrée à l'étude des derniers renversements de polarités enregistrés par des coulées volcaniques de l'île de Tahiti en Polynésie française.

RECORDS OF GEOMAGNETIC REVERSALS FROM VOLCANIC ISLANDS OF FRENCH POLYNESIA.
II. PALEOMAGNETIC STUDY OF A FLOW SEQUENCE (1.2-0.6 Ma) FROM THE ISLAND OF TAHITI AND DISCUSSION OF REVERSAL MODELS.

ANNICK CHAUVIN AND PIERRICK ROPERCH[1]

Laboratoire de Géophysique Interne et ORSTOM, Université de Rennes I, 35042 Rennes Cedex, France

ROBERT A. DUNCAN

College of Oceanography, Oregon State University, Corvallis 97330 Oregon, USA

submitted to Journal of Geophysical Research

Abstract:

A volcanic sequence of almost 700 meters thick has been sampled in the Punaruu valley on the island of Tahiti situated in the southern central Pacific ocean. Detailed paleomagnetic results have been obtained from 123 sites. Three reversals are recorded in this sequence. The available age determinations (K-Ar) indicate that the youngest reversal corresponds to the Matuyama-Brunhes transition while the two other transitions limit the Jaramillo normal polarity subchron. An apparent excursion R-T-R has been recovered lower in the volcanic sequence and K-Ar age determinations around 1.1 Ma. suggest that it corresponds to the Cobb Mountain event. No normal paleomagnetic directions have been found within this transition. The Matuyama-Brunhes and the lower Jaramillo transitions are defined by only a few intermediate directions while various intermediate directions are observed for the upper Jaramillo transitions and the Cobb excursion. We attribute these differences to variations in the rate of eruption of the volcanic rocks. The lower Jaramillo record is characterized by a steepening of the inclination, which might correspond only to the beginning of the reversal. This suggests a possible axisymmetric control of the field at this stage. However, in the other cases, no clear path is observed in the intermediate directions. Paleointensity determinations were attempted on 48 samples and reliable results have been obtained for 26 of them. Paleointensities for the transitional field range from 3 to 8 μT. This very low field strength was first suggested in the intensity of the natural remanent magnetization associated with intermediate directions. An analysis of the variation of the intensity of magnetization with the angular departure from the central axial field was performed together with other available data from Polynesia. Comparison of the distribution observed in Polynesia with previous studies from Iceland suggests a latitudinal dependence of the intensity of the nondipole field during stable periods as well as during transitions.

Introduction

The study of the secular variation of the Earth's magnetic field [*Le Mouel*, 1984; *Gire et al.*, 1986; *Gubbins*, 1987; *Bloxham*, 1988] has provided some insight, even if sometimes controversial, on fluid motion in the Earth's core, leading to a better understanding of the geodynamo. Paleomagnetic studies of the behavior of the geomagnetic field during polarity transitions constitute another important way to constrain the various models of the Earth's dynamo. In this paper, we will focus on the second aspect, in bringing some new data of reversals recorded by a sequence of volcanic flows from the island of Tahiti (French Polynesia).

Since the beginning of the study of reversals [*Sigurgeirsson*, 1957; *Van Zijl et al.*, 1962], a great number of paleomagnetic records of transitions have been obtained. The first major step was to recognize the non-dipole character of the transitional field [*Dagley and Lawley*, 1974; *Hillhouse and Cox*, 1976]. Because the transitional path was lying in a restricted sector of longitude, *Hillhouse and Cox* [1976] suggested that reversals recorded at one site might be controlled by a standing non-dipole field. Models with axial symmetry were then proposed by *Hoffman* [1977] and *Hoffman and Fuller* [1978]. However, evidence for non-axisymmetric components led to floodings models both north-south and east-west [*Hoffman*, 1979, 1981a]. Similar approaches, with analytical calculations of the Gauss coefficients, were proposed by *Williams and Fuller* [1981, 1988]. Such models have been under active consideration by the paleomagnetists because they have provided a guideline for the analysis and comparisons of the records of the intermediate field. However, in order to determine the morphology of the transitional field, more numerous paleomagnetic records with better resolution are required. Especially, widely spaced multiple records of individual reversals and records of successive reversals at the same site are necessary. The last polarity transitions (the Matuyama-Bruhnes, the upper and lower boundaries of the Jaramillo and Olduvai) are already the most documented; adding new records of these transitions will help to a better understanding and modelization of the behavior of the transitional field. Since *Hoffman* [1979] showed the necessity for additional data from the southern hemisphere, several records have been obtained from southern low latitudes [*Clement and Kent*, 1984; *Clement and Kent*, 1985; *Hoffman*, 1986] as well as from the northern hemisphere [*Clement and Kent*, 1986; *Liddicoat*, 1982; *Theyer et al.*, 1985; *Herrero-Bervera*, 1987; *Valet et al.*, 1988b]. However, most of these data come from sedimentary rocks and several authors [*Hoffman and Slade*, 1986; *Prévot et al.*, 1985b] have questioned the reliability of such records, particularly when they deal with low sedimentation rates. In a recent study of the Matuyama-Bruhnes reversal recorded at lake Tecopa, *Valet et al.* [1988a] have shown that a strong overprint in the following normal polarity period was not removed in a previous study done by *Hillhouse and Cox* [1976]. Because few studies have used thermal demagnetizations (Valet et al., 1988, Laj et al., 1988), to what extent the other available records are also altered is an unanswered question.

Only relative changes in paleointensity are obtained from sedimentary rocks. The variations of the magnetic properties in the sediments are generally recognized through the variations of an artificial remanence such as an isothermal or an anhysteretic, but this method also assumes that the NRM is not

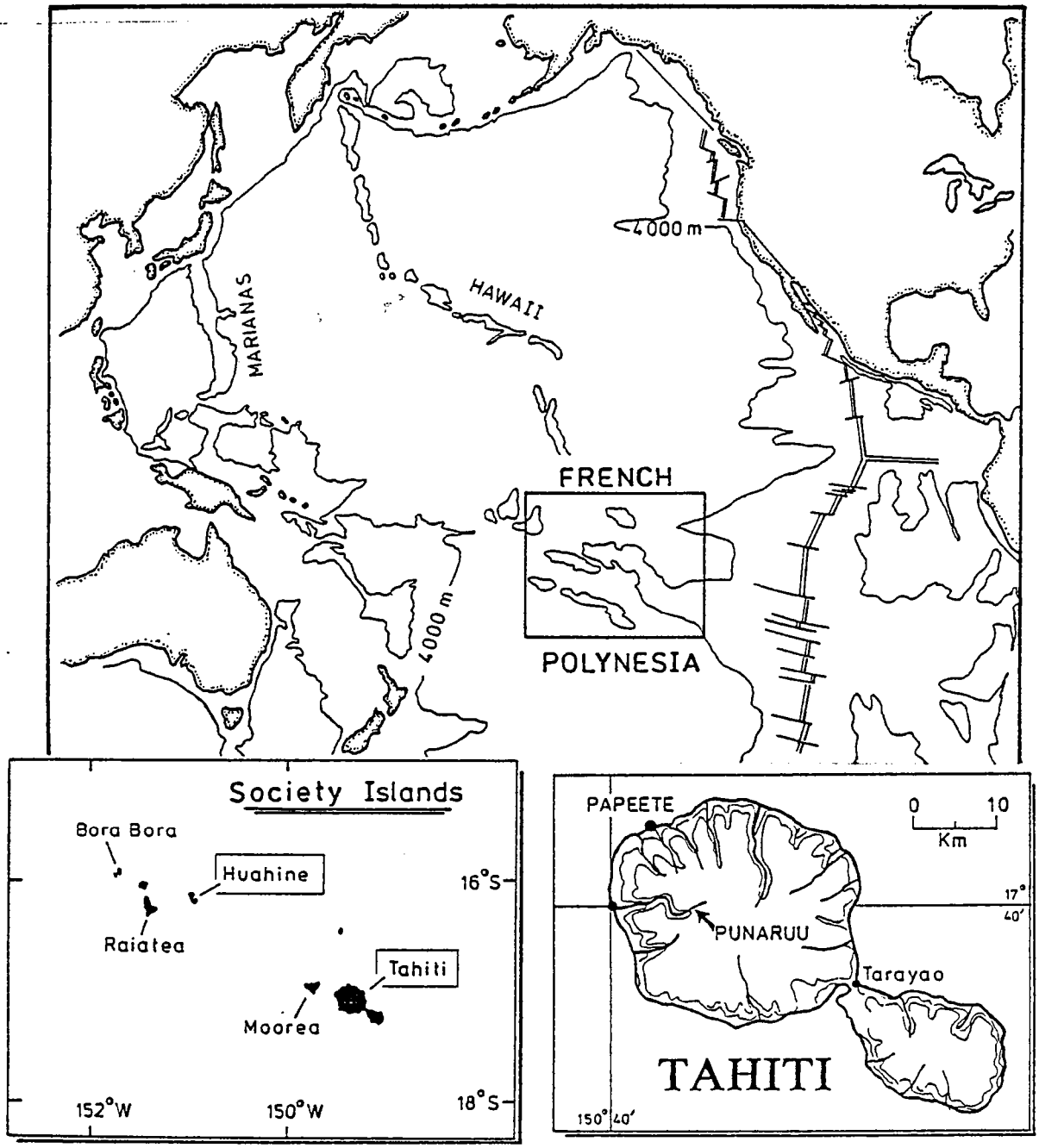

Fig. 1: A) Location of the island chains of French Polynesia and maps of the Society islands archipelago and the island of Tahiti. Hachures in the eastern Pacific encloses the present ridge configuration. Sea level is denoted by stippling and bathymetry is indicated by selected 4000 m. contours.

altered by a multicomponent magnetization. The normalization technique is also useless if geochemical alterations had occured during diagenetic processes [*Karlin and Levi*, 1985].

Most estimates of the time duration of reversals come from sedimentary sections. Because several studies show a significant decrease in intensity before any changes in directions, the estimates vary from a few Ka. (Ka=thousand years) to several Ka. depending on how the transition boundaries are defined.

While sediments provide only, in the best cases, average field directions and relative paleointensity changes, volcanic rocks generally enable a well determined paleofield direction and sometimes accurate determinations of the absolute paleointensity. However, with volcanic records of reversals, due to a poor knowledge of the rate of extrusion of the lava flows, the time resolution of the transition is generally not well established.

A common feature in all records is an important decrease of the paleointensity during transitions, but up to now most of the studies have focussed on the directional behavior during reversals rather than analyzing the field as a complete vector. When paleointensity data are added to the directional records, some unexpected characteristics of the intermediate field appear, which are not shown by directional data alone. The most complete description of the behavior of the geomagnetic field, in direction and intensity, comes from the study of the volcanic record of a Miocene age reverse to normal reversal at the Steen Mountains [*Mankinen et al.*, 1985, *Prévot et al.*, 1985a]. Very rapid field variations (as a few thousands gammas per year) have been suggested by these authors but have not yet been fully established. Apart from the large decrease in intensity during transition, which is the main characteristic, *Shaw* [1975,1977] has also suggested that occasionally, the intermediate field may reach some high values. On the other hand, high variations of the field without changes in direction were shown by *Shaw* [1977] as well as on paleointensities from the Steens Mountain [*Prévot et al.*, 1985b]. We will discuss later, that some paleointensities may not be valid due to several problems encountered in paleointensity experiments.

For all the reasons previously explained, in order to produce accurate reversal models, studies on volcanic rocks are necessary. However, it is not easy to discover a volcanic sequence that has recorded a detailed polarity reversal and generally, only partial records are found [*Bogue and Coe*, 1984].

Some islands of French Polynesia (south central Pacific ocean) provide the possibility to study the last polarity reversals. In this paper, we report paleomagnetic results obtained on a volcanic sequence almost 700 meters thick from the island of Tahiti. Within this section, four transitional zones have been found and, two of them have recorded various intermediate directions.

1 Geological setting

The Society archipelago, in the southern central Pacific ocean (Fig 1a), is composed of volcanic islands which are aligned in a direction NW-SE delineating the Pacific plate motion during the last 5 millions years [*Duncan and McDougall*, 1976]. The island of Tahiti is the largest one within Society Islands and is made of two islets (Tahiti Nui and Tahiti Iti). The Tahiti Nui volcano is a cone rising 6 000 meters high above the surrounding abyssal sea-floor, of which only one-third is subaerial. The erosion of the island has built up some radial valleys which enable the sampling of volcanic sequences. Few transitional paleomagnetic directions were first reported by one of us [*Duncan*, 1975] in the Punaruu valley, which is one of the deepest valleys of Tahiti Nui in its western part. This discovery suggested to

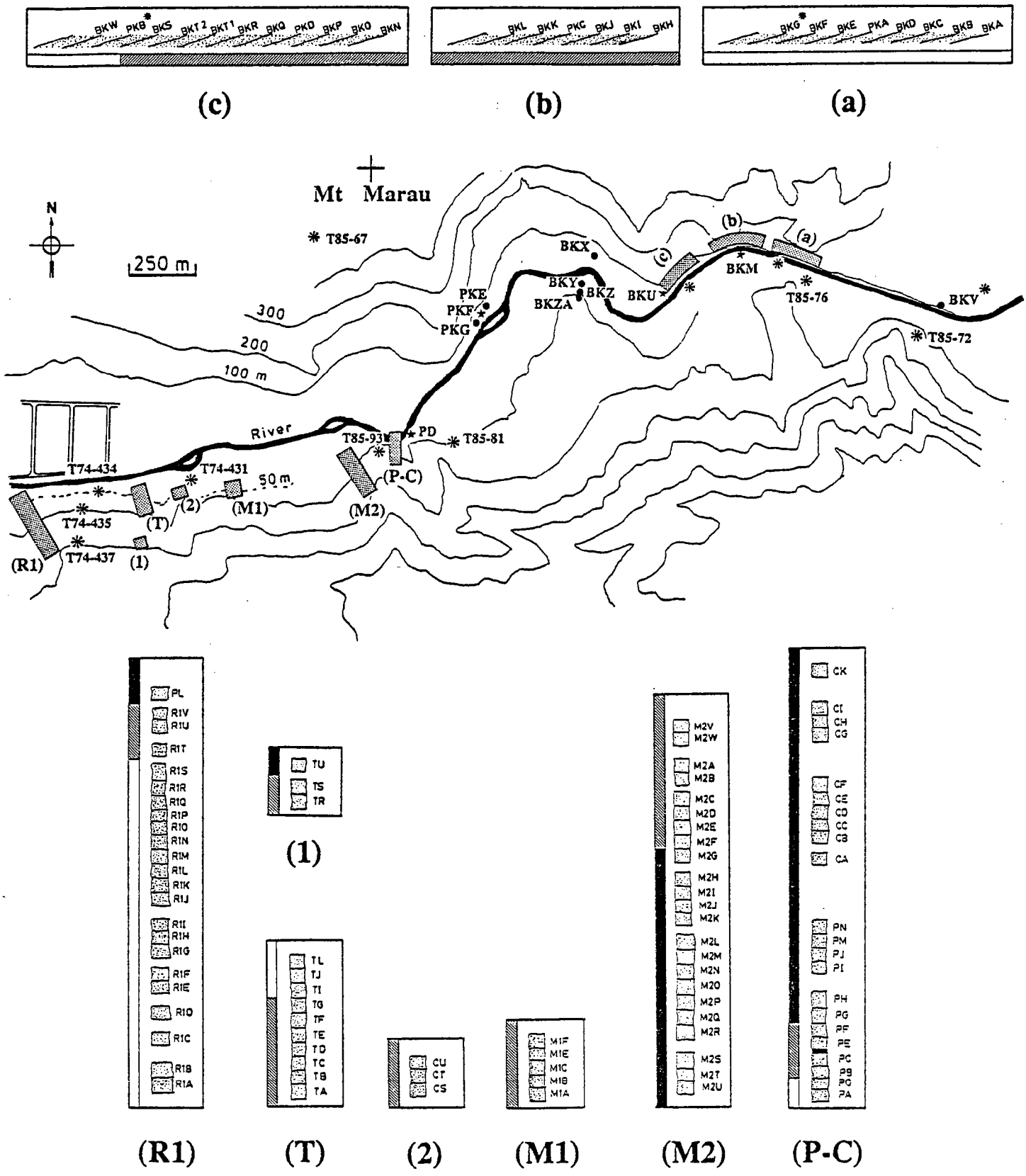

Fig. 1 B) Sampling map along the Punaru valley in the western part of the island of Tahiti. Flows are dipping toward the west. On the north side of the valley, the sampling was done along the river as indicated by the 3 sections a, b, c. Filled circles correspond to flows below (site BKV) and above sections a, b, c. Stars are the sampling sites of the dykes. On the southern border of the river, numerous cross sections of the hillside have been done and are indicated by letters referenced in the text. The magnetic polarity has been shown within each section. Gaps in the sampling are also indicated by discontinuities within each section. The location of the dated samples is also given.

us that some volcanic activity occurred during reversal boundaries and that this volcanic sequence might provide detailed behavior of the transitional field.

2. Geology and Geochronology of Volcanic Rocks from the Punaruu Valley

The thick succession of seaward-dipping lava flows exposed in the Punaruu Valley was erupted during the main phase of shield construction at the Tahiti Nui volcano. These are typically blocky 'aa' flows with rubbly oxidized top surfaces and massive interiors, easily traced for hundreds of meters along the canyon walls. The thickness of the flows varies between 1 and 4 m, with a mean of 3 m. Rapid erosion during periodic storms and active quarrying have exposed fresh outcrop surfaces. Compositionally these rocks are alkali basalts, but range considerably in phenocryst content from porphyritic (picrites and ankaramites) to aphyric varieties. *Brousse et al.* [1987] have produced a geological map and brief description of the volcanic succession exposed in the Punaruu Valley. Samples with T74 prefixes have been described by *Duncan* [1975]. Complete geochemical and mineralogical analyses of the dated samples will be reported elsewhere.

Samples selected for K-Ar dating were first examined in thin section to determine the state of alteration of the K-bearing phases. In most cases the rocks are petrographically fresh and well-crystallized. Samples which showed patchy groundmass alteration to clays or glassy mesostasis were excluded. Samples bearing cumulate olivine and rare small peridotite xenoliths were also eliminated because of the possibility of mantle-derived argon carried in xenocrysts.

After removal of any weathered surfaces, each sample was crushed to chips (0.5 to 1.0 mm size) and ultrasonically cleaned in distilled water. A representative split of this fraction was powdered and K-concentration was determined by atomic absorption spectrophotometric methods. Argon was extracted from the coarse chips by radio frequency inductive heating in a high vacuum glass line equipped with ^{38}Ar spike pipette and Ti-TiO_2 getters for removing active gases. The isotopic composition of argon was then measured mass spectrometrically using a model AEI MS-10S instrument with computer-controlled peak selection and digital data acquisition and reduction.

The age determinations on 12 samples from the Punaruu Valley section appear in Table 1. The positions of these dated samples are shown in Figures 1b and 2. With the exception of the age of sample T85-76 which appears to be slightly too young, the age succession is consistent with the stratigraphic order of the lava flows. The ages and magnetic polarities of the rocks are also compatible with the late Matuyama to early Brunhes portion of the magnetostratigraphic timescale (see later discussion of paleomagnetic transitions). This 700 m thick section was erupted between 1.2 and 0.7 Ma, yielding an average accumulation rate of 1.4 km per million years, or approximately one flow every 10^3 years. The evidence from the paleomagnetic studies, however, indicates that flows were erupted in pulses with significant time gaps, rather than at regular intervals.

3 Paleomagnetic sampling

All the paleomagnetic sampling has been done in the Punaruu valley and was carried out during two field trips. The first one was a preliminary sampling during which 150 cores from 25 lava flows were collected. Preliminary results, associated with the Jaramillo termination and the Brunhes onset, were

Table 1. K-AR Age Determinations for basalts from the Punaruu Valley, Tahiti.

Sample Number	%K	Radiogenic $^{40}Ar/g$ ($x10^{-7}cc$)	%Radiogenic ^{40}AR	Age±1σ (Ma)
BKV-185	0.83	1.7156	27.9	1.19±0.02
T85-72	0.86	1.5745	15.2	1.08±0.02
T85-76	1.03	1.7688	10.8	1.01±0.05
BKG-85	2.07	3.9120	24.4	1.09±0.02
PKB-14	1.16	2.2268	18.4	1.11±0.03
T85-81	1.03	1.8259	24.4	1.05±0.02
T85-93	1.28	2.1740	19.8	1.00±0.02
T74-431	1.62	2.8538	17.0	1.04±0.02
T74-434	1.16	1.8886	11.8	0.96±0.02
T74-435	1.34	2.0978	17.8	0.92±0.02
T74-437	1.66	2.1991	14.2	0.78±0.01
T85-67	2.19	2.3630	6.6	0.62±0.02

Age calculations based on the following decay and abundance constants:
$\lambda_\varepsilon=0.581x10^{-10}\ yr^{-1}$, $\lambda_\beta=4.962x10^{-10}yr^{-1}$, $^{40}K/K=1.167x10^{-4}$ mole/mole.

Table 1 K-Ar age determinations for basalts from the Punaruu valley, Tahiti.

reported by *Roperch and Chauvin* [1987]. The second field trip was more detailed and covers a distance of 4 km into the valley. This sampling corresponds to a volcanic sequence almost 700 meters thick.

A total of 788 cores have been drilled for 123 lava flows and 4 dykes, which means an average of 6 to 7 cores per volcanic unit. Cores were obtained with a gasoline-powered portable core drill, and then oriented using a magnetic compass and whenever possible by sun orientation. We have tried to distribute the samples throughout the flows, vertically or horizontally in order to minimize risks of systematic deviation of the paleomagnetic directions due to local block disturbances, but, in many cases, the location of the samples was controlled by accessibility. During the sampling we used a portative spinner magnetometer (LETI) in order to recognize the polarities of the flows and understand the stratigraphy. The intensity of the natural remanent magnetization (NRM) was often a better tool than the NRM direction to recognize transitional zones. Because of viscous components in the present day field, some transitional flows showed directions closed to a normal polarity but with very low magnetic intensity. The information, obtained with a portable spinner magnetometer, is more accurate than when using a fluxgate with oriented blocks but, obviously, is more time consuming.

The natural dip of the lava flows is close to 10 degrees toward the ocean. This fact allowed us to sample either along the river or by vertical sections (Fig. 1b).

Description of volcanic the sequence, sampling from bottom to top (figure 1b):

The first part of the sampling was done along the river. A lava flow (BKV) with a reversed direction was at the base of the sequence. Between BKV and the next flow (BKA), no outcrop was found. From BKA to BKG, a reverse polarity was observed. Following this reverse succession, there was a small gap in the sampling of a few tens of meters, followed by a transitional zone which contained 16 lava flows (from BKH to BKT2) and represented an horizontal extent of 350 m. One dyke (BKM) with a reversed direction cuts the transitional sequence and was sampled near flow BKL.

Immediately above BKT2, we found 3 lava flows (BKS,PKB,BKW) and one dyke (BKU) with reversed polarity. No normal direction was observed in this part of the volcanic sequence. No outcrop was available for the next 250 m and taking into account a slope of ten degrees, this corresponds to a vertical gap of almost 40 meters in the sequence. Then 4 flows with reversed directions were sampled: BKX on the north side of the river and BKY, BKZ, BKZA on the other side in an old quarry where the stratigraphic order was easy to recognize. Around 300 m away from the previous location, two other reversed flows PKE and PKG were sampled. The dyke PKF which cuts these two flows has a normal polarity. This sampling, done along the river, from flow BKV to PKG, corresponds to the lower part of our sequence.

The second part of the sampling was made on the southern part of the valley, by sections on the hillside whose slope is almost 100%. In all cases we tried to sample all the flows which could be observed on the field but it was necessary to do several small sections because of a lack of outcrops or because of topographic difficulties, like small cascades. There were no indications either in the geological, geochronological or paleomagnetic data for differences between the two sides of the river, neither fault nor tectonic is observed in the valley and young valley filling flows were generally easily recognized.

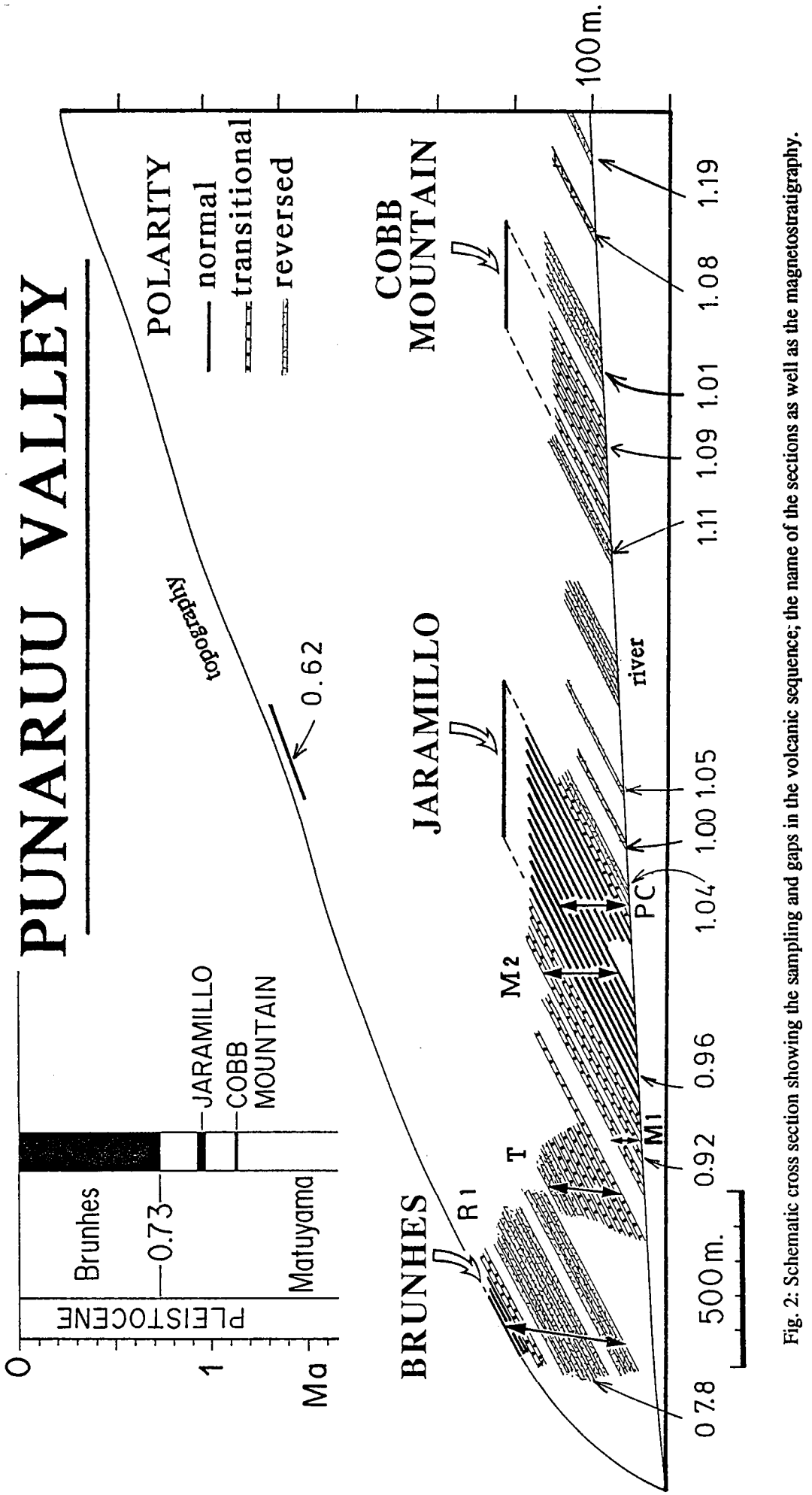

Fig. 2: Schematic cross section showing the sampling and gaps in the volcanic sequence; the name of the sections as well as the magnetostratigraphy.

The section P-C (flows PA to PN and CA to CK) begins near the river, something around 350 m away from the flow PKG. A reverse polarity was observed for the first two bottom flows and a transitional zone was recorded by the overlying flows (PB,PC,PE,PF). A small baked soil, 50cm thick, was interbedded between flows PC and PE but we were unable to sample it. No such well defined soil was seen elsewhere in our sequence. As it does not mark the transition from full reverse to full normal, but is interbedded between two flows having a similar direction, this kind of baked soil is not an indicator of a larger time span between two flows, in contrast to what we expected. A normal polarity was found above the transition up to an elevation of 125 meters (flows PG to PN and CA to CK).

The section M2 starts at an elevation of 30 m. Up to 120 m high above the sea level, (from M2U to M2G) only normal directions are observed. The seven top flows (M2E to M2V) of this section have transitional directions.

The section M1 is about 400 m away to the west from section M2 and is composed by 6 flows (M1A to M1F) with intermediate directions. The particular paleomagnetic directions recorded by the flows from the sections M1 are very similar to that observed on the flows CS, CT, CU (noted section 2 on Fig.1) which are situated 100 m westwards.

Section T is very close and just above flows CS, CT, CU and starts at an elevation of 30 m; 7 flows (from TA to TG) have transitional directions and the upper 2 flows (TJ and TL), at an elevation of 150 m, have a reverse polarity. We were unable to sample between altitudes of 150 to 250 m in this section. At 250 m (section 1, Fig.1), one flow of normal polarity (TU) was found overlying two flows (TR and TT) with intermediate directions.

The last section (R1) shows a new polarity transition. From an elevation of 50 m high above sea level to 170 m (flows R1A to R1S), only a reverse polarity is observed and is overlaid by a small transition zone of 20 m thick, composed of only 3 flows (R1T, R1U, R1V). The intermediate direction of the flow R1V is similar to that of flow TR which had been sampled at the top of the section T. Above the flow R1V, the last flow PL has a normal polarity as TU which was sampled at the top of the section 1.

From this sampling, a synthetic cross section of the valley has been constructed (Fig. 2, see section 5), which shows the stratigraphic order and the geomagnetic polarities recorded. According to the radiometric datings, and the polarities observed, we have sampled: the Brunhes-Matuyama reversal at the top of the volcanic sequence, followed by the upper and lower Jaramillo and the Cobb Mountain event.

4 Laboratory procedures

Remanence: Each core was cut in standard specimens (2.5 cm). Remanent magnetization was measured using a Schonstedt spinner magnetometer. Stepwise demagnetizations either thermal or by alternating field (af) were performed, at least on one sample of each core, using Schonstedt furnace and af demagnetizer. Most of the normal and reverse samples were cleaned only by af while samples from the transition zones were demagnetized with thermal or af techniques. Flows with intermediate directions have lower NRM intensities and even if the viscous remanent magnetization (VRM) overprint is almost the same as with normal or reverse magnetized flows, its relative importance to the initial NRM is greater. Af demagnetizations were more efficient in removing isothermal (IRM) components, while

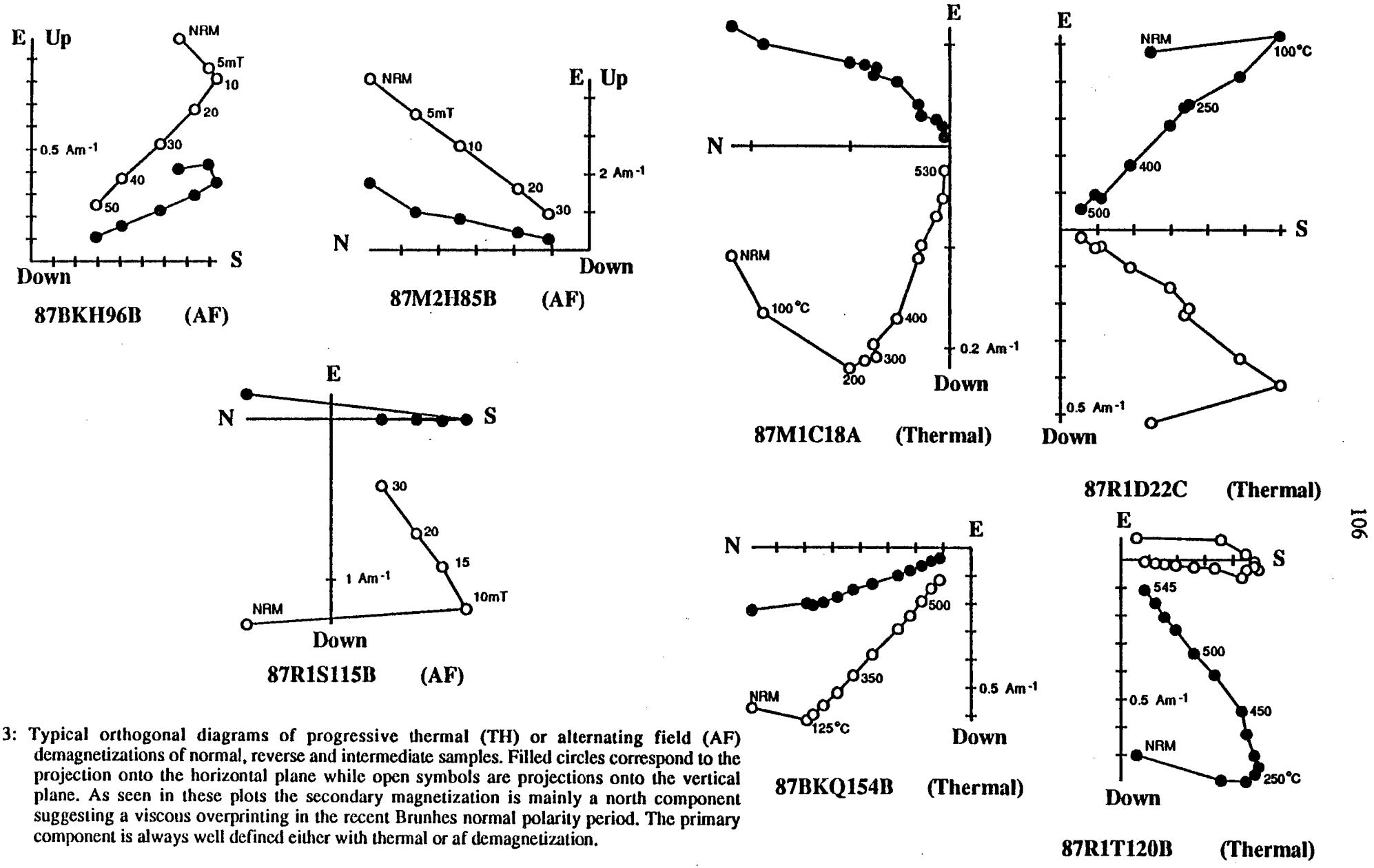

Fig. 3: Typical orthogonal diagrams of progressive thermal (TH) or alternating field (AF) demagnetizations of normal, reverse and intermediate samples. Filled circles correspond to the projection onto the horizontal plane while open symbols are projections onto the vertical plane. As seen in these plots the secondary magnetization is mainly a north component suggesting a viscous overprinting in the recent Brunhes normal polarity period. The primary component is always well defined either with thermal or af demagnetization.

thermal demagnetizations were better in cleaning viscous remanent magnetization (VRM) from weakly magnetized samples.

During stepwise thermal demagnetizations of some lava flows (in particular: M1B, M1D, M1F), samples showed VRM acquisition at room temperature, in the laboratory field during their transport from the zero field of the oven to the spinner magnetometer. The VRM acquisition was easily seen at temperatures above 300°C because of the very low intensity of the NRM. Above this temperature the VRM intensity acquired in the laboratory field was high enough to prevent the measurement of the primary magnetization until 15 to 30 mn of storage in the zero field of the spinner magnetometer, showing that time of VRM decay in zero field is greater than time of VRM acquisition in weak field. Some experiments were undertaken on these samples in order to find the best way to minimize this spurious effect and we observed that the VRM acquisition capacity on a short time scale is greatly reduced if the samples are kept in zero field a few hours after the heating, before any application of an external field.

This seems to indicate that the VRM properties for these samples are very sensitive to their previous magnetic history. Similar effects of the heating have already been described [*Plessard*, 1971, *Tivey and Johnson*, 1981]; they can be attributed to the presence of multidomain (MD) magnetic particles in the samples, since single-domain (SD) particles seems to have a VRM acquisition capacity independent of the previous magnetic treatment. Without a room shielded from the Earth's magnetic field, we took special care in taking the samples from the furnace and waiting a few minutes before performing the measurements. Primary components were identified easily and some typical demagnetization diagrams are illustrated in Fig. 3.

Susceptibility: Weak field susceptibilities were measured using the Bartington susceptibility-meter, at room temperature.

Strong field thermomagnetic measurements were performed in vacuum (10^{-2} Torr) or in air, using an automatic recording Curie balance. Heating and cooling rates were 8°C per minute, with an applied field of between 0.1 to 0.7 Tesla.

Paleointensity: Paleointensity determinations were performed using the original Thellier's double heating method [*Thellier E. and Thellier O.*, 1959], which is more accurate than several other methods for basalts [*Coe and Gromme*, 1973]. Samples were heated in a quartz tube surrounded by a coil which produces the external laboratory magnetic field. All this system was shielded from the geomagnetic field by 3 layers of mu-metal cylinders. Following *Khodair and Coe* [1975], the heatings were performed in vacuum (10^{-2} Torr), in order to minimize temperature alterations of the magnetic minerals of the samples.

As with the original Thellier method, at each temperature step, the two successive heatings and coolings were performed in presence of the artificial laboratory field, but the direction of this field was reversed between each heating. This method differs a little from the modified version proposed by *Coe* [1967a,b] for which the first heating of each temperature step was made in zero field and the second heating in the laboratory field. The artificial laboratory field was applied during all the temperature cycle [*Levi*, 1975]. The applied fields varied from 9 to 40 microteslas, in order to minimize differences between laboratory and ancient field strength [*Kono and Tanaka*, 1984].

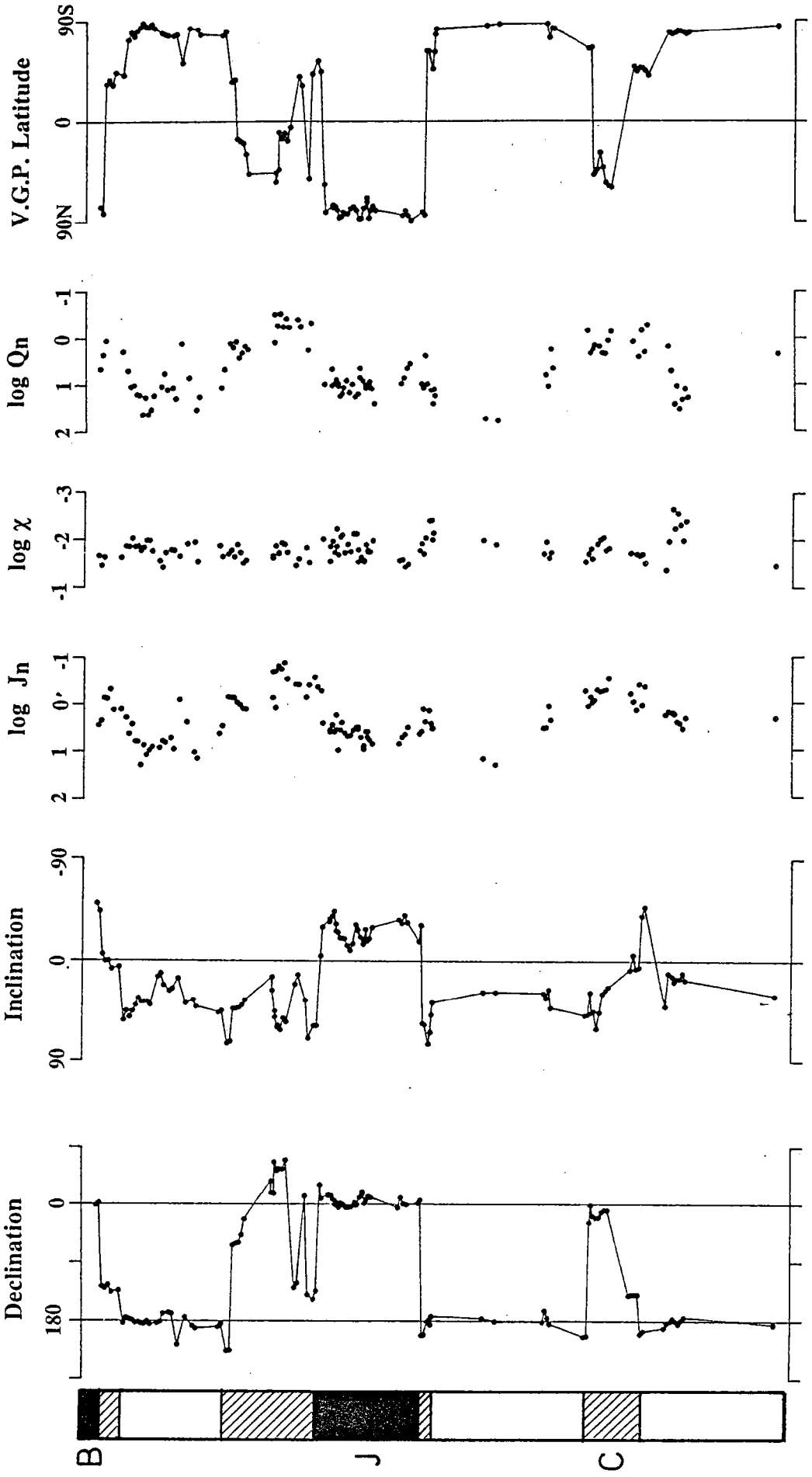

Fig. 4: Evolution of different magnetic parameters for each flow of the sequence against the calculated cumulative thickness. Jn: average NRM intensity after 10 mT; χ,Qn: mean susceptibility and Koenisberger ratio. The axial normal dipole inclination should be around -32.5° (32.5° for reverse). While the susceptibility appears to be equivalent throughout the section, large variations in intensity are seen with the low values always correlated to transition zones, identified on the VGP latitude plot. These low values are also well defined with the apparent Koenigsberger ratio.

5 Paleomagnetic results

Remanence directions:

When only stepwise af cleanings were used to demagnetize a lava flow, the mean direction was calculated at the one peak of the alternating field which provided the best grouping in the data. When both thermal and af cleanings were performed on one flow, primary remanence directions are obtained by interpretation of the Zijderveld diagrams. For these young lava flows, the primary component was considered as passing through the origin. In computing mean direction per flow, we omitted anomalous cores if field notes indicated possible orientation mistakes, or if their directions were at more than 2 times the standard deviation of the mean direction of the flow. The arithmetic mean of $\alpha 95$ for all the lava flows with normal or reverse polarity is 4.4±2., and 6.8±4. for flows with intermediate directions (with about 6 samples per flows), indicating that good determinations of paleomagnetic directions have been obtained, both outside and within polarity transitions. Only three flows did not provide any good results. In the case of the flow M2E, neither af nor thermal demagnetizations were able to isolate a stable primary remanence. This flow belongs to the upper Jaramillo transition, and has a very weak intensity of magnetization with an overprint of higher intensity than that of the primary direction. Another flow from the Jaramillo termination, TI, did show a strong overprint. Samples from this flow have an unusually high remanence intensity (more than 100 Am^{-1}) and show a very quick drop in intensity for small af peak values (5 to 10 mT). For higher af peaks, the decrease in intensity is lower, but the directions do not change up to 100 mT, which is the maximum field of our af demagnetizer. The scatter observed in the directions as well as the high intensity suggest that the overprint of this flow is an isothermal remanent magnetization (IRM) due to lightning. The last case of failure in the recovering of the primary direction corresponds to flow BKW, situated after the transitional zone of the Cobb event. It was obvious in the field that this flow was altered by weather. Demagnetization by af was unable to completely remove the secondary component of magnetization even if the evolution of the remanent vector suggested a primary direction close to the reverse polarity. On the other hand, during thermal demagnetizations the samples from this flow exploded in the oven for temperatures above 300°C. Thus no paleomagnetic direction was determined for this flow.

Paleomagnetic results are listed in Table 2. In Figure 4, mean inclinations, declinations, and virtual geomagnetic poles (VGP) per flow are plotted as a function of the stratigraphy of the valley. The altitudes reported in the right side of this figure have been calculated, knowing the thickness of the lava flows sampled, their average natural dip, their true altitude and their location on the field. They do not represent the elevation at which each flow was sampled, but only their stratigraphic height in the volcanic sequence which was reconstituted. In making Figure 4, an attempt to adjust relative position of points between the different vertical sections was made. The stratigraphic order of the flows has been well observed in the field, either for the part of the sampling along the river, or within each vertical sections. To match relative positions of the flows between the different vertical sections was generally easily done, since observations on the field were often sufficient. For example, taking into account the distance between section M1 and M2 (see Fig.1) and the dip of the flows toward the west, the top-most flow of section M2 (flow M2V) is stratigraphically beneath the first flow of section M1 (flow M1A).

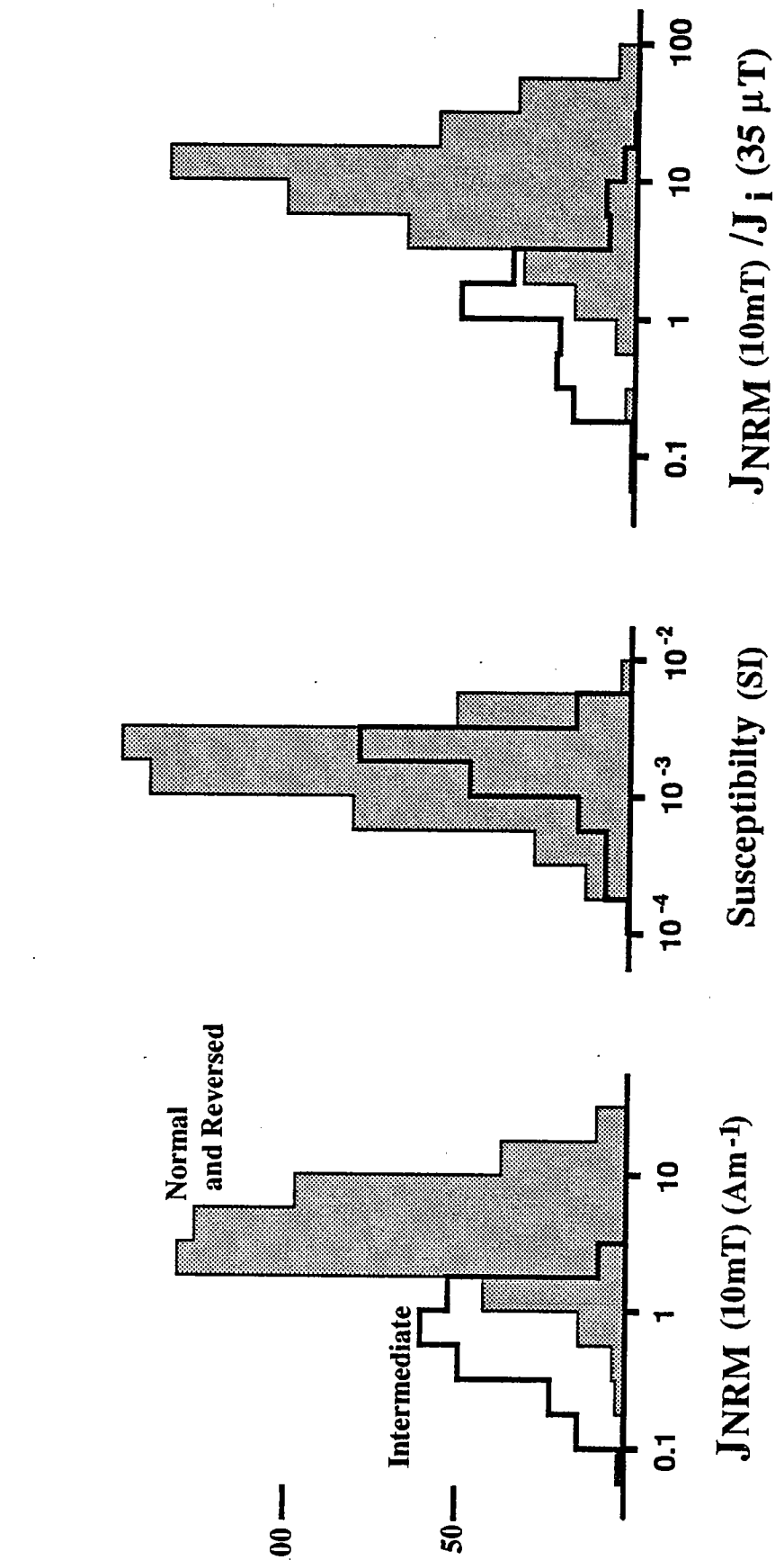

Fig. 5: Histograms showing the distribution of the NRM intensity (after 10 mT) (A), the susceptibility (B), and the ratio of the previous NRM with a calculated induced magnetization in a field of 35 μT (C) (this is an apparent Koenigsberger ratio). Samples have been separated into two populations intermediate and normal+reverse.

The same arguments are applied to sections T and R1 (Fig.1) and the flow TL (section T) is lower in the stratigraphy than flow R1A (beginning of section R1). This stratigraphy is in good agreement with the sequence of magnetic polarity obtained. In two cases, only paleomagnetic correlations have been used. First, section 2 (CS, CT, CU) and section M1, which are close to one another in the field, have similar paleomagnetic directions which suggest that flows CS, CT, CU are in the same stratigraphic level as flows M1A to M1D (CS: D=53.0, I=57.7; CT: D=66.7, I=50.2; M1D: D=56.6, I=59.8)

Correlations based on paleomagnetic directions are easier in the case of intermediate directions of the geomagnetic field, because they are less usual. On the contrary, it is more difficult to recognize and correlate directions during stable periods (reverse or normal) of the field. Our sections CA to CK and M2U to M2G both correspond to the Jaramillo normal subchron. Using the altitudes of the flows, their natural dip and the paleomagnetic directions, we have been able to correlate the two sections. However, the possibility that the same flow was sampled at two different sites, one in section C and the second in section M2 cannot be dismissed. The stratigraphic order chosen on the basis of the paleomagnetic data is indicated in Table 2.

Defining the boundaries of transitions in terms of directions is not so easy. Considering a direction to be transitional only when its corresponding VGP falls below a latitude of 50° [*Sigurgeirsson*, 1957], or 40° [*Wilson et al.*, 1972] is not always possible as can be seen for example with flows BKP, BKO and BKN (Fig. 4). These flows have purely transitional directions (Table 1) which correspond to an angular departure from the axial dipole higher than 50°. Their NRM intensities are also very weak, but their corresponding VGPs have a latitude higher than 50°. It seems that a better requirement for a direction to be considered intermediate is that the reversal angle (measure of the angular departure from the normal or reverse axial dipole) would be higher than 30°. This requirement was already proposed by *Hoffman* [1984] and we will see later that, from our data, this cutoff between intermediate and dipolar directions is not totally arbitrary.

Figure 4 shows that the thickness of the transitional zones is greatly variable. The upper Jaramillo transition has a thickness around 80 m while the normal subchron Jaramillo has been recorded only by a sequence of 120 m. Taking into account that a transition period is assumed to be 5 Ka. and, that the Jaramillo subchron is 60 Ka. long, great differences in the extrusion rate of the lava flows are then evident.

Magnetic properties:

NRM intensity and susceptibility

The stepwise af demagnetizations show that generally the secondary component of magnetization is cleaned at an af peak of 10 mT. In order to well define the distribution of the intensities of the primary directions, we report here the NRM intensities after 10 mT of af cleaning (J_{10}). The NRM intensities are widely distributed from less than 0.1 Am^{-1} up to 30 Am^{-1}, and samples with intermediate directions clearly have lower intensities of magnetization than normal and reverse samples. On the contrary, there is no apparent difference in weak field susceptibility for both populations (Fig.5); lowest values correspond to high-temperature oxidized samples. As a result, the distribution of the apparent

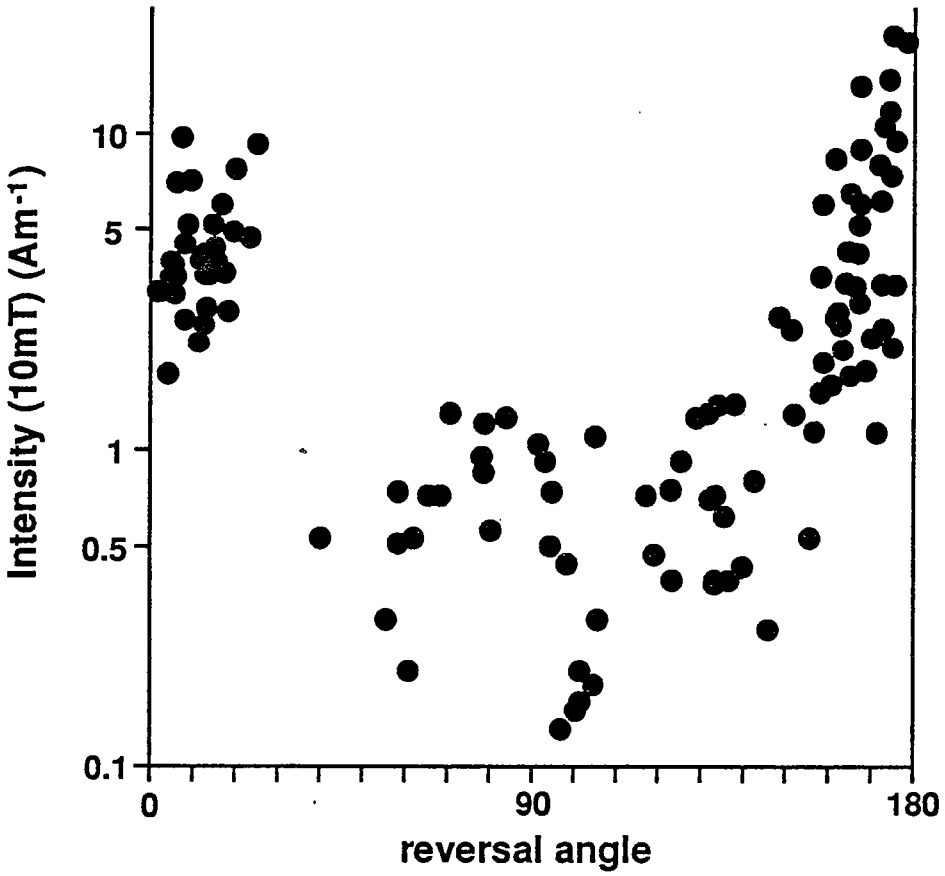

Fig. 6: Variations of the mean flow intensity of magnetization (after 10 mT) versus reversal angle. Intensity of magnetization is on a logarithmic scale.

Koenigsberger ratio, (NRM intensity after af cleaning at 10 mT divided by the product of the bulk susceptibility by an ambiant field of 35 μT), is similar to that of the intensities of magnetization.

Geometric mean values of NRM intensities (J_{10}), weak field susceptibilities and apparent Koenigsberger ratio calculated per flow are reported in Table 2 and are represented in Figure 4. This figure clearly shows that the average NRM intensities per flow is lower during transitional period than during normal or reverse periods. This fact is particularly clear when the transitional zone is well detailed. This pronounced decrease is also observed in the Koenigsberger ratio. But, on the contrary, no important changes in susceptibility occur within the section, and especially there are no differences in susceptibility between samples from the transitions, and samples with a normal or reversed direction. These results strongly suggest that the variations observed in intensity of magnetization are not mineralogically controlled but reflect changes in the geomagnetic field intensity. This is easily seen when the geometric averages NRM intensities, after 10 mT, per flows are displayed versus the reversal angle in Figure 6. The intensities for directions close to the normal polarity are distributed from 1.7 to 10 Am^{-1} with a mean value of about 4 Am^{-1}, while reverse polarity data show a distribution between 1 and 20 Am^{-1} with a mean value of about 6 Am^{-1}. Typically, full normal or reverse flows have NRM intensities higher than 1 Am^{-1}, while the transitional directions are always associated with weaker intensities of magnetization. Even if the scatter of the data is relatively important, with a deviation of one order of magnitude between some flows, the distinction with the full polarity state is very clear. In a study of a N-T-N excursion recorded on lava flows from the island of Huahine (Society island), a similar distribution of the intensities of magnetization is observed [Roperch and Duncan, this issue]. In that study, a normalization of the natural remanence by an anhysteretic magnetization did not modify the general pattern and demonstrated that the between flow intensity variations were not related to large differences in the magnetic properties. As the volcanism in Tahiti is similar to that of Huahine, a similar result is expected. A large decrease in the intensity of the geomagnetic field during the transition is expected and the ratio of the strength of the Earth's magnetic field between its intermediate state and its normal (non-transitional state) might be around one fifth to one tenth.

Nevertheless, we must emphasize that NRM intensity is a parameter which provides only a general trend of field variations if a great number of samples and flows are used. Details in the paleointensity changes between flows could not be resolve using NRM intensities alone. Absolute values of the geomagnetic intensity are necessary in order to better constrain paleofield variation during a reversal. Unlike the sedimentary and intrusive rocks, lava flows record a quasi instantaneous field, and they can provide accurate absolute paleointensities. In order to quantify the relative change in the geomagnetic field intensity reflected by the NRM data, some paleointensity determinations were attempted and will be presented below (see paragraph 8).

6 Statistical analysis of the distribution of the normal and reverse directions.

A previous study of paleosecular variation recorded on volcanic rocks from French Polynesia [*Duncan*, 1975] indicated an amplitude of dispersion of the paleomagnetic data in agreement with values predicted by secular variation models, with an angular standard deviation of the site VGP's about the geographical axis of 13.8°. This result was obtained from a sampling of 53 sites from 5 of the younger

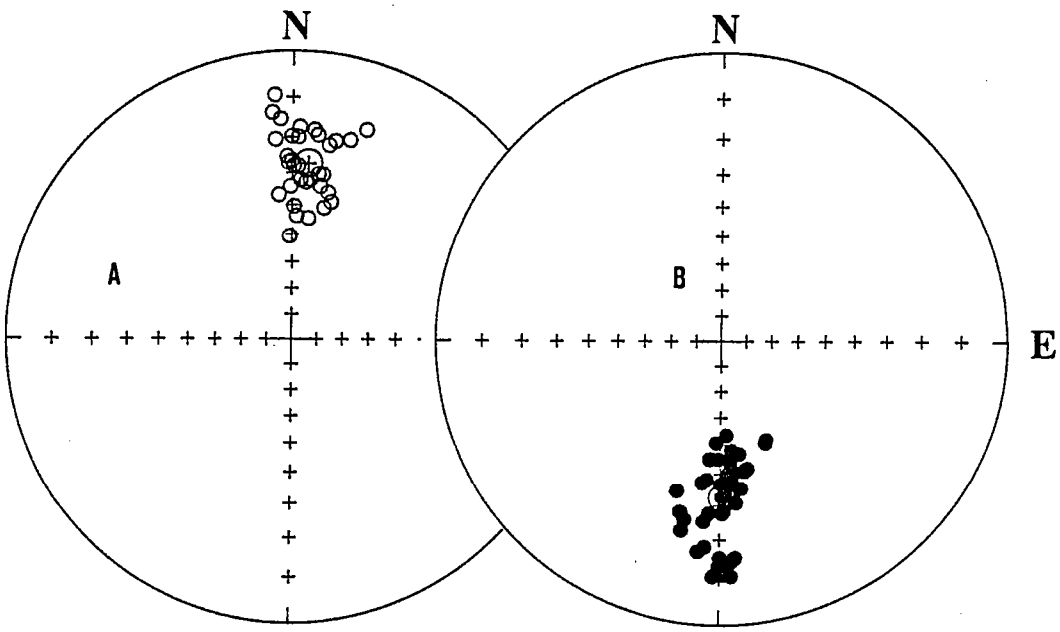

Fig. 7: Stereographic projections of all normal (A) and reversed (B) polarity directions observed in the volcanic sequence from Tahiti.

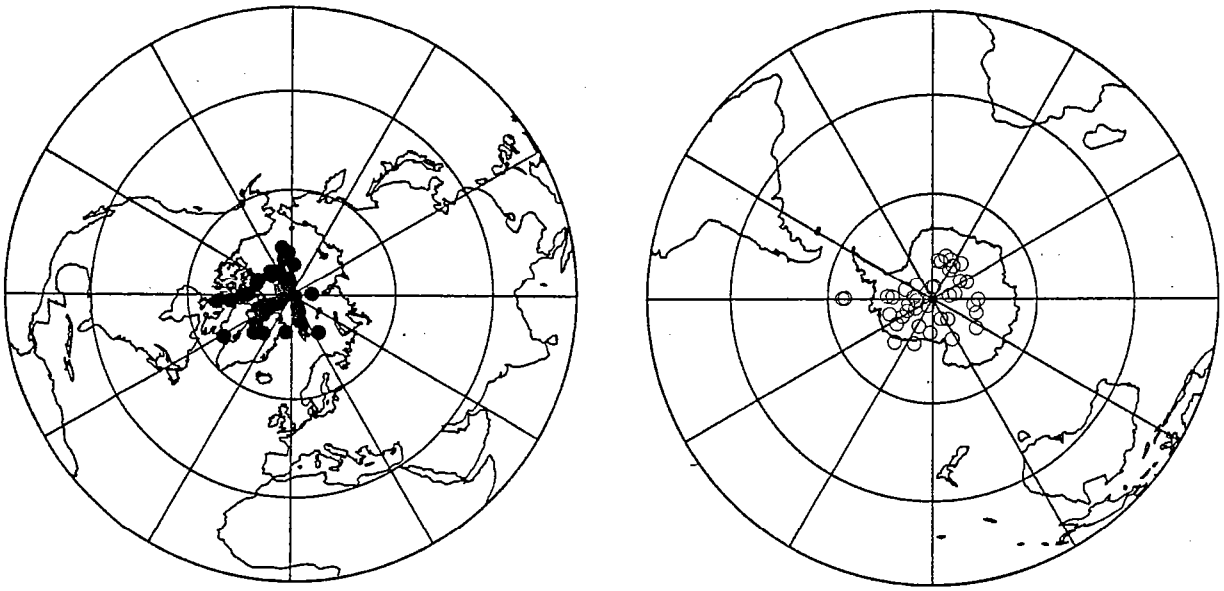

Fig. 8: Equal area projection of the VGP's corresponding to the previous directions shown on Figure 7 .

islands of the volcanic chain. In this case, all sites were geographically dispersed and then may be considered as independent. They also represent a larger time interval (4 Ma) than our sampling of one lava sequence from the Punaruu valley. A statistical analysis of the dispersion of the paleomagnetic directions may provide some insight on the sampling process of the magnetic field by such a volcanic sequence.

The normal polarity direction set is constituted by 31 flows erupted during the Jaramillo subchron, 2 during the Brunhes period and 2 dykes (Table 2). As most of the data correspond to the Jaramillo period they might represent a time interval around 60 Ka. (Figure.7a). The set of reversed directions is composed of 39 lava flows and 2 dykes (Fig.7b) and might represent a greater interval of time (about 350 Ka).

In a first step, paleomagnetic directions which are more than 30° away from the axial geocentric dipole have not been included in the analysis, since they have been considered as transitional. This is a criteria different from some other studies [*McFadden and McElhinny*, 1984; *McElhinny and Merrill*, 1975] for which a VGP latitude lower than 45° has been chosen as a cut-off level. The pattern of the directions (Figure.7 a,b) has a non Fisherian distribution, as it is commonly observed for sites at low latitudes, because of the movement of the dipole (dipole wobble). As a consequence, the distribution of the VGPs associated with the paleomagnetic directions is much more Fisherian (Figure 8 a and b).

The VGP mean for the flows of the Jaramillo is: long=263.9°, Lat=84.4°, with K=87.1, ST=8.7°, n=31 and α_{95}=2.8°. As it was discussed during the description of the sampling, two sections composed the Jaramillo; some sites between CA to CK perhaps correspond to flows already sampled in the section M2. Nevertheless, even if the ten flows between CA to CK are taken out of the computation, the result is not changed (mean VGP: l=266.8° L=85.0°, K= 83.1, α_{95}=3.5° and ST=8.9°). At the 95% confidence level, the mean VGP is distinguishable from the geographical axis, the low value of the angular standard deviation of the VGPs indicates an important grouping of the data. A low level of the non-dipole field activity, or a partial sampling of the cycles of secular variation because of a high rate of extrusion of the lavas flows can explain this result. Statistical analyses of volcanic flow sequences erupted over a very short time span could produce a biased estimate of the angular dispersion [*McElhinny and Merrill*, 1975]. In the case of the Jaramillo data set, whether the flows were erupted regularly over 60 Ka. or in one or a few short periods is an unanswered question. On the other hand, there is no substantial proof that the Earth's magnetic field can be averaged to a mean dipole, on a time period less than 50 Ka, for a single site.

For the reversed directions, the mean VGP is indistinguishable from the geographical axis at 95% confidence level, but the total standard deviation remains lower than the expected value at this latitude (mean VGP: l=268.0°, L=-88.9°, K=52.2, α_{95}=3.2°, n=39 and ST=11.2°). Such a statistics with a moderate number of samples, is very sensitive to the selection of the data. Adding 5 other flows, which have a VGP latitude of about 45-50°, but a reversal angle higher than 30°, the distribution provides an amount of dispersion in better agreement with the different models (which used such a cut-off level) for the secular variation. (l=246.0°, L=-86.4°, K=30.3, α_{95}=3.9°, ST=14.8°).

Computing the mean VGP with all the normal and reversed directions (VGP higher than 45°) gives an angular standard deviation very close to the expected value: l=327.9°, L=88.9°, α_{95}=2.7°, K=34.2,

Table 2

Site	n /N	AF/TH	Dec	Inc	k	α_{95}	∂	Lat	Long	P	J_{10}	χ	Q
TU	5/5	200	358.6	-50.6	117	7.1	18.1	76.3	35.6	N	2.74	2.16	4.56
PL	6/6	AF+TH	2.0	-43.6	92	7.0	11.2	82.0	17.5	N	2.18	3.45	2.27
TT	6/6	AF+TH	232.9	--5.5	900	2.2	117.0	-34.0	104.6	I	0.72	2.32	1.11
TR-TS	5/6	AF+TH	230.2	0.2	1055	2.4	122.9	-37.7	106.4	I	0.75	N.d	N.d
R1V	5/6	AF+TH	235.0	0.1	42	12.0	119.0	-33.1	108.6	I	0.47	N.d	N.d
R1U	4/5	AF+TH	224.5	7.3	702	3.5	131.7	-44.2	108.1	I	1.30	N.d	N.d
R1T	5/6	AF+TH	226.6	5.4	264	4.7	128.8	-41.9	107.9	I	1.26	2.36	1.92
R1S	6/6	AF+TH	176.7	53.4	101	6.7	159.0	-73.5	220.3	R	1.88	1.37	4.93
R1R	6/6	100	185.3	44.8	231	4.4	167.1	-80.0	182.1	R	4.18	1.40	10.74
R1Q	5/6	100	182.6	50.6	347	4.1	161.8	-76.2	201.3	R	2.61	0.93	10.10
R1P	6/6	100	181.1	44.9	579	2.8	167.6	-81.2	204.2	R	6.01	1.40	15.44
R1O	6/6	200	177.1	39.7	691	2.5	172.5	-84.4	239.5	R	6.14	1.34	16.39
R1N	6/6	100	178.2	33.3	405	3.3	178.3	-88.2	284.6	R	19.47	1.69	41.40
R1M	5/5	100	176.2	36.7	724	2.8	174.8	-85.5	262.6	R	7.37	1.45	18.20
R1L	5/5	200	175.2	36.5	907	2.5	174.4	-84.8	270.0	R	11.72	1.03	40.87
R1K	9/11	200	179.8	36.6	311	2.9	175.9	-87.3	214.6	R	9.48	1.04	32.7
R1J	6/6	200	174.9	39.4	1940	1.5	172.0	-83.3	255.7	R	7.98	1.73	16.53
R1I	6/6	100	176.9	14.2	367	3.5	161.4	-79.1	14.1	R	8.32	2.78	10.76
R1H	6/6	300	179.0	11.0	327	3.7	158.4	-77.8	25.9	R	5.99	3.77	5.71
R1G	7/8	200	191.6	21.6	115	5.6	165.0	-77.0	92.1	R	6.48	1.87	12.43
R1F	6/6	AF+TH	193.2	26.7	328	3.7	167.1	-76.8	106.7	R	5.15	1.63	11.37
R1E	4/5	AF+TH	191.3	24.7	66	11.4	167.4	-78.1	98.6	R	8.94	1.68	19.12
R1D	5/7	AF+TH	143.0	15.6	214	5.5	142.5	-52.7	310.9	I	0.80	2.23	1.3
R1C	5/6	200	185.8	37.8	835	2.6	172.9	-83.5	154.1	R	2.41	1.22	7.07
R1B	5/6	200	172.2	34.8	609	3.1	173.1	-82.5	288.2	R	10.52	1.13	33.45
R1A	4/5	100	168.4	40.9	994	2.9	167.5	-77.7	270.9	R	14.17	2.89	17.61
TL	5/5	200	170.9	46.3	368	4.0	164.6	-77.0	249.1	R	4.24	1.34	11.36
TJ	6/6	200	175.3	44.6	92	7.0	167.4	-80.4	236.7	R	2.92	2.26	4.64
TI			N.d	N.d									
TG	6/6	200	133.0	74.4	249	4.2	132.3	-35.6	236.6	I	0.70	1.98	1.28
TF	7/7	200	134.0	72.5	194	4.3	133.6	-37.6	239.5	I	0.72	1.67	1.55
TE	3/5	200	297.0	42.9	299	7.1	94.9	15.3	153.7	I	0.74	2.28	1.16
TD	3/4	200	299.6	42.6	354	6.6	93.3	17.5	154.6	I	0.92	1.27	2.61
TC	8/8	200	301.3	41.5	259	3.4	91.6	19.3	154.7	I	1.04	1.87	2.01
TB	5/8	200	312.7	39.2	128	6.8	84.1	28.9	159.5	I	1.26	3.07	1.47
TA	8/8	200	337.8	35.0	83	6.1	70.9	46.7	178.1	I	1.30	2.71	1.72
M1F	6/6	AF+TH	18.2	26.0	261	4.2	61.1	53.8	241.5	I	0.20	2.41	0.30
CU	3/5	AF+TH	37.2	14.1	75	14.3	58.6	45.6	269.7	I	0.74	2.17	1.22
M1E	4/5	AF+TH	17.0	44.9	126	8.2	79.0	42.8	231.5	I	1.21	N.d	N.d
M1D	6/6	AF+TH	51.6	59.8	123	6.1	101.6	14.5	248.5	I	0.16	1.93	0.30
CT	5/5	AF+TH	66.7	50.2	19	19.3	101.5	9.6	263.6	I	0.20	1.35	0.53
CS	4/5	AF+TH	53.0	57.7	20	20.9	100.6	15.1	251.1	I	0.15	1.88	0.29
M1C	6/6	AF+TH	56.1	62.0	101	6.7	104.7	10.3	248.5	I	0.18	1.16	0.56
M1B	6/7	AF+TH	55.9	51.2	19	15.8	97.1	17.0	258.0	I	0.13	1.25	0.38
M1A	6/7	AF+TH	69.8	54.8	77	7.7	105.8	5.3	260.9	I	0.29	1.83	0.57
M2V	6/7	AF+TH	231.1	20.5	34	11.6	133.2	-40.1	119.6	I	0.38	3.43	0.39
M2W	5/5	AF+TH	238.3	12.3	92	8.0	123.2	-32.0	116.8	I	0.39	2.51	0.55
M2A	6/6	AF+TH	12.7	35.0	120	6.1	68.6	51.0	229.8	I	0.72	1.46	1.76
M2B	6/6	AF+TH	220.4	69.6	172	5.1	136.7	-42.6	178.9	I	0.39	2.99	0.46
M2C	6/6	AF+TH	213.5	58.0	194	4.8	146.0	-54.1	163.3	I	0.27	N.d	N.d
M2D	5/6	AF+TH	226.3	58.1	98	7.8	139.9	-44.7	158.1	I	0.43	N.d	N.d
M2E			N.d	N.d									
M2F	5/5	AF+TH	30.7	-4.4	401	3.8	40.2	56.1	276.8	I	0.53	N.d	N.d
M2G	6/6	AF+TH	9.0	-29.8	884	2.3	8.2	81.2	290.6	N	2.57	0.96	9.65
M2H	6/7	200	15.8	-37.3	318	3.8	13.8	74.7	315.1	N	3.58	2.81	4.57
CK	6/7	200	13.7	-34.7	408	3.3	11.6	76.9	309.0	N	3.97	1.37	10.37
M2I	4/5)	100	13.6	-39.7	401	4.6	13.1	76.3	323.6	N	2.80	1.07	9.42
M2J	4/5	200	7.6	-44.0	137	7.9	12.9	79.3	350.8	N	3.92	1.82	7.73
M2K	5/6	300	4.9	-32.6	101	7.6	4.1	85.3	301.6	N	1.73	0.59	10.57

CI	5/5	200	359.8	-26.4	261	4.7	6.1	86.3	207.0	N	3.53	1.36	9.32
CH	4/5	200	358.3	-25.2	537	4.0	7.5	85.3	190.0	N	9.70	2.06	16.91
CG	4/4	200	355.0	-20.4	1005	2.9	12.9	81.4	175.7	N	3.58	0.86	14.95
M2L	6/6	100	1.6	-19.9	174	5.1	12.7	82.4	22.6	N	2.49	0.79	11.32
M2M	6/6	100	359.7	-19.7	462	3.1	12.8	82.4	208.3	N	4.17	1.85	8.07
M2N	5/6	300	354.7	-13.5	385	3.9	19.6	78.0	184.5	N	4.89	1.23	14.29
M2O	5/6	300	355.6	-9.4	1243	2.2	23.5	76.3	191.7	N	4.69	1.75	9.64
M2P	6/6	300	356.7	-15.2	379	3.4	17.6	79.5	192.3	N	3.62	0.74	17.55
M2Q	5/6	300	2.9	-32.0	334	4.2	2.5	87.2	293.8	N	3.17	0.74	15.29
CF	7/7	200	358.6	-26.9	247	3.8	5.8	86.3	189.0	N	3.11	1.61	6.92
M2R	6/6	100	0.4	-27.8	299	3.9	4.8	87.0	218.1	N	3.48	2.85	4.39
CE	6/8	200	10.7	-21.2	153	5.4	14.8	77.7	269.1	N	5.16	2.27	8.16
M2S	4/6	200	16.2	-18.6	2261	1.9	20.1	72.3	275.3	N	7.73	2.71	10.24
CD	5/5	200	19.6	-14.8	251	4.8	25.1	68.4	275.1	N	9.25	2.83	11.74
CC	4/4	200	1.9	-27.3	1395	2.5	5.0	86.6	243.0	N	3.92	1.26	11.18
CB	6/8	200	6.0	-17.8	140	5.7	15.7	79.8	246.1	N	3.93	1.65	8.55
M2T	7/7	200	7.1	-19.0	270	3.7	15.0	79.5	252.5	N	5.14	1.78	10.35
M2U	7/7	TH+AF	12.3	-19.8	1163	1.8	16.8	75.9	270.1	N	5.97	1.78	12.03
CA	5/5	200	10.6	-29.7	520	3.4	9.5	79.7	292.3	N	7.11	1.03	24.79
PN	7/7	200	354.6	-36.5	102	6.0	6.0	84.3	92.7	N	7.00	2.68	9.37
PM	6/7	100	10.4	-33.3	232	4.4	8.8	80.1	305.0	N	5.14	2.59	7.13
PJ	5/5	200	0.8	-40.4	413	3.8	7.9	84.6	22.8	N	4.47	3.64	4.40
PI	6/6	200	359.3	-34.0	210	4.6	1.6	88.8	65.9	N	3.16	3.21	3.53
PH	7/7	200	1.9	-17.3	278	3.6	15.3	81.0	222.6	N	4.37	1.66	9.45
PG	7/7	200	6.4	-31.6	258	3.8	5.5	83.9	296.0	N	3.84	1.18	11.66
PF	8/8	AF+TH	157.8	55.8	233	3.6	152.8	-62.9	252.6	I	1.29	1.95	2.38
PE	8/8	AF+TH	158.6	57.1	102	5.5	151.3	-62.6	249.4	I	2.40	0.90	9.55
PC	7/7	100	179.4	74.4	297	3.5	138.1	-46.9	211.0	I	1.39	0.39	12.83
PB	7/7	200	182.6	63.9	175	4.6	148.6	-62.0	206.7	I	2.63	0.38	24.75
PO	6/6	100	174.4	47.8	158	5.4	164.2	-77.7	234.3	R	3.36	0.98	12.31
PA	7/7	300	187.4	36.8	85	8.8	172.6	-82.5	143.7	R	3.33	0.71	16.78
PKG	4/5	AF+TH	183.8	27.5	407	4.6	174.0	-85.2	80.7	R	14.87	1.01	52.71
PKE	5/5	AF+TH	179.3	27.5	273	4.6	174.9	-86.8	18.3	R	20.37	1.25	58.41
BKZA	9/9	AF+TH	178.7	28.2	132	4.5	175.5	-87.0	5.6	R	3.32	1.93	6.19
BKZ	4/8	AF+TH	196.2	32.6	106	9.0	166.4	-74.6	123.2	R	3.27	1.09	10.83
BKY	6/7	AF+TH	185.2	25.0	757	2.4	171.2	-83.2	78.9	R	1.13	2.35	1.73
BKX	11/12	AF+TH	175.4	41.5	504	2.0	170.3	-82.5	244.7	R	2.25	1.80	4.48
BKW			N.d	N.d									
PKB	5/7	AF+TH	155.5	48.4	67	9.4	155.7	-64.8	268.5	R	0.53	2.82	0.68
BKS	7/7	AF+TH	156.5	47.6	492	2.7	156.7	-65.8	269.3	R	1.14	1.93	2.11
BKT2	6/6	AF+TH	332.4	27.7	70	8.0	65.7	47.7	168.9	I	0.72	1.51	1.71
BKT1	5/5	AF+TH	358.7	45.8	87	8.2	78.4	45.1	209.0	I	0.95	2.44	1.40
BKR	5/6	AF+TH	342.1	44.5	212	5.3	78.7	42.8	188.5	I	0.85	N.d	N.d
BKQ	6/6	AF+TH	339.6	60.5	31	12.3	94.5	27.9	193.4	I	0.50	1.19	1.51
PKD	5/6	AF+TH	339.9	45.8	213	5.3	80.4	41.0	186.7	I	0.56	0.97	2.07
BKP	7/7	AF+TH	348.1	28.7	992	1.9	62.3	55.0	190.3	I	0.53	0.87	2.18
BKO	7/7	AF+TH	351.4	25.5	596	2.5	58.6	57.7	194.8	I	0.51	1.63	1.12
BKN	7/7	AF+TH	351.2	22.6	185	4.5	65.8	59.3	193.5	I	0.29	1.48	0.70
BKL	5/7	AF+TH	219.7	7.3	41	12.0	135.4	-48.7	105.4	I	0.62	1.88	1.19
BKK	5/5	AF+TH	221.3	-5.7	313	4.3	125.2	-44.4	97.9	I	0.92	N.d	N.d
PKC	6/6	AF+TH	220.8	6.4	272	4.1	134.0	-47.5	105.5	I	1.38	1.96	2.53
BKJ	7/7	AF+TH	220.8	5.2	242	3.9	133.2	-47.2	104.6	I	0.39	2.11	0.66
BKI	6/6	AF+TH	160.0	-40.3	924	2.2	104.9	-44.9	4.2	I	1.10	1.98	1.99
BKH	8/8	AF+TH	164.3	-48.1	42	8.6	98.1	-40.8	12.4	I	0.44	3.00	0.52
BKG	9/9	AF+TH	169.8	40.2	349	2.8	168.8	-79.1	270.3	R	1.77	0.42	1.51
BKF	7/7	AF+TH	177.2	10.6	590	2.5	157.9	-77.3	17.8	R	1.51	1.06	5.14
BKE	7/7	AF+TH	180.3	13.0	280	3.6	160.5	-78.9	32.1	R	1.60	0.22	26.02
PKA	7/7	400	184.3	17.9	378	3.1	164.9	-80.5	57.3	R	1.71	0.56	10.90
BKD	6/6	AF+TH	180.0	15.2	318	3.8	162.7	-80.0	30.6	R	2.47	0.27	32.85
BKC	6/6	AF+TH	175.9	15.1	105	6.6	162.2	-79.2	8.3	R	2.72	0.47	20.71
BKB	7/7	AF+TH	181.7	10.6	332	3.3	158.0	-77.5	38.5	R	3.52	1.02	12.43
BKA	4/5	200	186.0	16.6	678	3.5	163.2	-79.1	63.7	R	2.07	0.40	18.67

Site	n /N	AF/TH	Dec	Inc	k	α_{95}	∂	Lat	Long	P	J_{10}	χ	Q
BKV	7/8	200	174.5	30.6	234	4.0	174.9	-84.6	312.9	R	2.10	3.43	2.20
DYKE													
PD	4/7	AF+TH	0.2	-36.5	69	11.1	N.d	87.4	26.5	N	N.d	N.d	N.d
BKM	6/6	AF+TH	191.7	42.2	212	4.6	N.d	-77.2	154.1	R	1.36	1.77	2.75
BKU	6/6	AF+TH	171.9	32.8	239	4.3	N.d	-82.3	298.2	R	0.62	0.25	8.81
PKF	5/5	AF+TH	24.0	-30.8	132	6.7	N.d	67.1	301.5	N	1.35	1.49	3.27

Table 2 n/N: number of samples used in the analysis/total number of samples collected; AF+TH indicate that thermal and af demagnetizations have been done, while a number refers to the af peak (Oe), at which the mean was calculated; D, I: mean declination and inclination; k: precision parameter of Fisher; α_{95}: 95% confidence cone about mean direction; ∂: reversal angle; Lat, Long: latitude and longitude respectively of VGP position; P: polarity of the flow (N: normal, R: reverse, I: intermediate); J_{10}: geometric mean NRM intensity after 10 mT; χ: geometric mean susceptibility (SI units); Q: geometric mean ratio of J_{10}/ (35 $\mu T^*\chi$).

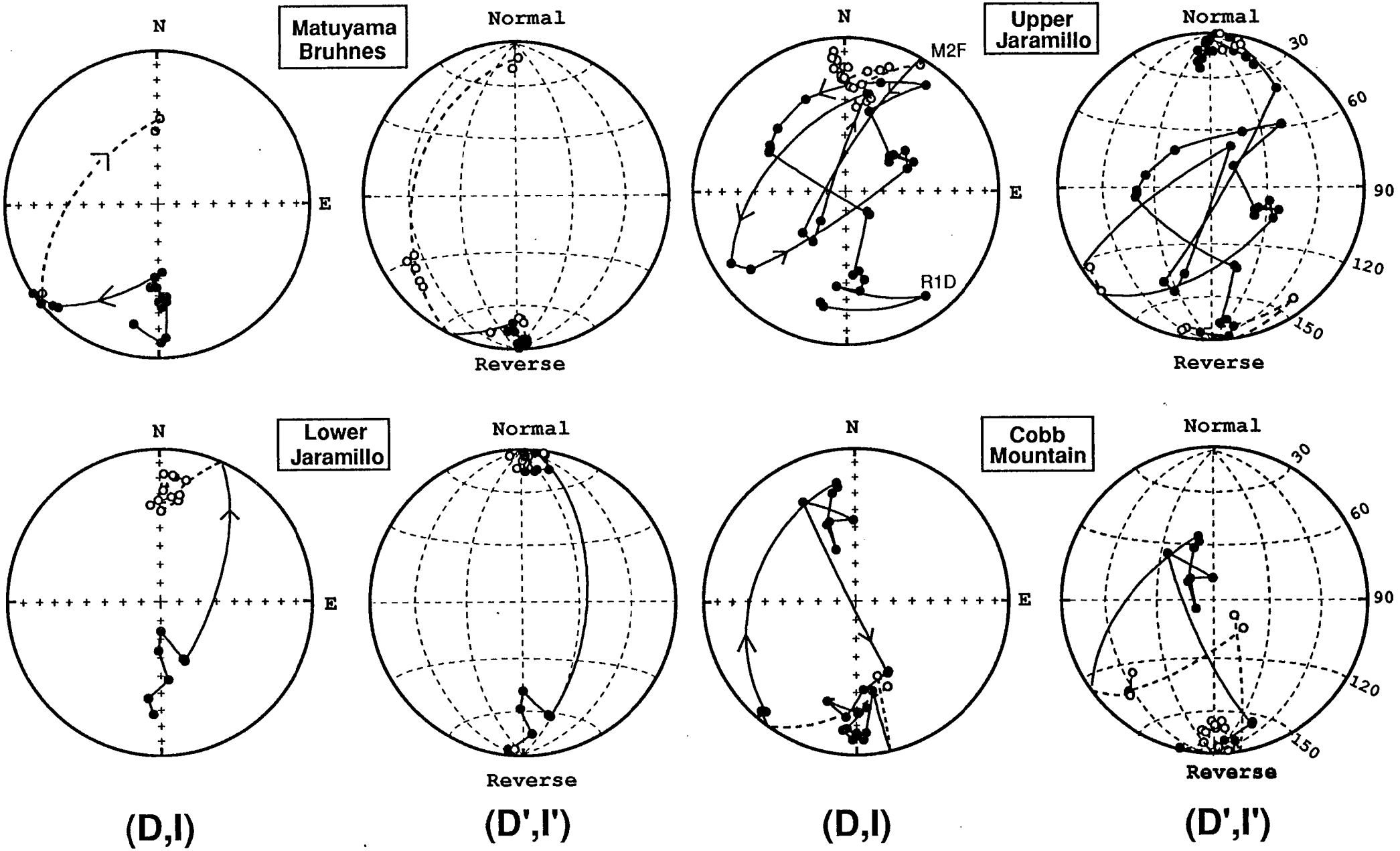

Fig. 9: For each transition, equal area projections of the directional paths before rotation (left) and rotated directions (D', I') [Hoffman, 1984] (right).

ST=14.0°. The angular standard deviation of the field is usually calculated with the following formula: $SF^2 = ST^2 - SW^2/n$, where ST is the total standard dispersion between sites, SW the within site dispersion and n the average number of sample per flows. The previous population of VGP gives a field dispersion SF=13.9° (SW=4.6°, n=5.9).

This study of the paleosecular variation provides the following conclusions:

The mean VGP associated with all the normal and reversed direction is indistinguishable from the geographical axis, thus, the dip of the flows is clearly not related to a tectonic process but results from their extrusion, and then no tectonic corrections are needed on the paleomagnetic directions.

The results from the Jaramillo indicate either that the Jaramillo represents a too short period of time to average the secular variation at this site or that the individual observations (i.e., each lava flow) are not independent in time.

Finally our estimate of the angular standard deviation of the VGP is identical to the value obtained by *Duncan* [1975] and is very close to the value given by the different models (The most recent (G) of *McFadden et al.* [1988] gives SF=13.4° for the latitude of Tahiti island).

7 Description of the transitions:

The directional path, before (D,I) and after rotation (D',I') following *Hoffman* [1984], for all the transitions found in our sequence, are displayed on stereoplots (Fig.9 a,b,c and d) while the virtual geomagnetic pole paths are shown in Figure 10.

a) Cobb Mountain (Fig. 9 and 10)

The paleosecular variation is not well recorded in the bottom of the section because several flows (BKA to BKF) have recorded a statistically indistinguishable direction with a low inclination. Only the two flows (BKV, and BKG) before and after this group have a different direction. As it has been discussed before, there is a small gap in the sampling of a few tens of meters between the last reversed direction (BKG) and the next (BKH) which is intermediate. Thus, this direction with negative inclination might not correspond to the beginning of the transition and lead only to an apparent far-sided VGP movement to position about 160° away from the site meridian. After that, southwest directions (flows BKJ to BKL) associated with shallowed inclinations have been recorded by 4 successive flows. The VGPs associated with these directions cannot be easily classified as near or far-sided. The followed directions (flows BKN to BKT2) are north but with positive inclinations between 20 and 60°; in the D', I' space they are situated in the near-sided quadrant, and are 90 to 60° away from the reverse polarity direction while the VGPs are less far from a normal polarity. Just above these intermediate directions, a direction only 25° away from the reversed polarity is recorded on two successive flows. Even if there are some gaps in the sampling, the following flows also have a reversed polarity. No normal directions have been observed, so this record is an apparent R-T-R excursion. K-Ar dating of some flows suggest that this excursion should be correlated to the Cobb Mountain event [*Mankinen et al.*, 1978].

b) Lower Jaramillo (Fig.9 and 10)

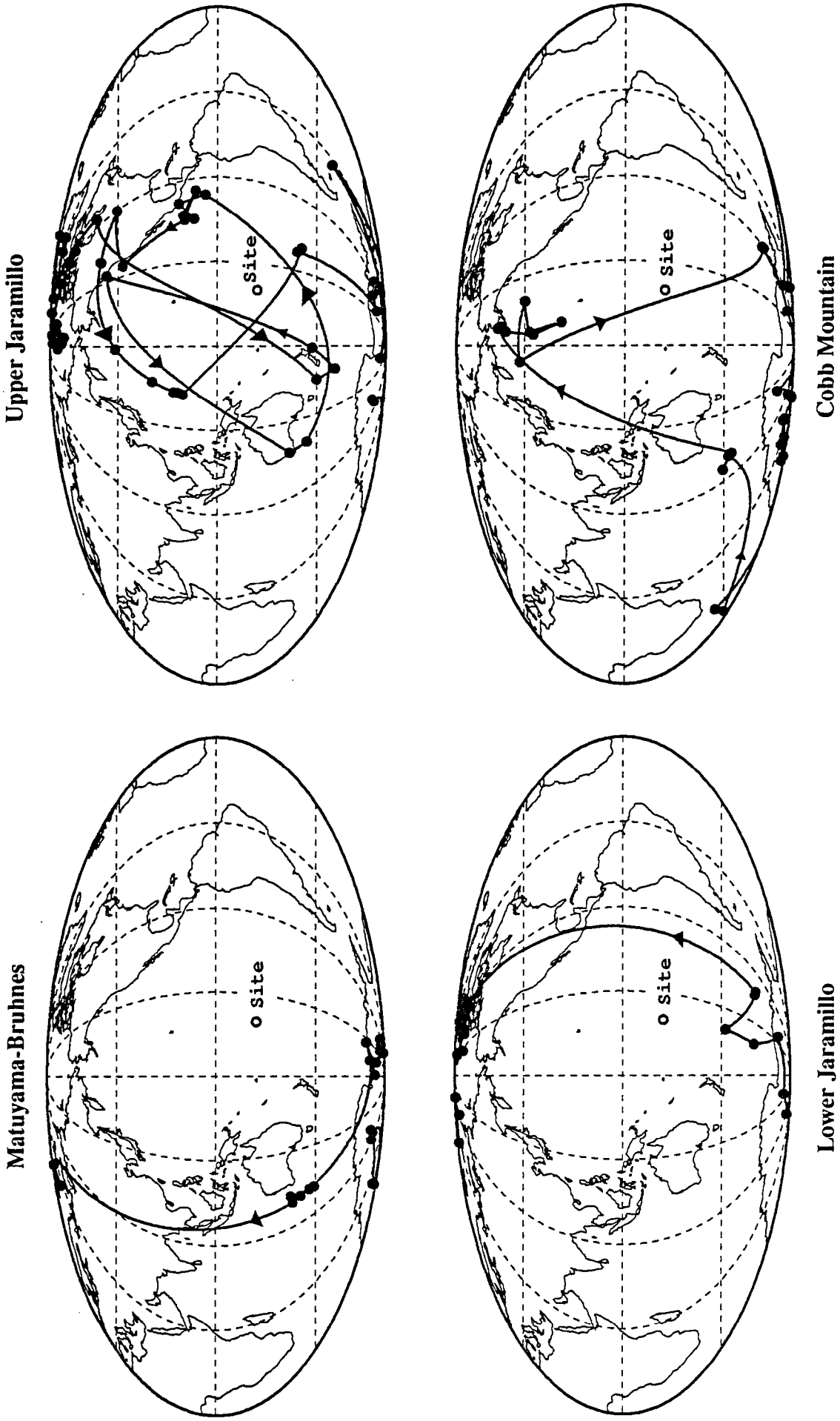

Fig. 10: Evolution of the PGV's during each transition plotted on a Mollweide projection. Same data sets as in Figure 9.

The transition is not very detailed, only 4 flows (Table 2) have a paleomagnetic direction which involves a maximum angular deviation from the geocentric axial dipole of 30 to 40° in the north/south vertical plane. In contrast with what is observed for the other transitions, the NRM intensity of these 4 flows cannot be distinguished from that of the underlying flows. This fact suggests that these flows recorded the beginning of the transition. No accurate paleointensities are available to confirm this interpretation.

c) Upper Jaramillo (Fig.9 and 10)

This reversal boundary is much more detailed and recorded by 23 flows. The first transitional direction (flow M2F) has a very shallow negative inclination, and shows a large swing of the field away from its secular variation pattern during the Jaramillo subchron. A different direction (southwest and steep positive inclination) is observed in the three following flows (M2D, M2C, M2B). The next transitional direction (M2A) is north with a moderate positive inclination and it is followed by two southwest directions (flow M2V, M2W). There is no gap in the sampling of these flows. Another transitional direction (east and positive steep inclination) has been recorded on six sites (M1A, M1B, M1C, CS, CT, M1D). The hypothesis that a gap in the sampling exits between section M2 and section M1 cannot be ruled out. Then, a passage of the directions to the north with a decrease in inclination is observed (M1E, CU, M1F). From flows TA to TE, in contrast with what was seen before, a regular shift in the direction is observed which seems to correspond to a better sampling in time of the field variation or a more regular behavior of the field. The end of the transition shows steep and southeast directions (flows TF and TG). The VGP associated with these intermediate directions are grossly near-sided except for two (flows M2V and M2W). All the transitional directions are associated with a weak NRM intensity.

The next 5 flows (TJ, TL, R1A to R1C) are purely reverse, with NRM intensities higher, and characteristic of the stable polarity state. But, just above these flows, the next one (R1D) has a remanent direction which goes out of the typical secular variation pattern, with an angular departure from the axial dipole of 37° and a low intensity of magnetization. This special direction has been obtained as well during thermal demagnetization as with af cleaning, and is clearly determined as shown by sample 87R1D22c on Figure 3. This site was clearly identified as a lava flow and not a sill. This result might indicate a period of dipolar instability in the nearly reestablished reverse polarity state.

Our record of the Upper Jaramillo is clearly characterized by : *i)* large changes between two intermediate directions (i.e., between the flows M2A and M2W), *ii)* progressive vector movement of the field, recorded by successive lava flows (flows CU to TE), *iii)* relative stability in intermediate positions (flows M1A to CT). The question is: are these properties related to the transitional field behavior or are they just an effect due to the sporadic extrusion of the lava flows?

Quick and large directional changes can be attributed first to gaps in the paleomagnetic sampling. We have seen that this is not the case for the 3 larger vector movements recorded by the flows of the top of section M2. On the contrary, perhaps this is the case between flows of section M2 and flows of section M1. On the other hand, gaps due to the extrusion rate are more difficult if not possible to verify.

We have some good evidence that the intensity of the Earth's magnetic field during the transition was very low, as shown by the NRM intensity, and also the paleointensity data (see next section). With a small magnetic vector, large and sudden changes in direction are easier to produce than with a normal geomagnetic field intensity. A simple analytical model of the reversal, in which the dipole term of the spherical harmonic expansion is reduced to zero while the other terms are allowed sinusoidal variations in 'realistic' agreement with the present non dipole field, gives a record also characterized by periods of progressive changes and periods of important and rapid directional variations when the magnetic field intensity is greatly reduced [*Roperch*, 1987]. Similar behavior is also observed in the recent reversal models proposed by *Williams et al.* [1988]. Other records of geomagnetic reversals on volcanic rocks [*Bogue and Coe*, 1984; *Prévot et al.*, 1985b; *Hoffman*, 1986] also give such impressions of irregular magnetic behavior during the transition. This argument might indicate that all the features of our record of the Upper Jaramillo are not only controlled by the sporadic volcanic activity, and that some of them reflect the irregular evolution with time of the field directions during intermediate states. Nevertheless, it is obvious that we do not have the complete evolution with time of the paleomagnetic directions during the transition, as it is always the case with volcanic rocks (Weeks et al., 1988).

d) Matuyama-Brunhes (Fig. 9 and 10)

Between the Jaramillo termination and the Matuyama-Brunhes reversal, as it was discussed before, one flow (R1D) has recorded a geomagnetic direction which moves away from regular secular variation amplitude. The following directions describe a counterclockwise loop finishing with a direction close to the purely reversed dipole. Before the Matuyama-Bruhnes boundary, a progressive increase in inclination is observed and we can speculate that this pattern has some similarities with the Lower Jaramillo. The transition is not detailed and only five lava flows have recorded intermediate directions which are southwest with a shallow inclination and 50° to 60° away from the geocentric axial dipole. As seen in the rotated space (D',I'), these directions are neither far-sided nor near-sided. Two normal directions on the top of the sequence (flows PL and TU) correspond to the Bruhnes polarity chron.

8 Paleointensity determinations

Method

The aim of the Thellier method is to compare partial thermoremanent magnetization (PTRM) acquisition and the decrease of the partial natural remanent magnetization (PNRM) with increasing temperature steps. Because of the law of additivity of the PTRM, the ratio PNRM/PTRM should be constant over each temperature interval and equal to the ratio of the ancient field strength and the laboratory field. This is true if no alteration of the magnetic minerals occur during the heating. So, only samples, for which their NRM is an original TRM, without important secondary magnetization, and showing no or little thermal instability, enable a paleointensity determination.

Sample selection:

In order to select the most suitable samples for the paleointensity measurements, we have used the three following criteria as a function of the NRM direction, the magnetic mineralogy and the thermal stability.

a) *NRM direction:* The NRM direction must be close to the mean direction of the flow obtained after af and/or thermal demagnetization. This allows us to reject samples carrying important viscous remanences (VRM). This criteria was particularly efficient on samples with a transitional direction, because, as the primary remanent magnetization has a very weak intensity, the overprint has a relative intensity more important than samples with a non-transitional direction.

b) *Grain size:* Multidomain grains cause non-ideal behavior during the Thellier experiment, and a concave up curvature of the points in the NRM-TRM diagram [*Levi*, 1977]. This effect prevents the use of the low-temperature part of the NRM-TRM diagram to calculate the paleointensity, since the slope of the line would be steeper than those provided by the ratio of the true paleointensity to the laboratory field.

Remanence stability to af demagnetization with a medium demagnetizing field above 30 mT, is used as indicators that the remanence is controlled by single (SD) or pseudo-single (PSD) domain particles. Of course, these experiments are performed on other specimens from the same core, and heterogeneousness of the magnetic properties over the core may sometimes occur.

c) *Thermal stability:* Thermal stability of our samples was investigated with strong field thermomagnetic experiments. The degree of alteration during the Js-T experiments has been estimated from the difference between the Curie point on heating and that on cooling and also from the change in the strong field induced magnetization (Js) at room temperature before and after heating. It is well known that volcanic rocks with a single high Curie temperature are good candidates for paleointensity determinations, because, generally, their highly oxidized state prevents a further oxidation during the laboratory experiment. Therefore, we have also used this criteria to select the samples, which is in good agreement with the previous one, since the magnetization of high Curie point samples is frequently carried by small grains (SD or PSD). Js-T experiments, performed on 111 samples (Figure 11), exhibit four types of curves. We assumed that the Curie temperature corresponds to the temperature of the inflection point of the Js-T curve. This method yields values generally lower than that obtained using a linear extrapolation of the Js-T curve as described by *Gromme et al.* [1969]. The temperature of the inflection point can be considered as the average of the broad distribution of the Curie point of the individual magnetic particles within a volcanic rock [*Prévot et al.*, 1983].

The first Js-T type curve is the most common encountered (76 samples) and shows a single ferrimagnetic phase, with a high temperature Curie point between 500 and 565° C. The type 1 curve can be divided into three groups, according to the relative discrepancy between the heating and cooling curves. Samples of group 1a are characterized by a decay of the strong field induced magnetization at room temperature, Js, after the heating, less than 10% and a decrease of the Curie temperature during the cooling of only a few degrees. This behavior has been found on 42 samples. Group 1b (13 samples) shows a decrease in Js greater than 10% after the heating and a more important drop of the Curie temperature during the cooling. The evolution of the samples is more pronounced when heatings are made in air than in a vacuum. The group 1c (21 samples) is characterized by an increase in the induced magnetization at room temperature after heating, since the cooling curves cross the heating curves, typically in the temperature interval 250-450°C. The magnetic phase producing the type 1 curve could be a Titanium-rich titanomagnetite which has been transformed to a Ti-poor titanomagnetite by high

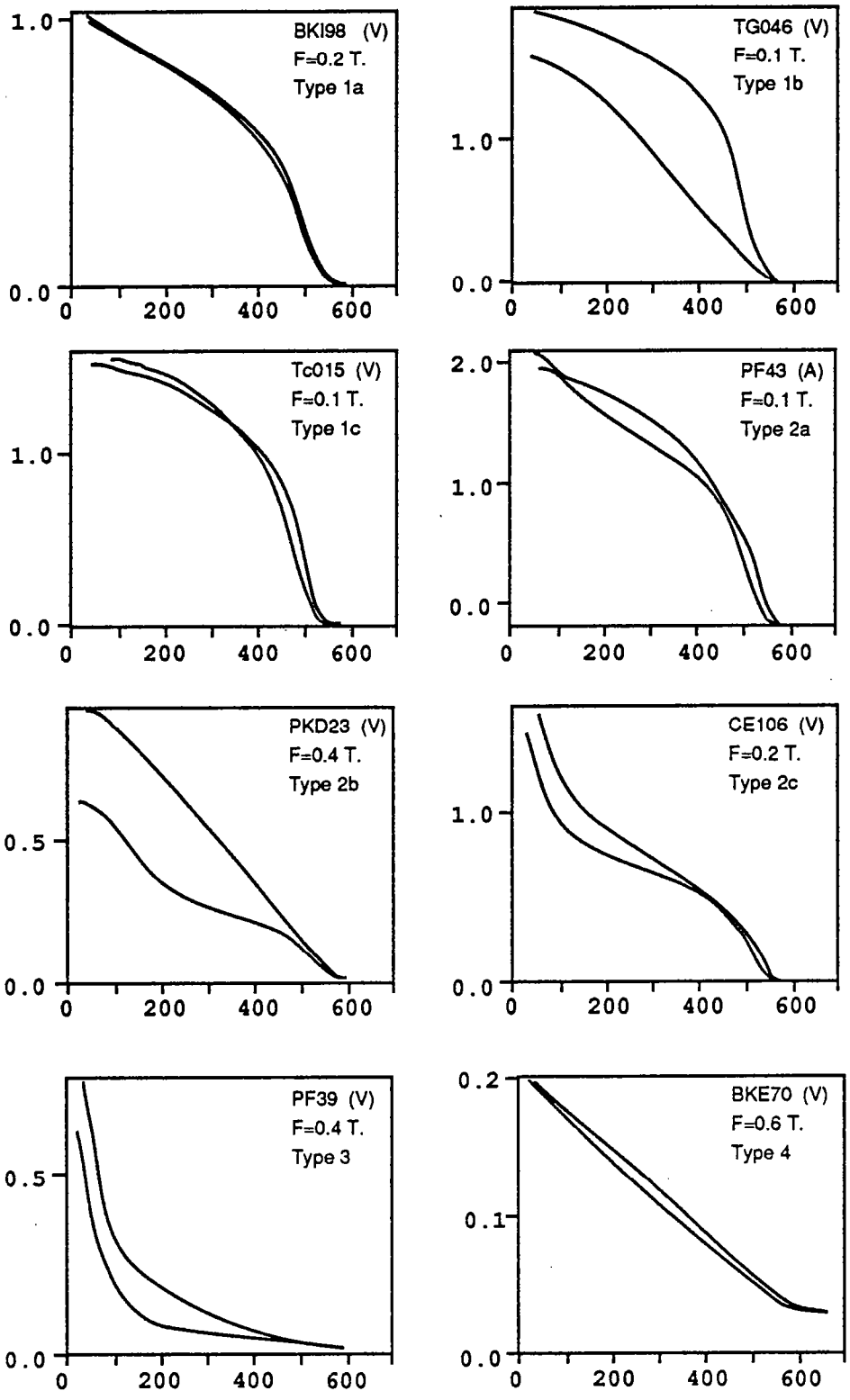

Fig. 11: The four different types of strong field thermomagnetic curves obtained on samples from the island of Tahiti. Analyses were done either in a vacuum (V) or in air (A) with various applied fields from 0.1 to 0.6 Teslas. Arrows indicate heating curves. The unit of the magnetic moment is given in Am^2Kg^{-1}.

temperature deuteric oxidation, or a primary low-Ti titanomagnetite. Discrepancy between the groups 1a, 1b and 1c might result either from low temperature oxidation (that is, maghemitization) which induces non-reversible behavior or minor variations in the magnetic grains or bulk rock [*Mankinen et al.*, 1985].

Type 2 curves were produced by 14 samples and they result from the presence of two ferrimagnetic minerals. Those curves could also be separated into 3 classes. In the case of the class 2a (8 samples), one magnetic phase commonly has a Curie point between 100 and 200°C, while the other phase has a Curie temperature higher than 500°C but, the heating and cooling curves are nearly reversible. In contrast to the previous class, class 2b (9 samples) shows irreversibility, the cooling curves always being above the heating curves. Class 2c curves (7 samples) are also characterized by two Curie points; one above 500° C but the second lower than 100°C and in some cases lower than the room temperature. In all cases, the Curie points of samples were changed only by a few degrees after the experiment. Bimodal Curie temperature samples are commonly observed in flows where high temperature deuteric oxidation has transformed only part of an originally Ti-rich titanomagnetite to a Ti-poor titanomagnetite containing ilmenite lamellae. The high temperature oxidation seems to be more important in the type 2a curve than in the two other categories. The non reproducibility of the heating and cooling curves of group 2b indicates a low temperature oxidation and the lower Curie point might be a cation deficient titanomaghemite but the disproportionation peak has been observed in only one sample. If the amount of low temperature oxidation was not very important, the disproportionation might be indistinguishable from the part of the curve representing the high Curie temperature phase.

Type 3 curves show only one ferrimagnetic mineral with a very low Curie temperature, below 75° C and sometime lower than the room temperature. Either in air or in a vacuum the cooling curves do not retrace the heating curves. Seven samples produce these kinds of curves. This behavior can be related to a Ti-rich titanomagnetite without initial high temperature oxidation and the nonreversibility of the curves is interpreted as the indication that a maghemitization of the titanomagnetites occurred.

Only 3 samples gave type 4 Js-T curves. In this case the Curie temperatures seem to be distributed between 25 and 550° C, indicating multiphase samples.

As the Js-T experiments were carried on selected samples, they do not represent the true distribution of the Curie points over all the flow sequence.

For the paleointensity measurements, we have used only samples exhibiting type 1 Js-T curves.

Interpretation of the NRM-TRM diagrams:

The paleointensity data are represented in this study in NRM-TRM diagrams [*Nagata et al.*, 1963] where the NRM (Y_i) remaining at each temperature step T_i is plotted against the TRM (X_i) acquired from T_i to room temperature in the laboratory field. Ideally all dots should be on a straight line whose slope gives the ratio between the intensity of the ancient geomagnetic field and the laboratory field. But in practice, generally, only one part of the diagram is linear. The temperature at which the secondary magnetizations, such as VRM, are cleaned, determines the lowest limit of the temperature interval which can be used for paleointensity determinations. Because a linear distribution of the points on the NRM-TRM diagram is not a proof of the absence of chemical or physical changes during the Thellier experiment [*Prévot et al.*, 1983], we have to check the stability of the partial TRM acquisition capacity

Table 3: Paleointensity results

Sample	D	I	Js-T	Tc	N	H_{lab}	J_{NRM}	∂T	f	g	q	r	R%	Fe±σFe	F_E±s.d.	<F_E>
R1N85	180.0	37.2	1a	531	15	34	18.8	200-570	0.899	0.891	40.8	0.997	2.6	38.8±0.8		
R1N84	181.1	36.7	1a	562	10	34	12.8	200-530	0.768	0.820	29.5	0.998	2.9	36.6±0.8	37.7±1.6	37.7
R1U128	237.5	9.0'	1a	522	5	9	1.2	370-500	0.434	0.674	8.3	0.998	1.7	3.6±0.1		
R1U127	231.0	8.5	1b	527	6	9	1.1	330-500	0.406	0.738	21.7	0.999	4.3	3.3±0.1	3.4±0.2	3.4
TR067	230.0	0.0	1c	524	14	10	0.3	250-540	0.852	0.909	30.6	0.996	2.8	3.2±0.1		
TR068	229.6	4.7	1a	520	7	20	0.4	350-495	0.328	0.819	4.5	0.991	5.3	3.7±0.2		
TS063	230.8	5.7	1a	560	11	20	0.8	200-505	0.170	0.829	1.8	0.971	28.6	3.8±0.3	3.6±0.3	3.3
CA084	14.0	-26.7	1b	565	9	34	3.5	200-515	0.582	0.857	11.5	0.993	11.9	54.3±2.4		54.3
M2C52	205.0	51.0	*1b	N.d	12	10	0.4	300-540	0.829	0.883	30.5	0.997	2.4	2.6±0.1		
M2C54	210.0	61.0	*1b	N.d	7	15	0.6	300-480	0.242	0.800	3.1	0.990	7.8	2.5±0.2	2.6±0.1	2.6
BKT170	345.0	56.0	1c	527	8	10	1.1	350-500	0.422	0.784	8.8	0.996	11.05	4.0±0.2		4.0
PKC16	222.7	11.8	1c	522	11	20	2.0	350-535	0.601	0.863	16.7	0.996	4.6	6.6±0.2		
PKC17	218.3	10.5	1a	531	13	10	2.0	200-520	0.667	0.867	15.1	0.992	12.0	6.2±0.2		
PKC18	225.8	8.1	1a	533	11	20	2.2	350-535	0.623	0.866	14.1	0.993	3.5	6.2±0.2	6.3±0.2	6.3
BKI97	158.5	-42.6	1a	531	11	20	2.3	350-535	0.518	0.880	9.4	0.990	4.6	6.6±0.3		
BKI98	154.5	-44.1	1a	513	12	20	2.4	200-515	0.386	0.871	9.8	0.994	7.7	8.0±0.3		
BKI99	158.0	-37.0	1a	542	9	10	1.0	350-510	0.495	0.841	5.2	0.977	14.1	8.7±0.7		
BKI100	148.2	-36.5	N.d	N.d	7	10	1.1	410-510	0.385	0.808	3.1	0.975	24.4	8.2±0.8	7.9±0.9	7.7
BKP147	346.5	29.2	*1b	N.d	13	9	0.8	200-550	0.738	0.867	23.6	0.996	18.0	9.0±0.2		
BKP144	348.0	27.6	*1b	N.d	10	9	0.8	200-530	0.558	0.870	12.8	0.994	13.5	8.7±0.3		
BKP148	347.8	25.1	1a	565	9	9	0.8	270-530	0.654	0.841	12.1	0.993	7.0	7.9±0.4		
BKP143	345.9	27.9	N.d	N.d	9	9	0.6	200-515	0.477	0.863	4.8	0.975	18.7	6.9±0.6	8.1±1.0	8.4
BKK114	224.4	-8.0	N.d	N.d	8	9	1.0	200-500	0.360	0.843	5.1	0.989	2.9	9.1±0.5		
BKK113	223.7	1.2	1c	511	11	10	0.8	250-510	0.468	0.840	8..1	0.989	3.2	3.9±0.2	6.5±3.7	6.1
BKB52	182.4	12.7	1a	550	9	34	4.5	200-510	0.469	0.835	8.4	0.992	10.4	28.5±1.3		
BKB47	182.5	8.5	1a	550	11	20	3.9	250-515	0.232	0.873	10.7	0.998	18.5	27.4±0.5	27.9±0.8	27.9

Table 3 D, I are the magnetic declination and inclination of the NRM left in the ∂T interval; Js-T is the type of the thermomagnetic curve; Tc is the Curie temperature of the sample; n is the number of points in the ∂T interval; H_{lab} is the intensity of the laboratory field in μT; J_{NRM} is the intensity of the natural remanence in Am^{-1}; ∂T is the interval of temperature used the determine the paleointensity; f, g, q, are NRM fraction, gap factor, and quality factor respectively (Coe et al., 1978); r is the linear correlation coefficient; R% is the maximum percentage of CRM; Fe is the paleointensity estimate for individual specimen in μT, σ(Fe) is its standard error, F_E is the unweighted average paleointensity of individual lava flow in μT, plus or minus its standard deviation; <F_E> is the weighted mean in μT.

as the heating temperature increases (PTRM checks). Any increase or decay in the TRM acquisition capacity indicates a physico-chemical alteration of the magnetic minerals. Generally, several PTRM checks were performed during each experiment using larger temperature intervals with increasing heating temperature. The acquisition of chemical remanent magnetization (CRM) during the heating in the laboratory field cannot always be detected by the PTRM checks [*Coe et al.*, 1978]. But when the laboratory field and the NRM are not parallel, a movement of the NRM direction toward that of the applied field shows an alteration in the TRM spectrum due to CRM build up. This is easily checked on the orthogonal plots of the NRM demagnetization in sample coordinates. At each temperature step, the first heating is the most efficient in producing chemical changes. This has been verified in measuring the bulk susceptibility at room temperature after both heatings at each step. Small changes in susceptibility are observed after the first heating of each temperature step, while the second heating does not modify the previous value of the susceptibility. As the first heating in the true Thellier method is made while the laboratory field is on, this method seems to be more adequate to detect CRM acquisition than the modified version by *Coe* [1967a] in which the first heating is made in zero field. Indeed, chemical alteration, in zero field, will not enable CRM acquisition. The maximum temperature step which defines the linear part of the NRM-TRM diagram used to calculate the paleointensity is the last temperature step before any evidence of PTRM capacity changes. The linear segment defined in the NRM-TRM diagram where overprint and magnetochemical changes are negligible must contain at least four to five points and span no less than 15% of the total NRM in order to be reliable [*Coe et al.*, 1978, *Prévot et al.*, 1985b]. Special difficulties in the interpretation of the NRM-TRM appear when a curvature of the plot is observed along all the temperature range, while no PRTM capacity alteration is observed. In this case, using the first part of the curve would result in overestimating the paleofield while the last part of the curve would give an underestimate of the paleointensity. This kind of curves can be explained if the magnetic carriers are multidomain grains [*Levi*, 1977] or if the NRM is not a pure TRM. The last hypothesis might be tested by comparing the blocking temperature spectrum and the Curie point [*Prévot*, 1985b]. We will see that in some cases, these two explanations are not valid.

In our experiments, a minimum of 11 temperature steps were performed. The statistical method developed by *Coe et al.* [1978] was used to obtain the slope b of the straight line, its corresponding relative standard error σ_b and the standard error $\sigma(Fe)$ about the paleofied intensity: Fe (σ(Fe)=Fe*σ_b). The validity of the paleointensity determinations were expressed using the quality factor q estimated from the NRM fraction used f, the gap factor g and the scattering of the plot about the linear segment. An indication of the potential for error caused by CRM acquisition is given for each sample by the factor R, as defined by *Coe et al.* [1984]. It represents the maximum error, in percent of the laboratory field, that CRM *would* cause in the paleointensity estimate. Within a single volcanic unit, the average paleointensity was calculated using the weighting factor w, defined by *Prévot et al.* [1985b], the uncertainty about the mean was expressed by the standard deviation of the unweighted average.

Results

Paleointensity determinations were attempted on 48 samples, 26 of which have given reliable results on 11 distinct lava flows (Table 3).

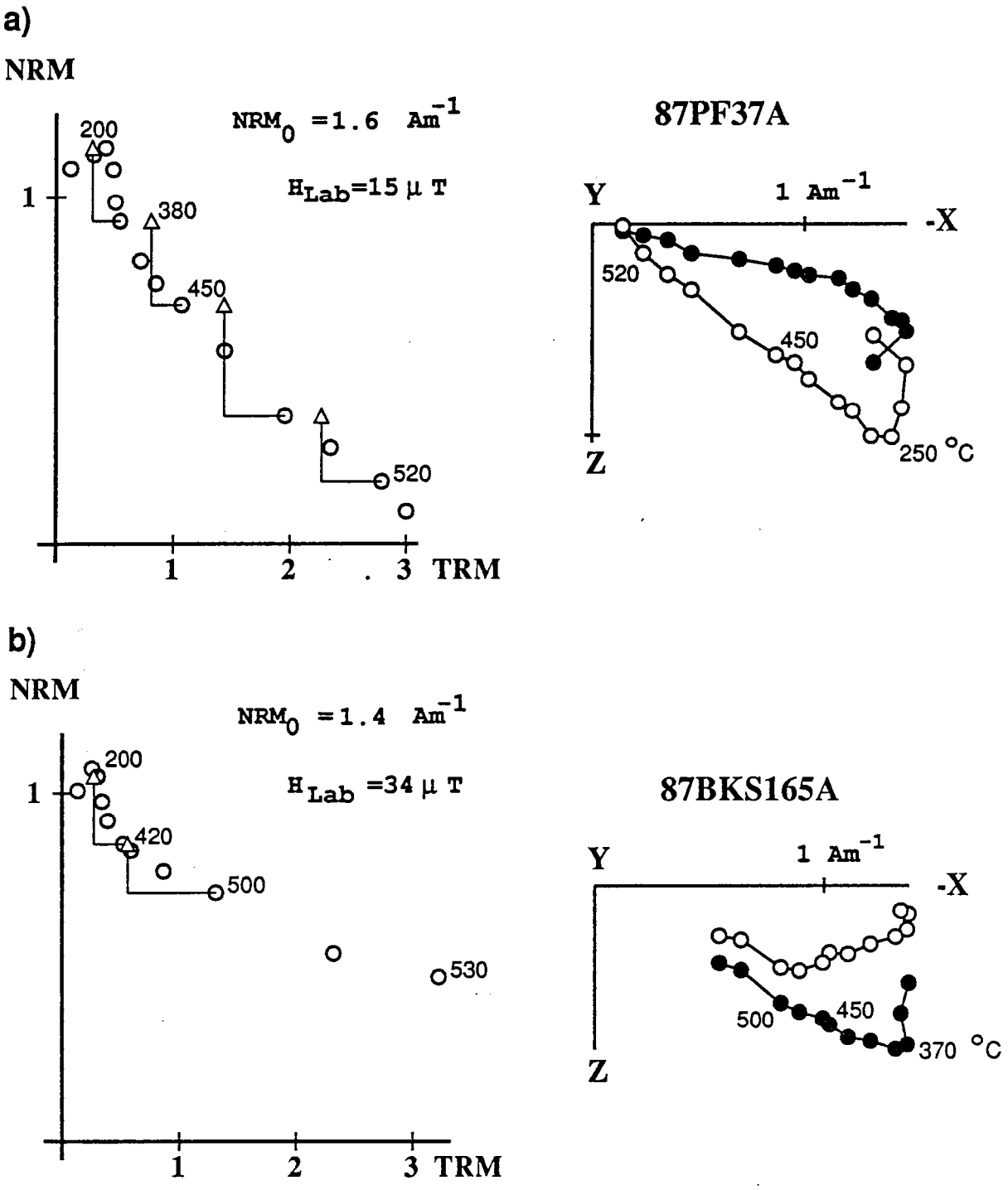

Fig. 12: NRM-TRM diagrams (normalized to the original remanence) showing non ideal behavior during paleointensity determination. Orthogonal plots in sample coordinates represent the evolution of the remanent vector during the experiment. NRM_0: initial remanent magnetization of the sample; H_L: intensity of the laboratory field in μT. Sample 87PF37A shows negative PTRM checks indicating that magnetic alteration occurred early in the experiment. Sample 87BKS165 shows acceptable PTRM checks, but the shape of the NRM-TRM plot also suggests non ideal behavior. The inclination moves toward the direction of the applied field which is vertical

Two types of non-ideal behavior occurred during the Thellier experiments. The first type is constituted by samples for which the evolution in the PTRM capacity begins at low temperature, generally just after the cleaning of the secondary component. Sample PF37a is one example (Figure 12a) for which the overprint is cleaned at 250°C, while the first PTRM check at 380°C shows a decrease in the TRM acquisition capacity, indicating that physico-chemical changes occurred. All the following PTRM checks suggest an increase in the TRM capacity, but the remanent direction is not altered. This might indicate that the variation in the TRM acquisition capacity does not result in an acquisition of CRM. If such evolutions are not detected, they will lead to an overestimated paleointensity in the lower temperature range followed by a possible underestimate in the higher temperature range. In the other case, sample BKS165 (Figure 12b), the PTRM checks are successful but the ratio NRM/TRM does not plot on a straight line; the shape of the plot indicates that the sample altered during heating in the laboratory field. The orthogonal vector plot, in samples coordinates, shows that the vertical component of the natural remanence moved slowly toward the direction of the applied field, which is vertical downward during the first heating of each temperature step. This indicates that alteration is producing a small component of chemical remanent magnetization, with higher blocking temperatures that persists during the next heating. Obviously in these two cases, the linear part of the NRM-TRM diagram is too short and not reliable; thus no paleointensity has been determined.

More common and more difficult to understand than the two previous examples is the evolution during the Thellier experiment shown by samples PKE29a and PE30c (Figure 13 a,b). No alteration of the magnetic mineral is shown either by the PTRM checks or by the evolution of the remanent vector. These samples have no secondary component of magnetization and high blocking temperatures in good agreement with their Curie points. But, all the dots are distributed on a concave up curve. Depending on whether the paleointensity is calculated on the first part or on the last part of the curve, the result can change by a factor of two. The curvature of the diagram can be expected if the remanence is carried by MD particles [*Levi*, 1977]. But as it has been said, only cores with medium demagnetizing field (MDF) greater than 30 mT were used. This value and the shape of the af demagnetization curves [*Dunlop*, 1983] indicate that the magnetic carriers are SD or PSD grains. Some mechanisms which could produce non-ideal behavior during the Thellier experiment have been discussed by *Coe* [1967b]. Among these, the effect of the demagnetizing field, which results from interaction of the grains on each other and the non-linearity of the TRM with field have been considered. The last case can be expected if the flow cooled in a field which was greatly higher or lower than the laboratory field. This curvature of the NRM-TRM plot is observed either in samples with a normal or reversed polarity and samples from transitional zones. In each paleointensity experiment, we have tried to work with a realistic laboratory field, that is, a field close to the expected strength of the Earth's magnetic field, so the large differences from the ideal behavior that we observe would indicate an important non-linearity of the acquisition of TRM, greater than what is expected from different studies [*Day*, 1977].

Effect of the demagnetizing field can be expected if the lava flow is strongly magnetized but, the NRM intensity of our samples is not particularly high, and, even low in the case of intermediate directions. Thus, these two mechanisms are unsuccessful in explaining our data. Such effects, as high concentration of magnetic particles, impurities or movement of dislocation in the crystals or change of

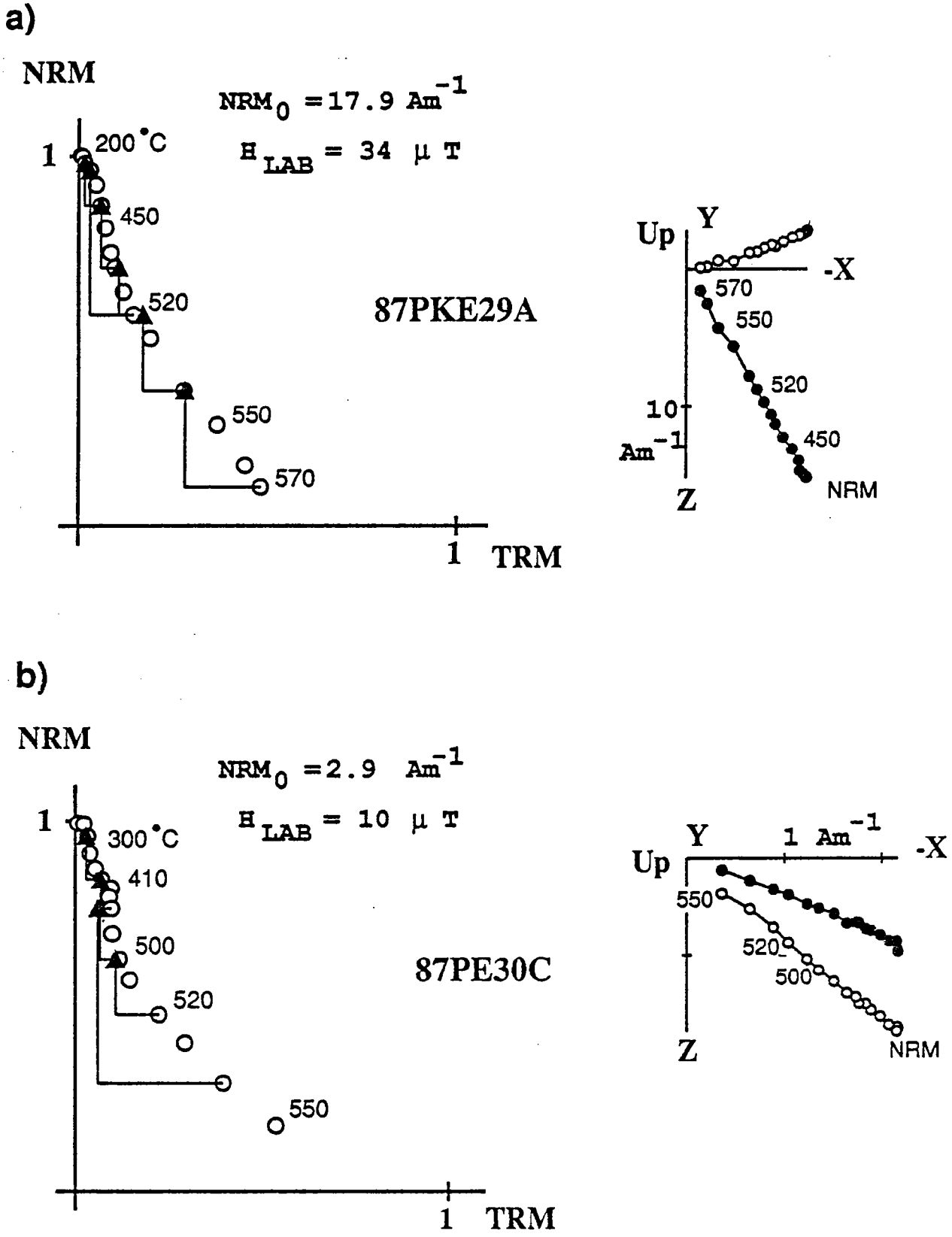

Fig. 13: Typical non-ideal behavior in Thellier and Thellier paleointensitiy experiments, NRM-TRM diagrams and orthogonal vector plot in sample coordinates. Samples 87PKE29A and 87PE30C show concave up behavior with positive PTRM checks. These two samples have high unblocking temperature and almost no VRM components as seen on the orthogonal plots. On the other hand, they have high and medium intensities of magnetization indicating that the curvature might not be related to the internal demagnetizing field. Selecting only part of the curves will result in high or low paleointensities.

the stress induced by heating might be considered but are not easily identified. Even if the true mechanism responsible for this curvature is not yet fully understood, it appears necessary to perform the experiment with numerous temperature steps up to a complete demagnetization of the NRM, because a straight line might be fitted only on a few points from a small portion of a large curvature of the NRM-TRM plot. All the samples showing this behavior have been rejected. We notice also that the Js-T curves are unable to predict such special behavior, obviously because the induced magnetization is less sensitive to as many factors as the TRM.

Nevertheless, more than half of our selected samples have provided reliable results. Most of them are determined with 5 to 15 points, a NRM fraction typically close to 50%, and a quality factor q around 10. The highest temperatures used are generally close to the Curie point, and at least near 500°C, which indicate a good thermal stability of the samples. The laboratory Koenigsberger ratio (Q_l) [*Prévot et al.*, 1985b] has been calculated for each sample, and the average value is 13.8, with data extended from 5 to 63. The mean Q_l is similar to the one obtained by *Prévot et al.* [1985b] in the most stable samples from the Steens Mountain. Some paleointensity diagrams are shown in Figure 14 and results are summarized in Table 3 and Figure 15. On Figure 14, the demagnetization diagram of the NRM during the Thellier experiment is also shown. We notice that the NRM is determined by substracting two opposite partial TRMs at each step. Thus, the very low noise observed on the orthogonal projections enhances the quality of these experiments.

Four paleointensity determinations have been obtained on two reverse polarity flows; the flow R1N which precedes the Matuyama-Bruhnes reversal and the flow BKB before the Cobb Mountain transition. Only one experiment has been successful on one flow from the Jaramillo normal polarity subchron (flow CA). The results are close to the expected value at this latitude, from 27.1 to 54.3 μT and are in good agreement with those obtained in previous studies [*Senanayake et al.*, 1982].

Twenty-one paleointensity results from 8 distinct lava flows were obtained from 3 transitional zones: 14 paleointensity values from the Cobb Mountain transition (5 flows), 2 results from the Upper Jaramillo (1 flow) and 5 results from the Matuyama-Brunhes (2 flows). For the Cobb Mountain transition, the paleofields obtained are between 4 and 8.4 μT. A lower value was obtained for the Upper Jaramillo transition with a field strength for the flow M2C of 2.6 μT. The two flows from the Matuyama-Bruhnes transition also give very low paleointensities from 3.4 to 3.6 μT. Good consistency between samples from the same flow is observed, except in the case of the flow BKK. Our results shows a very weak geomagnetic field during each transition, the greater transitional paleointensity obtained is 8.4 μT and the lower is 2.6 μT. Inspecting Table 2 and Table 3, we can see that some transitional flows which have different NRM intensity, give in fact the same paleointensity. This is, for example, the case for the flows R1U and TR. The discrepancy in the NRM intensities can be easily explained by the difference in the oxidation state of the two flows. If the Js-T curve indicates that the magnetic carriers in these two lava flows are Ti-poor titanomagnetites resulting probably from a deuteric oxidation, the lower value of Js for the flow TR and also its red color show that this flow has been more strongly high-temperature oxidized, with probable formation of hematite. Therefore, small differences in NRM intensities may also reflect some differences in the magnetic mineralogy.

NRM

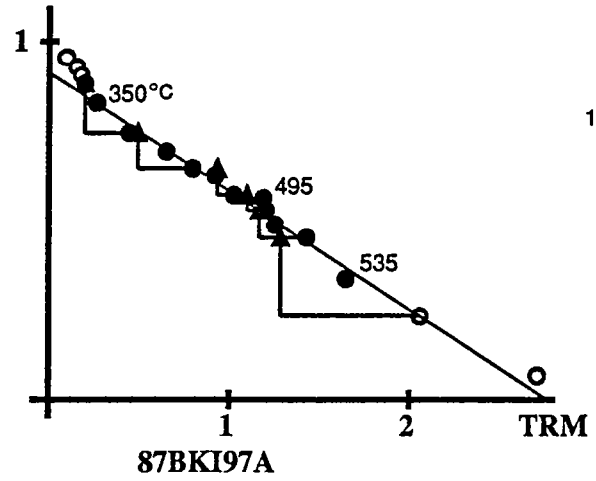

87BKI97A

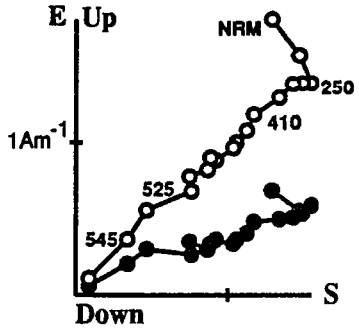

87BKI97A (IS)

NRM

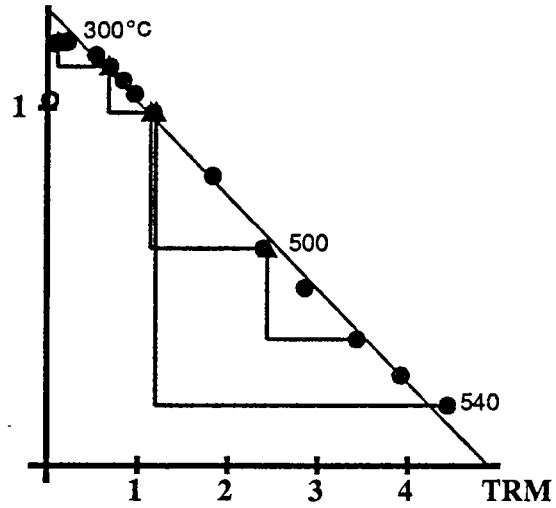

87M2C52A

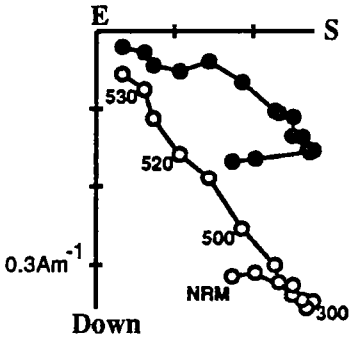

87M2C52A (IS)

NRM

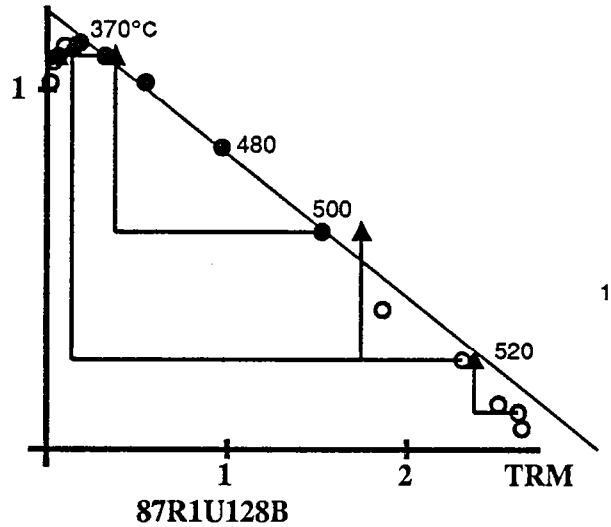

87R1U128B

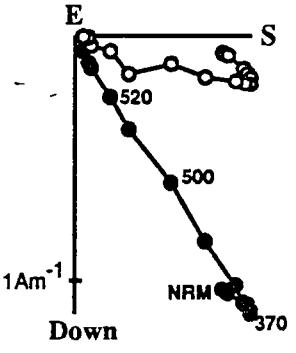

87R1U128B (IS)

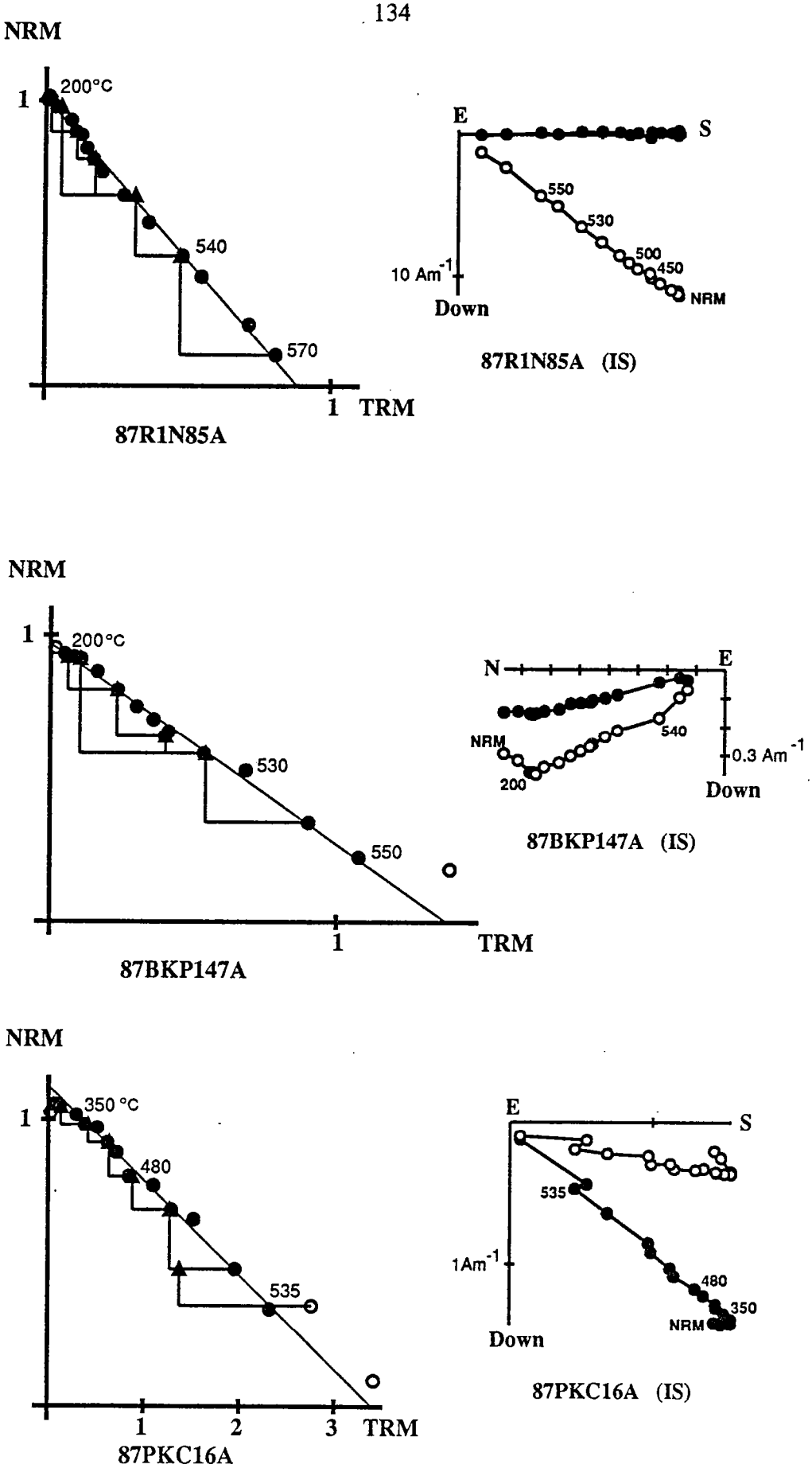

Fig. 14: Arai-diagrams of very accurate paleointensity determinations where the paleointensity is determined using a large portion of the NRM left. NRM_0 is the initial intensity of magnetization of the sample, Q the quality factor, H_{lab} the laboratory field and H the paleointensity obtained (in μT). Here, the orthogonal plots show the evolution of the remanent vector in geographical (in situ) coordinates.

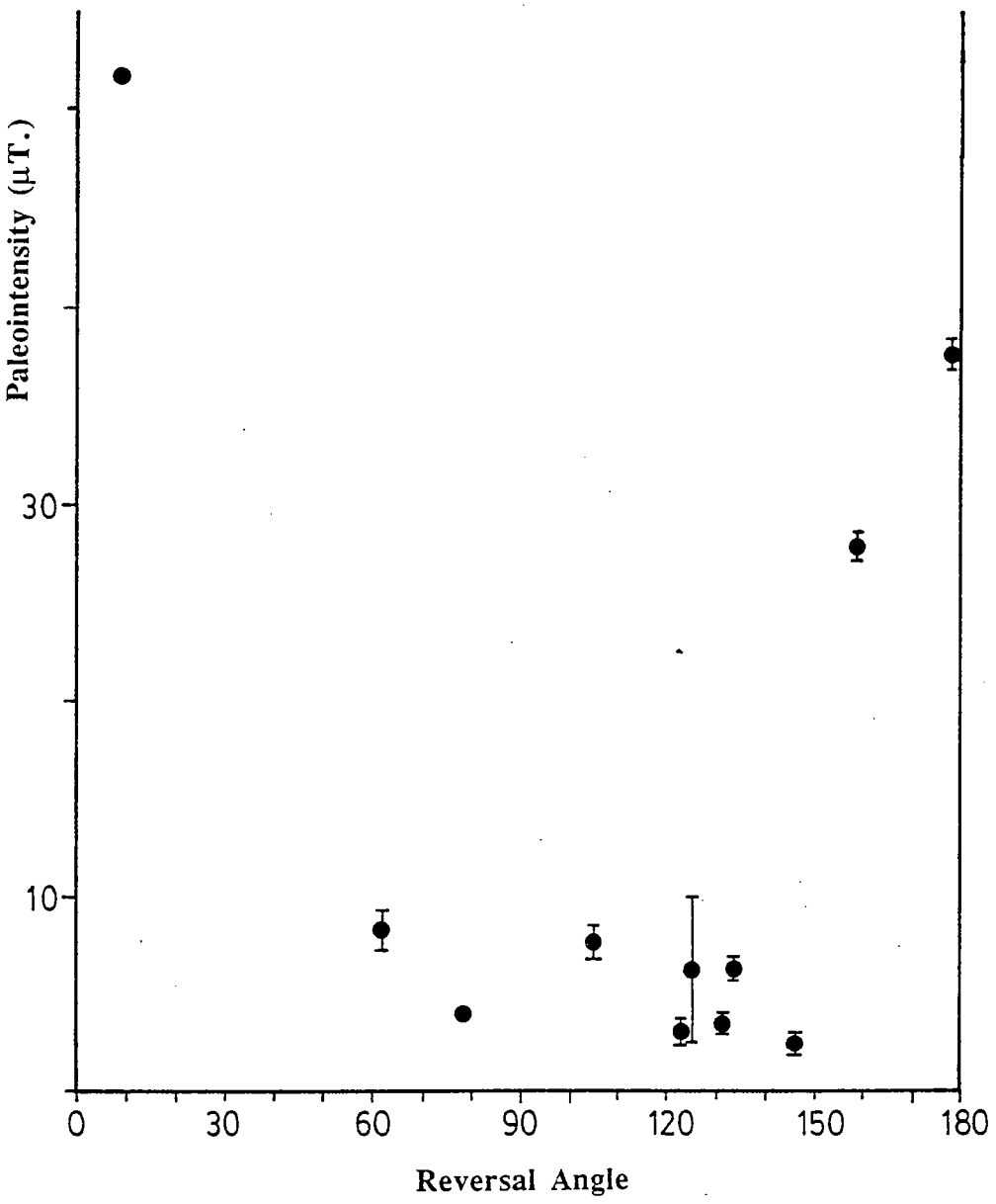

Fig. 15: Diagram showing the evolution of the mean paleointensities per flow with their standard deviation bars, versus the angular departure from the axial normal dipole. Paleointensities obtained from the intermediate flows are below 10 μT.

The ratio of the non-transitional intensity and the intensity of the field during its intermediate state varies from one fourth to less than one tenth.

9 Discussion

The Cobb event: Excursion or short normal polarity event?

An apparent R-R excursion of the Earth's magnetic field, dated around 1.1 Ma, is recorded in the volcanic sequence from Tahiti. Several paleomagnetic reports from marine or terrestrial sediments and volcanic rocks have suggested that a complete reversal of polarity occurred at that time but this event has not yet been classified in the main polarity time scales [*Mankinen and Dalrymple*, 1979; *Harland et al.*, 1982]. Therefore, a review of available data appears to be necessary.

The study of marine magnetic anomalies has enabled the recognition of the main features of the polarity sequence but short events with time duration of the order of 10,000 years are difficult to recognize. On half of 14 magnetic profiles from a survey over the east Pacific Rise Crest, *Rea and Blakely* [1975] have identified a small positive magnetic anomaly centered around 1.1 Ma. They argue that the identification of this short magnetic anomaly as a geomagnetic event was only tentative, because this brief period of normal polarity does not show up well in their average profile.

Magnetostratigraphic studies of marine sediment cores and from pliocene continental deposits have, in some cases, revealed the existence of a short event before the Jaramillo subchron. But, discontinuous sampling of the core as well as the time averaging process in the acquisition of the magnetic remanence have often given poor magnetic signatures.

An anomalous change in inclination before the Jaramillo normal subchron was found in one marine sediment core from the north Pacific [*Ninkovich et al*, 1966] and transitional directions were reported from two deep-sea calcareous sediments from the Melanesian basin [*Kawai et al.*, 1977; *Sueishi et al.*, 1979]. In this last case, the excursion has been dated at 1.06 Ma, according to the depth of the major boundaries of polarity epoches and the sedimentation rate.

A complete reversal was suggested in one deep-sea core from the equatorial Pacific [*Forster and Opdyke*, 1970] and four cores from the Southern Ocean [*Watkins*, 1968], from which the normal polarity zone was dated around 1.07 Ma.

Kochegura and Zubakov [1978] summarized the results of their magnetostratigraphic studies of the marine and loess deposits of the Ponto-Caspian zone of USSR, and showed a normal polarity period just before the Jaramillo, occurring around 1.1 Ma; but no information on their paleomagnetic data are presented, making the quality of these results difficult to assess.

More recently, in the vicinity of the magnetozone correlated to the Jaramillo, several intervals of anomalous directions of magnetization have been observed on deep-sea cores from the Caribbean site 502 [*Kent and Spariosu*, 1982]. The most detailed record of an event of normal polarity preceding the Jaramillo sub-chron was obtained from sediment cores from the north Atlantic [*Clement and Kent*, 1986]. It has been dated around 1.16 Ma, according to a constant sedimentation rate, and the depths of the the major polarity chrons, and its time duration is estimated to be 11,600 years. Nevertheless, the normal period in this record is disrupted by very shallow inclinations and the authors argue that the proximity of this large directional swing to the upper transitional zone, and the occurrence within an

intensity minima, suggest that they are part of the transitional behavior. Thus, the true normal period might be as short as 5,000 years.

Some normal or intermediate directions have also been found, in several places, on volcanic flows dated around 1.1 Ma., but the imprecision in radiometric dating was often great enough to not dismiss the possibility of dealing with the Jaramillo subchron.

The name Cobb Mountain was given by *Mankinen et al.*[1978] to an event which, for the first time, was found in a volcanic unit, a composite rhyolite and dacite dome, situated in northern California. K-Ar datings have given an age of 1.12±0.02 Ma. Transitional directions were clearly recorded on 5 sites of rhyolites, while the normal polarity was only defined by a strong normal overprint at one particular locality, where the rock is completely devitrified. Because no evidence of late hydrothermal alteration was found on the Cobb Mountain, *Mankinen et al.* argue that this devitrification was caused by deuteric alteration which could have started shortly after eruption. Therefore the NRM direction was considered as representing a complete change from reversed to normal polarity during the cooling of the rhyolite.

One intermediate polarity lava flow dated by K-Ar at 1.13 ±0.08 Ma and six flows with a normal polarity with age from 1.07 to 1.37 Ma have been reported by *Briden et al.* [1979] in their study of volcanic rocks from the islands of St. Vincent and La Guadeloupe, in the Lesser Antilles. In the island of Madeira, one normally magnetized basalt dated at 1.15 Ma has been found by *Watkins and Abdel-Monem* [1971]. Using the new constants in K-Ar datings [*Mankinen and Dalrymple*, 1979], this age became 1.18 Ma.

More recently two basalts flows in Cosa Range, California with a normal polarity have given an age about 1.08 Ma, close to the previous one obtained on the Cobb Mountain [*Mankinen and Gromme*, 1982]. However the age uncertainties are quite large for these two flows (around 12%).

Normal polarities from volcanic units with ages around 1.05 Ma. have also been reported by *Fleck et al.*, [1972] in south Argentina, *Abdel-Monem et al.*, [1972] in the island of Tenerife and *McDougall and Chamalaun* [1966] in the island of La Reunion. However it should be noticed that no information concerning the polarity of the flows above and below was available. Thus, the interpretation must rely only on the K-Ar results.

A normal polarity period, preceding the Jaramillo, was found in an ash layer and adjacent sediments from the deposits of the Osaka group (Japan) [*Maenaka*, 1979]. The ash horizon has given a fission track age of 1.1±0.01 Ma. But, the use of only one level of af cleaning might have not been sufficient to remove a possible strong normal overprint.

This review shows the difficulty in identifying a short geomagnetic event either in sediment or volcanic units. However, there is now strong evidence for a worldwide geomagnetic feature of either a short event or an excursion around 1.1 Ma. Our data from the Punaru valley suggest that the field did not reach a full normal polarity. Nevertheless, the detailed record from core 609b [*Clement and Kent*, 1987] suggests a very short time for the normal period. Therefore, such a short normal polarity might correspond to a hiatus in the volcanic activity at that time and only the transitional boundaries were recorded.

Comparison of the transitional field characteristics with other available records:

A comparison of the intermediate states of the field observed at different sites for a single reversal may provide a clue to the understanding of the geomagnetic process. To do that, a review of the other records are necessary. We will not argue in detail about the reliability of previously published data sets. Nevertheless, we think that not enough caution has been taken in interpreting some sedimentary records.

1 The Cobb Mountain

As discussed before, the most detailed record concerning the Cobb event was reported from hydraulic piston cored sediments by *Clement and Kent* [1987]. This record has one main characteristic in that while the declination exhibits very short transition for both the onset and the termination of the normal polarity period, large variations in inclination occurs before and after the transitions as defined by the declination. We already mentioned in the discussion about the nature of the Cobb that an important shallowing of the inclination is also reported in the normal polarity period as defined with the declination pattern by Clement and Kent. The VGPs associated with these intermediate directions are almost confined in the meridian plane containing the site and show a well defined antisymmetry between the onset and the termination.

In the record from French Polynesia, we observed three different groups of intermediate directions. Obviously, they represent only a few snapshots of the transition (if it is an excursion) or (we cannot rule out this possibility) for one or both transitions limiting an eventual normal polarity event. Two groups satisfied the criteria of axysymmetry. On the other hand, the VGPs associated with our intermediate directions clearly disagree with those obtained by *Mankinen et al.*[1978] on the Cobb Mountain.

Reliable paleointensities have been obtained for these flows with fields from 4 to 8 μT. There is no evidence for a strong intermediate state. In the hypothesis of an excursion, these data show that the intermediate field during the Cobb Mountain has similar characteristics to those observed during polarity reversal, supporting the interpretation of excursions as aborted reversals (*Hoffman, 1981b*).

2 Lower and Upper Jaramillo

Up to now, deep-sea sedimentary core records of the transitions delimiting the Jaramillo have been obtained in the Indian Ocean [*Opdyke et al.*, 1973, *Clement and Kent*, 1984, 1985], in the north Atlantic ocean [*Clement and Kent*, 1986] and Pacific ocean [*Hammond et al.*, 1979; *Herrero-Bervera and Theyer*, 1986, *Theyer et al.*, 1985]. From volcanic records, a few intermediate directions come from the study of *Mankinen et al.* [1981] on Clear Lake (California).

Data from deep-sea cores from the Pacific ocean are, in our opinion, difficult to interpret, simply because of the very low sedimentation rates as low as 6 mm/10^3 years [*Hammond et al.* 1979] or 7.8 mm/10^3 years [*Theyer et al.*, 1985]. If the remanence is a DRM, as detailed as can be the sampling technique, each sample represents an average of the paleomagnetic signal over a great period of time; in the case of a PDRM (post-detrital remanent magnetization), the transition can be completely missed or the directions observed can differ completely from the true configuration of the intermediate geomagnetic field [*Valet*, 1985; *Hoffman and Slade*, 1986].

Records of the lower Jaramillo from the terrestrial sediments were described by *Gurarii* [1981], from the territory of western Turkmenia (USSR) but, since the remanence is carried by two magnetic minerals, hematite and magnetite, the nature of the magnetic remanence (detrital and chemical) is unclear.

Herrero-Bervera and Theyer [1986] have presented a non-axisymmetric behavior of the field during the upper Jaramillo recorded by deep-sea sediments from a site near Hawaii (sedimentation rate 35 mm/10^3 years). This record is mostly characterized by oscillations between reverse and normal. This behavior may question the possibility that antipodal magnetizations are present in the samples. Assuming that their record is reliable will lead to the conclusion that transitional fields recorded at a site at a low north latitude in the same longitudinal band as the Society islands have no common features with those recorded at Tahiti.

Following *Opdyke et al.* [1973], the record of the Upper Jaramillo transition in deep-sea sediments from the Indian Ocean [*Opdyke et al.*, 1973 and later *Clement and Kent*, 1985] showed evidence of bioturbation, which might well have acted to smooth the transition.

The sediments from the north Atlantic ocean [*Clement and Kent*, 1986], which are characterized by a sedimentation rate of 82 mm/10^3 years, have given a record of the Upper Jaramillo in which full normal polarity directions are not observed at the base of the sampling zone, and therefore the lower boundary of the transition is not defined. So we are beside the disappointing conclusion that no fully reliable data are available for comparison with our detailed record from the Upper Jaramillo.

Only one accurate paleointensity was obtained for the upper Jaramillo transition (Table 3) showing a field strength close to 2.6 μT, but all the NRM intensity data indicate that the intensity of the field might have stayed particularly low during this reversal.

As it was already pointed out, an intermediate direction associated to a low NRM intensity is observed on the flow R1D which follows the Jaramillo termination transition. This direction has an angular departure of almost 40° from the full reversed polarity.

This is not the first time that a brief polarity fluctuation is described close to that polarity boundary. *Clement and Kent* [1986] observed a 60° swing in the inclination just after the upper Jaramillo transition. On the lava flows of the Clear Lake zone (California) [*Mankinen et al.*, 1981] a sequence of intermediate polarity lava, younger than the reversed lava showing the end of the Jaramillo termination has been found. The K-Ar age obtained on one of the intermediate flows (0.90 ± 0.02 Ma) is indistinguishable from the age of the end of the upper Jaramillo transition, suggesting that the brief intermediate state observed is part of the reversal boundary, and represents what is generally called a rebound effect [*Prévot et al.*, 1985b; *Laj et al*, 1987, 1988]. Our data from flow R1D can be interpreted in this way. However we must notice that some data from Clear Lake and deep-sea sediments from the Southern ocean [*Watkins*, 1968], suggest that a polarity event might also have occured at about 0.83-0.85 Ma, which could also explain the direction of flow R1D. Without an estimate of the age of this flow, we cannot choose between these two hypotheses.

Only a few intermediate directions are present in our record, but it is the first time that absolute paleointensity data have been obtained for this reversal. At least for the part of the transition recorded in the Tahiti section, the field was low (3μT).

There are multiple sedimentary records of this reversal. A strong dependence of the VGP path during the reversal with the longitude of the observation sites was first pointed out by *Fuller et al.* [1979]. However, careful examination of the data convinced us that some sediments have not accurately recorded the weak geomagnetic field and that the geometry of the transitional field might not be as simple as recently proposed by *Hoffman* [1988].

In the case of the Japanese record [*Niitsuma et al.*, 1971], the NRM intensity data are scattered and no clear variation of the intensity can be observed. With sediments from the mid-northern and equatorial Pacific [*Clement et al.*, 1982], dissimilar VGP paths have been obtained from two nearby cores, and an increased dispersion in directions is observed within the transitional zone. These observations suggested to *Clement et al.* that some sedimentological factors have probably distorted the magnetization of these sediments characterized by a low sedimentation rate (7 to 11 mm/10^3 years).

The accuracy of some paleomagnetic techniques to clearly isolate the primary remanent direction (if it still exists and has not been replaced by subsequent geochemical processes [*Karlin et al.*, 1987]) constitutes one of the major problems. The lake Tecopa record [*Hillhouse and Cox*, 1976] has been considered during a long time as one of the most reliable records of the last polarity reversal. However, a resampling of the section and new data obtained by thermal demagnetization [*Valet et al.*, 1988a] shows clearly that strong magnetic overprints are not removed by af demagnetizations. The previous intermediate directions were the result of a superimposition of reverse and normal components of magnetization, and were of no meaning for the understanding of the reversal. Although *Valet et al.* [1988] clearly shows that af demagnetization did not isolate a primary component, they do not demonstrate in a convincing manner that the intermediate directions isolated by thermal demagnetization are meaningful.

Recently, data from the equatorial Atlantic ocean (site 664) have been reported on deep-sea sedimentary cores [*Valet et al.*, 1988c]. In comparing the VGP path they obtained with deep-sea core results from a site of the same longitude (site 609), but situated at a mid-northern latitude [*Clement and Kent*, 1986], *Valet et al.* show that the two records provide antipodal VGP paths, located over America (site 609) and Asia (site 664), a fact that cannot be reconciled with a simple axial geometry of the transitional field.

Obviously, even for this 'well' documented reversal, a close look at the data shows that more accurate paleomagnetic records are still needed for a better description of the transitional field.

The second part of this discussion will include some of the results obtained on the island of Huahine [*Roperch and Duncan*, this issue).

Zonal and non-zonal components:

East and west intermediate directions are more numerous in the record of the N-T-N excursion of Huahine than in the record from Tahiti which shows less deviations from the North/South vertical plane. *Prévot at al.* [1985b), suggested that non zonal components are as important as the components lying

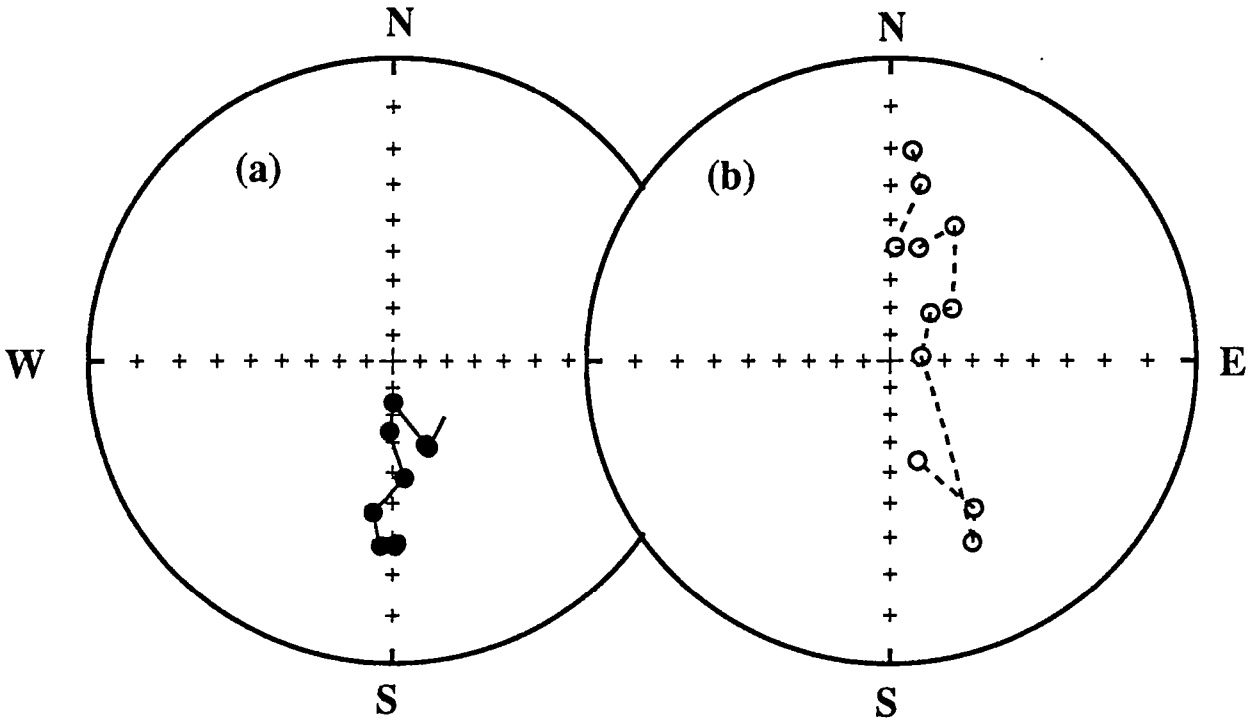

Fig. 16: Equal area projections of paleomagnetic directions observed at the beginning of the N-N Huahine excursion (b) and the lower Jaramillo transition (a) recorded at Tahiti. In these two cases, the directions go through high inclinations, leading us to suggest that the beginning of a transition might be controlled by axisymmetric components of the field.

Table 4 Average NRM intensities

	Tahiti			Huahine			Tahiti+Huahine		
∂(°)	N	Jn	err	N	Jn	err	N	Jn	err
10	29	4.9	0.93	16	4.8	0.48	45	4.8	0.63
20	34	3.7	0.42	12	2.8	0.52	46	3.5	0.34
30	11	2.6	0.88	5	1.2	0.58	16	2.0	0.66
40	3	0.8	0.72	15	0.7	0.47	18	0.7	0.40
50	11	0.7	0.12	5	0.9	0.33	16	0.7	0.14
60	7	0.6	0.13	4	0.5	0.38	11	0.6	0.15
70	6	0.5	0.08	5	1.1	0.23	11	0.7	0.14
80	10	0.4	0.15	14	0.7	0.24	24	0.6	0.15
90	8	0.6	0.13	25	0.8	0.20	33	0.8	0.15

VGP	Tahiti			Huahine			Tahiti+Huahine		
latitude	N	Jn	err	N	Jn	err	N	Jn	err
90	38	4.3	0.75	20	3.9	0.49	58	4.2	0.52
80	31	4.0	0.48	13	1.9	0.50	44	3.2	0.38
70	6	1.9	1.30	5	0.6	0.46	11	1.1	0.78
60	8	0.4	0.08	11	1.0	0.61	19	0.7	0.37
50	19	0.8	0.08	5	0.8	0.30	24	0.8	0.09
40	6	0.6	0.06	7	0.7	0.27	13	0.6	0.15
30	2	0.8	0.38	9	0.4	0.11	11	0.5	0.11
20	7	0.3	0.15	24	0.9	0.19	31	0.7	0.16
10	2	0.2	0.04	7	0.3	0.41	9	0.9	0.37

Table 4 Geometric means of NRM intensities (at 10 mT), by 10° intervals in reversal angles (∂) and in VGPs latitude, plus or minus standard errors.

within the geographical meridian during transitions. However, from our data from Polynesia, we might speculate that transitions may have two different configurations for the beginning and the middle of the reversal.

As it is often the case for transitions recorded in lava sequence, the timing of the reversal is not well controlled. However for the record from Huahine, and the record of the lower Jaramillo at Tahiti, it seems that the beginning of these two transitions have been well sampled by the lava flows. In the two cases (Fig.16), the first part of the transition is strongly axisymmetric, while in the case of the excursion, the following part of the record is less controlled [*Roperch and Duncan*, this issue]. The path through high inclinations observed for these two opposite reversals may be fit with a decaying dipole and a growing quadrupole field having the same sign than the initial dipole.

Some other volcanic records show less clearly a trend toward axisymmetry at the onset of reversal [*Prévot at al.*, 1985b] and *Hoffman* has noticed the same predominance of the zonal terms at the beginning of some records of the Matuyama-Bruhnes reversal [*Hoffman*, 1982, 1985]. *Williams and Fuller* [1988] have suggested that the energy of the decreasing dipole is redistributed in the other low order zonal harmonics. Our data lead us to speculate that a significant difference in the transitional field geometry might exist between the beginning of the reversal controlled by axisymmetric components and the following phase, more complex. This hypothesis might find some theoretical support, since *Hide* [1981]. suggested that decaying magnetic fields may have an axis of symmetry while growing, or steady fields might exhibit large departures from axial symmetry. On the other hand, *Merrill and McFadden* [1988] argue that a reversal may occur if the axial dipole field is low and the quadrupole family field is high. In this case, the quadrupole family may be dominated by the axial quadrupole field.

Variation in the intensity:

a) Intensity of the NRM versus directions or VGPs

As it has already been said, the NRM intensities (at 10 mT) can reflect in average the variations in the geomagnetic field intensity. All the NRM intensity data from Huahine and Tahiti have been grouped by ten degree intervals in reversal angles and VGP's latitudes; then, arithmetic and geometric mean values were calculated for each group (Fig.17 a, b). The standard error bars have been reported for the arithmetic means. Differences between arithmetic and geometric averages underline the scatter in each data set. As the NRM intensity depends on the strength of the geomagnetic field and the magnetic mineralogy of rocks, it seems reasonable to add simply the two data sets from Huahine and from Tahiti. Indeed, these data are from the same geographical area and the volcanic rocks which compose these two islands come from the same kind of magma. In Table 4 are reported the average values, within each reversal angle group, of the NRM data for Tahiti, Huahine and for the both islands. In combining the two data sets the number of lava flows used is quite large (220), and we hope it is sufficient to assume that short-term field paleointensity variations and NRM intensity fluctuations due to rock magnetic properties have been averaged. An important drop in intensity is observed for reversal angles between 0 and 30° or VGP's latitudes higher than 70-60°. For higher reversal angles (i.e., lower VGP's latitudes), the intensities stay very low, lower or around 1 A/m. The same result is obtained using either the data from Huahine or Tahiti, giving us some confidence in the observed distribution. This behavior in the

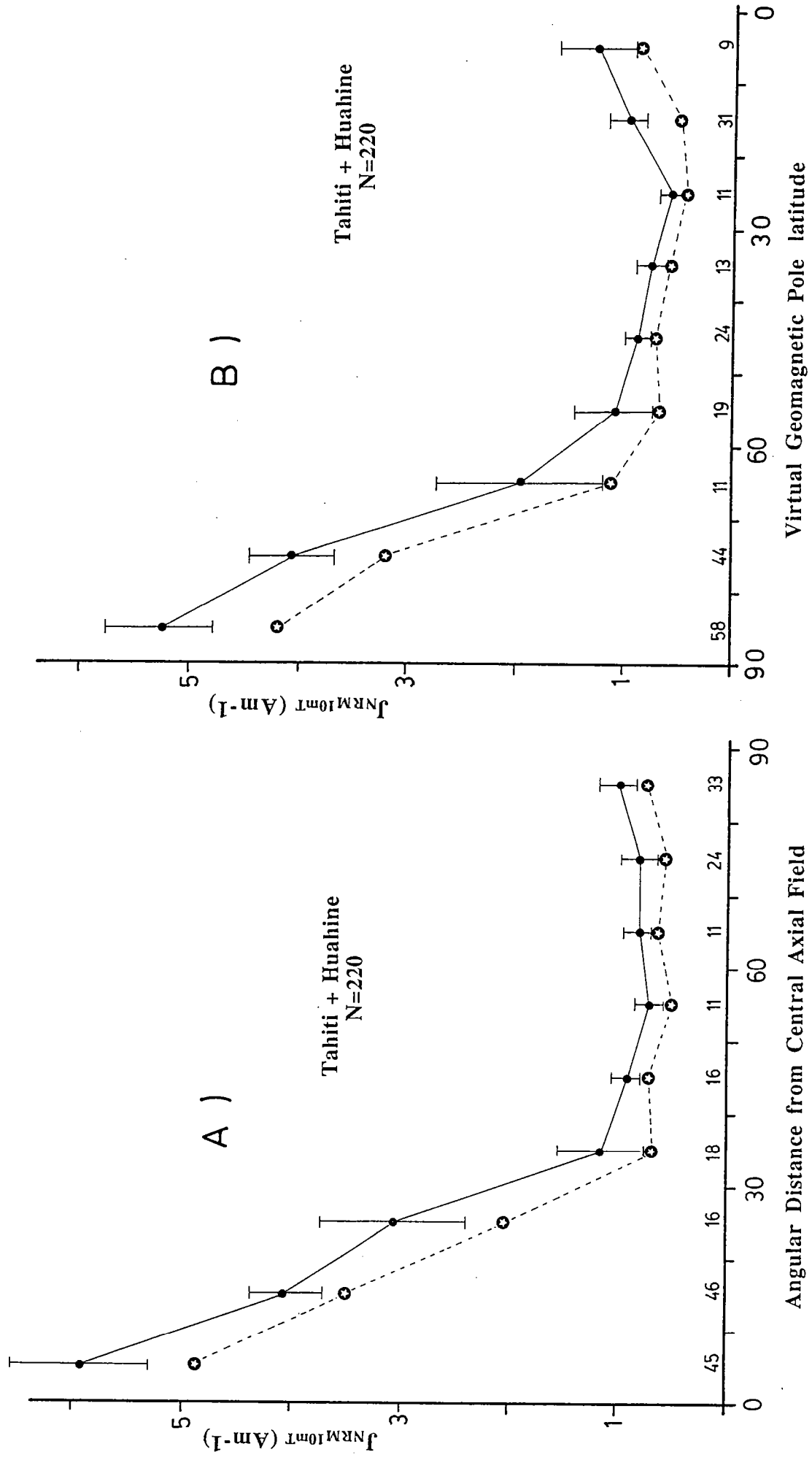

Fig. 17: Diagrams showing the variations of the mean NRM intensity (after 10 mT) averaged for group of flows from Polynesia, versus the angular departure from central axial field (A) or versus virtual geomagnetic pole latitude (B). The reversed directions have been inverted and added with the normal one. The arithmetic means (black dots) are shown with their standard error bars while open circles refer to geometric means. The number of flows available in each interval is also indicated.

NRM intensities suggest that for reversal angles higher than 30°, the geomagnetic field is purely transitional, at this latitude, and that the mean intensity of the field stays very weak during all the transitional periods. However, we must emphasize that this representation enables only the recognition of average field variations and for example, these values do not show what was the maximum reached during the transitions.

A similar study has been done on a data set of more than two thousands lava flows from Iceland by *Kristjansson and McDougall* [1982] and *Kristjansson* [1985]. Comparison of results from these two sites at different latitudes deserves consideration. For this reason, both geometric mean values have been normalized by the intensity observed within the 0-10° interval in reversal angles or VGP's colatitudes (Fig.18). With respect to the deviations from the axial dipole direction, the decrease in intensity observed in Polynesia is also observed in Iceland with a cut-off level between transitional and stable period around 30 to 40° departure from the central axial dipole. But, the main difference is that, in average, the intensity of the transitional geomagnetic field appears to be higher in Iceland than in a site of low latitude like Polynesia; the ratio of the transitional field intensity to its strength during stable periods might be around 25-30% in Iceland and 10-20% in Polynesia. As the intensity of the normal and reversed field is higher in Iceland than in Polynesia, this indicates significant differences between the average paleointensity during transitions between these two sites. One well established feature of paleosecular variation is that the non-dipole field is also latitudinal dependant. Thus, our suggestion that average paleointensity during transitions could vary with latitude, may not be irrelevant.

While, in Polynesia, the decrease of the relative mean intensity with decreasing VGP's latitude is similar to that defined with directions, the drop in intensity with VGP colatitude is particularly smooth in Iceland. This smooth variation observed in Iceland might result from the VGP calculation process because of a higher non dipole field. As seen from Polynesia, the dipole wobble is not large and a discussion of the average properties of the Earth's magnetic field using the VGP calculation is not appropriate particularly at high latitude [*Kristjansson*, 1985]. However, that our data set is around ten times less than that from Iceland, and this can explain the quite large error bars observed in some cases.

Because the average field during periods just before and after the reversal may not be representative of the average field during longer stable periods, like a chron or a subchron, a bias is perhaps introduced in our data. Indeed, a great percentage of them came from transitional zones, especially in the case of Huahine, while the sampling in Tahiti is more regular and covers an interval of time around 400 to 500 Ka. Certainly, the shape of our curves can change with increasing the number of data, but we think that this changes would not be important enough to modify significantly the major trend of our present observation and its interpretation.

Absolute paleointensities versus reversals:

Our absolute paleointensity data range from 2 to 8μT with an average around 5-6 μT. More determinations are still needed, but it seems that paleointensities determined at Tahiti are significantly lower than the average intensity during the transition of the Steens Mountains, which is close to 11 μT [*Prévot et al.*, 1985a]. In view of the paleointensity determinations, and the previous discussion about the variations in the NRM intensities with angular departures from the central axial dipole, it seems that

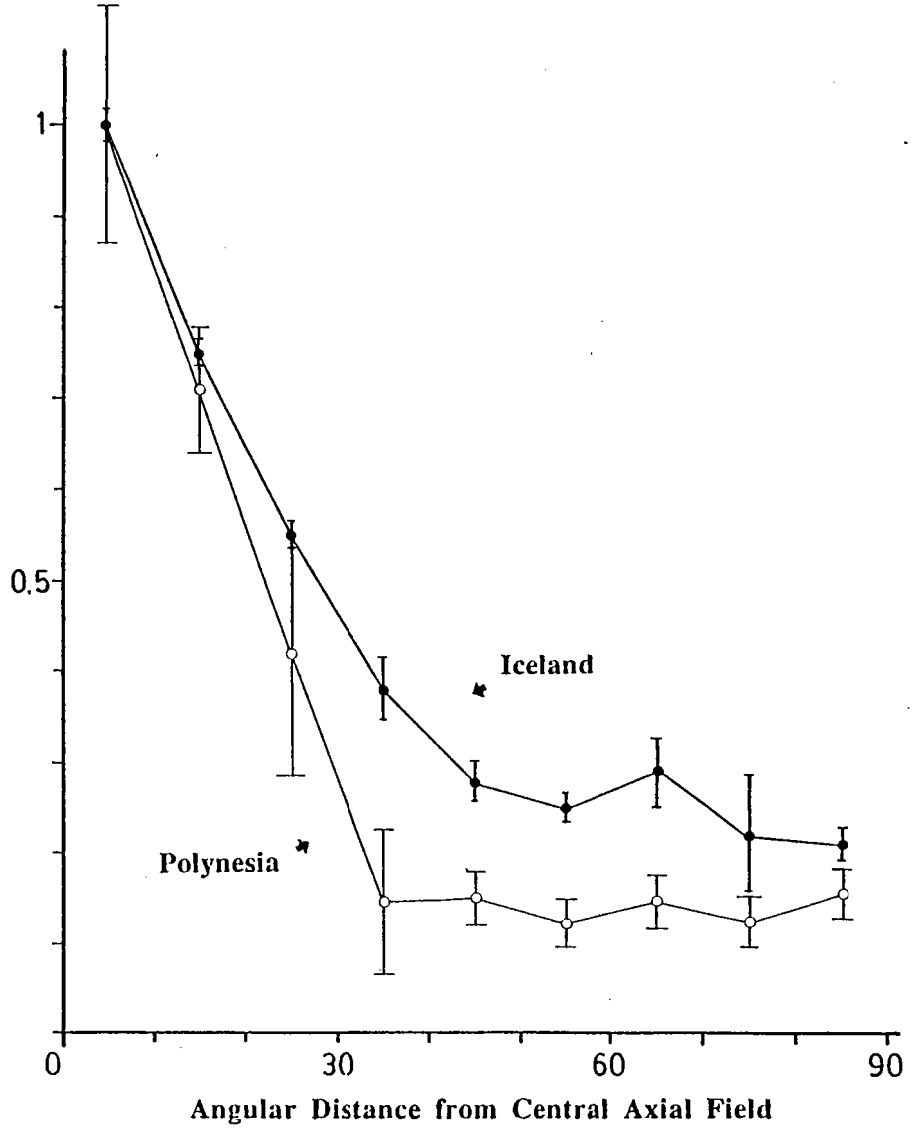

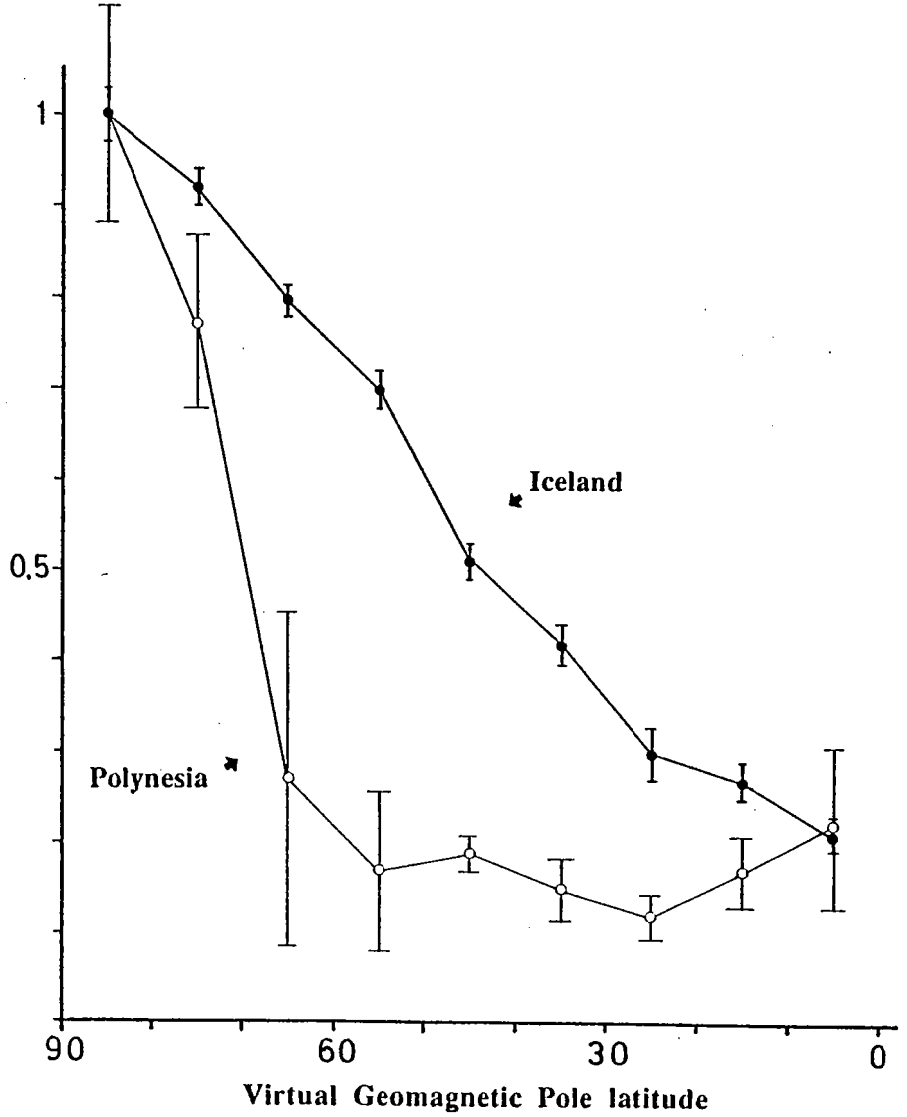

Fig. 18: Comparison of the variations of the average geometric mean values of intensity of magnetization (after 10 mT) from Polynesia and Iceland versus the reversal angle (A) and the VGP latitudes (B). Data from Iceland are extracted from *Kristjansson* [1985]. In order to enable comparison, each data set has been normalized with their respective first value in the 0-10° interval. The arithmetic standard errors have also been normalized.

the average intensity of the field, during transitions might be latitudinaly dependent, with possibly higher values at high latitudes than at low latitudes in contrary to what was suggested by *Prévot et al.* [1985a]. If our speculation is right, this means that the field does not lose all its structure during transition, and that the latitudinal asymmetry observed in the non-dipole is conserved.

However, few data from studies of reversals in Hawaii [*Bogue and Coe*, 1984] and from three excursions recorded by lava of Oahu [*Coe et al.*, 1984] indicates stronger paleointensities than those observed in Polynesia. Obviously, the small number of accurate available data limits the discussion. *Shaw* [1975,1977] reported high paleointensities during transitions while *Lawley* [1970] indicated weak field (around 5 μT) during Neogene polarity transitions recorded in Iceland, but obviously results obtained by total TRM methods are questionable because they may give erroneous results if thermal alterations of the samples are not detected.

Very low intensities of the field, as low as 3 μT have some implications. With such low magnetic vectors, large variations in direction may occur more easily than with a strong field because they do not correspond to large total vector changes.

Alteration of the geomagnetic signal by the recording medium.

It is well known that the irregular extrusion rate of lava flows and the smoothing processes in sediments and intrusion may alter significantly the record of geomagnetic reversal paths [*Weeks et al*, 1988]. However, we must emphasize that volcanic rocks record accurately the magnetic field even if providing only partial records or snapshots of a reversal. On the contrary, *Hoffman and Slade* [1986] demonstrated clearly that smoothing effects may provide reversal features without relation to the initial magnetic signal.

An other question is the meaning of a paleomagnetic vector with respect to the initial magnetic field of internal origin. Particularly, records of low intensity fields may be damaged by any kind of local perturbations.

One possibility is the addition of a crustal magnetic signal to the one of internal origin. The intensity of the magnetic anomaly developed by an island like Tahiti remains very low compared to the strength of the geomagnetic field during normal or reversed periods. Giving an average remanent intensity to the volcanic rocks between 5 to 10 A/m, an homogeneous volcanic cone of the size of Tahiti can develop, at its surface, a local magnetic field between 0.5 to 1 μT, which are low values. The induced magnetization by the Earth's field is negligible in view of our Koenigsberger ratios; this is particularly true when the inducing field is already low. This means that during a transition, with a geomagnetic field close to 3 μT, at least two third of the magnetic field recorded has a geomagnetic origin. Obviously, because magnetic anomalies have strong dependence with the shape of the body, short wavelength variations could exist. In the case of our data, we do not think that local effects play a major role because similar directions were recorded several hundreds meters apart.

We do not know what the implications are of such low paleointensities on the complicated processes of remanence acquisition in sedimentary rocks. One can speculate that in some cases, it would be difficult for a sediment to adequately record such a low field, simply because the magnetic strength responsible for the DRM (detrital remanent magnetization) becomes very weak. Thus, some sediments

may not be able to record the middle part of a transition but, in the better cases, only the beginning and the end of a transition when the field decays or grows toward the other polarity. The fact that several records have a shallow inclination in the middle of the reversal may indicate that the sedimentary process may control the remanence in some cases.

Implications for and from theoretical studies:

Recently, a new interest in the reversal process has been triggered by the development of models which seems sufficiently specific to be testable against the paleomagnetic data. Combining detailed studies of the recent field and inversion methods, *Bloxham and Gubbins* [1985] have produced maps of the radial component of the field at the core-mantle boundary (CMB) from 1715 to 1980. Static features, associated to the main standing field generated by the dynamo and rapidly drifting features are observed [*Gubbins and Bloxham*, 1987]. The development of reverse flux patches in the middle southern Atlantic hemisphere is possibly explained by expulsion of toroidal flux by fluid upwelling [*Bloxham*, 1986]. *Gubbins* [1987] suggests that the location of these reverse flux zones would be tied to mantle temperature anomalies, and that their growth provide a mechanism for polarity reversals. However, the large decrease of the paleointensity during reversals is one of the best established characteristics which suggests a general breakdown of the dipole. Thus, the growing of one reverse flux zones may not systematically provide low intensities everywhere.

This model predicts also that all reversals should be similar (i.e., have the same transitional field) within the life-time of mantle convection pattern (10^8 years). Some sedimentary records seems to provide a negative test for this model [*Laj et al.*, 1988], even if there are indications in records from Crete that the reversal process may remain invariant over several polarity intervals [*Valet and Laj*, 1984]. Different transitions from Polynesia exhibit some common features. Particularly south west directions with shallow inclination are observed in 4 out of 5 reversal records. But it is obvious that more data are needed to be significant.

Comparing his theory with available paleomagnetic data, *Gubbins* [1988] argues that reverse flux features have been absent within the northern hemisphere during the last 5 Ma. This idea of constant location of region where reversals are initiated is quite equivalent to the common starting point for a reversal model of the type suggested by *Hoffman* [1979]. However models which assume that the field reverses in a progressive way, through spreading of the reversal over the core, may not be adequate to explain rebound effects as a part of the transitional field behavior.

The location of our site, in central Pacific ocean, does not help much in constraining Gubbins's theory since most of the expected perturbations should be in the Indian ocean. Comparing our results with data from this area would be helpful.

Even if there is no clear paleomagnetic data supporting Gubbins's scheme of reversal, there is now strong evidence that thermal and topography variations at the core-mantle boundary are constraining field variations, particularly in the long-term changes in the mean reversal rate [*Mc Fadden and Merrill*, 1984; *Courtillot and Besse*, 1987].

Geomagnetic polarity reversals in a turbulent core were investigated by *Olson* [1983] using the α^2 dynamo model. *Olson* considers that changes in the sign of helicity in an α^2 dynamo can provide two

types of reversals, 'component reversals' when only the poloidal or the toroidal field reverse or 'full reversal' when the two field components reverse. Following *Olson*, reversals would be the result of the competition between two source powers of the dynamo: heat lost at the CMB and progressive crystallization of the solid inner core. Over a brief interval, the contribution from inner core growth may exceed the contribution from heat lost at the CMB, causing a transient reversal of helicity.

The mathematical analysis from *Olson* predicts the variation of the dipole intensity for a field reversal with a reasonable time duration, but it does not define the non-dipole configuration of the field during the transition. *Clement* [1987] used the dipole time evolution equations from *Olson*'s theory and assumed that the energy lost by the dipole field is partitioned to low degree non-dipole fields [*Williams and Fuller*, 1981] for modeling records of two reversals from both northern and southern hemispheres. The fit to the data is strongly dependent on the way the dipole energy is distributed to the other terms. The attempt made by *Clement* [1987] was not successful for the intensity pattern which should be the main parameter for a rigorous test of *Olson*'s hypothesis on the variation of the dipole intensity.

The two previous theories assume that polarity reversals result from disturbances perturbing the movement in the core which produce the stable main field. This hypothesis is in agreement with the conclusion of the analysis of the geomagnetic reversal sequence made by *Mc Fadden and Merrill* [1986] which indicates that the triggering effect of reversal might be independent of the process producing the main field.

Our data show, like other volcanic ans sedimentary records, that the intensity of the geomagnetic field at the earth surface is considerably reduced (one fifth to one tenth) during the transition. It seems reasonable to think that the field intensity is also reduced in the core and that the magnetic energy lost is transferred into kinematic energy [*Prévot et al.*, 1985a], increasing the level of turbulence within the liquid core. This effect has been suggested in order to explain the large and quick directional changes observed in some record of polarity reversal. In particular, the 'geomagnetic impulses' occurring during the Steen Mountain transition imply a rate of change of the field components considerably larger than the maximum rate calculated for the recent secular variation [*Prévot at al.*, 1985a]. Resampling of several flows and detail thermal demagnetizations associated to a cooling model of the lava flows, might indicate even quicker directional changes of the geomagnetic field [*Coe and Prévot*, 1988]. We have not found such a behavior in our volcanic sequences. Nevertheless, the great number of different intermediate directions found either at Huahine or for the Upper Jaramillo shows that important directional field variations occurred.

10 Conclusion

Four transitional zones have been sampled in a volcanic sequence of 120 lava flows in one valley of the island of Tahiti. According to the radiometric datings, they correspond to the Cobb Mountain, the lower and upper Jaramillo and the Matuyama-Bruhnes transitions.

This study might indicate that the Cobb Mountain corresponds to a Reverse to Reverse excursion of the Earth's magnetic field, occurring around 1.1 Ma.

Combining data from the island of Tahiti with the record of a Normal to Normal excursion in lavas from the island of Huahine [*Roperch and Duncan*, this issue], the non-zonal components of the field appear important during the transition. Nevertheless, the beginning of two transitions (the lower Jaramillo and the N-N excursion from Huahine), seems to indicate that the onset of a reversal could be more axisymmetric than the following phase. An increase of the quadrupole field at the onset of the reversal may fit the observed high inclination path.

NRM intensity data show that the intensity of the transitional field, at this latitude was very low during all the intermediate period. This fact is confirmed by some reliable paleointensity determinations, which indicate a paleofield strength around 3 to 8 μT. Comparison between average NRM intensity from Iceland and Polynesia might indicate a lower averaged transitional field (i.e. non-dipole field) at low latitude than at high latitude.

The response of the different paleomagnetic recorders to such low and rapid changing fields needs to be investigated in order to provide more reliable paleomagnetic records of the transitional field.

The main features of a polarity transition, i.e., short duration, non-dipole configuration and large drop in intensity, are now well established. However, these characteristics provide little evidence for a clear understanding of the processes occuring in the liquid earth's core which lead to geomagnetic reversals. Other reversal records with a better worldwide coverage of the same transition, absolute paleointensities and a more critical judgment on the data quality are needed to clearly establish some other features of reversals of geomagnetic field (i.e. axisymmetry at the onset, latitudinal dependency of the intensity of the intermediate field, ultra rapid field variations), and then to make further progress in the comprehension of the reversal process.

References

Abdel-Monem, A., N.D., Watkins and Gast P.W., Potassium-Argon ages, volcanic stratigraphy and geomagnetic polarity history of the Canary islands: tenerife, la Palma and Hierro, *American Journal of Science*, 272, 805-825, 1972.

Bloxham, J., The expulsion of magnetic flux from the Earth's core, *Geophys. J. R. astr. Soc.*, 87, 669-678, 1986

Bloxham, J., The dynamical regime of fluid flow at the core surface. *Geophys. Res. Lett., 15*, 585-588. 1988.

Bloxham, J. and D. Gubbins, The secular variation of earth's magnetic field, *Nature*, 317, 777-781, 1985.

Bogue, S.W.., and R.S. Coe, Transitional paleointensities from Kauai, Hawaii, and geomagnetic reversals models. *Jounal of Geophysical Research., 89*, 10341-10354, 1984.

Briden, J.C., D.C. Rex, A.M., Faller and J.F., Tromblin, K_Ar geochronology and palaeomagnetism of volcanic rocks in the lesser Antilles island arc, *Phil. Trans. R. Soc. London*, A291, 485-528, 1979.

Brousse et al. Carte Géologique de Tahiti

Clement, B.V., Paleomagnetic evidence of reversals resulting from helicity fluctuations in a turbulent core, *Journal of Geophysical Research*, 92, 10629-10638, 1987.

Clement, B.M., D.V., Kent and N., Opdyke, Brunhes-Matuyama polarity transition in three deep-sea sediments cores, *Phil. Trans. R. Soc. London*, A306, 113-119, 1982.

Clement, B.M. and D.V. Kent, A detailed record of the Lower Jaramillo polarity transition from the southern hemisphere, deep-sea sediments cores, *Journal of Geophysical Research*, 89, 1049-1058, 1984

Clement, B.M., and D.V., Kent, A comparison of two sequential geomagnetic polarity transitions (Upper Olduvai and Lower Jaramillo) from the southern Hemisphere, *Physics of the earth and Planetary Interiors*, 39, 301-313, 1985

Clement, B.M. and D.V. Kent, Geomagnetic polarity transition records from five hydraulic piston core sites in the north Atlantic, *Init .Report .DSDP .Proj.*, 94, 831-852, 1986.

Clement, B.M. and D.V., Kent, Short polarity intervals within the Matutyama: transitional field records from hydraulic piston cored sediments from the north Atlantic. *Earth and Planetary Science Letters*, 81, 253-264, 1987.

Coe, R.S., Paleointensities of the Earth's magnetic field determination from tertiary and quaternary rocks, *Jounal of Geophysical Research, 72*, 3247-3262, 1967a.

Coe, R.S., The determination of paleointensities of the Earth's magnetic field with emphasis on mechanisms which could cause non-ideal behavior in Thellier's method. *J. geomag. Geoelectr., 19*, 157-179, 1967b.

Coe, R.S. and C.S., Gromme, A comparison of three methods of determining geomagnetic paleointensities, *J. Geomag. Geoelectr.*, 25, 415-435, 1973

Coe, R.S., C.S., Gromme and E.A., Mankinen, Geomagnetic paleointensities from radiocarbon dated lava flows on Hawai and the question of the Pacific non-dipole low, *Journal of Geophysical Research*, 83, 1740-1756, 1978.

Coe, R.S., S., Gromme and E.A., Mankinen, Geomagnetic paleointensities from excursion sequences in lavas on Oahu, Hawaii, *Journal of Geophysical Research*, 89, 1059-1069, 1984.

Coe, R.S. and M., Prévot, Evidence of very rapid field variation during reversals, *NATO Adv.Study.Inst.on Geomag.and Paleomag.*, Newcastle, 1988.

Coutillot, V. and J. Besse, Magnetic field reversals, Polar wander and Core-Mantle coupling, *Science*, 237, 1140-1147, 1987.

Dagley, P. and E. Lawley, Paleomagnetic evidence for the transitional behavior of the geomagnetic field, *Geophys. J. R. astr. Soc.*, 36, 577-598, 1974

Day, R., TRM and its variation with grain size, *J. Geomag. Geoelectr.*, 29, 233-265, 1977

Duncan, R.A., Paleosecular variation at the Society islands, French Polynesia, *Geophys. J. Roy. Astr. Soc., 41*, 245-254, 1975.

Duncan, R. A. and I. McDougall , Linear volcanism in French Polynesia , *J . Volc. Geother. Res. ,1*, 197-227, 1976.

Dunlop, D.J., Determination of domain structure in igneous rocks by alternative field and others methods, *Earth and Planetary Science Letters*, 63, 353-367, 1983.

Fleck R.J., J.H., Mercer, A.E.M., Nairn and D.N. Peterson, Chronology of the late Pliocene and early Pleistocene glacial and magnetic events in southern Argentina, *Earth and Planetary Science Letters*, 16, 15-22, 1972.

Forster J.H. and N., Opdyke, Upper Miocene to recent magnetic stratigrapy in deep-sea sediments, *Journal of Geophysical Research*, 75, 4465-4473, 1970.

Fuller, M., I., Williams and K.A., Hoffman, Palaeomagnetic records of geomagnetic field reversals and the morphology of the transitional fields, Reviews of Geophysics and Space Physics, 17, 179-203, 1979.

Gire, C., J.L. Le Mouel and T. Madden, Motions at the core surface derived from SV data, *Geophys. J. R. astr. Soc., 84*, 1-29, 1986

Gromme, S., T.L. Wright and D.L. Peck, Magnetic properties and oxidation of iron-titanium oxide minerals in Alae and Makapuki lava lakes, Hawaii, *Journal of Geophysical Research 74*, 5277-5293, 1969.

Gurarii, G.Z., The Matuyama-Jaramillo geomagnetic inversion in western Turkmenia, *Izvestiya, Earth Physics*, 17, 212-218, 1981.

Gubbins, D., Mechanism for geomagnetic polarity reversals, *Nature, 326*, 167-169., 1987.

Gubbins, D., Thermal core-mantle interactions and time-averaged paleomagnetic field, *Journal of Geophysical Research*, 93, 3413-3420, 1988.

Gubbins, D. and J., Bloxham, Morphology of the geomagnetic field and implications for the geodynamo, *Nature*, 325, 509-511, 1987.

Hammond, S.K., S.M., Seylo and F. Theyer, Geomagnetic polarity transitions in two oriented sediment cores from the Northwest Pacific, *Earth and Planetary Science Letters*, 44, 167-175, 1979.

Harland, W.B., A.V. Cox, P.G. Llewellyn, C.A.G. Pickton, A.G. Smith and R. Walters, A geologic time scale; Cambridge University Press, 1982.

Herrero-Bervera, E. and F., Theyer, Non-axisymmetric behavior of Olduvai and Jaramillo polarity transitions recorded in north central pacific deep-sea sediments, *Nature*, 322, 159-162, 1986.

Herrero-Bervera, E., F., Theyer, and C.E. Hesley, Olduvai onset polarity transition: Two detailed paleomagnetic records from the north central Pacific sediments, *Physics of the Earth and Planetary Interiors*, 49, 325-342, 1987.

Hide, R, Self exciting dynamo and geomagnetic polarity transition, *Nature*, 293, 728-729, 1981.

Hillhouse, J. and A., Cox, Brunhes-Matuyama polarity transition, *Earth and planetary Science Letters*, 29, 51-64, 1976.

Hoffman, K.A., Polarity transition records and the geomagnetic dynamo, *Science*, 4296, 1329-1332, 1977.

Hoffman, K.A., Behavior of the geodynamo during reversal: a phenomenological model, Earth Planet. Sci. Lett., 44, 7-17, 1979.

Hoffman, K.A., Quantitative description of the geomagnetic field during the Matuyama-Bruhnes polarity transition, *Physics of the Earth and Planetary Interiors*, 24, 229-235, 1981a.

Hoffman, K.A., Palaeomagnetic excursions, aborted reversals and transitional fields, Nature, 294, 67-69, 1981b

Hoffman, K.A., The testing of the geomagnetic reversal models/ recent developments, *Phil. Trans. R. Soc. London*, A306, 147-159, 1982.

Hoffman, K.A., A method for the display and analysis of transitional paleomagnetic data, *Journal of Geophysical Research, 89*, 6285-6292, 1984.

Hoffman, K.A., Transitional behavior of the Geomagnetic field, *J. Geomag. Geoelectr.*, 37, 139-146, 1985.

Hoffman, K.A., Transitional field behavior from southern hemisphere lavas: evidence for two-stage reversals of the geodynamo, *Nature*, 320, 228-232, 1986.

Hoffman, K.A., Ancient magnetic reversals: Clues to the geodynamo, *Scientific American*, 258, 76-83, 1988.

Hoffman, K.A. and M., Fuller, Transitional fields configurations and geomagnetic reversals, *Nature*, 273, 715-718, 1978.

Hoffman, K.A. and S.B, Slade, Polarity transition records and the acquisition of remanence: a cautionary note, *Geophys. Res. Lett.*, 13, 483-486, 1986.

Karlin, R. and S., Levi, Geochemical and sedimentological control of the magnetic properties of hemipelagic sediments, *J. Geophys. Res.*, 90, 10, 373-10,392, 1985.

Karlin, R., M. Lyle and G.R. Heath, Authigenic magnetite formation in suboxic marine sediments, *Nature*, 326, 490-493, 1987.

Kawai, N. T., Sato, T. Sueishi and K., Kobayashi, Paleomagnetic study of deep-sea sediments from the Melanesian basin, *J. Geomag. Geoelectr.*, 29, 211-223, 1977.

Kent, D.V and D.J., Spariosu, Magnetostratigraphy of Carribbean site 502 hydraulic piston cores, *Init. Rep. DSDP Proj.*, 68, 419-433, 1982.

Khodair, A.A. and R.S. Coe, 1975, Determination of geomagnetic paleointensities in vacuum. *Geophys. J. R. astr. Soc., 42*, 107-115, 1975.

Kochegura, V.V. and A. Zubakov, Palaeomagnetic time scale of the Ponto-Caspien Plio-Pleistocene deposits, *Palaeogeography, Palaeoclimatology, Palaeoecology*, 23, 151-160, 1978

Kono, M., and H. Tanaka, Analysis of the Thellier's method of paleointensity determination 1- estimation of statistical errors, *J. Geomag. Geoelectr.., 36*, 267-284, 1984.

Kristjansson, L., Some statistical properties of paleomagnetic directions in Icelandic lava flows, *Geophys. J. R. astr. Soc.*, 80, 57-71, 1985.

Kristjansson, L. and I., Mc Dougall, Some aspects of the late Tertiary geomagnetic field in Iceland, *Geophys. J. R. Soc.*, 68, 273-294, 1982.

Laj. C., Guitton, S. and C. Kissel, Rapid change and near stationary of the geomagnetic field during a polarity reversal, *Nature, 330*, 145-148, 1987

Laj, C., S., Guitton, C., Kissel and A. Mazaud, Paleomagnetic records of sequential field reversals from the same geographical region at different epoch, *Journal of Geophysical Research*, 1988, in press.

Lawley, E.H, The intensity of the geomagnetic field in Iceland during Neogene polarity transitions and systematic deviations, *Earth and Planetary Science Letters*, 10, 145-149, 1970.

Le Mouel, J.L., Outer-core geostophic flow and secular variation of Earth's geomagnetic field, *Nature*, 311, 734-735, 1984.

Levi, S., Comparison of two methods of performing the Thellier experiment (or, how the Thellier method should not be done.), *J. Geomag. Geoelectr., 27*, 245-255, 1975.

Levi, S., The effect of magnetite particle size on paleointensity determinations of the geomagnetic field, *Phys. earth Planet. int., 13*, 245-259, 1977.

Liddicoat, J.C, Gauss-Matuyama polarity transition, *Phil. Trans. R. Soc. Lond.*, A306, 121-128, 1982.

Maenaka, K., paleomagnetic study of sediments around the Komyoike volcanic ash horizon in Osaka group, Senpoku area, Osaka prefecture, Japan, *Geophys. Res. Lett.*, 6, 257-260, 1979.

Mankinen, E.A., J.M., Donnelly, and C.S.,Gromme, Geomagnetic polarity event recorded and 1.1 Ma BP on Cobb Mountain, Clear Lake volcanic field, California, *Geology*, 6, 653-656, 1978.

Mankinen, E.A. and G.B, Dalrymple , Revised geomagnetic polarity time scale for the interval 0-5 Ma BP, *Journal of Geophysical Research*, 84, 615-626, 1979.

Mankinen, E.A., J.M., Donnelly-Nolan, C.S., Gromme and B.C., Hearn JR, Paleomagnetism of the Clear Lake volcanics and new limits of the age of the Jaramillo normal polarity event, *U.S.Geol.Surv.Prof.Paper*, 1141, 67-82, 1981.

Mankinen, E.A. and C.S., Gromme, , Paleomagnetic data from the Coso Range, California and the current status of the Cobb Mountain normal geomagnetic event, *Geophys. Res. lett.*, 9, 1279-1282, 1982.

Mankinen, E.A., M., Prévot, C.S., Gromme, and R.S. Coe, The Steens Mountain (Oregon) geomagnetic polarity transition. 1- Directional history, duration of episodes and rock magnetism. *J. Geophys. Res.*, 90,10393-10416. 1985.

McDougall, I. and F.H., Chamalaun, Geomagnetic polarity scale of time, *Nature*, 212, 1415-1418, 1966.

McElhinny, M.W. and R.T Merrill, Geomagnetic secular variation over the past 5. Ma, *Rev. Geophys. Space Phys., 13*, 687-708, 1975.

McFadden, P.L. and M.W., McElhinny, A physical model for paleosecular variation. *Geophys. J. R. astr. Soc., 78*, 809-830, 1984.

McFadden, P.L. and R.T. Merrill, Lower mantle convection and geomagnetism, *Journal of Geophysical Research*, 89, 3354-3362, 1984.

McFadden, P.L. and M.T., Merrill, Geodynamo energy source constraints from paleomagnetic data, *Physics of the Earth and planetary Interiors*, 43, 22-33, 1986.

McFadden, P.L., R.T., Merrill and M.W. McElhinny, Dipole/Quadrupole family modeling of paleosecular variation, *Journal of Geophysical Research*, 93, 11583-11588, 1988.

Merrill, R.T. and P.L., McFadden, Secular variation and the origin of geomagnetic field reversals, *Journal of Geophysical Research*, 93, 11589-11598, 1988.

Niitsuma, N.D., Paleomagnetic and paleoenvironmental study of sediments recording Matuyama-Brunhes geomagnetic reversal, *Tohoku Univ. Sci. Rep. Geol.*, 43, 1-39, 1971.

Ninkovich, D., N., Opdyke, B.C, Heezen and J.H., Foster, Paleomagnetic stratigraphy, rates of deposition and tephrachronology in north Pacific deep-sea sediments, *Earth and Planetary Science Letters*, 1, 476-492, 1966.

Olson, P., Geomagnetic polarity reversals in a turbulent core, *Physics of the Earth and Planetary Interiors*, 33, 260-274, 1983.

Opdyke, N.D., D.V., Kent and W. Lowrie, Details of magnetic polarity transitions recorded in high deposition rate, deep-sea core, *Earth and Planetary Science Letters*, 20, 315-324, 1973.

Plessard, C., Modifications des propriétés magnétiques, en particulier de trainage, après réchauffement d'une roche préalablement stabilisée thermiquement. *C.R. acad. Sc., Paris, 273*, 97-100,1971.

Prévot, M., E.A. Mankinen, S. Gromme and A. Lecaille, High paleointensities of the geomagnetic field from thermomagnetic studies on rift valley pillow basalts from the mid-Atlantic ridge., *Journal of Geophysical Research, 88*, 2316-2326, 1983.

Prévot, M., E.A. Mankinen, C.S. Gromme and R.S. Coe, How the geomagnetic field vector reverse polarity, *Nature, 316*, 230-234, 1985a.

Prévot, M., E.A., Mankinen, R.S., Coe and C.S., Gromme, The steens Mountain geomagnetic polarity transition 2. Field intensity variation and discussion of reversal models, *Journal of geophysical Research*, 90, 10417-10448, 1985b

Rea, D.K. and Blakely, R.J., Short-wavelength magnetic anomalies in a region of rapid seafloor spreading, *Nature*, 255, 126-128, 1975.

Roperch, P., Comportement du champ magnétique terrestre au cours de transitions de polarité, Thèse, *Travaux et documents ORSTOM*, TDM 26, 209 pp., 1987.

Roperch, P., and A. Chauvin, Transitional geomagnetic field behavior: Volcanic records from French Polynesia, *Geophys. Res. Lett., 14*, 151-154., 1987.

Roperch, P. and R.A., Duncan, Records of geomagnetic reversals from volcanic islands (French polynesia). I Paleomagnetic study of a polarity transition recorded on a lava sequence from the island of Huahine., this issue.

Senanayake, W.E., M.W. Mc Elhinny and P.L. Mc Fadden, Comparison between the Thellier's and Shaw's paleointensity methods using basalts less than 5 millions years old, *J. Geomag. Geoelectr.*, 34, 141-161, 1982.

Shaw, J., Strong geomagnetic fields during a single Icelandic polarity transition, *Geophys. J. R. astr. Soc.*, 40, 345-350, 1975

Shaw, J., Further evidence for a strong intermediate state of the paleomagnetic field, *Geophys. J. R. astr. Soc.*, 48, 263-269, 1977

Sigurgeirsson, T., Directions of magnetization in Icelandic basalts, *Adv. Phys.*, 6, 240-246, 1957.

Sueishi, T., T. Sato, N., Kawai and K., Kobayashi, Short geomagnetic episode in the Matuyama Epoch, *Physics of the Earth and Planetary Interiors*, 19, 1-11, 1979.

Thellier, E. and O. Thellier, Sur l'intensité du champ magnétique terrestre dans le passé historique et géologique, *Ann. Geophys., 15*, 285-376, 1959.

Theyer, F., E., Herrero-Bervera and V;, Hsu, The zonal harmonic model of polarity transitions/ a test using successive reversals, *Journal of Geophysical Research*, 90, 1963-1982, 1985.

Tivey, M., and Johnson H.P., Characterization of viscous remanent magnetization in single and multidomain magnetite grains, *Geophys. Res., Lett., 18*, 217-220, 1981.

Valet, J.P., Inversions géomagnétiques du Miocene superieur en Crete. Modalités de renversement et caracteristiques du champ de transition, Thèse , 195 p., Universite d'Orsay, France, 1985

Valet, J.P. and C., Laj, Invariant and changing transitional field configurations in a sequence of geomagnetic reversals, *Nature*, 311, 552-555, 1984.

Valet, J.P., L., Tauxe and D.R., Clark, The Matuyama-Bruhnes transition recorded from the lake Tecopa sediments (California), *Earth and Planetary Science Letters*, 87, 463-472, 1988a

Valet, J.P., C., Laj and C.G, Langereis, Sequential geomagnetic reversals recorded in Upper Tortonian marine clays in western Crete (Greece), *Journal of Geophysical Research*, 93, 1131-1151, 1988b.

Valet, J.P., L., Tauxe and J.,Bloemendhal, The Matuyama-Bruhnes geomagnetic reversal from two deep-sea cores of the east-equatorial Atlantic, *Proc. ODP*, 108, 1988c(In review).

Van Zijl, J.S.V., K.W.T. Graham and A.L. Hales, The paleomagnetism of the Stormberg Lavas of South Africa; I: Evidence for a genuine reversal of the earth's field in Triassic-Jurassic Times., *Geophys. J. R. Astr. Soc.*, 7, 169-182, 1962.

Watkins, N.D., Short period geomagnetic events in deep-sea sedimentary cores, *Earth and Planetary Science Letters*, 4, 341-349, 1968.

Watkins, N.D. and A. Abdel-Monem, detection of the Gilsa geomagnetic polarity event on the island of Madeira, *Geological Society of America Bulletin*, 82, 191-198, 1971.

Weeks, R.J., M. Fuller and I. Williams, The effects of recording medium upon reversal records, *Geophys. Res. Lett.*, 15, 1255-1258, 1988.

Williams, I. and M., Fuller, Zonal harmonic models of reversal transition fields, *Journal of Geophysical Research*, 86, 11657-11665, 1981.

Williams, I., R., Weeks and M. Fuller, A model for transition field during geomagnetic reversals, *Nature*, 332, 719-720, 1988.

Wilson, R.L., P. Dagley and A.G., McCormack, Paleomagnetic evidence about the source of the geomagnetic field, , *Geophys. J. R. astr. Soc.*, 28, 213-224, 1972.

Résumé et Conclusions

Références Bibliographiques

RÉSUMÉ ET CONCLUSIONS

Le travail présenté dans ce mémoire avait pour principal objectif l'étude du comportement du champ géomagnétique, en direction et en intensité, aux cours de périodes stables et de transition. Dans ce but, plusieurs études paléomagnétiques ont été effectuées sur des coulées volcaniques d'âges s'échelonnant de 5 Ka à 1.1 Ma., échantillonnées à La Réunion (Ocean Indien), Tahiti (Polynésie française), en Islande et dans la Chaîne des Puys.

Pour la recherche de la paléointensité, j'ai utilisé la méthode de Thellier. Les particularités de cette méthode, nécessitant une sélection des échantillons, m'ont conduit à mener une étude approfondie des propriétés magnétiques des coulées échantillonnées.

Principaux résultats

1) Variation Séculaire sur la période 0-120 Ka

Une étude de la variation séculaire dans la période récente à porter sur 2 empilements volcaniques du Piton de la Fournaise (La Réunion), d'âge respectifs 5-11 Ka et 82-98 Ka.

Les paléointensités obtenues sur le plus jeune site sont en accord avec la courbe globale des variations du dipôle déterminée à partir d'autres points du globe. Les données acquises sur la séquence la plus ancienne constituent les premières données d'intensité obtenues sur cette gamme d'âges.

Pour les deux empilements étudiés, l'ensemble des paléointensités obtenues (de 21 à 54 μT) ainsi que la variation séculaire observée dans les directions concordent avec des intensités des champs dipôle et non-dipôle comparables avec les valeurs actuelles.

Par contre, un résultat tout à fait différent a été obtenu sur des laves de directions intermédiaires d'Islande et de la Chaîne des Puys, datées entre 40 et 50 Ka. Les déterminations de paléointensité effectuées sur ces coulées confirment le caractère géomagnétique de l'excursion du Laschamp et la très forte baisse (de 75 à 90%) de l'intensité du champ qui lui est associée.

2) Renversements de polarité les plus récents

Une séquence de 123 coulées échantillonnées à Tahiti a fourni des enregistrements détaillés des transitions du Jaramillo supérieur (0.96 Ma) et du Cobb Mountain (1.1 Ma), alors que les transitions du Jaramillo inférieur et de Brunhes-Matuyama (0.73 Ma) n'ont été enregistrées que par quelques coulées.

Sur cet enregistrement le Cobb apparait comme une excursion inverse-transitionel-inverse et non pas comme un épisode de polarité normale au sein de la période essentiellement inverse du Matuyama.

Les données acquises à Tahiti, combinées à d'autres déjà obtenues en Polynésie suggèrent une domination des termes axisymmétriques du champ au début des renversements.

L'intensité du champ de transition, à cette latitude, parait très faible, comme l'indiquent les paléointensités obtenues (3 à 8 μT). Cette observation combinée à une analyse de l'intensité d'aimantation des coulées, pourrait indiquer une variation de l'intensité moyenne du champ de transition avec la latitude.

Les hypothèses d'une domination des termes axisymmétriques du champ au début des renversements et d'une variation avec la latitude dans l'intensité du champ de transition, peuvent apporter des contraintes au modèles de géodynamo et méritent donc d'être testées par de nouvelles études paléomagnétiques.

REFERENCES BIBLIOGRAPHIQUES

AITKEN M.J., A.L. ALLSOP, G.D.BUSSELL et M.B. WINTER, comment on: "the lack of reproducibility in experimentally determined intensities of the Earth's magnetic field", by D. Walton, *Reviews of Geophysics*, 26, 23-25, 1988.

BARBETTI M.F. et M.W. McELHINNY, The lake Mungo geomagnetic excursion, *Phil. Trans. Soc. London*, A281, 515, 1976.

BERGGREN W.A., D.V. KENT, J.J. FLYNN et A. COUVERING. Cenozoic geochronology, *Geol., Soc. Am. Bull.*, 96, 1407-1418, 1985.

BONHOMMET, N. AND J; BABKINE, Sur la présence de directions inversées dans la Chaîne des Puys, *C. R. Acad. Sci. Paris*, 264, 92-94, 1967.

CHAMPION, D.E., M.A., LANPHERE AND M.A., KUNTZ, Evidence for a new geomagnetic reversal from Lava flows in Indaho: Discussion of short polarity reversals in the Brunhes and late Matuyama polarity chrons, *J. Geophys. Res.*, 93, 11667-11680, 1988.

CLEMENT B.M. et D.V. KENT, Latitudinal dependency of geomagnetic polarity transition duration, *Nature*, 310, 488-491, 1984.

COE, R.S., S. GROMME AND E.A. MANKINEN, Geomagnetic paleointensities from radiocarbon dated lava flows on Hawaii and the question of the pacific non-dipole low, *J. Geophys. Res.*, 83, 1740-1756, 1978.

COE, R.S., S. GROMME AND E.A. MANKINEN, Geomagnetic paleointensities from excursion sequences in lavas on Oahu, Hawaii, *J. Geophys. Res.*, 89, 1059-1069, 1984.

COURTILLOT V. et J.L. LE MOUEL. On the long period variation of the Earth's magnetic field from 2 months to 20 years, *J. Geophys. Res.*,81, 2941-2950, 1976.

COURTILLOT V, J. DUCRUIX et J.L. LE MOUEL, Sur une accélération récente de la variation séculaire du champ magnétique terrestre, *C. R. A cad. Sci., Paris*, Ser. D, 287, 1095-1098, 1978.

COURTILLOT V. et J.L. LE MOUEL. Geomagnetic secular variation impulses a review of observational evidence and geophysical consequences, *Nature*. 311, 709-716, 1984.

COURTILLOT V. et J. BESSE. Magnetic field reversals, polar wander, and core-mantle coupling, *Science*, V.237, 1140, 1987.

COURTILLOT V. et J.L. LE MOUEL. Time variations of the Earth's magnetic field : from daily to secular, *Ann. Rev. Earth Planet. Sci.*, 16, 389-476, 1988.

COX A. Lengths of geomagnetic polarity intervals, *J. Geophys. Res.*, 73, 3247, 1968.

COX A Geomagnetic reversals, *Science*, 163, 237, 1969.

COX A. The frequency of geomagnetic reversals and the symmetry of the non dipole field, *Rev. Geophys. Sp. Phys.*, 13, 35-51 1975.

COX A. Magnetostratigraphic time scale, in a geologic time scale (W.B. Harland et al. eds) p. 63, *Cambridge University Press*, Cambridge, 1982.

COX A., R.R. DOELL et G.B. DALRYMPLE. Geomagnetic polarity epochs and Pleistocene geochronometry.*Nature*, 198, 1049, 1963.

CREER K.M., P.W READMAN et A.M. JACOBS. Palaeomagnetic and palaeontological dating of a section at Gioia Tauro, Italy : identification of the Blake event, *Earth Planet. Sci. Lett.*, 50, 289-300, 1980.

DENHAM et COX. Evidence that the Laschamp polarity event did not occur 13300-30400 years ago, *Earth Planet. Sci. Lett.*,13, 181-190, 1971.

DODSON M.H., E. McCLELLAND BROWN, Magnetic blocking temperatures of single domain grains during slow cooling, *J. Geophys. Res.*, 85, 2625-2637, 1980.

FOX J.M.W. et M.J. AITKEN, Cooling-rate dependence of thermoremanent magnetization, *Nature*, 283, 462-463, 1980.

GILLOT, P.Y., J. LABEYRIE, C. LAJ, G. VALLADAS, G. GUERIN, G. POUPEAU AND G. DELIBRIAS, Age of the Laschamp paleomagnetic excursion revisited, *Earth Planet. Sci. Lett.*, 42, 444-450, 1979.

GIRE C.. Sur la variation séculaire du champ magnétique terrestre et les mouvements des couches externes du noyau fluide. *Thèse Paris VII*, 1985.

GIRE C., LE MOUEL J.L. et T. MADDEN. Motions at the core surface derived from SV data, *Geophys. J. R. Astr. Soc.*, 84, 1-29, 1985.

GUERIN, G., La thermoluminescence des plagioclases. Méthode de datation du volcanisme. Applications au domaine volcanique français: Chaîne des Puys, Mont Dore et Cezallier, Bas Vivarais, *Thèse, Paris*, 1983.

HALGEDAHL S.L., R. DAY et M. FULLER, The effect of cooling rate on the intensity of weak field TRM in single domain magnetite, *J. Geophys. Res.*, 85, 3690-3698, 1980.

HARRISON C.G.A. Secular variation and excursions of the earth's magnetic field, *J. Geophys. Res.*, 85, 3511-3522, 1980.

HEIRTZLER J.R., G.O. DICKSON, E.M. HERRON, W.C. PITTMAN II et X. LE PICHON. Marine magnetic anomalies, geomagnetic field reversals and notions of the ocean floor and continents.*J. Geophys. Res.*,, 73, 2119, 1968.

HELLER F. Self reversal of natural remanent magnetization in the Olby-Laschamp lavas, *Nature*, 284, 334-335, 1980.

HELLER et N. PETERSEN. The Laschamp excursion, *Phil. Trans. R. Soc.*, London, A306, 169-177, 1982.

HOFFMAN K.A. Palaeomagnetic excursions, aborded reversals and transitionnal fields, *Nature*, 294, 67-69, 1981.

IRVING E. et G. PULLAIAH. Reversals of the geomagnetic field, magnetostratigraphy, and relative magnitude of paleosecular variation in the Phanerozoic, *Earth Sci. Rev.*, 12, 35, 1976.

KRISTJANSSON, L., Some statistical properties of paleomagnetic directions in Icelandic lava flows, *Geophys. J. R. astr. Soc.*, 80, 57-71, 1985.

KRISTJANSSON, L. AND A. GUDMUNDSSON, Geomagnetic excursion in late-glacial basalts outcrops in south-western Iceland, *Geophys. Res. Lett.*, 7, 337-340, 1980.

McFADDEN P.L., R.T. MERRILL, W. LOWRIE etD.V. KENT, The relative stabilities of the reverse and normal polarity states of the Earth's magnetic field, *Earth. Plant. Sci. Lett.*, 82, 373-383, 1987.

MERRILL R.T. et McELHINNY, The Earth's magnetic field, its history, origin and planetary perspective, *Academic Press, International Geophysics series*, 32, 1983

MERRILL R.T. et P.L. McFADDEN, Secular variation and the origin of geomagnetic fied reversals, *J. Geophys. Res.*, 93, 11589-11597, 1988.

MULLER R.A. et D.E. MORRIS. Geomagnetic reversal from impacts on the Earth, *Geophys. Res. Let.*, 13, 1177-1180, 1986.

NAIDU P.S. The geomagnetic field reversal independent ?, *J. Geomg. Geoelect.*, 26, 101, 1974.

NESS G., S. LEVI et R. COUCH. Marine magnetic anomalies time scales for the Cenozoic and Late Cretaceous : a precis, critique and synthesis, *Rev. Geophys. Space Phys.*, 18, 753, 1980.

PAL P.C. et K.M. CREER, Geomagnetic reversal spurts and episodes of extraterrestrial catastrophism, *Nature*, 320, 148-150, 1986.

PHILLIPS J.D. Time variation and asymmetry in the statistics of geomagnetic reversal sequences, *J. Geophys. Res.*, 82, 835, 1977.

RAMPINO M.R. et R.B. STOTHERS, Terrestrial mass extinction, cometary impacts and the sun's motion perpendicuar to the galactic plane, *Nature*, 308, 709-712, 1984.

ROPERCH, P. et A. CHAUVIN, Transitional field behavior: Records from French Polynesia, *Geophys. Res. Lett.*, 14, 151-154, 1987.

ROPERCH, P., N. BONHOMMET AND S. LEVI, Paleointensity of the earth's magnetic field during the Laschamp excursion, and its geomagnetic implications, *Earth Planet. Sci. Lett.*, 88, 209-219, 1988.

SALIS, J.S., Variation seculaire de champ magnetique terrestre- Directions et paléointensité- sur la période 7000-70000 ans BP, dans la Chaîne de Puys, Thèse, *Mémoires et Documents du CAESS*, Rennes, 1987.

STOTHERS R.B. Periodicity of the Earth's magnetic reversals, *Nature*, 322, 444, 1986.

THELLIER, E. and O. THELLIER, Sur l'intensité du champ magnétique terrestre dans le passé historique et géologique, *Ann. Geophys.*, 15, 285-376, 1959

TUCHOLKA P., FONTUGUE M. et P. GUICHARD and M. PATERNE. The Blake magnetic polarity episode in cores from the Mediterranean Sea, *Earth Planet. Sci. Lett.*, 86, 320-326, 1987.

VEROSUB K.L. Geomagnetic excursions : a critical assessment of evidence as recorded in sediments of the Brunhes epoch, *Phil. Trans. R. Soc.,*London, A306, 161-168, 1982.

VEROSUB K.L., S.K. BANERJEE. Geomagnetic excursions and their paleomagnetic record, *Rev. Geophys. Sp. Phys.*, 15, 145-155, 1977.

WALTON D., The lack of reproducibility in experimentally determined intensities of the earth's magnetic fiedl, *Reviews of Gepohysics*, 26, 15-22, 1988.

KRISTJANSSON, L. AND I., MC DOUGALL, Some aspects of the late Tertiary geomagnetic field in Iceland, *Geophys. J. R. Soc.*, 68, 273-294, 1982.

LA BRECQUE J.L., D.V. KENT et S.C. CANDE. Revised magnetic polarity time scale for Late Cretaceous and Cenozoic time, *Geology*,5, 330, 1977.

LE MOUEL J.L. , C. GIRE et T. MADDEN. Motions at the core surface in the geostrophic approximation, *Phys. Earth Planet. Int.*, 39, 270-287, 1985.

LEVI, S., H. AUDUSSON, R.A. DUNCAN AND L. KRISTJANSSON, The geomagnetic excursion of Skalamaelifell Iceland: additional evidence for unstable geomagnetic behavior circa 40 Ka ago, *EOS, Trans. Amer. Geophys. Union*, 68, 1249, 1987.

LIDDICOAT et COE. Mono lake geomagnetic excursion, *J. Geophys. Res.*, 84, 261-271, 1979.

LOWRIE W. et W. ALVAREZ. One hundred million years of geomagnetic polarity history, *Geology*, 9, 392, 1981.

LUND S.P., LIDDICOAT J.C., K.R. LAJOIE, T.L. HENYEY et S.W. ROBINSON. Paleomagnetic evidence for long-term (10^4 year) memory and periodic behavior in the Earth's core dynamo process, *Geophys. Res. Lett.*, 15, 1101-1104, 1988.

LUTZ T.M. The magnetic reversal record is not periodic, *Nature*, 317, 404-407, 1985.

LUTZ T.M. et G.S. WATSON. Effects of long-term variation on the frequency spectrum of the geomagnetic reversal record, *Nature*, 334, 240, 1988.

MANKINEN E.A. et G.B. DALRYMPLE. Revised geomagnetic polarity time scale for the interval O.5 m.y. BP*J. Geophys. Res.*, 84, 615, 1979.

MANKINEN E.A., M. PREVOT, C.S. GROMME et R.S. COE, The steens mountain (Oregon) geomagnetic polarity transition. I Directional history, durations of episodes and rock magnetism, *J. Geophys. Res.*, 90, 10393-10416, 1985.

MARSHALL, M., A. CHAUVIN AND N. BONHOMMET, Preliminary paleointensity measurements and detailed magnetic analysis of basalts from the Skalamaelifell excursion, southwest Iceland, *J. Geophys. Res.*, 93, 11681-11698, 1988.

MAZAUD A. , C. LAJ, L. de SEZE et K.L. VEROSUB. 15-Myr periodicity in the frequency of geomagnetic reversals since 100 Myr, *Nature*, 304, 328, 1983.

McCLELLAND-BROWN E., Experiments on TRM intensity dependence on cooling rate, *Gepohys. Res. Lett.*, 11, 205-208, 1984.

McDOUGALL I. The present status of the geomagnetic polarity time-scale. in The Earth : its origin, structure and evolution (N.W. Mc Elhinny, ed.), p. 543. *Academic Press*, London and New York, 1979.

McDOUGALL I. Status of geomagnetic polarity time scale, *J. Geomg. Geolelect.*, 37, 129-137, 1985.

McFADDEN et R.T. MERRILL. Lower mantle convection and geomagnetism, *J. Geophys. Res.*, 89, 3354-3362, 1984.

McFADDEN, P.L. et R.T. MERRILL, Geodynamo energy sources constraints from paleomagnetic data, *Phys. Earth. Planet. Int.*, 43, 22-33, 1986.

WÖRM H.U., M. JACKSON, P. KELSO et S.K. BANERJEE, Thermal demagnetization of partial thermoremanent magnetization, *J. Geophys. Res.*, 93, 12196-12204, 1988.

ANNEXE 1

I - Preliminary paleointensity measurements and detailed magnetic analyses of basalts from the Skalamaelifell excursion, southwest Iceland.

II - Transitional geomagnetic field behavior: volcanic records from French Polynesia.

JOURNAL OF GEOPHYSICAL RESEARCH, VOL. 93, NO. B10, PAGES 11,681-11,698, OCTOBER 10, 1988

PRELIMINARY PALEOINTENSITY MEASUREMENTS AND DETAILED MAGNETIC ANALYSES OF BASALTS FROM THE SKALAMAELIFELL EXCURSION, SOUTHWEST ICELAND

Monte Marshall[1], Annick Chauvin, and Norbert Bonhommet

Laboratoire de Geophysique Intern, Universite de Rennes I, Rennes, France

Abstract. Among the many excursions reported in the late Brunhes, the Skalamaelifell excursion, recorded in 22 flows in three hills of assumed late Wisconsin basalts in the active rift zone of the Reykjanes peninsula, is one of the most reliable. It is characterized by a single, well-defined transitional direction (D=260, I=-16). Paleointensity (PI) measurements, using the Thellier method as modified by Coe in a vacuum with partial thermoremanent magnetization checks, were made on six samples from the excursion flows. For comparison, 10 samples from the adjacent and probably nearly contemporaneous normally magnetized flows were also measured. Because of sample scarcity, four of the excursion samples and seven of the normal samples had been already af demagnetized to 20 mT in Iceland. The samples, however, were chosen because of their high coercivity and lack of viscous remanent magnetization. They retained 70-95% of their natural remanent magnetization (NRM) after 20 mT demagnetization, and their remanence directions were stable during the 20 mT demagnetization and during 2-6 years of storage following it. Saturation magnetization (J_s) measurements suggest that the reason for the low NRM of the excursion samples was a paleofield one fourth to one tenth that of the normal basalts. The mean PI from four excursion samples is 4.3 ± 0.6 μT, whereas the mean PI of the five normal samples considered reliable is 30 ± 9 μT. The quality of the NRM-thermoremanent magnetization (TRM) data correlated well with the reversibility of the J_s-T curves. The PI differences agree, in general, with those predicted by the NRM/J_s data, especially when comparing the means of the two groups, which average the effects of different grain sizes. A prior, partial alternating field (af) demagnetization of one sample in each of two pairs from the same cores caused the PI to be underestimated by only 10%. Continuous af demagnetization during the NRM-TRM measurements of one sample in another pair that had nonlinear TRM-TRM plots, even in the undemagnetized sample, caused the PI to be overestimated by 40%. These results, combined with other studies, suggest that the effect of partial af demagnetization on high-coercivity samples depends on when the demagnetization is done, i.e., only prior to or during the NRM-TRM measurements, and, probably more importantly, the thermochemical stability of the sample. If correct, this increases the usefulness for PI determinations of old, hard to recollect, partially demagnetized collections. The very low PI of 4 μT is similar to that found for excursions and transitions in Iceland and other places. However, its virtual geomagnetic pole lies 90° from a north-south vertical plane through the sites, which rules out a purely axisymmetric model for the excursion. The low normal intensities are similar to those found in the Chaine des Puys (France) and elsewhere for the period 10,0000-50,000 years B.P.. Given its very low PI and a direction only 70° from complete reversal, the Skalamaelifell excursion is most likely the result of nondipole fields and an unusually weak dipole field, such as that observed in France for the 10,000-year interval, 35,000-45,000 years B.P., surrounding the Laschamp excursion.

Introduction

This paper reporting measurements made to estimate the intensity of the Earth's magnetic field during the Skalamaelifell excursion is dedicated to Allan Cox. Among his many contributions to paleomagnetism and geomagnetism, Allan Cox and his colleagues established the existence and timing of reversals by the worldwide correlation of volcanic rocks having the same polarity and age. In the last two decades much research has been focused on the more localized, small-scale changes of the geomagnetic field (ordinary secular variation) and on intermediate-scale changes such as extreme secular variation and short-lived or aborted reversals, called excursions.

The core processes and resultant configuration of the geomagnetic field at the Earth's surface during the geologically brief, intermediate-scale excursions are still unknown. As pointed

[1]Permanently at Department of Geological Sciences, San Diego State University, San Diego, California.

Paper number 7B3053.
0148-0227/88/007B-3053$05.00

out by Verosub [1982], there is probably a continuous spectrum of field behavior between ordinary secular variation and complete, long-duration reversals. Therefore, as viewed from the rock record, excursions can be defined as departures of the local field direction, or its corresponding virtual geomagnetic pole (VGP), from the values for a geocentric, axial dipole greater than some semiarbitrary limit.

The first evidence of the existence of more than ordinary secular variation during a period of constant polarity was the discovery of reversed directions in a series of late Quaternary lava flows in southcentral France, now known as the Laschamp excursion [Bonhommet and Babkine, 1967]. In the following 10 years, about 16 excursions were found, mostly in sediments, for the time interval since about 40,000 years B.P. [Barbetti and McElhinny, 1976]. Because of age uncertainties, how many of these excursions are due to the same geomagnetic fluctuation is uncertain. Moreover, whether the abnormal magnetization directions found in many of the sediments are a real record of a field change or are just the result of other factors such as deformation during coring or unusual depositional conditions is questionable [Verosub, 1982].

Despite the above problems, the study and possible correlation of geomagnetic excursions is crucial to both our understanding of the core-mantle processes involved and also to the use of excursions as regional or even worldwide stratigraphic markers. Measurements of the paleofield intensity (PI) during excursions are important for both. Are all excursions characterized by the anomalously low PI values usually found in the intermediate directions during polarity transitions? How many excursions are due to unusually large standing or drifting nondipole fields superimposed on a normal strength dipole, as opposed to normal dipole fields in a time of unusually weak dipole fields?

Unlike the remanence in sediments, the thermoremanence in igneous rocks is fairly well understood and often reproducible in the laboratory, sometimes allowing the accurate determination of PI values. Unfortunately, only three of the more than 16 sites that have possibly recorded geomagnetic excursions in the past 50,000 years are igneous. These are the Laschamp excursion and two sites in Iceland, the "Maelifell event" of Pierce and Clark [1978] and the "Skalamaelifell excursion" of Kristjansson and Gudmundsson [1980]. Since the PI during the Laschamp excursion has already been measured [Roperch and Bonhommet, 1982], we have chosen to make PI measurements on the more extensively sampled Skalamaelifell excursion flows.

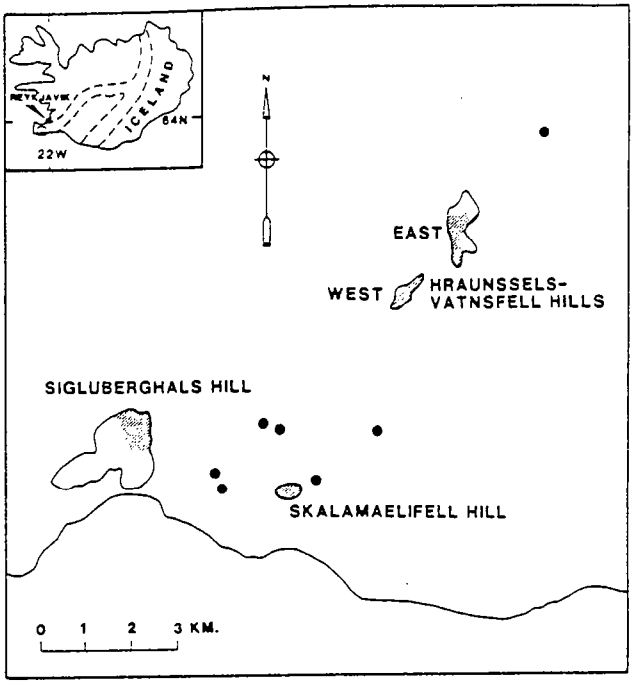

Fig. 1. Map of sample localities on the south coast of the Reykjanes peninsula. Hachured areas are portions of three volcanic hills in which the excursion basalts were found. Four of our excursion samples (14B-2P, 14C-3, G6, and G12) were taken from Sigluberghals Hill, two (M7 and MK36P) are from Skalamaelifell Hill. Solid circles are the seven normal sites used in this study. Inset map of Iceland shows sampled area (the square on the Reykjanes peninsula) and boundaries of current rifting and volcanism. Extent of excursion outcrops, samples, and sample locations kindly provided by L. Kristjansson personal communication, (1985).

The Skalamaelifell Excursion

In a search for reversely magnetized basalts in the axial zone of the Mid-Atlantic rift system on the Reykjanes peninsula, southwest Iceland, Kristjansson and Gudmundsson [1980] found three basaltic hills with stable remanent directions having shallow upward inclinations and westerly declinations (Figure 1). The average remanence intensity of the excursion flows was found to be about one tenth that of the surrounding, normally magnetized basalts. Given the similarity of remanent directions in the three hills, the rarity of such intermediate directions, and the closeness of the three hills (2-8 km apart), they concluded that the lavas of all three hills were probably erupted within 100 years of each other. They assigned a tentative age of late Wisconsin, i.e., 12,000 to 30,000 years

B.P., to this excursion. Given the probable brevity of the Skalamaelifell excursion and the uncertainty of its age, they hesitate to correlate it to any other late Quaternary excursion. Since a viscous remanence (VRM) with a steep positive inclination was found in most of the cores, L. Kristjansson kindly sent us portions of some of the most stably magnetized cores, as well as their demagnetization data, from their 1980 and subsequent studies.

Samples

Paleointensity measurements were made on 16 samples from the Skalamaelifell area (Figure 1 and Table 1). Six of the samples are from six of the excursion flows. For purposes of comparison, PI measurements were made on 10 samples from seven of the surrounding, normally magnetized basalt flows. The flows are commonly 2-4 m thick, are separated by ash or scoria, and usually outcrop as discontinuous exposures surrounded by volcanic rubble. Little can be said about the stratigraphic relationships between the various outcrops. Of the normal samples, MK4, BL17, and MK28 are probably older than the excursion samples, whereas MK13 and HV15 are possibly younger than the excursion (L. Kristjansson, personal communication, 1988). All six of the excursion samples are from the collection of 55 cores used by Kristjansson and Gudmundsson [1980] in their study. The 10 normal samples are from more recent studies in this area.

Valid PI measurements require that the remanence in a sample is thermoremanent magnetization (TRM) and, preferably, that the samples are not already partially demagnetized. The very limited number and general presence of VRM in cores from this area necessitated the use of samples whose high coercivity and lack of appreciable VRM was known by having been partially demagnetized to 20 mT (200 Oe) in Iceland. Two of the six excursion samples (14B-2P and MK36P), however, and three of the 10 normal samples (BL16P, BL17P, and BL19P) are undemagnetized portions of the core adjacent to that partially demagnetized in Iceland. The undemagnetized samples are highlighted by a "P" at the end of the sample name. In the case of the three normal "P" samples, the adjacent, partially demagnetized samples were available so that we could compare the effect of partial af demagnetization on PI determinations.

Magnetic Properties

In order to better understand and evaluate the results of the paleointensity measurements, an analysis of the remanence and other magnetic properties is useful (Table 1).

Remanent Magnetization

The remanence directions of the excursion samples are closely grouped and inclined slightly upward and to the west (Figure 2). The mean, af-cleaned direction of the six excursion cores is D=262, I=-22, α_{95}=6, almost identical to the mean of the 55 cores (D=260, I=-16, α_{95}=3) in the study by Kristjansson and Gudmundsson [1980] from which they were selected. The af-cleaned directions of the seven normal cores are more scattered than those of the excursion cores and, with one exception, point steeply down to the NE. Their mean is D=31, I=69, α_{95}=9, a value about 30° clockwise and 7° shallower than that of a geocentric, axial dipole field at this latitude. The few normal flows have obviously not sampled the full azimuthal range of secular variation, but the angular departure of directions from that of an axial dipole ranges from 4° to 27°, with an average of 12°. Such dispersion is within the range of ordinary secular variation for Iceland [Cox, 1970; Doell, 1972].

The natural remanence intensities (J_{nrm}) of the two groups are quite different. The mean natural remanent magnetization (NRM) intensity of the 10 normal samples used in this study, 9 ± 7 A/m, is 5 times that of the six excursion samples, 2 ± 1 A/m (Table 1). However, the intensities vary by a factor of 10 within each group. The normal J_{nrm} ranges from 3 to 20 A/m, and the values tend to cluster into two groups. Six of the normal samples have a J_{nrm} of 3-6 A/m,with an average value of 4 A/m, essentially the same as that of the 18 normal samples reported by Kristjansson and Gudmundson [1980] from this area and a value typical of Tertiary Icelandic basalts [Kristjansson, 1984]. The other four normal J_{nrm} range from 12 to 20 A/m, higher than average. The J_{nrm} of the excursion samples ranges from 0.3 to 4 A/m, making two of the excursion samples more intensely magnetized that the two weakest normal samples.

In order to compare better the thermoremanence intensity of Iceland basalts by eliminating most of the viscous and lightning-produced secondary remanence, magnetization intensities after 10-mT af demagnetization are the values traditionally reported. Since they were chosen for their high coercivities, the J_{10} values of the present samples are not significantly less that the J_{nrm} (Table 1). The J_{10} of the four partially demagnetized excursion samples ranges from 0.3 to 4 A/m, which places them among the most intensely magnetized of the collection of 55 excursion samples, whose mean J_{10} is 0.4 A/m [Kristjansson and Gudmundson, 1980]. In a study of over 2000 Icelandic basalt flows

Table 1. Sample Magnetization Data

Sample	D_I	I_I	D_R	I_R	J_{nrm}	J_{10}	δDIR	J_{20}/J_{nrm}	δDIRS	K	Q	J_s	H_s	J_{nrm}/J_s
								Excursion						
14B-2P	--	--	266	-19	0.63	--	--	--	--	0.46	2.5	0.48	2.5	1.3
14B-2*	264	-18	--	--	1.1+	1.1+	6+	0.93+	--	--	--	--	--	--
14C-3	269	-29	282	-33	1.8	1.7	7	0.93	12	1.08	3.0	1.26	3.0	1.4
G6	262	-24	264	-27	0.97	0.88	11	0.78	4	0.72	2.4	1.01	3.0	0.96
G12	258	-26	258	-31	3.3	3.0	8	0.80	5	1.43	4.2	1.31	2.0	2.5
M7	265	-15	269	-20	3.7	3.6	4	0.89	6	1.54	4.4	1.40	3.0	2.6
MK36P	--	--	256	0	0.34	--	--	--	--	0.97	0.6	0.98	3.0	0.35
MK36*	256	-17	--	--	0.36+	0.33+	26+	0.77+	--	--	--	--	--	--
Mean	262	-22	265	-22	1.8±1.4	2.3±1.2	7±3	0.85±0.07	7±4	1.03±0.4	2.8±1.4	1.07±0.34	2.7±0.4	1.5±0.9
								Normal						
HV15	32	+67	17	72	17	15	11	0.78	8	1.40	22	0.50	4.0	34+
BL16P	--	--	37	70	2.8	--	--	--	--	0.50	10	0.48	3.5	5.8
BL16	23	66	31	62	3.3	3.0	1	0.71	6	0.56	11	0.52	3.5	6.3
BL17P	--	--	74	62	5.1	--	--	--		0.67	14	0.85	4.0	6.0
BL17	79	63	81	65	5.9	5.5	2	0.81	2	0.73	15	0.89	4.0	6.6
BL19P	--	--	32	77	15	--	--	--	--	1.53	18	0.96	3.0	16
BL19	33	69	32	70	20	19	2	0.79	1	1.72	21	1.01	3.0	20
MK4	5	70	7	72	3.1	2.8	1	0.68	3	0.51	11	0.43	3.5	7.2
MK13	355	80	350	80	2.5	2.3	0	0.75	1	0.38	12	0.45	3.5	5.5
MK28	26	57	28	61	12	12	0	0.84	4	1.17	19	1.05	3.0	12
Mean	31	69	37	71	9±7	9±7	1±1	0.76±0.06	4±3	0.92±0.5	15±4	0.74±0.26	3.5±0.4	9.5±5

D_I and I_I (in degrees), cleaned remanence declination and inclination, respectively, after 20-mT (200 Oe) af demagnetization in Iceland; D_R and I_R (in degrees), remanence declination and inclination, respectively, measured at Rennes at start of PI measurements; J_{nrm}, natural remanence intensity before demagnetization or heating, in ampress per meter (10^{-3} emu/cm^3); J_{10}, remanence intensity after 10-mT af demagnetization in Iceland; δ DIR, change in remanence direction during af demagnetization to 20 mT in Iceland; J_{20}/nrm, ratio of remanence remaining after 20-mT af demagnetization in Iceland to that before demagnetization; δ DIRS, change in remanence direction of the partially (20 mT) demagnetized cores after 2-7 years storage in the Earth's field in Iceland and Rennes; K, magnetic susceptibility, X 10^{-3}/cm^3, cgs; Q, Koenigsberger ratio, J_{nrm}/KH, H=55 μT (0.55 Oe); J_s, saturation magnetization, A m^2/kg (emu/g); H_S, field required for saturation, 10^{-1} T (kG).

* Have Iceland data only;

\+ Not used in calculating mean.

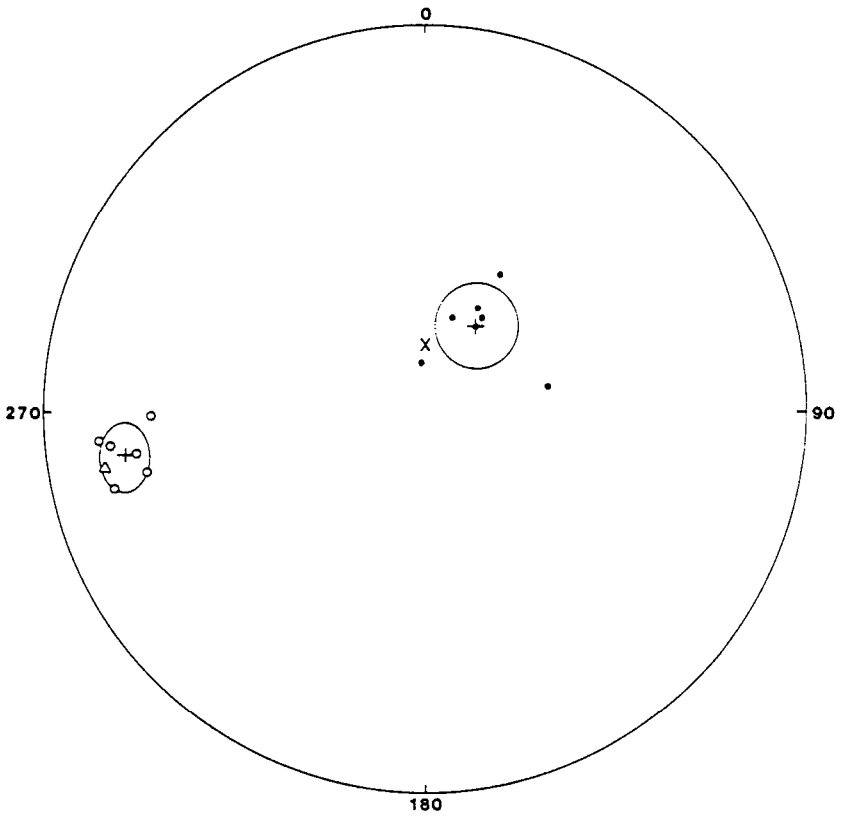

Fig. 2. Equal-area projection of the cleaned (at 20 mT) remanence directions of the six excursion and seven normal cores. Open circles, upper hemisphere; solid circles, lower hemisphere; plus, average directions of the two groups with their alpha 95 confidence limits; cross, direction at this latitude (64o N) of a geocentric, axial dipole field; delta, mean direction of the excursion samples studied by Kristjansson and Gudmundsson [1980].

Kristjansson [1985] found that the mean remanence, expressed as J_{10}, decreased systematically as its direction departed from that of an axial dipole field. For angular departures of 70°, as is the case for the excursion samples, the average J_{10} is 1 A/m. The 55 Skalamaelifell excursion basalt samples thus have only half the remanence intensity, on average, of Icelandic basalts with similarly nonaxial directions and one tenth that of "normal", axial dipole basalts. In addition to differences in the geomagnetic field strength when the basalts were erupted, the differences in J_{nrm} both between and within the two groups are probably due to a number of other factors, such as differences in amount, size, and composition of the magnetic grains. Given our sample selection criterion of using only the more stable samples during af demagnetization and the fact that both remanence coercivity and intensity increase with decreasing grain size, our samples probably represent the finer-grained basalts.

The high coercivity and lack of a significant VRM component in the NRM of our samples is shown by the small intensity and direction change during their partial af demagnetization and subsequent storage in Iceland. The directional change during the 20-mT af demagnetization in Iceland, δDIR, of the four partially demagnetized excursion samples used in this study was 11° or less (Table 1). All but 1° of these directional changes occurred by 10 mT (15 mT for MK36). The undemagnetized excursion sample 14B-2P is likely to be equally stable since the δDIR of the adjacent sample, 14B-2 is only 6°. Undemagnetized sample MK36P should be the least stable of all since the δDIR of MK36 is 26°. The normal group is even more stable, and the seven partially demagnetized samples have a δDIR of 2° or less. On average, the samples retained about 80% of their NRM after demagnetization to 20 mT (Table 1). Except for MK36, the excursion samples have slightly higher coercivities than the normal samples and retain 80-95% of their NRM after 20-mT af demagnetization. Further evidence of their high coercivities is the very small change, 5° on average, in the remanence direction

after being demagnetized to 20 mT, stored in the Earth's field for 2 (the normal samples) to 6 (the excursion samples) years in Iceland and then stored in the Earth's field at Rennes for 1 year (δDIRS, Table 1). The almost total lack of any VRM and the very high percent of NRM remaining even after 20-mT af demagnetization strongly suggests that all of the 11 partially demagnetized samples, and most of the five, adjacent undemagnetized samples (with the possible exception of MK36P) are good candidates for PI measurements.

Magnetic Susceptibility K and Koenigsberger Ratio Q

Unlike the NRM values, the magnetic susceptibilities of the samples vary by only a factor of 4, and there is no significant difference between the means of the excursion and the normal samples (Table 1). For rocks with the same magnetic mineralogy, as will be seen to be the case in the present samples, any departure from a simple linear increase of NRM with increasing K is probably due to differences in either grain size and/or paleofield intensities when the samples cooled. A plot of J_{nrm} versus K of the samples shows that the two sample sets cluster fairly closely along two distinct lines (Figure 3). The slope of a single, best fit, straight line thru the normal values is 5-6 times greater than that through the excursion values. The difference in the J_{nrm} between BL19 and BL19P, samples from the same core, shows the effect of different grain sizes. Such a distinctly different grouping of the normal and excursion sample sets is probably not due to some fortuitous, systematic grain size variation but suggests that the paleofield during the excursion was, on average, about one fifth that during the eruption of the normal flows. Using the tenfold difference in average J_{nrm} and the similarity of K values between the two groups, Kristjansson and Gudmundsson [1980] suggested that the excursion paleofield might have been only one tenth that of the normal flows.

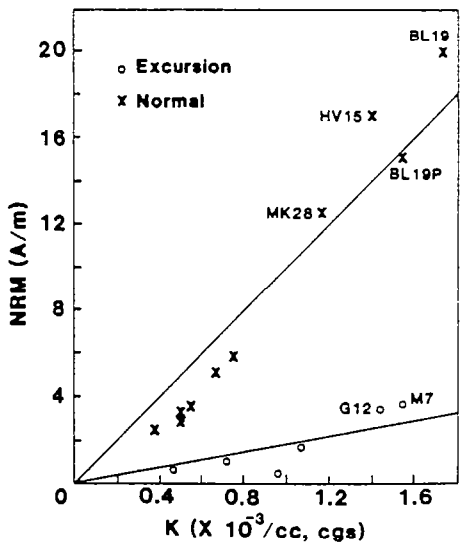

Fig. 3. Plot of NRM intensity versus magnetic susceptibility K of our samples.

The Koenigsberger ratio, or ratio of remanent to induced magnetization, is, in effect, the slope of the NRM versus K plots in Figure 3. The Q of the normal samples ranges from 10 to 22, with a mean of 15 (Table 1). That of the excursion samples ranges from 0.6 to 4.4, with a mean of 3, one fifth that of the normal samples. The four normal samples with the highest J_{nrm} and K have Q values of about 20, whereas the four weakest have Q values of about 10. A similar trend exists in the excursion samples where the two samples with the highest J_{nrm} and K also have the larger Q values.

Saturation Magnetization J_s

Saturation magnetization is a parameter useful in estimating the amount of ferromagnetic minerals in a rock since it depends only on the percent and composition, which determines the spontaneous magnetization, of the magnetic grains. As will be seen next, Curie temperature measurements indicate that the magnetic mineralogy in all the samples except HV15 is single phase, almost pure magnetite. Like the magnetic susceptibility, the J_s values for the two groups overlap; the J_s ranges from 0.5 to 1.4 A m^2/kg (emu/g) in the excursion samples and from 0.4 to 1.0 A m^2/kg in the normal samples (Table 1). The excursion mean J_s, 1.1 A m^2/kg, is somewhat greater than the normal mean, 0.7 A m^2/kg. Given the range in values and limited number of samples, this difference is probably not significant.

The J_s values prove, as was strongly suggested in the J_{nrm} versus K plot, that the low NRM intensities of the excursion basalts are not due simply to a lesser percent of magnetic grains. A plot of J_{nrm} versus J_s shows the same grouping seen in the J_{nrm} versus K plot (Figure 4). Most of the normal samples plot along a line whose slope is 4 times greater than that of the excursion samples. And, as above, four of the normal samples (HV15, BL19, Bl19P, and MK28) and two of the excursion samples (G12 and M7) have a higher than average J_{nrm} for their magnetite content. The J_{nrm}/J_s ratio of the three most strongly magnetized normal samples is about 10 times that of most of the excursion samples (Table 1). Excursion sample MK36P has an unusually low J_{nrm}/J_s ratio. How much of the variation in the J_{nrm}/J_s ratios is caused by differences in grain

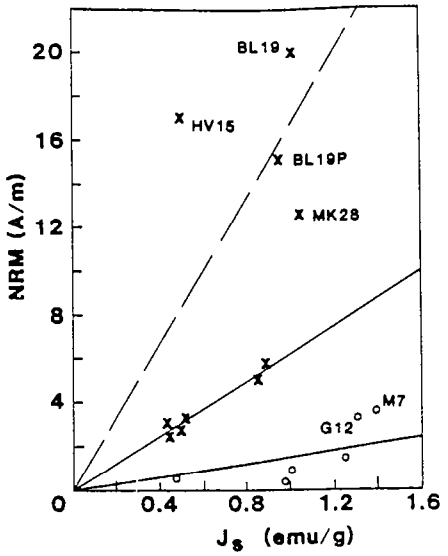

Fig. 4. Plot of NRM intensity versus saturation magnetization, J_s, of our samples. Circles and crosses as in Figure 3.

size, e.g., BL19 versus BL19P, and how much to paleofield differences still remains unresolved, however. Measures of the field required for saturation, H_s, suggest that the average coercivity of the normal samples 0.35 T (3.5 kG) is slightly higher than that (0.27 T) of the excursion samples (Table 1). However, the difference is small and not statistically significant. Saturation measurements reflect simple percentages of magnetite grains, whereas a disproportionately large amount of the NRM may be carried in a few percent of the magnetite grains that are small enough to be psuedo-single or even single domain. It should be noted here that since J_{nrm} is normalized by volume and J_s by weight, values of J_{nrm}/J_s can be affected by variations in sample porosity. This effect is not significant since the porosity of the samples ranged from 0 to 20%, with an average value of 10% for both groups.

Curie Temperature T_c

Thermomagnetic (J_s-T) curves are one of the most useful measurements in PI studies. In addition to suggesting magnetic mineralogy and oxidation state, T_c values are the upper limit of the blocking temperature spectrum of a sample. In their PI study of the Steens Mountain basalts, Mankinen et al. [1985] classified J_s-T behavior according to the differences in form between the heating and cooling curves. As would be expected, those samples showing the least difference, i.e., the least mineralogical change during heating, provided the most concordant PI data [Prevot et al., 1985].

J_s-T curves for our samples were measured, in vacuo, on a continuously recording magnetic balance in fields of about 0.3 T (3 kG), a value usually greater than H_s. In order to better define the temperature at which any mineralogical changes begin, our heating runs were interrupted several times, usually at a temperature between 300° and 400°C and again between 450° and 550°C. At these points the sample was allowed to cool about 40°C, and the heating was then resumed.

Excepting sample HV15, the J_s-T curves of the samples exhibit a single Curie temperature between 555° and 575°C, typical of almost pure magnetite (Table 2). The J_s-T curves of most of the samples were almost reversible. The T_c on heating was within 5° of that on cooling, and the J_s was, on average, 20% higher than that before the heating (Table 2).

The thermomagnetic behavior of our samples can be divided into five categories on the basis of the reversibilty of the J_s-T curves: primarily on the difference in J_s (T) between heating and cooling and, secondarily, on any differences in J_s (T) during the intermediate cooling and heating cycles mentioned above. The J_s on cooling from about 620°C of nine samples was continuously greater than that on cooling. The intermediate temperature cycling showed that the J_s of five of these samples (called here type A) began to increase by several percent at temperatures of 300°-400°C (Table 2 and Figure 5a). In the four other samples (type B), no increase in J_s was detected during the heating even at about 500°C (Figure 5b). The J_s of the remaining seven samples was less during part or all of the final cooling than that during heating. In four of the samples (type C), the J_s curve at the beginning of the final cooling was less than that on heating but crossed over and remained greater for temperatures less than 200° to 500°C (Figure 5c). Interestingly, the intermediate thermal cycling of these samples showed a small (about 5%) decrease in J_s at temperatures greater than about 400°C. A larger decrease of 10-20 % during intermediate thermal cycling was observed in two samples (type D), and the final cooling curve remained below the heating curve to room temperature (Figure 5d). The type D cooling curves lack a well- defined Curie temperature, and their linearity suggests a range of magnetic mineral composition. The most complicated J_s-T behavior is shown by sample HV15, which apparently contains three magnetic minerals with Curie temperatures of about 240°, 460°, and 560°C (Figure 5e). However, only two Curie temperatures, at about 290° and 560°C, remain upon cooling.

The reason(s) for the irreversible

TABLE 2. J_S-T Measurements

Sample	$T_C(H)$	$T_C(C)$	$\frac{J_S(C)}{J_S(H)}$	T_{CY}	$\delta J_S(T)$	Type
14B-2P	565	570	1.4	350-385	REV	A
				475-520	+11	
14C-3	565	565	1.3	385-410	REV	A
				450-480	" "	
				515-540	+ 6	
G6	570	570	1.4	265-320	+ 2	A
				395-490	+ 2	
G12	555	560	1.4	360-380	+ 1	A
				415-490	+ 6	
M7	560	560	1.2	225-380	+ 3	A
				350-480	+ 3	
MK36P	570	565	1.06	330-385	REV	C
				475-510	- 4	
				525-545	- 4	
HV15	240	290	1.2	215-280	REV	E
	465	560		290-395	+ 6	
	560					
BL16P	575	575	1.2	285-330	REV	C
				440-485	- 4	
BL16	570	570	1.2	285-330	REV	C
				440-485	- 6	
BL17P	570	565	0.99	220-230	+ 2	D
				340-460	- 9	
BL17	570	565	0.97	305-400	+ 1	D
				450-505	-20	
BL19P	575	575	1.3	290-330	REV	B
				440-482	REV	
BL19	570	570	1.4	290-330	REV	B
				440-485	REV	
MK4	560	560	1.2	215-410	REV	B
				495-540	REV	
MK13	565	560	1.03	160-255	REV	C
				315-430	- 3	
				420-550	-10	
MK28	565	565	1.1	225-330	REV	B
				305-440	REV	
				415-545	REV	

$T_C(H)$ and $T_C(C)$, Curie temperature measured on the heating and cooling curves, respectively; $J_S(C)/J_S(H)$, ratio of saturation magnetization after cooling to that before heating; T_{CY}, temperature interval of intermediate thermal cycling (see text for explanation of experimental procedure); $\delta J_S(T)$, change, in percent, of J_S at the lowest temperature of each intermediate cycle compared with that measured on initial heating to the same temperature; REV, J_S-T curve reversible during the given cycle; Type, category of J_S-T behavior (see text and Figure 5).

behavior of even samples with apparently a single, high-temperature Curie point is/are not obvious. In weathered basalts, disproportionation of thermally unstable, cation-deficient spinels such as titanomaghemite or maghemite apparently cause most of the irreversible behavior when samples are heated in a vacuum. Both J_S and T_C increase dramatically when titanomaghemite disproportionates during heating to magnetite and ilmenite and other nonmagnetic phases [Marshall and Cox, 1972; Marshall, 1978; Gromme et al., 1979]. However, if the oxygen fugacity is sufficiently low during the J_S-T run, the newly exsolved magnetite will be reduced at temperatures above about 600°C and remixes to form titanomagnetites with T_C and J_S values significantly less than those produced by the exsolution during the heating cycle [Marshall and Cox, 1972]. Even the finely intergrown magnetite and ilmenite produced by deuteric oxidation in lavas can be reduced and remixed during the J_S-

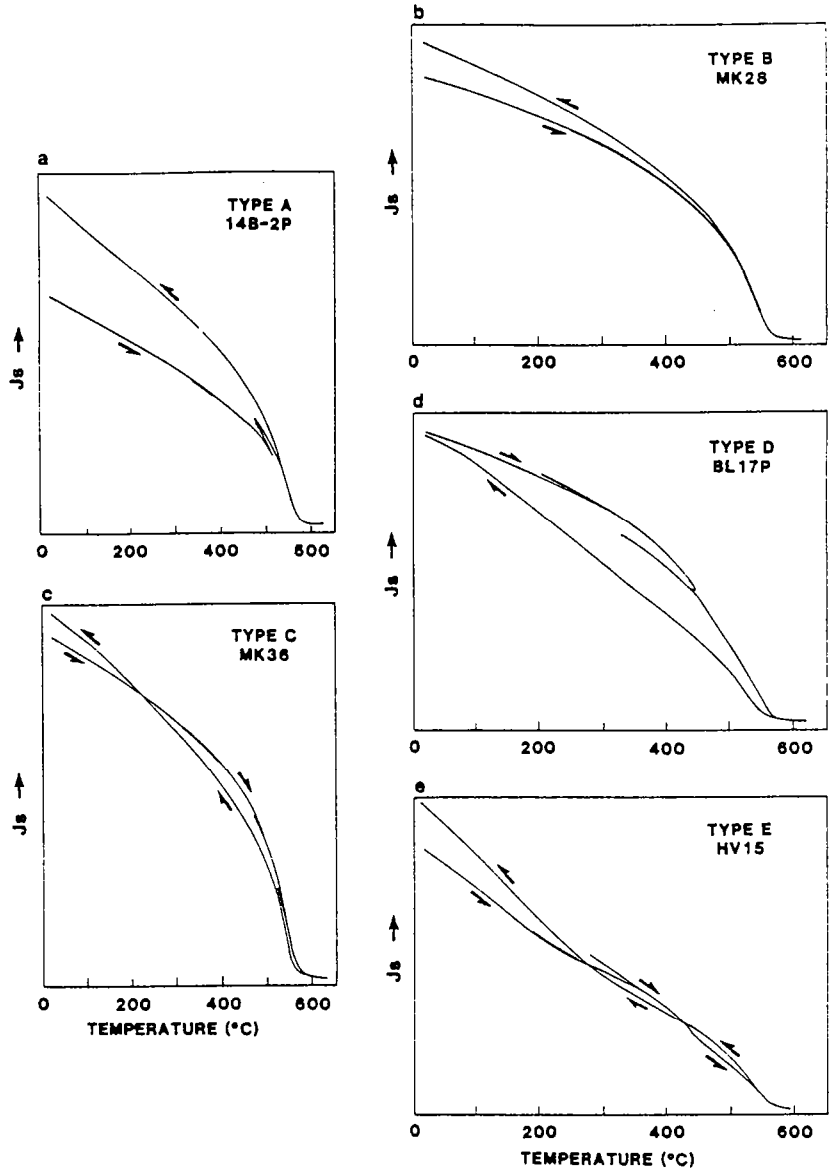

Fig. 5. Types of J_s-T curves observed in our samples. Heating and cooling curves designated by arrows. All runs were made on samples sealed in evacuated (less than 10^{-2} mbar) glass ampules and heated to about 620°C at 8°C/min. Darkened portions and spikes on the heating curves show the results of thermal cycling, i.e., allowing the sample to cool 25°-125°C during the heating cycle. Curie temperatures were estimated using the intersection of tangential lines method of Gromme et al. [1969].

T measurement (Gromme et al., 1969, Figure 3). The young age of our basalts and almost linear cooling curve of our type D basalts suggests that much of the decrease in J_s is due to such partial reduction and remixing of magnetite and ilmenite. Some of the decrease in Js seen in our samples and in many of the Miocene Steens Mountain basalts (type 2 of Mankinen et al.[1985] could be the result of the disproportionation of maghemite. Theoretically, its exsolution into magnetite and hematite should leave the T_c unchanged and decrease the J_s since the spontaneous magnetization of maghemite is similar to that of magnetite and the spontaneous magnetization of hematite is less than 1% that of magnetite.

Paleointensity Measurements

Laboratory Procedures

The paleointensity measurements were made using the Thellier and Thellier [1959] method as modified by Coe [1967a,b]. The samples were heated in an evacuated (pressure less than 10^{-2} mbar) quartz tube inside a mu-metal shield.

They were heated progressively in a series of 13-15 steps from 100° to 570°-580°C. Each step consisted of two heatings and coolings, each lasting about 2 hours, to the same temperature. The first heating and cooling was done in zero field; the second heating and cooling was in an applied field of 25 μT. The normal and excursion samples were heated together and a 25-μT field was chosen as a probable intermediate paleointensity. The remanence was measured after each cooling. The first measurement yields the decrease due to heating of the natural remanence, $J_n(T)$, whether it be the total NRM as for the "P" samples or the partial NRM remaining after 20-mT af demagnetization in Iceland. The vector difference between the first and second measurements yields the TRM acquired during cooling from the same temperature in a 25 μT field. In order to evaluate better the effects of af demagnetization on our PI values, half of the samples already partially demagnetized at 20 mT in Iceland were demagnetized at 20 mT, prior to measurement, after each cooling in the 25-μT field (the underlined samples in Table 3). The remaining samples were not demagnetized.

If the NRM is entirely TRM in origin, a plot of the NRM remaining versus the TRM acquired at each step will, ideally, yield a straight line whose slope is the ratio of the paleointensity to that used in the lab. In practice, the data frequently depart from linearity due to magnetochemical and physical changes during the heating [Prevot et al., 1985]. As a check on any magnetochemical or physical changes we have made four partial TRM (PTRM) checks. After the double heating and cooling at certain steps, the TRM destroyed by a third heating and cooling, in zero field, to a previous step about 50°C lower than that of the current step is compared to the TRM initially acquired at the lower step. This reveals any change in the TRM acquisition capacity in the interval from room temperature to the lower temperature step due to heating to the higher temperature.

Paleointensity Results

The paleointensity measurements show that the geomagnetic field during the excursion was considerably less than that when the normal basalts were erupted. The excursion PI values range from 3.4 to 5.0 μT, whereas the normal values range from 19 to 47 μT (Table 3). When looked at in detail, the various parameters measured during the course of the PI runs reveal some interesting relationships and magnetic behaviors. The blocking temperatures of all the samples are quite high. The samples typically retain over 90% of the NRM until 300°-450°C and half of their NRM until 450°-550°C. The average median demagnetizing temperature for both groups is about 520°C (Table 3). As would be expected from the directional stability discussed earlier, the orthogonal vector diagrams typically show a linear decrease of the remanence toward the origin. The only significant exception is sample MK36P, whose NRM direction varied erratically above 470°C. Its companion core showed the greatest change in direction during af demagnetization in Iceland (Table 1), yet its af "cleaned" direction was not significantly different from that of the other excursion samples. The erratic behavior coincides with unusually large increases in PTRM capacity at temperatures above about 470°C.

Most of the NRM-TRM plots are linear over an average temperature interval of 160°C. Figure 6 shows NRM-TRM plots of three excursion basalts that are typical in their linearity of most of the excursion and normal samples. The lowest useable temperature ranges from 250° to 510° with an average of about 400°C, whereas the highest useable temperature is, on average, about 560°C (Table 3). More importantly, the useable fraction f of the NRM is quite large and ranges from 40 to 96%, or 65% on average. The PI values are based on a least squares fit line through an average of eight points. The values of q, a quality factor which varies directly with f and N and inversely with scatter in the data, range between 2 and 54, with an average of 18, values similar to those obtained by Coe et al. [1978] in a study of late Quaternary Hawaiian basalts.

Considering the large fraction of the NRM whose decay usually yields very linear NRM-TRM plots, the PI values are apparently quite reliable. However, as Prevot et al. [1985] and others have shown, a good, linear fit of the NRM-TRM data is a necessary but not sufficient condition for accurate PI estimates. The PTRM checks show that most of the samples have very little change in their PTRM capacity, whereas that in some increases as much as 75% (Table 3). Often the PTRM capacity of a sample decreases at one temperature and increases at another. These checks can be used to assess the probable reliability of the PI values. The PTRM checks fall into two groups, based on the average change in the PTRM capacity over the last two or three temperature intervals. So little NRM was lost and TRM acquired by the first check at 280°-300°C in all the samples and even by 400°-440°C for many that the first and often second check is not meaningful. The changes in most samples average to less than 10%. This includes all the excursion samples, except MK36P, and all normal samples except HV15, BL17, and BL17P. These samples exhibit an average increase in PTRM capacity greater than

TABLE 3. Paleointensity Results

Sample	MDT	A	B	C	Type	T_{min} - T_{max}		N	f	g	σ	q	Fe ± σ(Fe)
						Excursion							
14B-2P	530	+15	-10	-10	A	340	540	8	0.56	0.82	0.019	24	4.6±0.09
14C-3	550	-	0	+10	A	510	555	4	0.37	0.62	0.125	2	5.0±0.62
G6	540	-5	+5	+ 5	A	250	555	11	0.64	0.84	0.027	21	4.6±0.12
G12	535	-	0	+ 5	A	400	555	8	0.72	0.80	0.027	21	3.4±0.09
M7	545	-	0	0	A	440	555	7	0.63	0.68	0.017	25	3.7±0.06
MK36P	500	+35	+45	+50	C	340	495	5	0.39	0.72	0.127	2	3.4±0.44+
Mean	535±20					380±90	540±25	7±2	0.55±0.14			16±11	4.1±0.6 <Fe>4.3
						Normal							
HV15	550	-	-	+25	E	490	570	6	0.57	0.71	0.047	9	24.9±1.2+
BL16P	495	-	-25	0	C	495	570	6	0.56	0.76	0.069	8	25.8±1.8+
BL16	480	-	0	+15	C	490	570	6	0.44	0.74	0.168	4	35.9±6.0+
BL17P	520	-	+55	+25	D	400	555	8	0.77	0.82	0.036	17	23.4±0.8+
BL17	520	-	+75	+20	D	280	570	11	0.96	0.86	0.027	31	19.1±0.5+
BL19P	520	+10	0	+ 5	B	340	570	10	0.93	0.87	0.015	54	33.5±0.5
BL19	530	+ 5	+10	+ 5	B	440	570	8	0.74	0.84	0.019	33	29.3±0.5
MK4	450	+10	0	0	B	300	570	11	0.89	0.88	0.051	15	47.4±2.4
MK13	490	-	+20	+ 5	C	400	570	9	0.89	0.85	0.079	9	22.2±1.8
MK28	540	-	-10	+ 5	B	440	570	8	0.82	0.78	0.071	9	38.2±2.7
Mean	510±30					410±80	570±5	8±2	0.75±0.20			19±16	34±9.5 <Fe>30

The underlined samples are those, already af demagnetized to 20 mT in Iceland, which continued to be af demagnetized at 20 mT after each TRM acquisition step; MDT, mean demagnetizing temperature, temperature at which the sample loses one half of its initial remanence, whether that is the total NRM as in the case of the "P" samples, or the 68-93% of the original NRM that remained after 20-mT af demagnetization in Iceland; columns A - C are PTRM checks during each NRM-TRM run (values are changes, in percent, of the PTRM capacity; see text for explanation of the laboratory procedure), temperatures are A, 495°-400°; B, 525°-470°; C, 555°-495°C for all samples except those underlined, in which case they are A, 490°-440°; B, 540°-490°; C, 570°-540°C; Type, J_S-T behavior type as in Figure 5; T_{min}-T_{max}, temperature range, in °C, over which the NRM-TRM points are essentially linear and therefore used for computing the best fit slope and corresponding PI value; N, number of NRM-TRM points in the useful temperature range above; f, fraction of the NRM with blocking temperatures in the T_{min}-T_{max} interval; g, gap factor, a measure of the evenness of spacing of the N points, g approaches 1 as the spacing becomes uniform; σ is a measure of the relative uncertainty of the slope determination and is the standard deviation of the least squares, best fit line through the N points, normalized by the slope value; q, quality factor, an estimate of the reliability of the PI value, = fg/σ, (f, g, σ, q [after Coe, et al., 1978]); Fe, the estimated paleointensity in microteslas; σ(Fe), the standard error of Fe; [Fe] is the weighted mean PI value [after Prevot et al., 1985].

+ Not used in computing mean value.

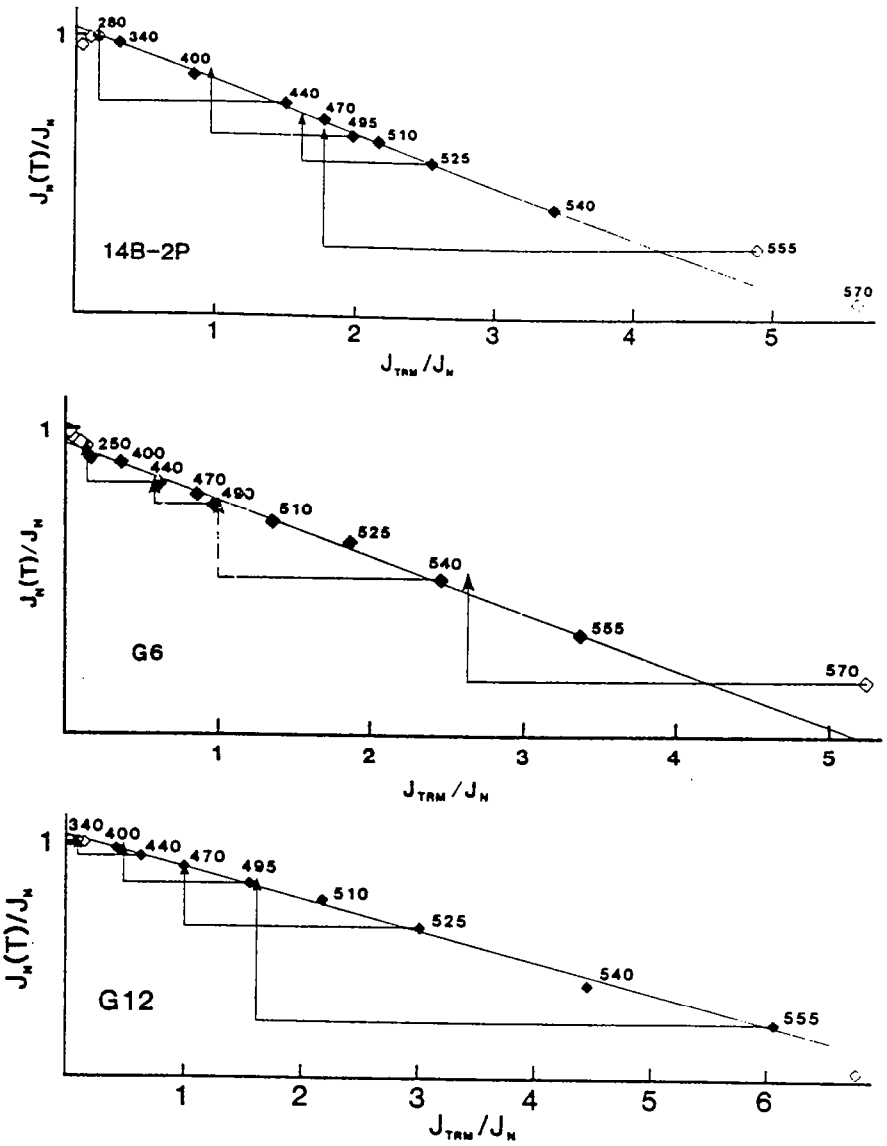

Fig. 6. NRM-TRM plots for three of the excursion samples. $J_N(T)$, the NRM remaining and J_{TRM}, the TRM acquired during each pair of heating steps (temperatures in degrees celsius); both are normalized by the remanence intensity J_N at the beginning of the heatings. Triangles are the PTRM checks. The lines connect each of the triangles to the NRM-TRM values measured at the double heating step immediately prior to the check. The abscissa of the triangles shows only that portion of the TRM from the last high- temperature step that was acquired during cooling from the same, lower temperature as that of the point laterally adjacent to the triangle and assumes the same NRM value as the earlier step. A shift of the triangle to the right of its corresponding point indicates an increase in PTRM capacity, a left shift indicates a decrease in PTRM capacity of the interval from room temperature to this temperature due to heating to the higher temperature. Sample 14B-2P has not been demagnetized, samples G12 and G6 were partially af demagnetized to 20 mT in Iceland, but only G6 was af demagnetized during the NRM-TRM runs. Solid diamonds are points used to calculate the PI.

25%. Prevot et al. [1985] have shown that a progressive increase in PTRM capacity will shallow the NRM-TRM slope, yielding an underestimated PI. A progressive 50% increase in the PTRM capacity, similar to that seen in MK36P, would yield a PI that is two thirds or 50% less than the true value. The large increase seen in samples BL17 and BL17P, however, decreases with increasing temperature not only proportionately but absolutely as well. A systematic decrease in the amount of PTRM added at progressively higher temperatures may

well steepen the NRM-TRM slope and yield an overestimated rather than underestimated PI. Nevertheless, considering the uncertainties, the PI values obtained from samples MK36P, HV15, BL17, and BL17P are probably less accurate than the PI values measured on samples in the first group.

The correlation between the degree of PTRM changes and the type of J_s-T behavior is good. All the samples in the first group are either type A, B, or C; that is, have fairly reversible J_s-T curves with a 3-40% increase in J_s on cooling (Figure 5). They also showed little or no changes in J_s(T) during the intermediate thermal cycling. As will be discussed shortly, the NRM-TRM behavior of two of the type C samples, BL16 and BL16P, is not at all ideal below about 500°C. The two type D (BL17 and 17P) and the one type E (HV-15) samples all show large increases in PTRM capacity.

Interestingly the two type D samples, which exhibited the largest increase in PTRM capacity, also had the largest decrease in J_s(T) during the thermal cycling. Both the experimental conditions and the magnetic properties measured in the J_s-T runs are different from those measured in the NRM-TRM experiments. In J_s-T runs the samples are usually subjected to only one heating and cooling lasting several hours, whereas in the NRM-TRM runs the samples are subjected to ten or more thermal cycles and spend at least an order of magnitude more time in each temperature interval. To the extent that the field in the J_s-T measurements approaches saturation, any changes in J_s are of a chemical nature, i.e., changes in the spontaneous magnetization. The NRM-TRM measurements are affected by both chemical and physical changes, such as changes in crystal dislocations and impurities, which can change the blocking temperature spectrum or PTRM capacity. From the limited number of samples in this study, as well as similar results from other studies [Coe et al., 1978; Gromme et al., 1979, Prevot et al., 1985], fairly reproducible J_s-T curves are, like linearity in NRM-TRM plots, a necessary but not sufficient condition for good PI results.

Effect of af Demagnetization

The samples in this study subjected to af demagnetization fall into two categories: five which were af demagnetized only once (in Iceland to 20 mT) and six which continued to be demagnetized to 20 mT after each TRM acquisition step (these are the underlined samples in Table 3). Some experiments have shown that af demagnetization can seriously degrade the results of PI measurements but the reason why is not well understood. Doell and Smith [1969] found that a single partial af demagnetization prior to some thermal PI methods can be helpful, despite the fact that their data show that partial af demagnetization can affect some of the high blocking temperature NRM. Coe and Gromme [1973] have shown that af demagnetization, when done after each step in the NRM-TRM measurement, steepens the slope and can yield PI values that are overestimated by several to as much as 65%. No PTRM checks were made in that study, but the amount of overestimation depends directly on the degree to which the NRM-TRM plot is nonlinear, both that of the af demagnetized sample and the undemagnetized sample used for comparison. The af demagnetized points generally track the undemagnetized points but at lower TRM values. In samples having large increases in PTRM capacity, as shown by the progressive displacement of the points above 400°C to the right of the slope for the known PI, the line defined by the demagnetized sample data at the lower temperature steps yields PI estimates that are 45-65% too large. However, when the TRM of the undemagnetized sample increases linearly to temperatures of almost 580°C, i.e., with little NRM remaining, the demagnetized sample data are linear as well and yield PI values that are overestimated by only about 5-15%.

Like the studies quoted above, we have only a few samples that can be used for direct comparison of the effects of af demagnetization. These are the three pairs of normal samples consisting of an undemagnetized ("P") sample and a demagnetized sample from the same core. The two pairs, BL17 and BL17P and BL19 and BL19P show the effects of only a single, 20-mT demagnetization prior to the NRM-TRM measurements. The PI values of samples BL17 and BL19 are both about 9% less than that derived from BL17P and BL19P, respectively (Table 3). Samples BL19 and BL19P are well suited for showing the effect on "ideal" samples, since their NRM-TRM plots are almost perfectly linear from about 400° to 570°C, they have q values of 33 and 54, respectively, and have good PTRM checks (Figure 7). Samples BL17 and 17P show the effect of prior af demagnetization on less ideal samples. Their NRM-TRM plots are almost as linear (q=17 and 31) from 400° to 570°C, but the PTRM checks reveal large increases in PTRM capacity (Table 3). Despite this difference, the effect of prior af demagnetization is minimal.

Unfortunately, the only sample pair on which to directly observe the effect of continuous af demagnetization, BL16 and BL16P, exhibit non-ideal NRM-TRM behavior (Figure 7). At temperatures below 490°C the TRM remains almost constant, while the NRM continues to decrease, yielding an almost vertical slope. The reason for this unusual behavior is unknown. Since a line through the low-temperature points would yield an unrealistically high PI

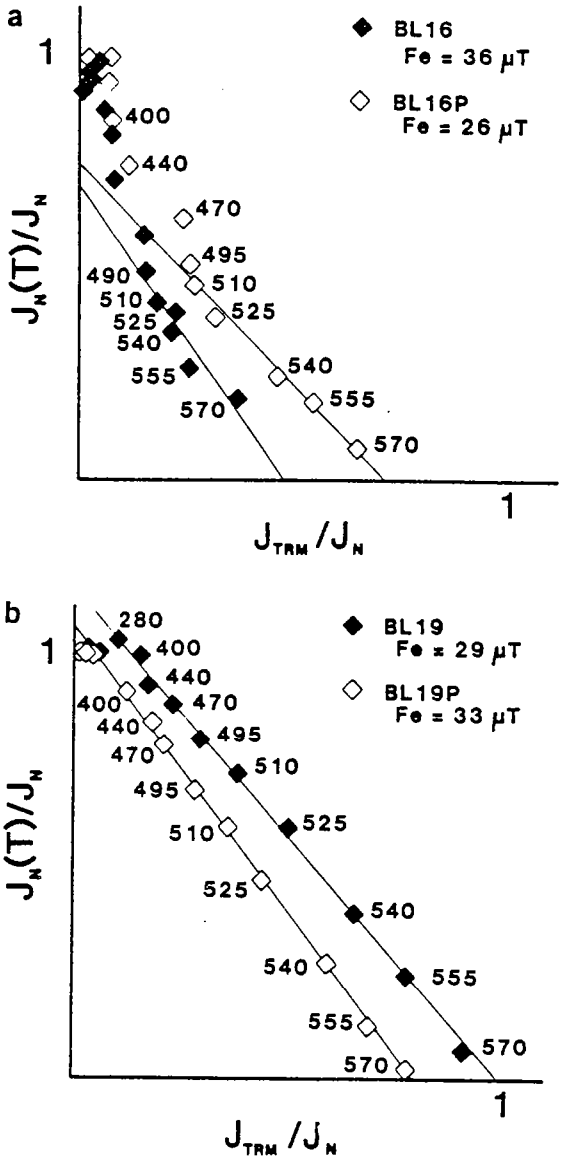

Fig. 7. NRM-TRM diagrams that illustrate the effect of af demagnetization on PI measurements of pairs of samples from the same cores. Samples BL16P and BL19P were never af demagnetized. Sample BL16, from the same core as BL16P, was demagnetized to 20 mT in Iceland and also prior to each TRM acquisition measurement during the NRM-TRM run. Sample BL19, from the same core as BL19P, was only demagnetized once to 20 mT in Iceland and not demagnetized during the NRM-TRM run. PTRM checks not shown for the sake of clarity. See Table 3 for the results of the checks.

and the high-temperature PTRM checks are good, the PI defined by the high-temperature points is probably closer to the true value. The slope of BL16 is considerably steeper than that of BL16P and yields a 40% greater PI. Although the study by Coe and Gromme [1973] shows overestimated PI's for demagnetized samples having large, nonlinear TRM increases at high temperatures, the conclusion seems to be the same; continuous af demagnetization degrades the NRM-TRM behavior of rocks which have poor linearity even when not af demagnetized and causes substantially (about 50%) overestimated paleointensities.

In light of these results, the PI values from the other five, continuously af demagnetized, samples need to be examined closely. The NRM of sample 14C-3 increased during the initial steps to an intensity 13% greater at 440°C than that at room temperature. Whether this unusual increase is due to the af demagnetization or possibly some chemical remanent magnetization (CRM) formed in a normal field is unknown. Even though the NRM-TRM plot becomes fairly linear at this temperature, the orthogonal vector diagram is only linear above 510°C. Because of this unusual increase in NRM, and the relatively low N, f, and q values, the PI of 14C-3 is somewhat suspect. The other continuously demagnetized excursion sample, G6, has a NRM-TRM plot that is quite linear from 250°-555°C (Figure 6). Assuming that the results of Coe and Gromme [1973] discussed above apply to G6, its PI estimate is probably overestimated by only several percent.

Turning to the remaining three, continuously af demagnetized normal samples, the NRM-TRM plot of HV15 is similar to that of BL16. Given its unusual J_S-T behavior (Figure 5e) and poor PTRM checks, it too is suspect. The remaining two samples, MK4 and MK28 are fairly linear over a wide temperature range and f interval, about 85%, and have good PTRM checks. Following the same reasoning as for sample G6, their PI values should not be overestimated by more than 10%.

Summary and Conclusions

The Skalamaelifell excursion discovered by Kristjansson and Gudmundsson [1980] in southwest Iceland, of assumed late Wisconsin age, is one of the best documented late Quaternary excursions. Recorded in volcanic rocks, it offers the best possibility of an accurate PI estimate. Because of sizeable VRM components found in many of their samples and the remoteness of the sites on the Reykjanes peninsula, we were limited to six samples of the excursion basalts and 10 of the surrounding normally magnetized basalts for comparison. In order to have little or no VRM, we used samples whose remanence directions had changed only a few degrees during 20mT af "cleaning" in Iceland. When measured in Rennes, the directions of the samples, which had been stored in the Earth's field for 2-6 years after 20-

mT demagnetization, had changed less than 7°. The high coercivity, especially of the excursion samples, is also shown by the retention of 85% of their NRM after the 20-mT demagnetization. Five of the 16 samples, two excursion samples and three normal samples, had not been demagnetized but were assumed to lack appreciable VRM because of the stability during demagnetization of adjacent samples in the same core. For the three undemagnetized normal samples we had the adjacent, demagnetized samples as well, and this made possible a comparison of the effects of af demagnetization on PI measurements.

The average remanence direction of our excursion samples (D=262, I=-22) is the same as that of the collection of 55 cores from which they were taken and which was used by Kristjansson and Gudmundsson [1980] in their study. The average remanence intensity, 2 A/m, is about 5 times that of the collection mean. Since our samples were selected for their unusually high coercivity, they are probably finer grained and therefore have a greater fraction of highly magnetized single or pseudo-single domain grains. The remanence intensity of the normal samples, like that of the excursion samples, has a tenfold range but averages 9 A/m, 5 times more intense than our excursion samples.

Unlike the large difference in mean J_{nrm}, the magnetic susceptibility and saturation magnetization of the two groups are almost identical. The J_s values show that the large differences in J_{nrm} between the two groups is not due to differences in magnetic mineral amount. The normalized NRM, J_{nrm}/J_s, of the normal samples is about 6 times greater on average than that of the excursion samples, and there is a threefold range within each group. This suggests that the PI during the eruption of the normal lavas most likely was 4-10 times greater than that during the excursion. The scatter within the two groups is probably due to grain size differences and/or secondary differences in the PI.

Curie temperature measurements indicate that the magnetic mineral in all but one of the samples is almost pure magnetite. The J_s-T behavior of the samples falls into six categories based mainly on the kind and degree of irreversibility of the J_s-T cooling curves. The cooling curves of the majority of the samples lie above the heating curves, and the J_s increases 10-40% after cooling. Five (type A) samples exhibit this increase even during the heating phase, whereas the other four (type B) do not. All but one of the rest show a decrease in J_s somewhere during cooling. The cooling curve of four samples above 200°C is less than the heating curve but crosses the heating curve so that the final J_s is 3-20 % greater than the initial (type C). The cooling curve of two of the samples remains entirely below the heating curve and, perhaps more importantly, is almost linear from 500° to 100°C (type D). Thermal cycling of the type D samples shows a 10-20% decrease in J_s at high temperatures even during heating. Sample HV15 is unique in that it exhibits three Curie temperatures on heating and two on cooling. The intermediate T_c phase, which disappears on cooling, is probably titanomaghemite which exsolves to magnetite on heating.

The reasons for the irreversibility of the J_s-T curves are not clear. The thermal cycling during heating shows that some of these changes begin at temperatures as low as 400° to 500°C. The use of fields great enough to saturate most of the samples at room temperature would seem to rule out physical changes affecting the coercivity. The probable young age would seem to rule out extensive chemical changes due to weathering. Yet the J_s-T curve of sample HV15 suggests it contains titanomaghemite, a product of the low-temperature oxidation of titanomagnetite. Increases in J_s during heating are frequently found to be the result of the disproportionation of titanomaghemite to a fine intergrowth of magnetite and ilmenite. Given a sufficiently low oxygen fugacity in the sample, decreases in J_s have been shown to result from the reduction at temperatures above about 600°C of the magnetite-ilmenite intergrowths and remixing to form a more Ti-rich titanomagnetite. This can occur whether the magnetite-ilmenite just formed during the disproportionation of titanomaghemite or formed naturally during the subsolidus oxidation of titanomagnetite. A further possible cause of a J_s decrease is the disproportionation of maghemite, a product of the low-temperature oxidation of magnetite, to magnetite and hematite.

Regardless of the mechanisms, the reversibility of J_s-T curves in this study is a good predictor of the linearity of TRM acquisition in NRM-TRM measurements. The NRM-TRM plots were almost always very linear, and the PTRM checks were very good for samples exhibiting the most reversible J_s-T behavior (types A and B). They were less good for samples whose cooling curves crossed over their heating curves (type C). The NRM of two of the type C samples, BL16 and BL16P, decreased about 30% before any significant TRM acquisition. Although their NRM-TRM plots were linear, the two type D samples exhibited large increases in PTRM capacity. The PTRM checks were also poor for the type E sample.

The results of the NRM-TRM measurements confirm the suspicion that the geomagnetic field was much weaker

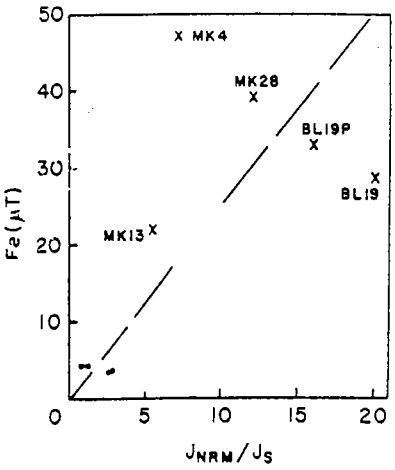

Fig. 8. Plot of PI values versus NRM intensity normalized by the saturation magnetization J_s. Solid circles and crosses are excursion and normal samples, respectively.

during the excursion than when the normal basalts were erupted. The estimated paleointensity of the four excursion samples which are considered reliable ranges from 3.4 to 4.6 μT, with arithmetic and weighted means of 4.1 and 4.3 μT, respectively. The PI values of the five normal samples considered reliable have a much greater range, from 22 to 47 μT and arithmetic and weighted means of 34 and 30 μT, respectively. The average PI of the normal basalts is 7 times that of the excursion samples.

This difference in paleointensity is similar to that predicted by the J_s data. The average J_{nrm}/J_s value of the normal basalts is 6 times that of the excursion samples. A plot of PI versus J_{nrm}/J_s shows a general increase in the normalized Jnrm with paleointensity (Figure 8). Some of the scatter is probably due to errors in the PI estimates but most probably results from differences in grain size. This is best seen in the BL19 sample pair, which have essentially the same PI values but differ by 25% in their J_{nrm}/J_s ratios. Thus normalized J_{nrm} values appear to be good indicators of relative PIs, but only when enough data are used to average differences in grain size.

NRM-TRM measurements on two pairs of samples from two cores, where one sample of each pair had been partially demagnetized to 20 mT and the other not, suggest that partial af demagnetization prior to NRM-TRM measurements does not seriously degrade PI results. The prior demagnetization of one sample of each pair resulted in a PI underestimated by only 10% as compared with the undemagnetized sample. The results from another pair of samples from the same core showed that continuous af demagnetization during the NRM-TRM measurement of samples with nonlinear behavior at low temperatures serious degrades the measurement and yields a PI overestimated by 40%. The effect of af demagnetization on PI estimates of high-coercivity samples, i.e., samples which acquire almost no VRM and retain at least 80% of their NRM after af demagnetization, thus seems to depend both on when the af demagnetization is done and on the thermochemical stability of the sample. Thermochemical stability may be the more important, since, in the study of Coe and Gromme [1973], even continuous af demagnetization caused only a 5% change in the PI of a sample whose NRM-TRM plot remained linear to 600°C. Many more measurements need to be made to test these conclusions. If correct, good PI values can be obtained from high-coercivity, partially af demagnetized samples from old collections taken in remote or not easily resampleable sites. An additional confirmation of this is the fact that the PI estimated from eight undemagnetized samples from the Skalamaelifell excursion, 4-5 μT, is the same as our estimate based on one undemagnetized and three partially demagnetized samples [Levi et al., 1987].

Finally, we turn to what is known of the Skalamaelifell excursion and the significance of our PI values. The collection of 55 cores from 22 flows from which our excursion samples were taken all had virtually the same direction, southwest and up [Kristjansson and Gudmundsson, 1980]. This direction is about 110° from that of a normal axial dipole direction, or two thirds toward being totally reversed. None of the flows sampled had a direction intermediate between this and that of the adjacent normal flows. The virtual geomagnetic pole (VGP) of the excursion flows (254E, 12S) is 90° from the meridian through the sample sites. The estimated PI of 4.3 μT is less than one tenth that of a dipole field at the sites. The mean PI estimated from the adjacent normal flows, 30 μT, is also significantly lower than expected. Because of poor exposures the stratigraphic relation between the excursion and the adjacent normal flows is uncertain. However, of the five normal PI values considered most reliable, the two samples (MK4 and MK28) from flows that probably underlie and therefore predate the excursion have the highest PIs (39 and 47 μT). Sample MK13 from a flow possibly younger than the excursion has the lowest PI (22 μT).

The excursion PI is quite similar to the mean value of 5 μT found by Lawley [1970] for 27 upper Tertiary Icelandic excursion or transition basalts and is about half the value, 8 μT, found for the Laschamp excursion [Roperch and Bonhommet, 1982]. Such low PIs are in marked contrast to the PI values several

times greater than the present field obtained for the other well-studied, late Quaternary Lake Mungo excursion [Barbetti and McElhinny, 1982). However, PI values of transitional fields during successful and even aborted reversals are commonly of the order of 5-10 μT [Hoffman, 1985; Prevot et al., 1985; and Coe et al., 1984]. Unlike the transitions and aborted reversals studied by Coe et al. [1984] and Hoffman [1986], the direction and VGP of the Skalamaelifell excursion, like those of Lake Mungo, are far from the meridional plane, ruling out any purely axisymmetric model for the excursion.

The dipole field for the period 50,000 to 10,000 years B.P. was about half its present value, and the period spanning the Laschamp excurison between 45,000 and 35,000 years B.P. was marked by unusually large secular variation [McElhinny and Senanayake, 1982; Salis, 1987]. Given a direction two thirds reversed and very low PI, the Skalamaelifell excursion was probably due to nondipole fields of about historical intensity and an unusually weak axial dipole field, a field configuration like that of the short-lived reversal at Laschamp and the well-documented, late Pliocence aborted reversal studied by Coe et al. [1984] on Oahu. The limited exposures have thus far concealed, or left unrecorded, any intermediate or more completely reversed parts of the excursion. But the very rapid changes in dipole field strength and direction observed in the Steens Mountain reversal show that such aborted reversals can occur in time spans measured in years and at rates 15-50 times faster than historic nondipole changes.

Acknowledgements. We would like to thank Leo Kristjansson for very generously selecting and sending us the samples, site information, and Icelandic demagnetization data used in this study. We gratefully acknowledge the considerable improvement of this article due to the suggestions of Sherman Gromme, the associate editor, and the editor, Ken Hoffman. I (M.M.) thank all those in the Laboratoire de Geophysique, especially Bastien Salis, Madame LeSolliec, and Francoise Calza, who helped with the measurements, gave much helpful advice, and endured my French. I also gratefully acknowledge the financial support of the Centre National de Recherche Scientifique during my sabbatical year at Rennes. Finally, I thank with sadness my thesis advisor, Allan Cox, for his support, wisdom, and direction. One example of this was a phone call to me on the night before my Ph.D. defense. I was anguishing over a small part of the data for one of my conclusions. He encouraged me not to forget the forest for the trees, to present my conclusions as I saw them, and, if I was truly concerned, to redo the measurement before publishing. I was much relieved by his thoughtfulness and had a good, if scary, defense and later verified the data.

References

Barbetti, M. F.,and M. W. McElhinny, The Lake Mungo geomagnetic excursion, Philos. Trans. R. Soc. London, Ser. A, 281, 515-542, 1976.

Bonhommet, N., and J. Babkine, Sur la presence d'aimantations inverses dans la Chaine des Puys, C.R. Acad. Sci., Ser. 2 264, 92-94, 1967.

Coe, R. S., Paleo-intensities of the Earth's magnetic field determined from Tertiary and Quaternary rocks, J. Geophys. Res., 72, 3247-3262, 1967a.

Coe, R.S., The determination of paleo-intensities of the Earth's magnetic field with emphasis on mechanisms which could cause non-ideal behavior in Thellier's method, J. Geomagn. Geoelectr., 19, 157-179, 1967b.

Coe, R.S., and C.S. Gromme, A comparison of three methods of determining geomagnetic paleointensities, J. Geomagn. Geoelectr., 25, 425-435, 1973.

Coe, R. S., S. Gromme, and E.A. Mankinen, Geomagnetic paleointensities from radiocarbon-dated lava flows on Hawaii and the question of the Pacific nondipole low, J. Geophys. Res., 83, 1740-1756, 1978.

Coe, R.S., S. Gromme, and E. A. Mankinen, Geomagnetic paleointensities from excursion sequences in lavas on Oahu, Hawaii, J. Geophys Res., 89, 1059-1069, 1984.

Cox, A., Latitude dependence of the angular dispersion of the geomagnetic field, Geophys. J. R. Astron. Soc., 20, 253-269, 1970.

Doell, R.R., Paleomagnetic studies of Icelandic lava flows, Geophys. J. R. Astron. Soc., 26, 459-479, 1972.

Doell, R. R., and P. J. Smith, On the use of magnetic cleaning in paleointensity studies, J. Geomagn. Geoelectr., 21, 579-594, 1969.

Gromme, C.S., T.L. Wright, and D.L. Peck, Magnetic properties and oxidation of iron-titanium oxide minerals in Alae and Makaopuhi lava lakes, Hawaii, J. Geophys. Res., 74, 5277-5293, 1969.

Gromme, C.S., E. A. Mankinen, M. Marshall, and R. S. Coe, Geomagnetic paleointensities by the Thelliers' method from submarine pillow basalts: Effects of seafloor weathering, J. Geophys. Res., 84., 3553-3575, 1979.

Hoffman, K.A., Transitional behavior of the geomagnetic field, J. Geomagn. Geoelectr., 37 139-146, 1985.

Hoffman, K.A., Transitional field behavior from Southern Hemisphere lavas: Evidence for two-stage

reversals of the geodynamo, Nature, 320, 228-232, 1986.

Kristjansson, L., Notes on paleomagnetic sampling in Iceland, Jokull, 34 67-76, 1984.

Kristjansson, L., Some statistical properties of paleomagnetic directions in Icelandic lava flows, Geophys. J. R. Astron. Soc., 80, 57-71, 1985.

Kristjansson, L., and A. Gudmundsson, Geomagnetic excursion in late-glacial basalt outcrops in southwestern Iceland, Geophys. Res. Lett., 7, 337-340, 1980.

Lawley, E. A., The intensity of the geomagnetic field in Iceland during Neogene polarity transitions and systematic deviations, Earth Planet. Sci. Lett., 10, 145-149, 1970.

Levi, S., H. Audunsson, R.A. Duncan, and L. Kristjansson, The geomagnetic excursion at Skalamaelifell, Iceland: Additional evidence for unstable geomagnetic behavior circa 40 ka ago, Eos Trans. AGU, 68, 1249, 1987.

Mankinen, E. A., M. Prevot, C. S. Gromme, and R. S. Coe, The Steens Mountain (Oregon) geomagnetic polarity tansition, 1, Directional history, duration of episodes, and rock magnetism, J. Geophys. Res., 90, 10,393-10,416, 1985.77, 6459-6469, 1972.

Marshall, M., The magnetic properties of some DSDP basalts from the North Pacific and inferences for Pacific plate tectonics, J. Geophys. Res., 83, 289-308, 1978.

Marshall, M., and A. Cox, Magnetic changes in pillow basalt due to seafloor weathering, J. Geophys. Res., 77, 6459-6469, 1972.

McElhinny, M. W., and W.E. Senanayake, Variations in the geomagnetic dipole, I, The past 50,000 years, J. Geomagn. Geoelectr., 34, 39-51, 1982.

Pierce, J. W., and M.J. Clark, Evidence from Iceland on geomagnetic reversal during the Wisconsin Ice Age, Nature, 273, 456-458, 1978.

Prevot, M., E. A. Mankinen, R. S. Coe, and C. S. Gromme, The Steens Mountain (Oregon) geomagnetic polarity transition, 2, Field intensity variations and discussion of reversal models, J. Geophys. Res., 90, 10,417-10,448, 1985

Roperch, P., and N. Bonhommet, Baked contact test and paleointensity results from the Laschamp-Olby flows, Eos Trans. AGU, 63, 1283, 1982.

Salis, J.S., Variation seculaire du champ magnetique terrestre--Direction et paleointensite--Sur la periode 7.000-70.000 ans BP, dans la Chaine des Puys, Mem. Doc. 11 Cent. Armoricain d'Etud. Struct. des Socles, Rennes, France, 1987.

Thellier, E., and O. Thellier, Sur l'intensite du champ magnetique terrestre dans le passe historique et geologique, Ann. Geophys., 15, 285-376, 1959.

Verosub, K.L., Geomagnetic excursions: A critical assessment of the evidence as recorded in sediments of the Brunhes Epoch, Philos. Trans. R. Soc. London, Ser.A., 306, 161-168, 1982.

N. Bonhommet and A. Chauvin, Laboratoire de Geophysique Intern, Universite de Rennes I, 35042 Rennes, France

M. Marshall, Department of Geological Sciences, San Diego State University, San Diego, CA 92182.

(Received October 12, 1987;
revised March 31, 1988;
accepted April 11, 1988.)

GEOPHYSICAL RESEARCH LETTERS, VOL. 14, NO. 2, PAGES 151-154, FEBRUARY 1987

TRANSITIONAL GEOMAGNETIC FIELD BEHAVIOR: VOLCANIC RECORDS FROM FRENCH POLYNESIA

Pierrick Roperch and Annick Chauvin

ORSTOM et Laboratoire de Géophysique Interne, Université de Rennes 1
35042 Rennes Cédex, France.

Abstract. Here we report the behavior of the earth's magnetic field for transitions recorded on volcanic islands from Polynesia in the South Central Pacific Ocean. Detailed transitional fields are observed on Huahine Island; the data suggest the record of an excursion N-N following the Kaena event. The Jaramillo termination and the Brunhes onset are recorded in a volcanic sequence from Tahiti Island. The transitional field is mainly characterized by low intensities. While the beginning of the transition appears to be consistent with the zonal model of reversal, large deviations from a north-south planar distribution of the intermediate directions show that non dipolar fields without preferential axisymmetry control the middle of the transition.

Introduction

In the past few years numerous papers have been devoted to the description of the magnetic field during reversals. However, very few transition studies are situated in the southern hemisphere (Van Zijl et al., 1962, Clement and Kent, 1984, Hoffman, 1986) and new data are necessary to provide accurate reversal models. On the other hand, most of the studies deal with sedimentary records (Hillhouse and Cox, 1976, Hoffman and Fuller, 1978, Fuller et al., 1979, Valet and Laj, 1981, Williams and Fuller; 1982, Valet et al.,1983, Clement and Kent, 1984, Theyer et al., 1985) and the need for volcanic records which provide accurate spot readings of the paleofield has become more apparent (Hoffman and Slade, 1986). However, volcanic records are rarely enough detailed to describe completely the reversal (Shaw, 1975, Bogue and Coe, 1982). Except in the Steens Mountain data (Prevot et al.,1985a,b), few transitional directions have been observed. A common feature of the volcanic results is that a similar direction can be recorded in successive flows, followed by large changes to another intermediate position. This can be explained either by a jerky behavior of the transitional field or, more probably, by irregularities in the extrusion rate of the flows. The fact that the magnetic field is highly nondipolar during reversals is, at the moment, the main result obtained from paleomagnetic studies of transitions. For this reason, Hoffman (1984) has suggested the description of transitional fields using directions rather than in terms of their virtual geomagnetic pole. The rotated space (D',I') has been chosen for the display of the directions on Figures 1 and 3.

Paper number 6L7047.
0094-8276/87/006L-7047$03.00

Volcanic islands in the Society Archipelago (French Polynesia) were sampled for a paleomagnetic secular variation study (Duncan, 1975). This sampling showed the existence of possible transition zones. Therefore, we have revisited two areas: 1) an excursion was found to be recorded in the south part of Huahine island (16.7S,209E). Radiometric dating for this volcano gave an age close to the Gauss-Matuyama boundary (2.5My) (Duncan and Mc Dougall, 1976). However, new radiometric K-Ar dating on some flows which have recorded the intermediate fields (Bellon, Duncan, personal communication) suggest an age close to the Kaena event . The sampling consists of two main sections of flows with a stratigraphical order. A dispersed sampling for which no chronological order is available was also carried out in the same area over 4 kilometers. No reversed polarity is observed. Although the possibility to have a gap in our sampling or a gap in the volcanic activity which leads to a complete missing of the short reversed event Kaena should not be completely discarded, we think that our data from Huahine might represent an excursion N-N younger than the Kaena termination. 2) A sequence of 25 flows has been sampled on Tahiti. The upper boundary of the Jaramillo event and the Matuyama-Bruhnes boundary are recorded in this sequence (Duncan and Mc Dougall, 1976). For both islands, volcanic flows are 1 to 2 meters thick. On Huahine, flows are originally dipping 10 degrees away from the center of the volcano. The characteristic directions for all the flows have been obtained after A.F. cleaning. Thermal demagnetizations were performed on some specimens to control the primary thermoremanent character of the magnetization. In view of the difficulties in obtaining reliable paleointensities, a simple comparison of the intensities of the magnetization was performed after A.F. cleaning at 10 mT which is generally sufficient to remove secondary components. Such a method gives a qualitative and relative estimate of field intensity changes and has been used previously for the statistical analysis of the Icelandic data (Kristjansson and Mc Dougall, 1982).

Results

HUAHINE ISLAND: The directional behavior for each of the two volcanic sections in Huahine is shown on Figures 1a and 1b. The first phase of the transition is seen on both sections. The beginning of the two records is identical. This first part seems to correspond to a complete reversal and the path seems to possess an high degree of symmetry. However, the directions close to the reversed dipole direction are associated with a very low intensity of magnetization (Figure 2a). This property suggests that the fully reversed field is not observed. Moreover,

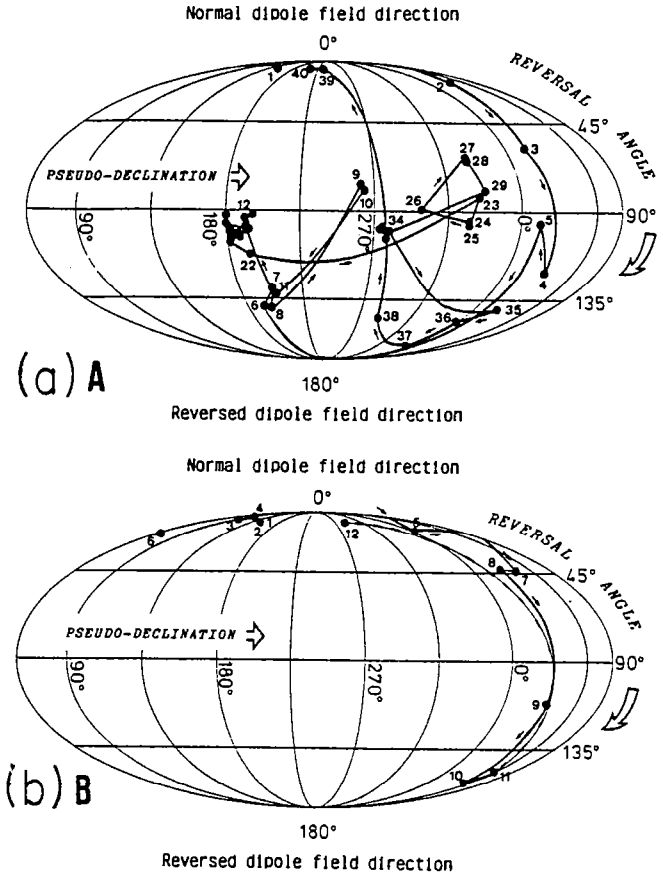

Fig. 1. Directional records for two sections of successive flows in Huahine Island:
1a: section A ; 1b: section B
Directions are rotated about the east-west horizontal axis to bring the dipole field directions coincident with the poles of the projection (Hoffman, 1984). A purely axisymmetrical field would have a pseudo-declination equal to 0 or 180 degrees which correspond to far-sided or near-sided VGP paths, respectively.

in section A, the field returns to intermediate stages where no clear organization is found. For section B, due to a gap in the sampling between flows B11 and B12, the record jumps directly to a normal direction and the great circle joining the directions B11 to B12 does not correspond to the real path. For section A, the transition ends also with a normal polarity. Moreover, the sills and dikes found in the transitional zone have recorded either an intermediate direction or a normal direction. This observation is in good agreement with the record of an excursion from Normal to Normal.

A major characteristic of the intermediate field is represented by the very low intensity of the magnetization (Figure 2a). While the intensity of magnetization before and after the excursion is distributed around 5 A/m, most of the intermediate flows have an arithmetic mean intensity lower than 1 A/m. Normalizations of the natural remanence by anhysteretic magnetization show that the between flows intensity changes are not related to changes in the magnetic properties. The same relative intensity variations are observed before (Figure 2a) and after the normalizations by the anhysteretic magnetizations (Figure 2b), this property give some confidence for an extrapolation to the relative paleofield variation.

TAHITI: A section of 200 meters was sampled in the Punaru valley. Important gaps in the sampling exist at 2 levels:
- the sequence of normal flows (T1 to T10) has been sampled 600 meters north of the section (T11 to T25) which starts directly with intermediate directions. Although the flows T1 to T10 appear to be stratigraphically lower than T11, no correlation using paleomagnetic direction is available.
- Only two flows have recorded the reverse interval between the Jaramillo termination and the Bruhnes onset. An important lapse of time may occur between T22 and T23.
Nevertheless, 13 transitional directions are obtained and they give an interesting comparison with those from the excursion recorded on Huahine. In the rotated space (Hoffman, 1984),

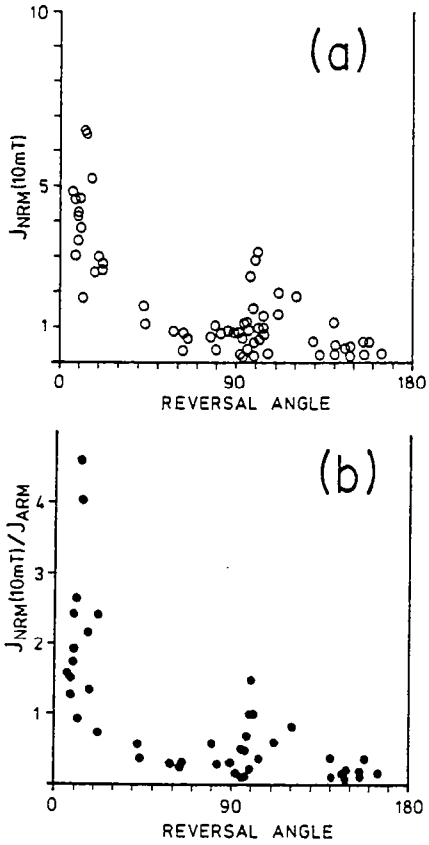

Fig. 2. Variation of the intensity of the magnetization per flow versus reversal angle. All data from Huahine (67 flows)
a) An arithmetic mean intensity was calculated for each flow after an alternating field demagnetization at 10 milliteslas. Intensity unit in A/m.
b) An anhysteretic remanence acquired in the laboratory field with an a.c. field of 70 mT. was given to each specimen and was then used to normalize the NRM (at 10mT.). A mean ratio is calculated per flow and represented by the black dots. This has been done for 44 flows.

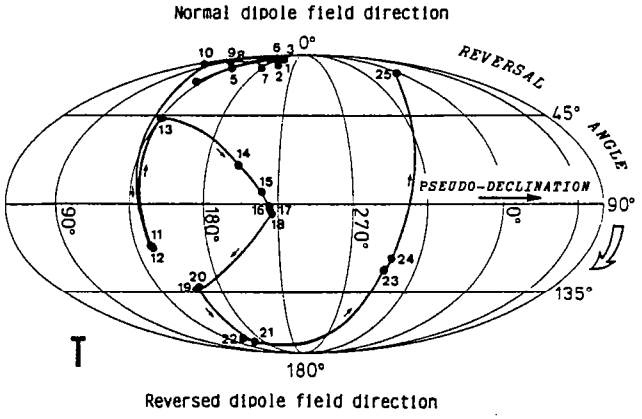

Fig. 3. Directional record for a sequence of flows from Tahiti (T). Same conventions as in Figure 1.

the directional path (Figure 3) for the first reversal from normal to reverse appears to be grossly near-sided. The stable reverse state is only determined by two flows of which the intensities of the magnetizations are of the same order as for flows with a normal polarity (Figure 4). The two flows which have recorded the Matuyama-Bruhnes reversal have intermediate directions which do not provide a clear correlation with those from the previous transition. Finally, a large decrease in the intensity of magnetization (i.e. the paleofield) appears once again during the transition, what we believe is an important characteristic of the transitional field (Figure 4).

Discussion

After the first recognition of the non dipolar character of the field during transition (Hillhouse and Cox, 1976), it was first claimed that the transitional field was mainly dominated by axisymmetric quadrupole or octupolar terms (Hoffman and Fuller, 1978, Williams and Fuller, 1982). A phenomenological model which describes qualitatively the reversal was developed by Hoffman (1979). Properties inherent to the magnetization acquisition processes in sediments might have induced such interpretations (Larson and Walker, 1985, Hoffman and Slade, 1986). Data from volcanic rocks show that non axisymmetric components are not negligible (Prevot et al., 1985a,b). The random distribution of the transitional directions recorded by Icelandic lava flows (Kristjansson and Mc Dougall, 1982, Kristjansson, 1985) constitute one of the best examples. The large deviations from the near-sided or far-sided configurations observed in our data confirm that non-zonal components play an important role during transitions. However, a significant difference in the transitional field geometry might exist between the onset and the following phases of the transition. For example, the onset of the excursion recorded at Huahine is mostly coincident with the zonal far-sided field behavior (Figures 1a and 1b). Although the onset of the first reversal recorded on Tahiti is not so clearly defined than the one from Huahine, a zonal dominance cannot be rejected. The possibility that the onset of a reversal should show less departures from axial symmetry than the following phases was already suggested by Hoffman (1982). On an other hand this hypothesis might find some theoretical support (Hide, 1982).

The recent complete vector description of the Steens Mountain reversal indicates that rapid changes of the magnetic field may occur and a such behavior might be related to an increase of the fluid velocity in the core (Prevot et al., 1985b). Such impulses cannot be discarded in order to explain the major changes in the polynesian records, even if we believe that the extrusion rate of lava flows for this kind of volcanism is an uncontrolled parameter. Recently, Hoffman (1986) has put forward evidence for two-stage reversals of the geodynamo. As viewed from an equatorial southern latitude, no such behavior is clearly seen.

Apart from discussions concerning the directional behavior, the large intensity changes appear to be at least as important. If we relate the intensity of the magnetization to the paleofield, after the decrease of the dipole field, the earth's surface magnetic field is dominated by non dipole fields which can have very low intensities. The transitional field intensity amounts to about 20% of that of the paleofield occuring during stable polarity.

Excursions are often interpreted as reversal attempts which have not been successful (Harrison, 1980, Hoffman, 1981, Coe at al., 1984) or sometimes, excursions appear to precede or to follow a successful reversal. An example of this is seen in the Steens Mountain record (Prevot et al., 1985a,b). Taking into account the new K-Ar dating, a link between the excursion recorded on Huahine island and the Kaena event might exist. However, the Island of Huahine does not provide a very clear magnetostratigraphy showing the Mammoth and Kaena reverse events inside the Gauss normal epoch. Thus, it is difficult to discuss the alternative hypothesis between an excursion linked to reversal or an independent excursion. In the case of this last hypothesis, the similar characteristics of the intermediate fields observed at Huahine with those recorded during full reversals should support the aborted reversal hypothesis.

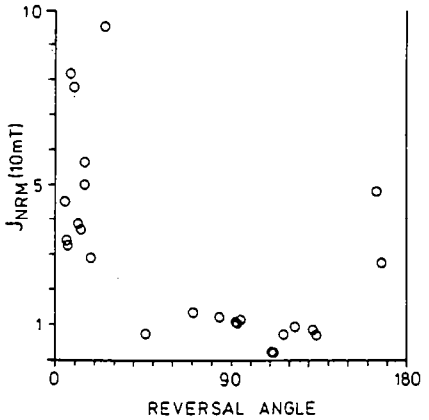

Fig. 4. Intensity of magnetization versus reversal angle. Data from Tahiti. Same conventions as in Figure 2a.

Acknowledgements. We thank Dr H. Bellon and Dr R.A. Duncan for providing us K-Ar dating for Huahine. We thank Drs N. Bonhommet, C. Laj, H. Perroud, M. Prevot and an anonymous reviewer for critically reading an earlier version of this paper and making many valuable suggestions. We thank L. Chungue and B. Dabet for efficient help in collecting samples. This work is a contribution ORSTOM A06.

References

Bogue, S.W., and R.S. Coe, Successive paleomagnetic reversal records from Kauai, Nature, 295, 399-401, 1982.

Clement, B.M. and D.V. Kent, A detailed record of the lower Jaramillo polarity transition from a southern hemisphere, deep sea sediment core, J. Geophys. Res., 89, 1049-1058, 1984.

Coe, R.S., C.S. Gromme and E.A. Mankinen, Geomagnetic paleointensities from excursion sequences in lavas on Oahu, Hawai, J. Geophys. Res., 89, 1059-1069, 1984.

Duncan, R.A., Paleosecular variation at the society islands, French Polynesia, Geophys. J. Roy. Astr. Soc., 41, 245-254, 1975.

Duncan, R.A. and I. Mc Dougall, Linear volcanism in French Polynesia, J. Volc. Geother. Res. 1, 197-227, 1976.

Fuller, M., I. Williams and K.A. Hoffman, Paleomagnetic records of geomagnetic field reversals and morphology of the transitional fields, Rev. Geophys. Space Phys. ,17, 179-202, 1979.

Harrison, C.G.A., Secular variation and excursions of the earth's magnetic field, J. Geophys. Res., 85, 3511-3522, 1980.

Hide, R., On the role of rotation in the generation of magnetic fields by fluid motions, Phil. Trans. R. Soc. Lond., A306, 223-234, 1982.

Hillhouse, J. and A. Cox, Brunhes-Matuyama polarity transition, Earth Planet. Sci. Lett.,29, 51-64, 1976.

Hoffman, K.A., Behaviour of the geodynamo during reversal: a phenomenological model, Earth Planet. Sci. Lett., 44, 7-17, 1979.

Hoffman, K.A., Paleomagnetic excursions, aborted reversals and transitional fields , Nature, 294, 67-69, 1981.

Hoffman, K.A.,The testing of geomagnetic reversal models:recent development, Phil. Trans. R. Soc. Lond., A306, 147-158, 1982.

Hoffman, K.A., A method for the display and analysis of transitional paleomagnetic data, J. Geophys. Res., 89, 6285-6292, 1984.

Hoffman, K.A., Transitional field behaviour from southern hemisphere lavas: evidence for two stage reversals of the geodynamo, Nature, 320, 228-232, 1986.

Hoffman, K.A. and M. Fuller, Transitional field configurations and geomagnetic reversal, Nature, 273, 715-718, 1978.

Hoffman, K.A. and S.B. Slade, Polarity transition records and the acquisition of remanence: a cautionary note, Geophys. Res. Lett., 13, 483-486, 1986.

Kristjansson, L., Some statistical properties of paleomagnetic directions in Icelandic lava flows, Geophys. J. Roy. Astr. Soc., 80, 57-71, 1985.

Kristjansson, L. and I. McDougall, Some aspects of the late tertiary geomagnetic field in Iceland, Geophys. J. Roy. Astr. Soc., 68, 273-294, 1982.

Larson, E.E. and T.R. Walker, Comment on "Paleomagnetism of a polarity transition in the lower(?) triassic Chugwater formation, Wyoming" by Emilio Herrero-Bervera and Charles E. Hesley, J. Geophys. Res., 90, 2060-2062, 1985.

Prevot, M., E.A. Mankinen, R.S. Coe and C.S. Gromme, The Steens mountain (Oregon) geomagnetic polarity transition II Field intensity variations and discussion of reversals models, J. Geophys. Res., 90, 10417-10448, 1985a.

Prevot, M., E.A. Mankinen, C.S. Gromme and R.S. Coe, How the geomagnetic field vector reverse polarity, Nature, 316, 230-234, 1985b.

Shaw, J., Strong geomagnetic fields during a single icelandic polarity transition, Geophys. J. Roy. Astr. Soc., 40, 345-350, 1975.

Theyer, F., E. Herrero-Bervera and U. Hsu., The zonal harmonic model of polarity transition: a test using successive reversals, J. Geophys. Res., 90, 1963-1982, 1985.

Valet, J.P. and C. Laj, Paleomagnetic record of two successive miocene geomagnetic reversals in western Crete, Earth Planet. Sci. Lett., 54, 53-63, 1981.

Valet, J.P., C. Laj and C. Langeris, Two different R-N geomagnetic reversals with identical VGP paths recorded at the same site, Nature, 304, 330-332, 1983.

Van Zijl, J.S.V., K.W.T. Graham, and A.L. Hales, The paleomagnetism of the Stormberg lavas,II, The behavior of the magnetic field during a reversal, Geophys. J. R. Astr. Soc., 7, 169-182, 1962.

Williams, I. and M. Fuller, Zonal harmonic models of reversal transition fields, J. Geophys. Res., 87, 9408-9418, 1982.

A. Chauvin and P. Roperch, ORSTOM et Laboratoire de Géophysique Interne, Université de Rennes 1, 35042 Rennes Cédex, France.

(Received September 9, 1986;
revised December 4, 1986;
accepted December 4, 1986.)

ANNEXE 2

Diagrammes ARN-ATR

Echantillons de la Réunion

Site A

Coulée	RA1	échantillons	RA01-RA05
''	RA2	"	RA06-RA10
''	RA3	"	RA11-RA18
''	RA4	"	RA19-RA23
''	RA5	"	RA24-RA28
''	RA6	"	RA29-RA34
''	RA7	"	RA35-RA40
''	RA8	"	RA41-RA46
''	RA9	"	RA47-RA52
''	RA10	"	RA53-RA58
''	RA11	"	RA59-RA66
''	RA12	"	RA67-RA72
''	RA13	"	RA73-RA77
''	RA14	"	RA78-RA83
''	RA15	"	RA84-RA90
''	RA16	"	RA91-RA97
''	RA17	"	RA98-RA105

Site B

Coulée	RB1	échantillons	RB106-RB111
''	RB2	"	RB112-RB117
''	RB3	"	RB118-RB122
''	RB3'	"	RB123-RB127
''	RB4	"	RB128-RB134
''	RB5	"	RB135-RB139
''	RB6	"	RB140-RB145
''	RB7	"	RB146-RB152
''	RB8	"	RB153-RB157
''	RB9	"	RB158-RB162
''	RB10	"	RB163-RB167
''	RB11	"	RB168-RB172
''	RB12	"	RB173-RB177

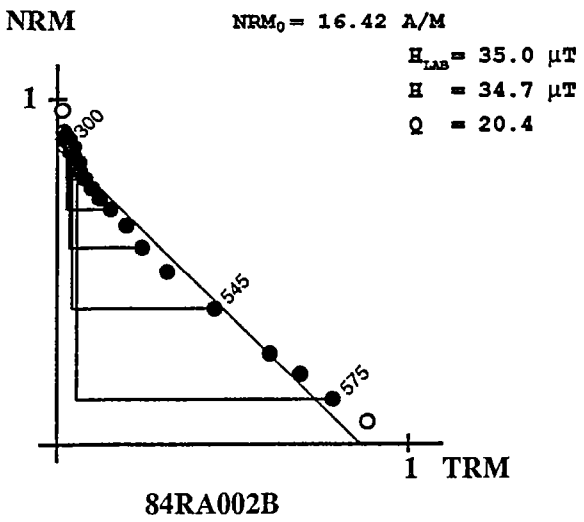

84RA002B

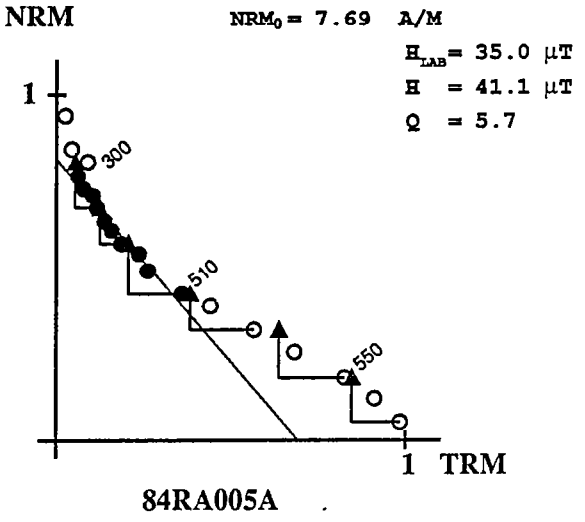

84RA005A

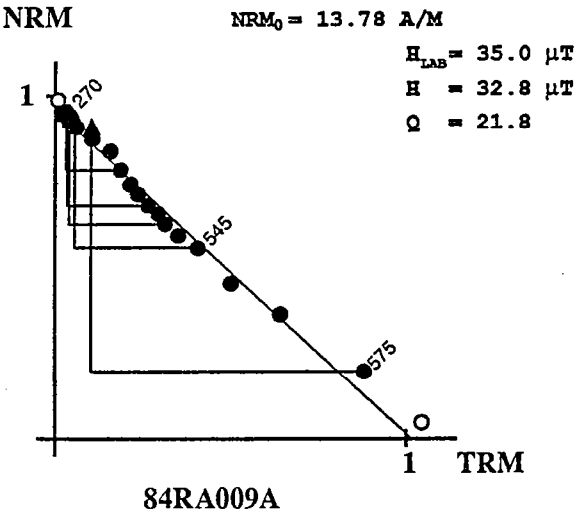

84RA009A

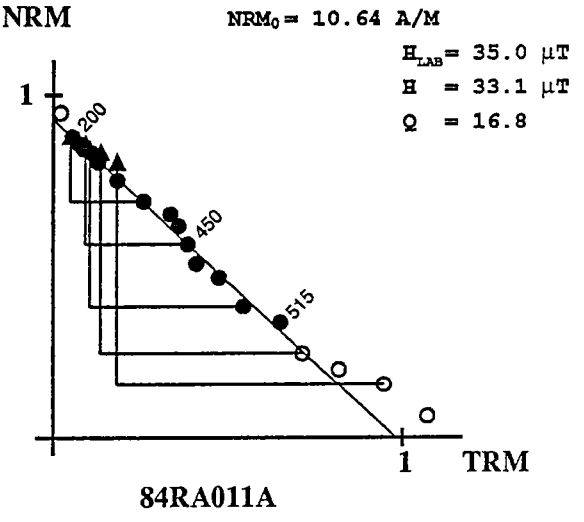

84RA011A

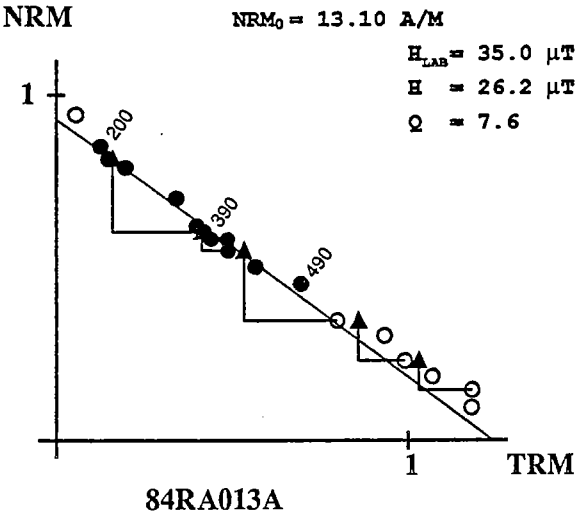

84RA013A

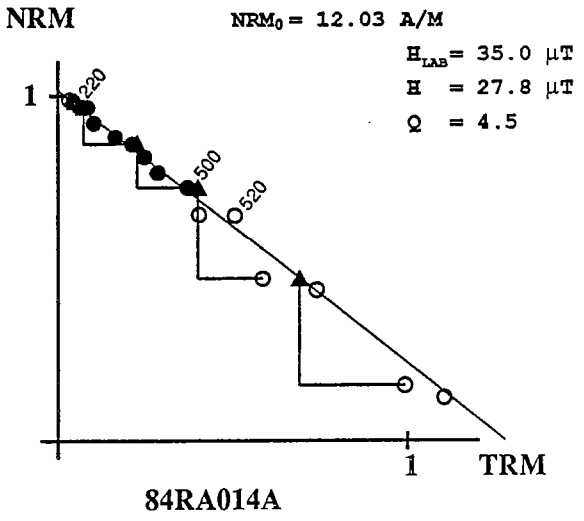

84RA014A

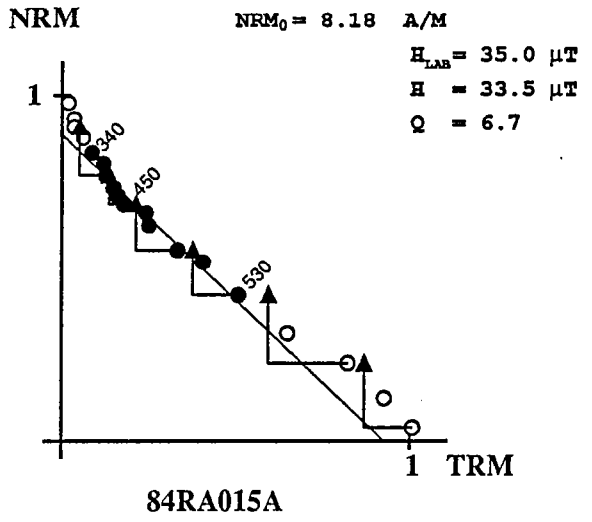

84RA015A

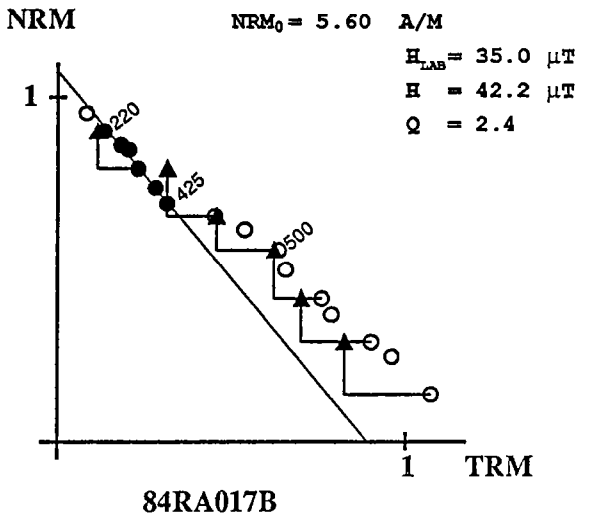

84RA017B

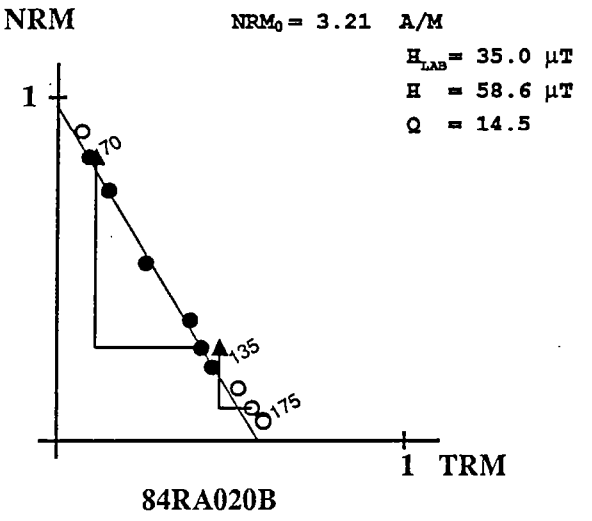

84RA020B

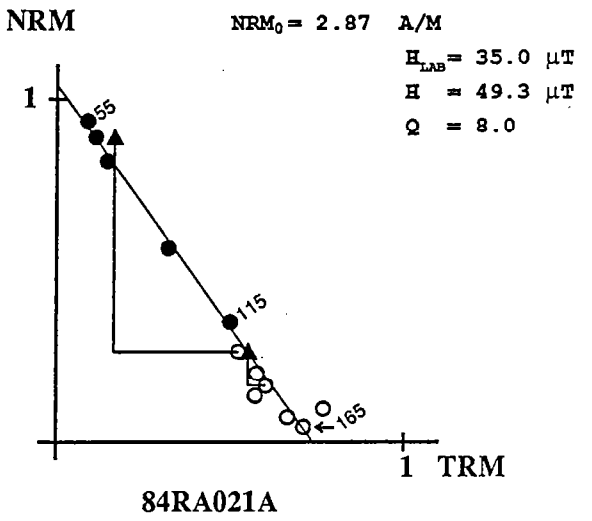

84RA021A

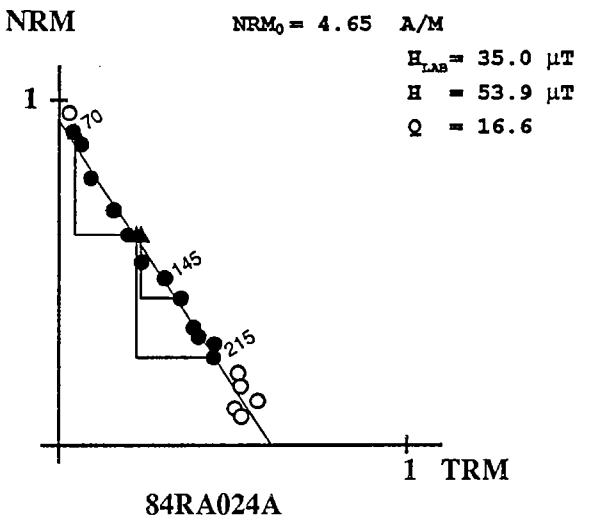

84RA024A

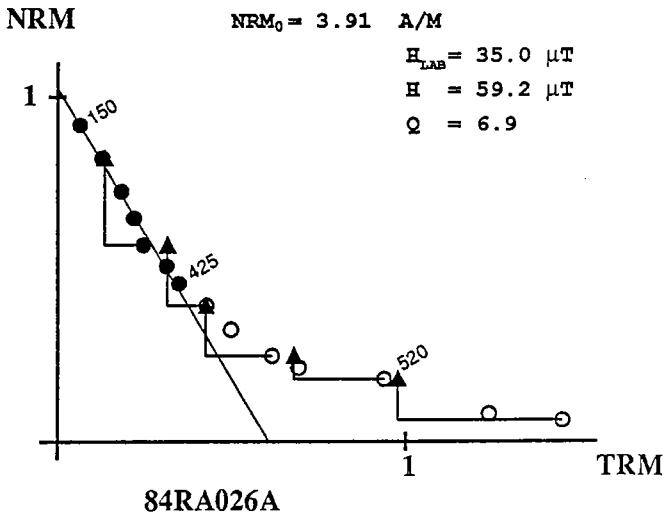

84RA026A

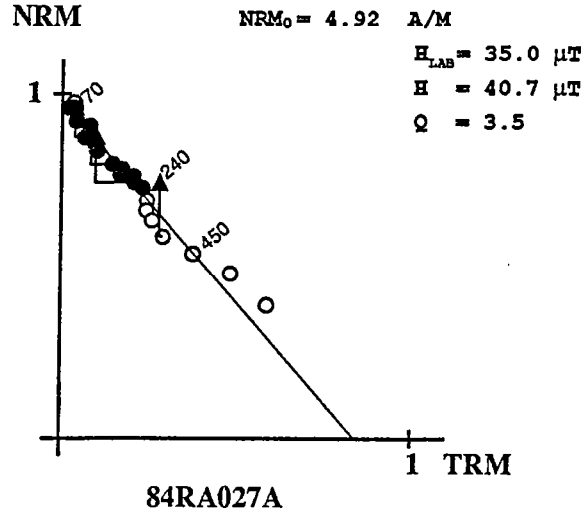

84RA027A

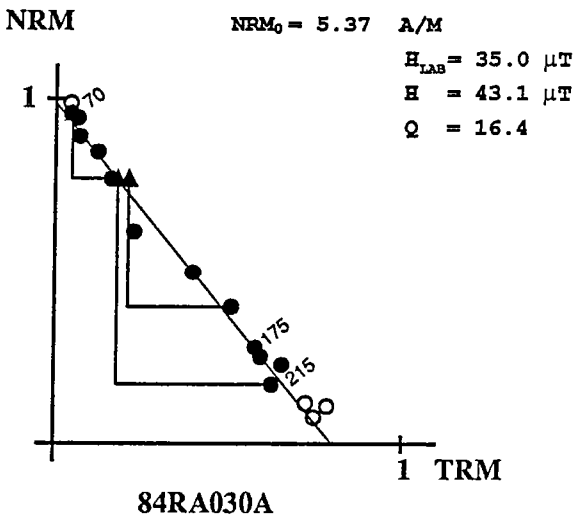

84RA030A

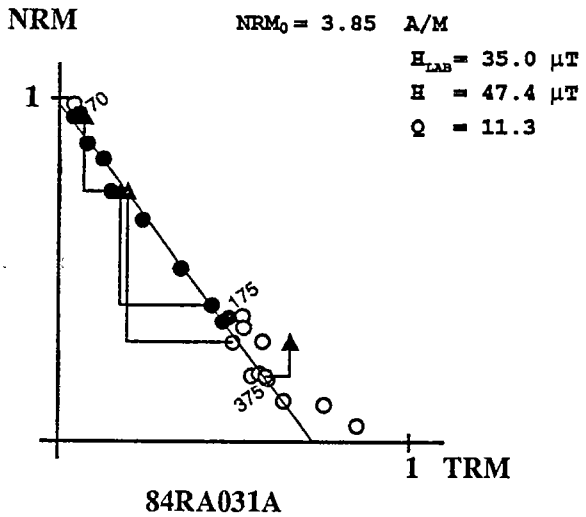

84RA031A

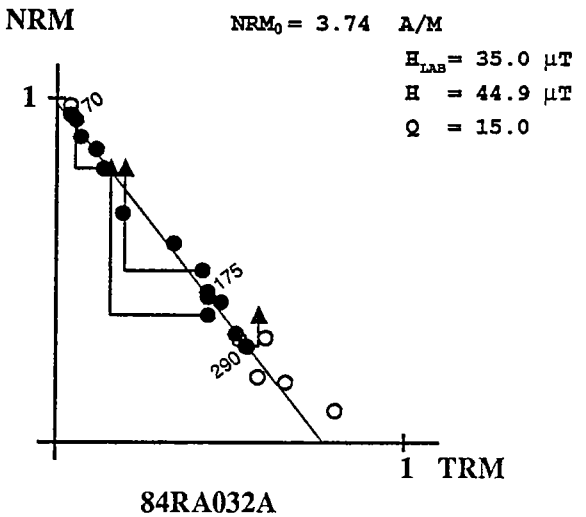

84RA032A

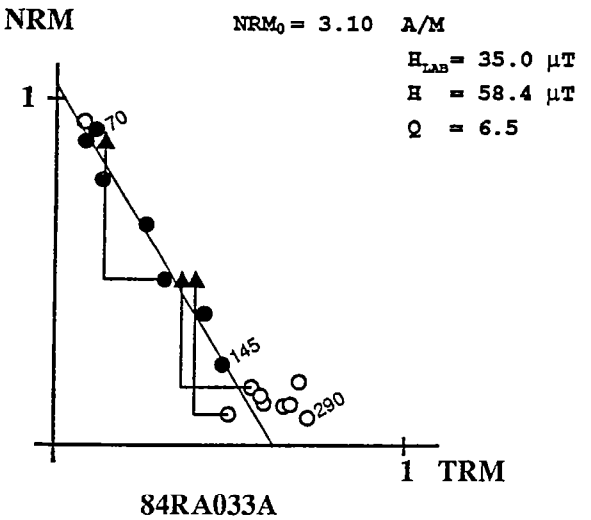

84RA033A

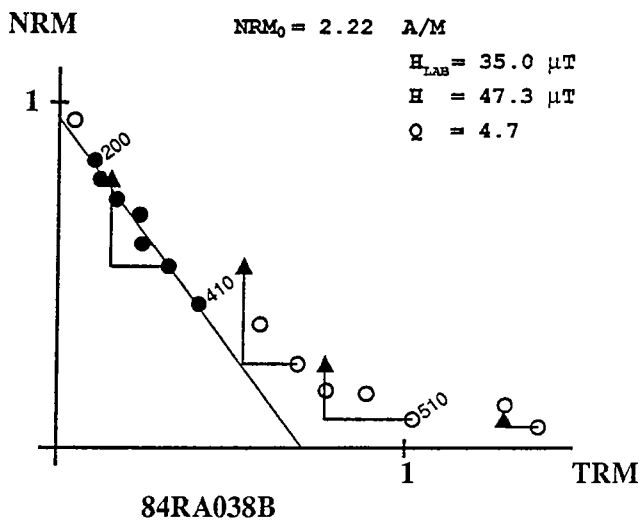

84RA038B

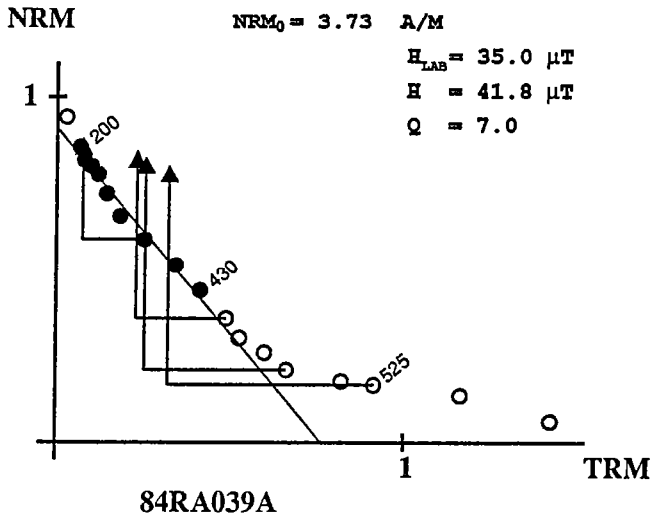

84RA039A

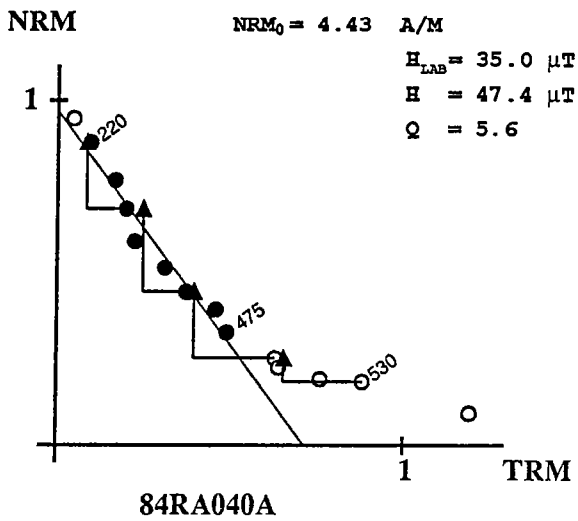

84RA040A

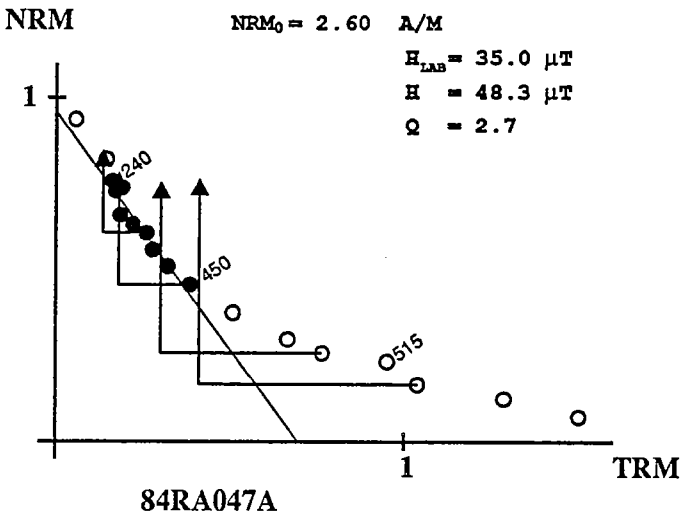

84RA047A

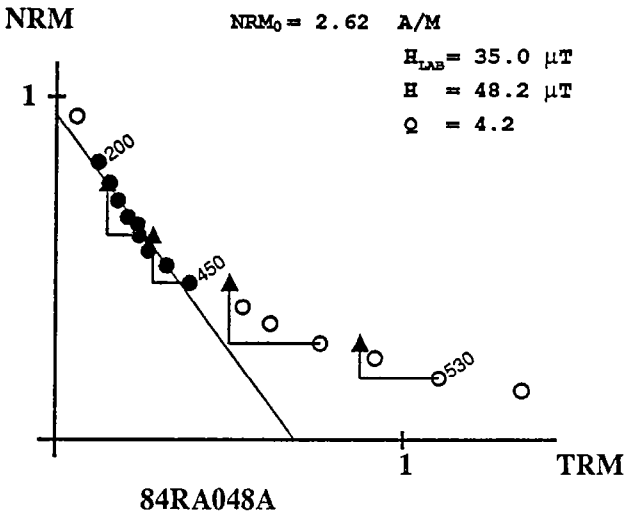

84RA048A

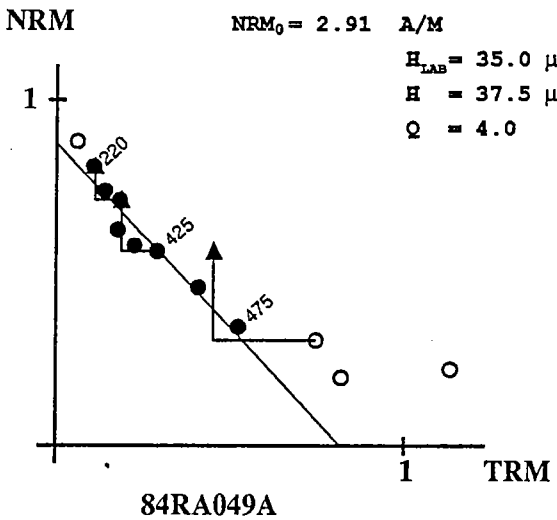

84RA049A

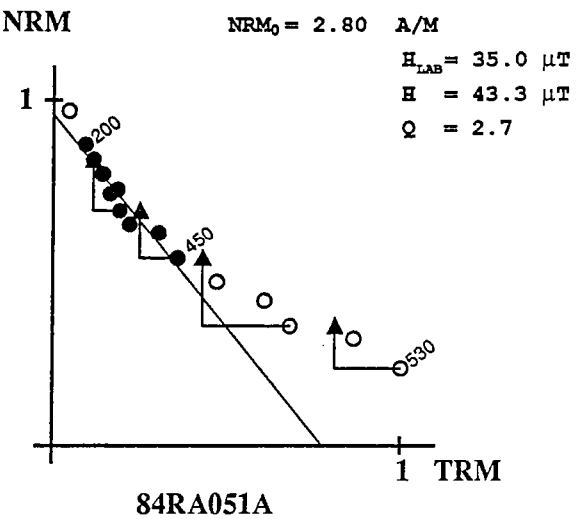

84RA051A

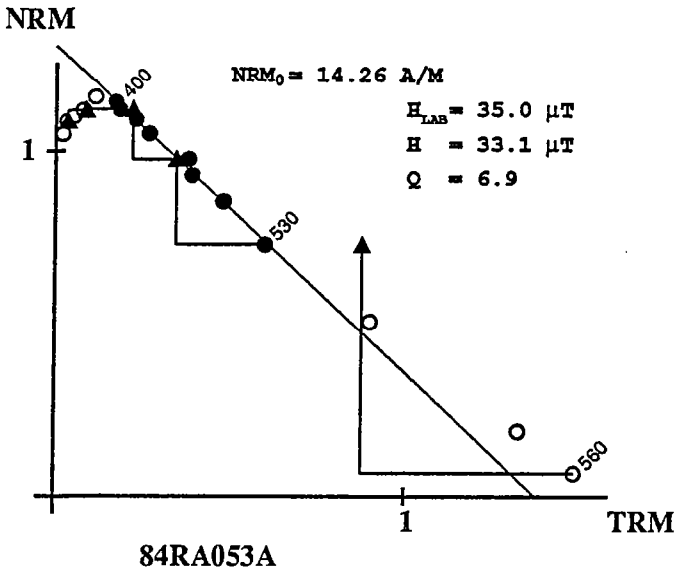

84RA053A

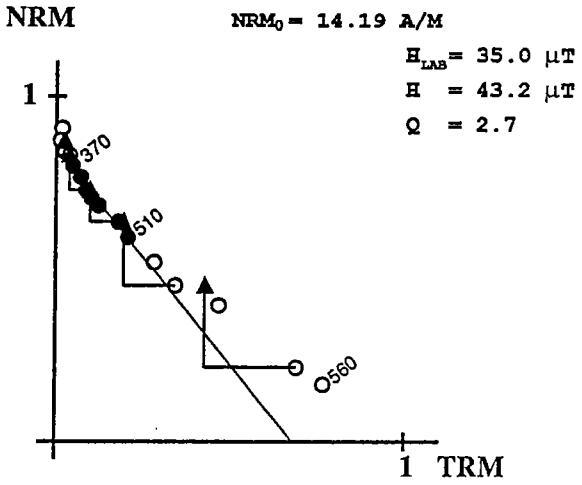

84RA057A

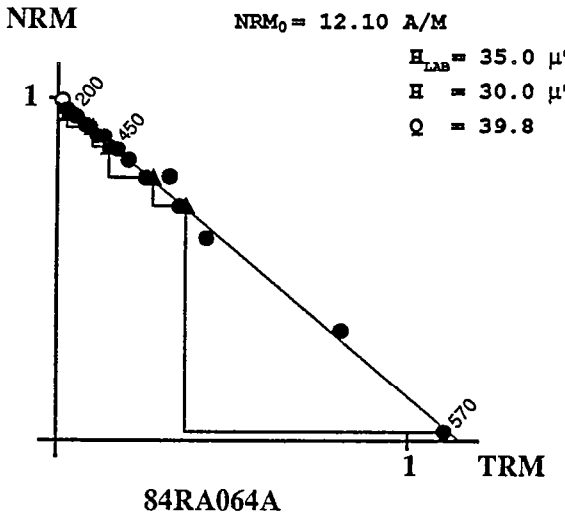

84RA064A

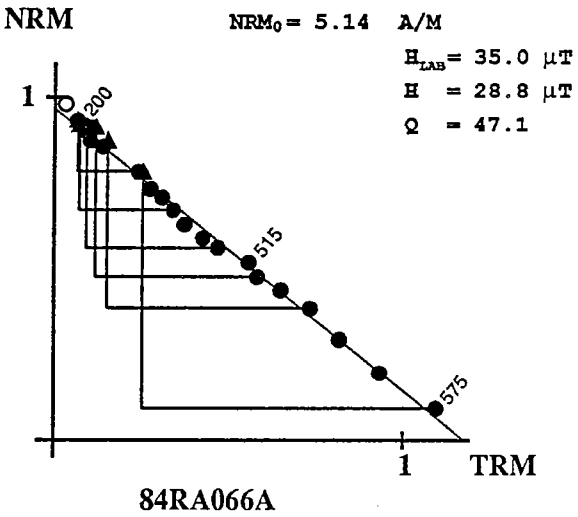

84RA066A

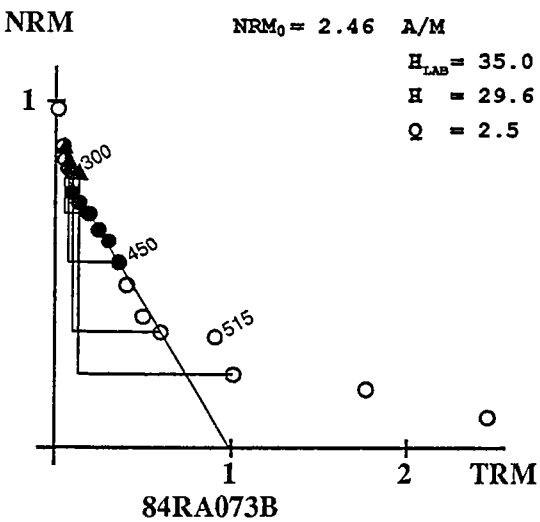

84RA073B

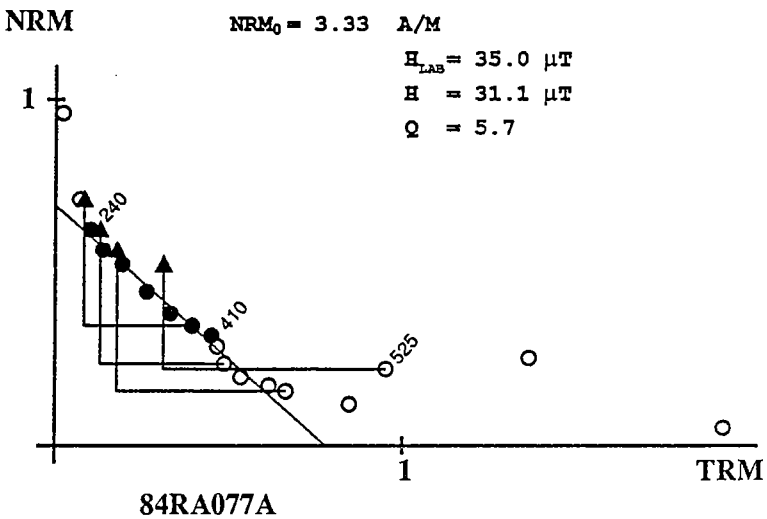

84RA077A

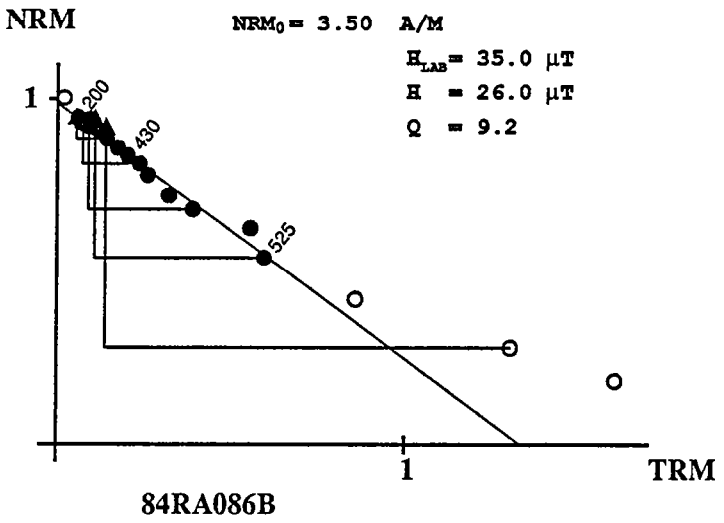

84RA086B

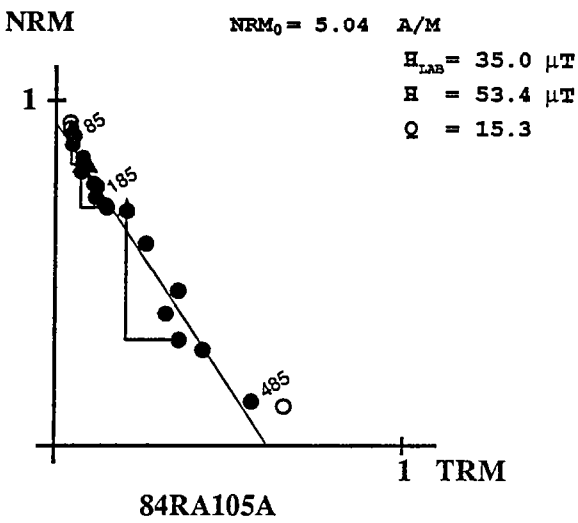

84RA105A

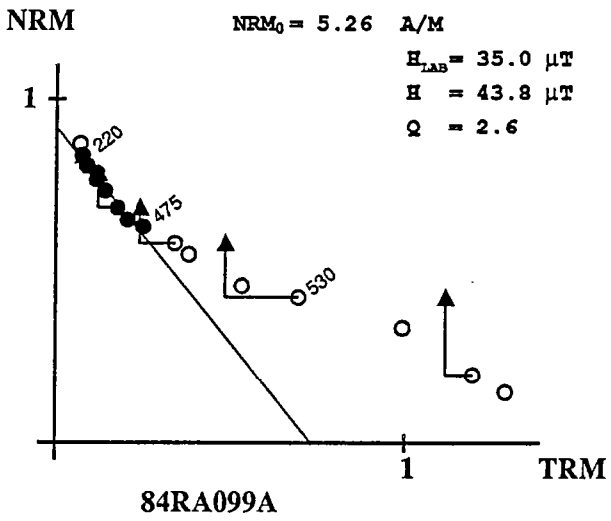

84RA099A

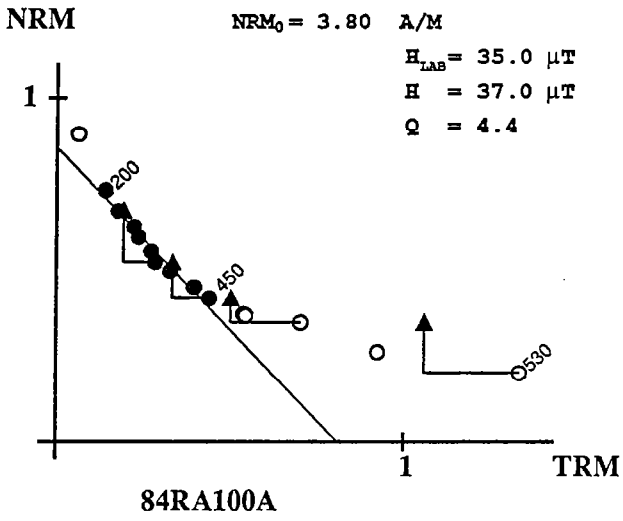

84RA100A

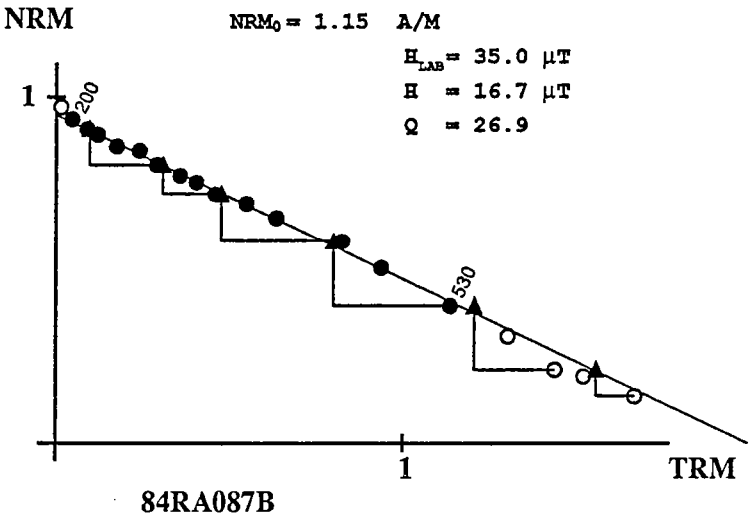

84RA087B

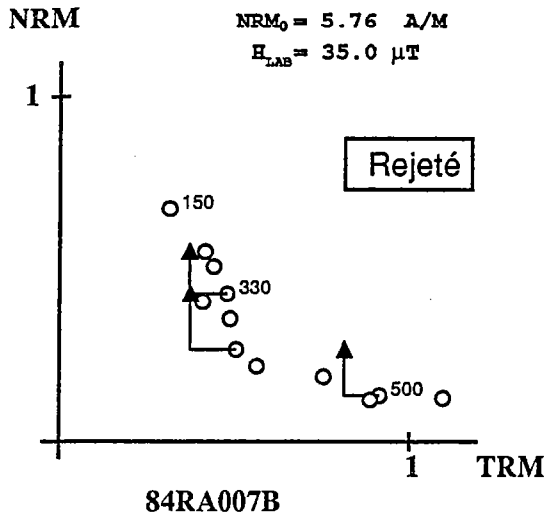

84RA007B

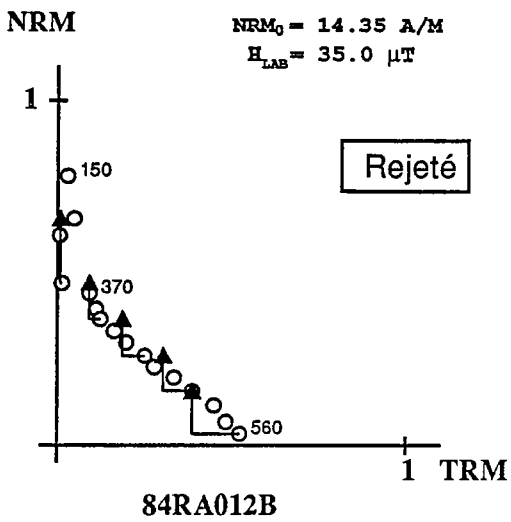

84RA012B

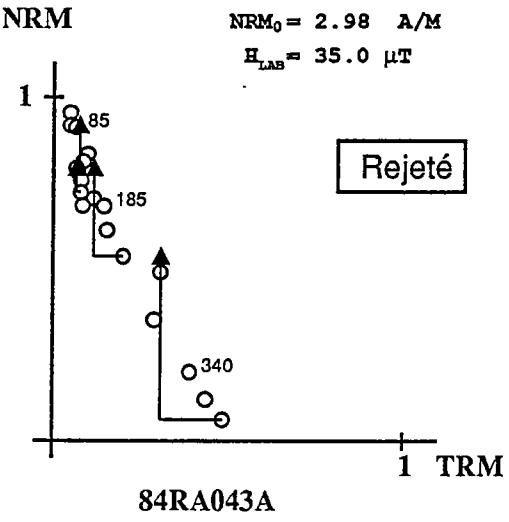

84RA043A

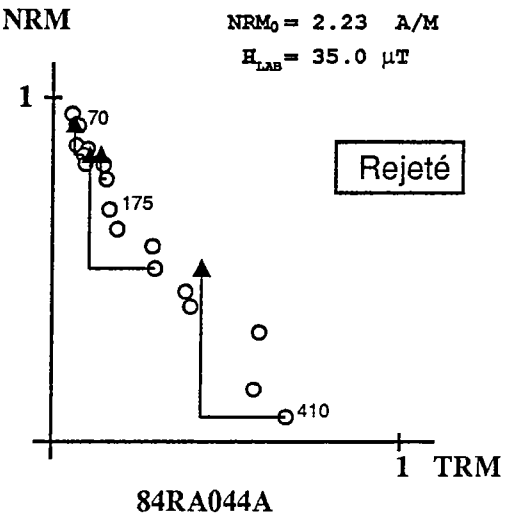

84RA044A

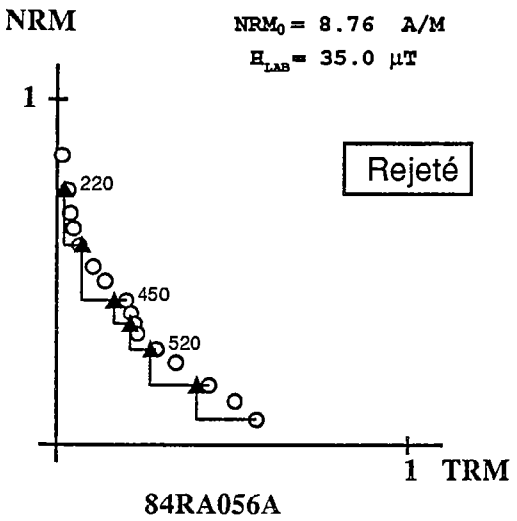

84RA056A

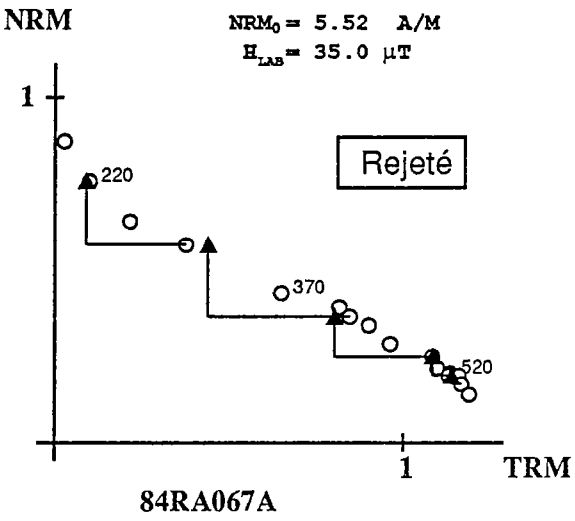

84RA067A

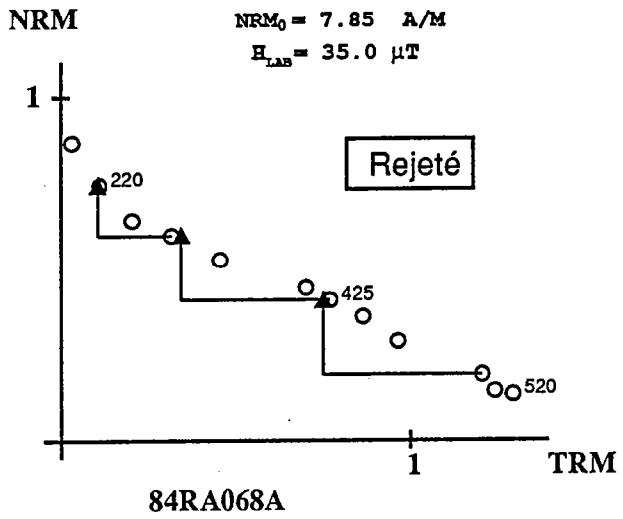

84RA068A

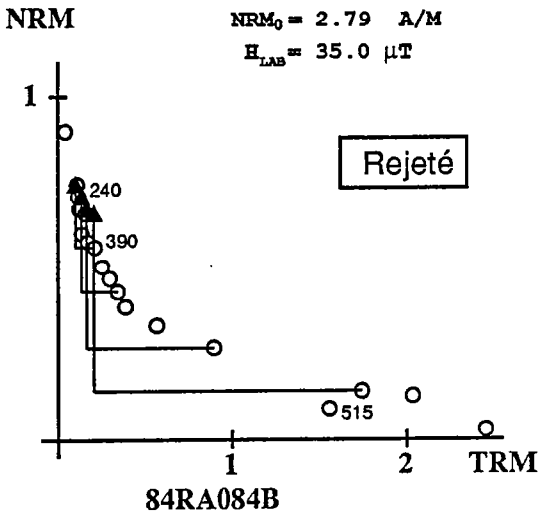

84RA084B

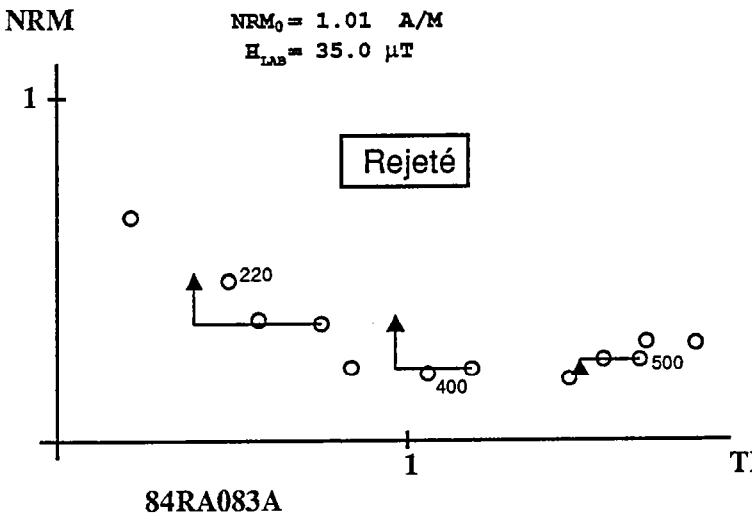

84RA083A

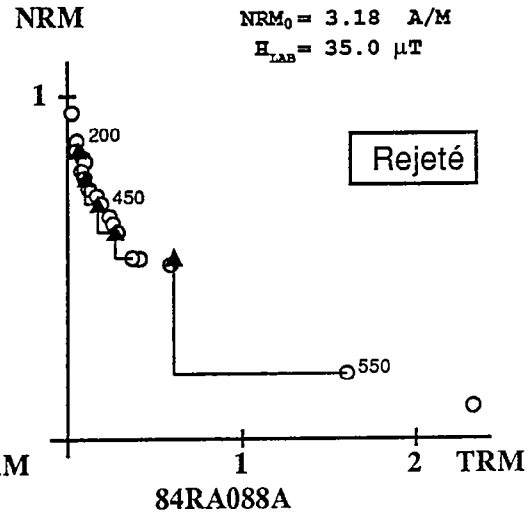

84RA088A

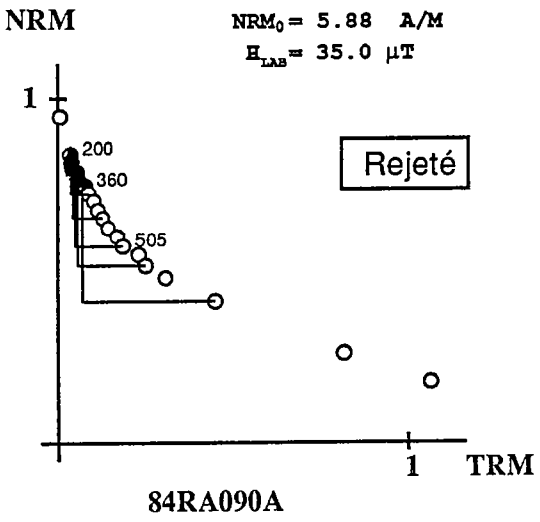

84RA090A

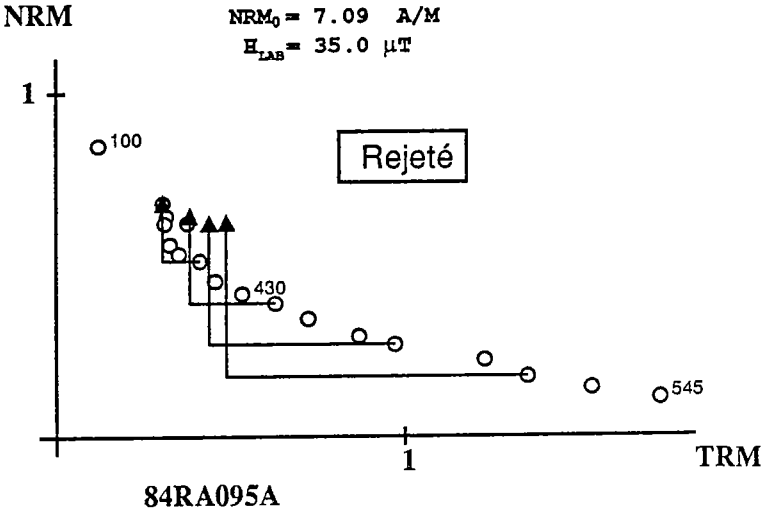

84RA095A

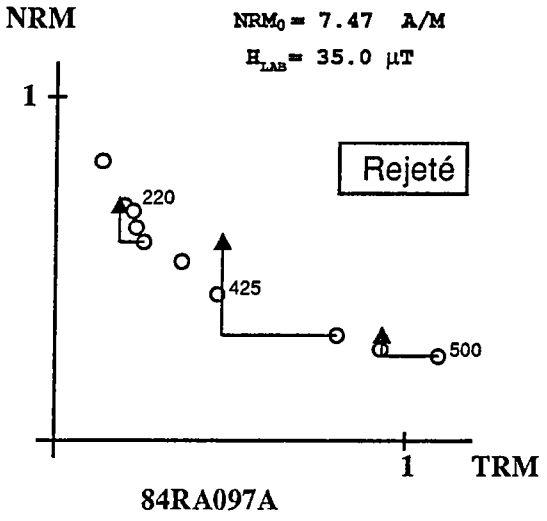

84RA097A

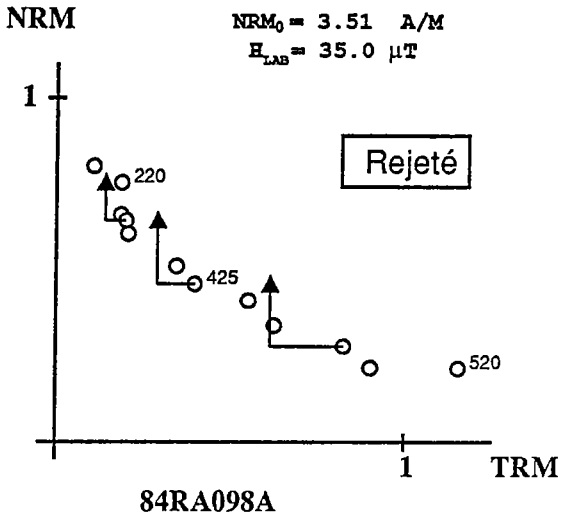

84RA098A

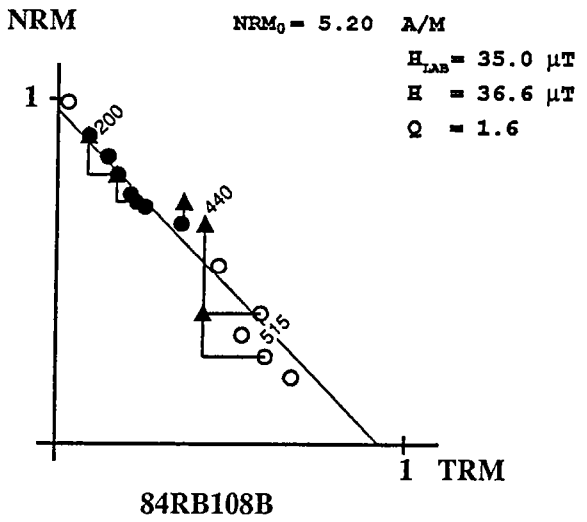

84RB108B

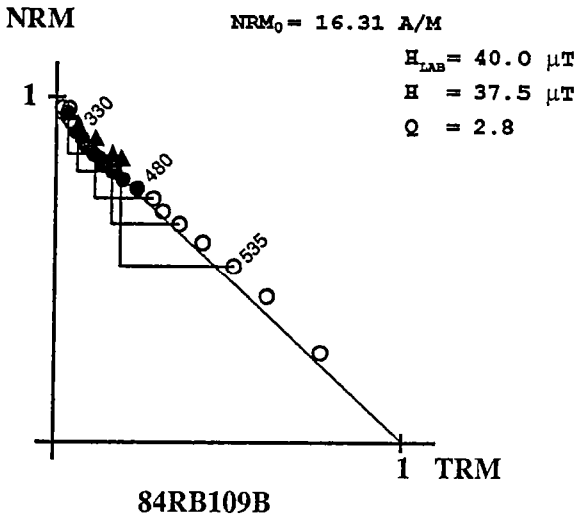

84RB109B

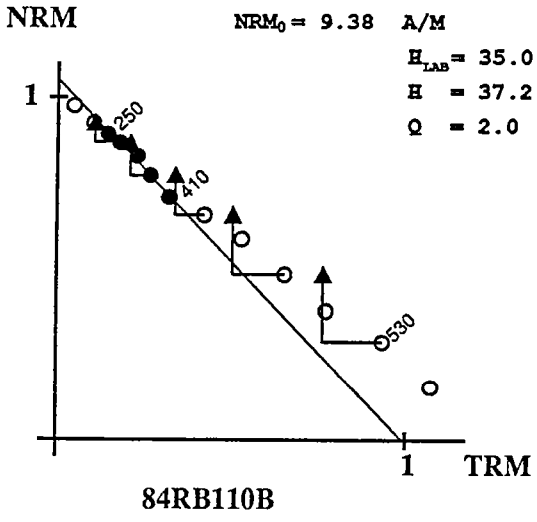

84RB110B

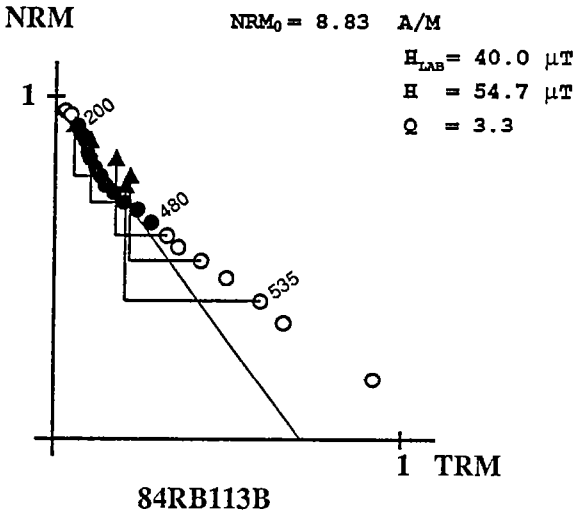

84RB113B

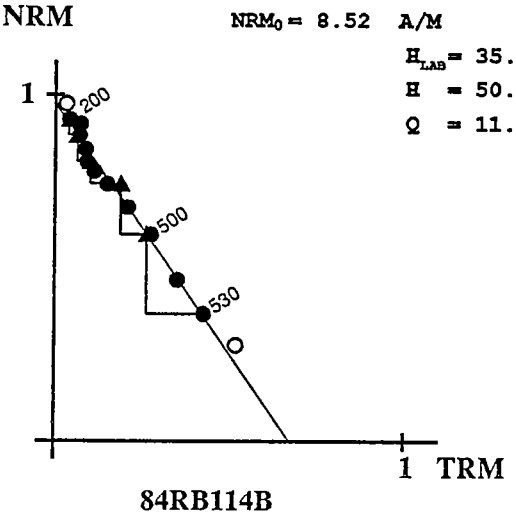

84RB114B

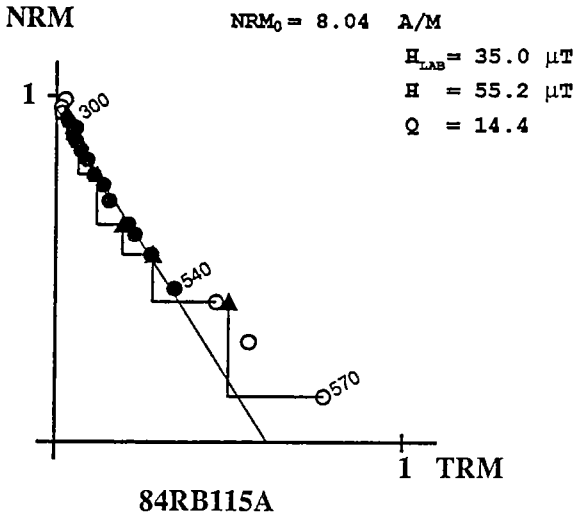

84RB115A

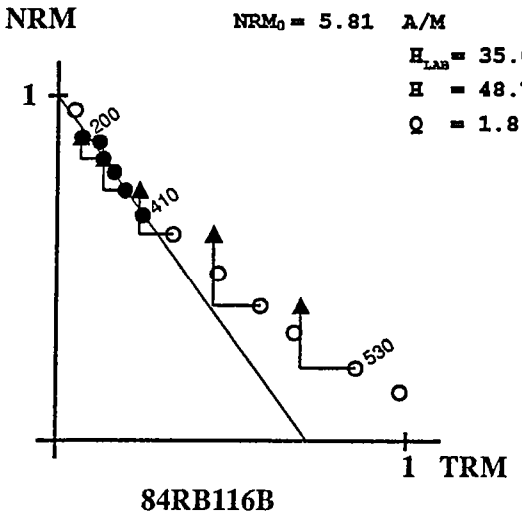

84RB116B

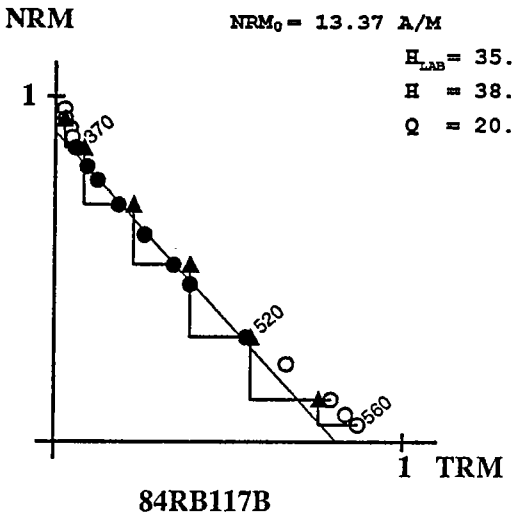

84RB117B

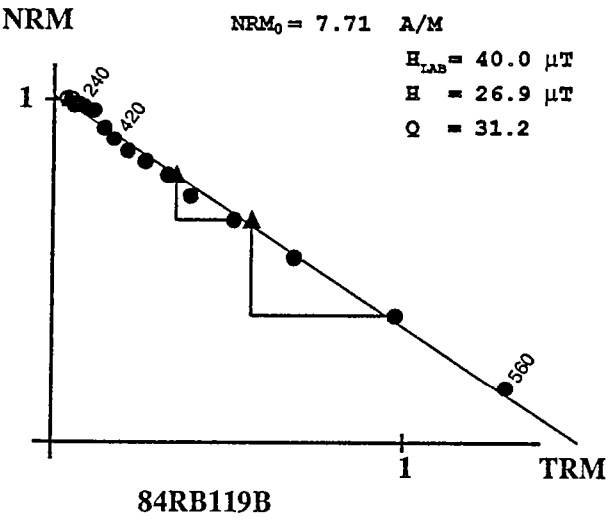

84RB119B

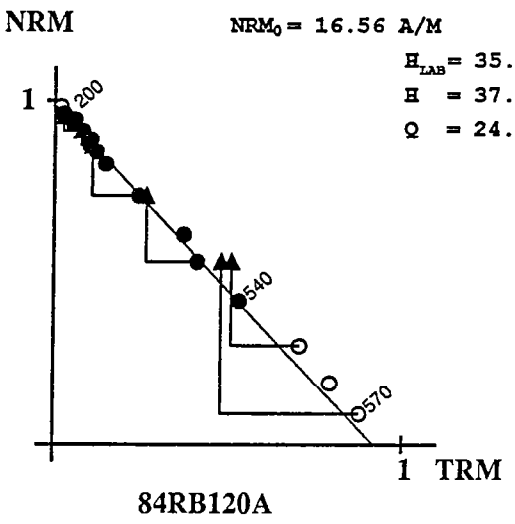

84RB120A

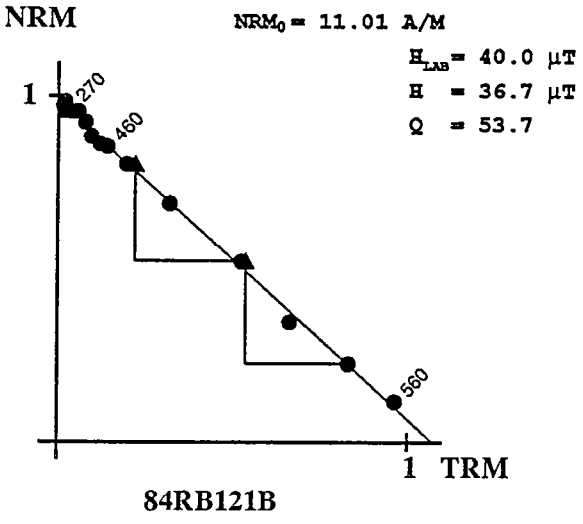

84RB121B

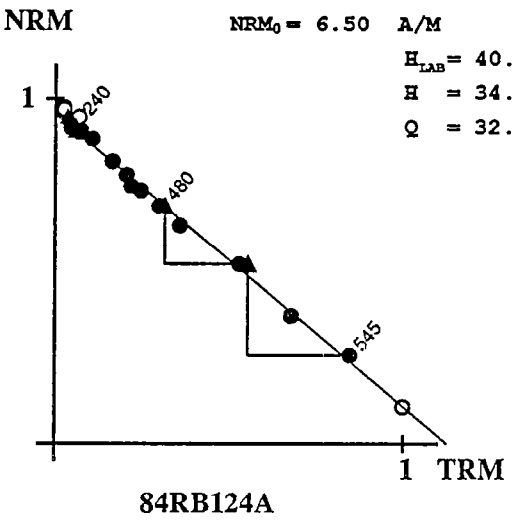

84RB124A

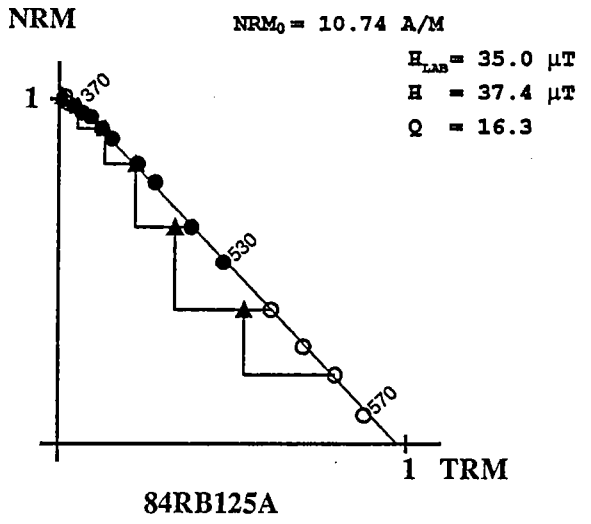

84RB125A

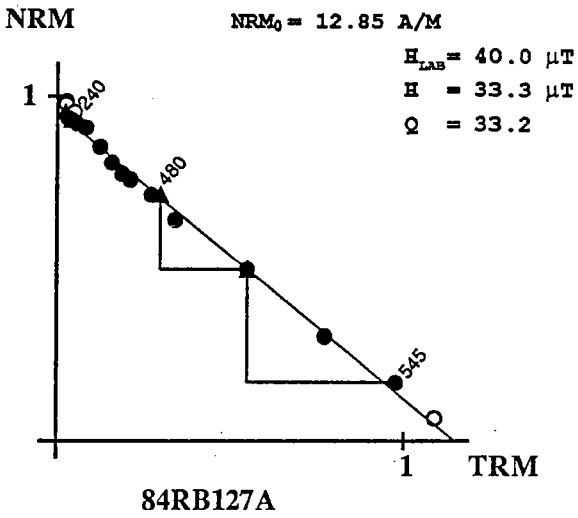

84RB127A

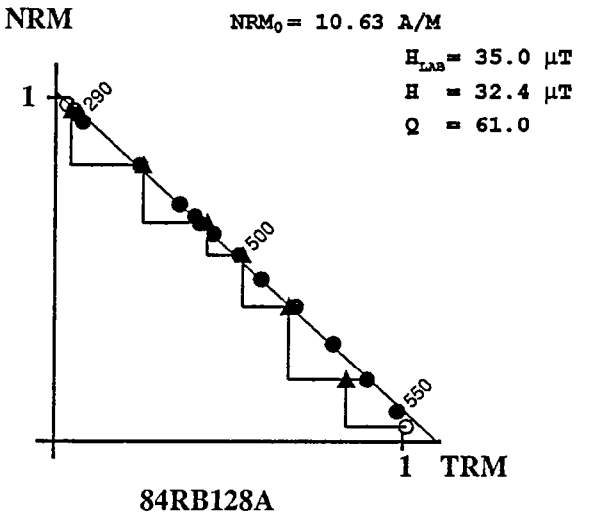

84RB128A

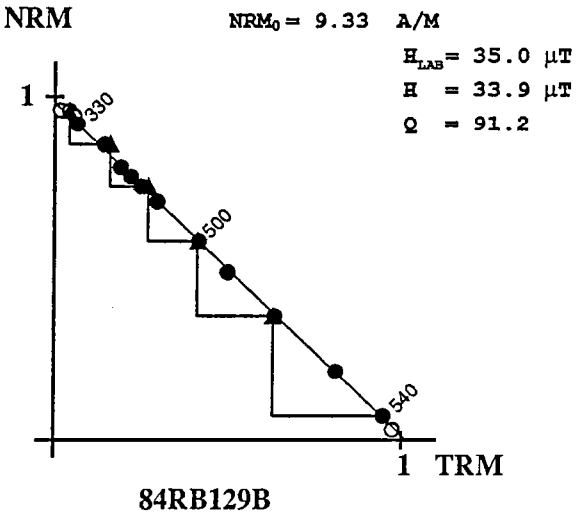

84RB129B

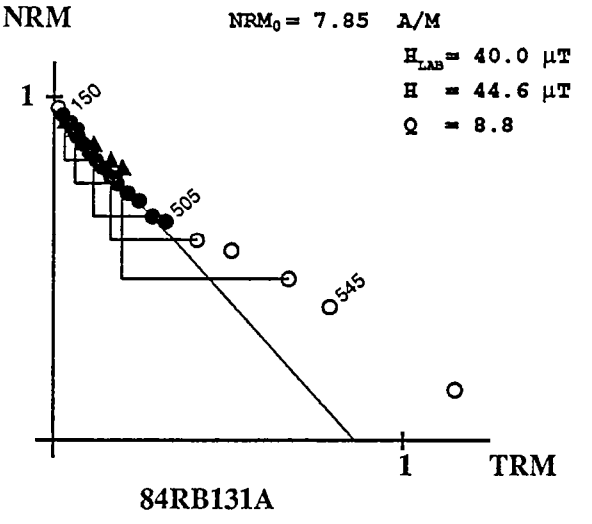

84RB131A

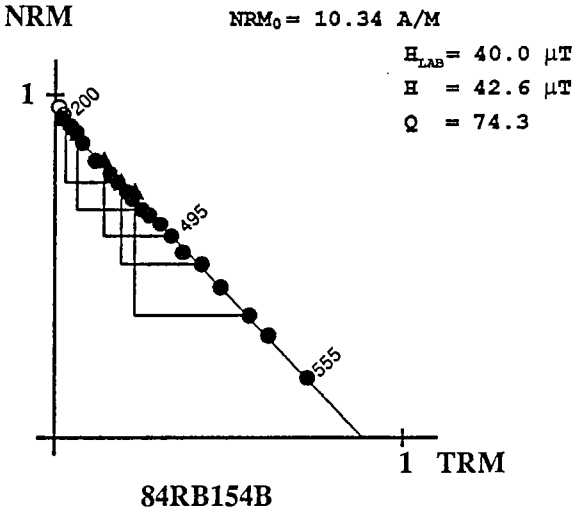

84RB154B

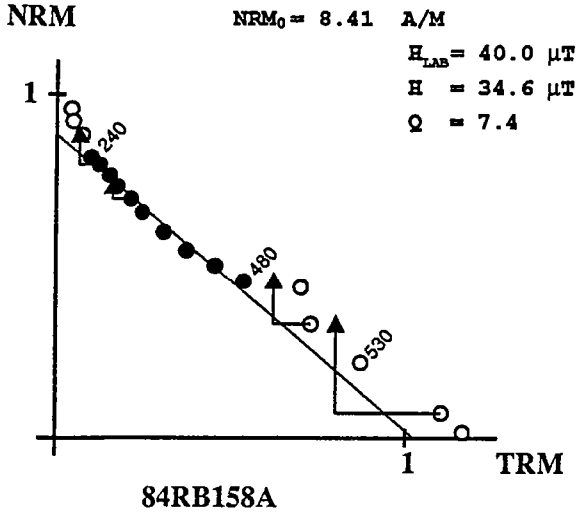

84RB158A

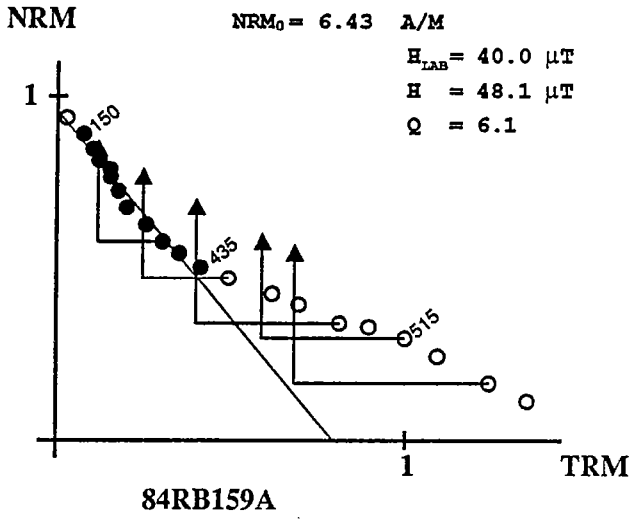

84RB159A

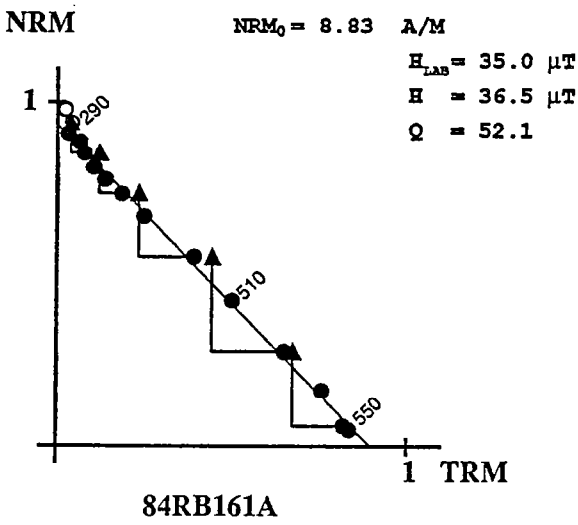

84RB161A

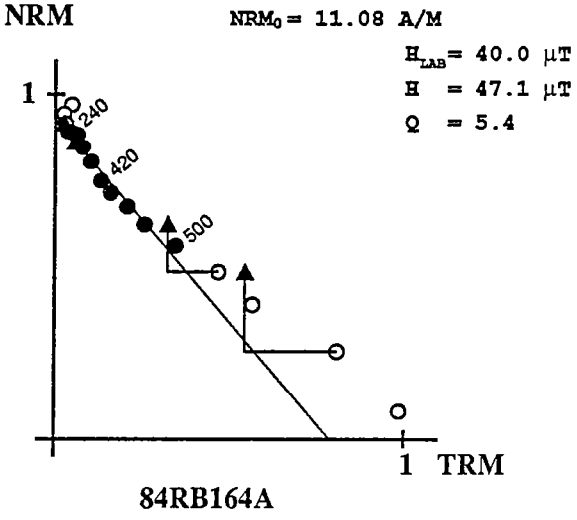

84RB164A

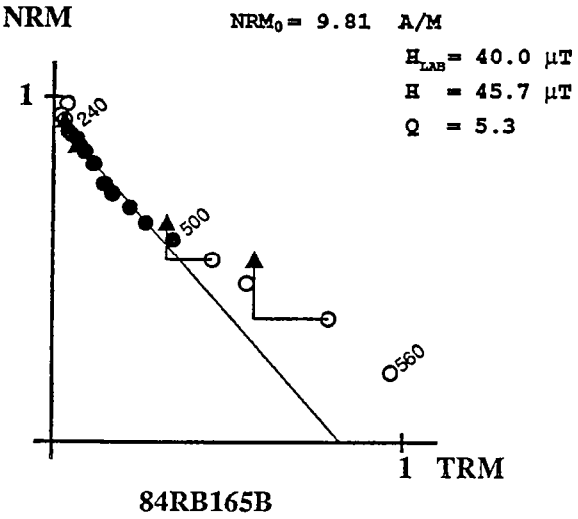

84RB165B

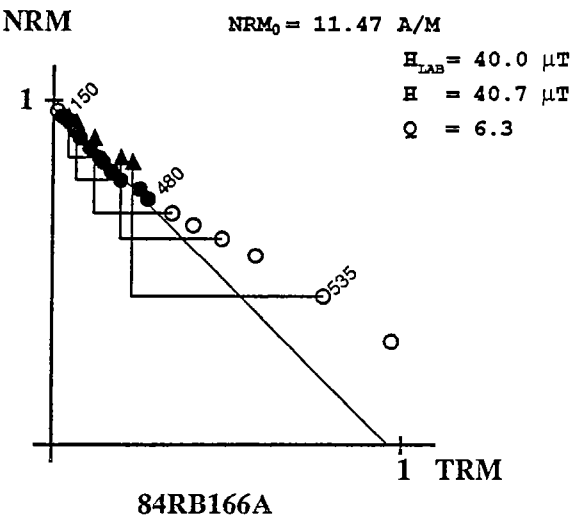

84RB166A

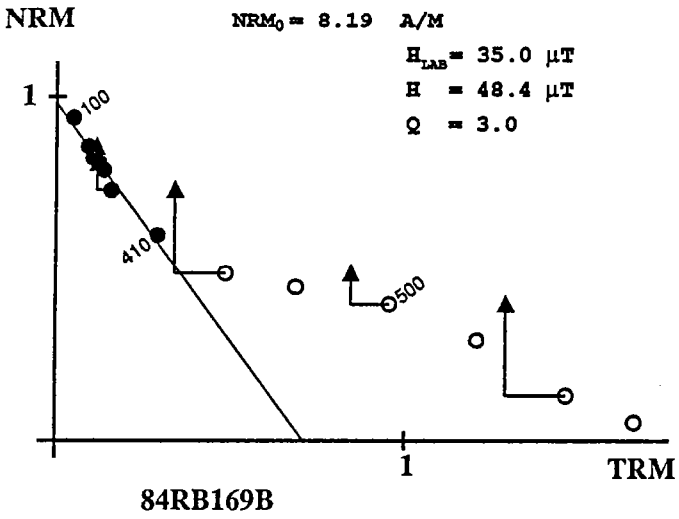

84RB169B

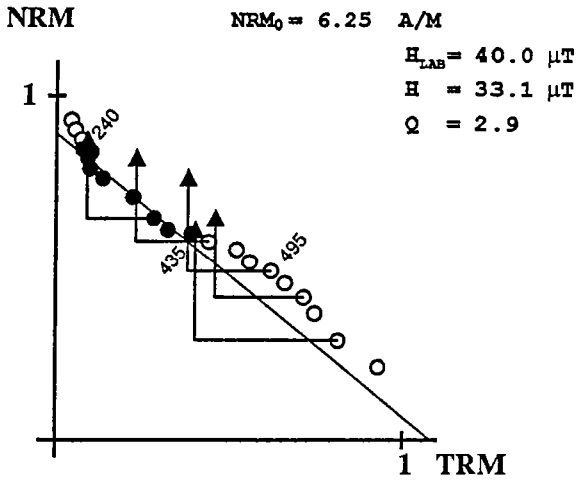

84RB170B

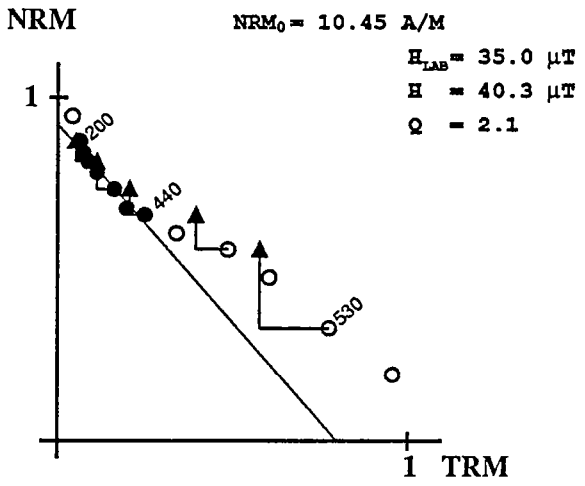

84RB171B

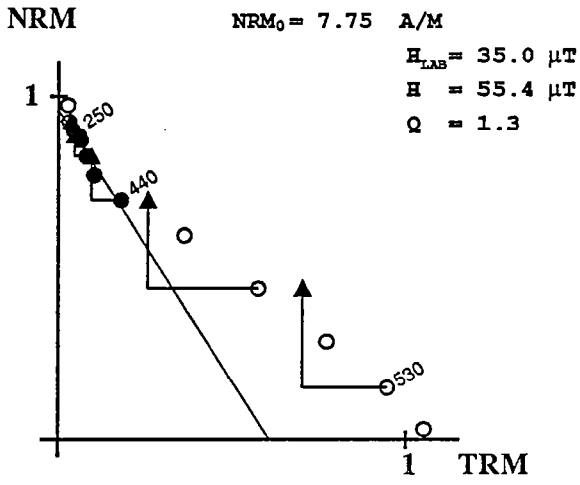

84RB173B

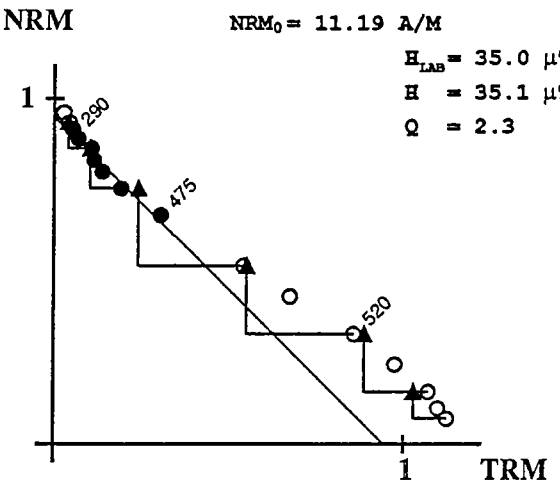

84RB175A

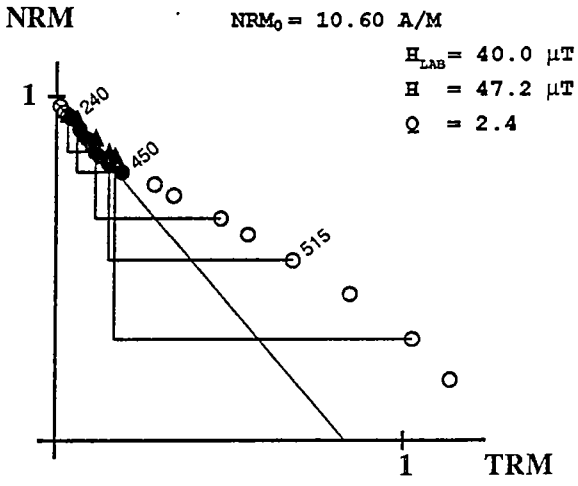

84RB176A

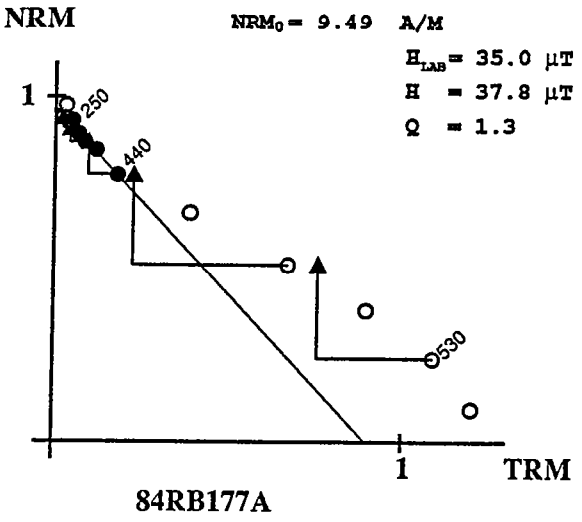

84RB177A

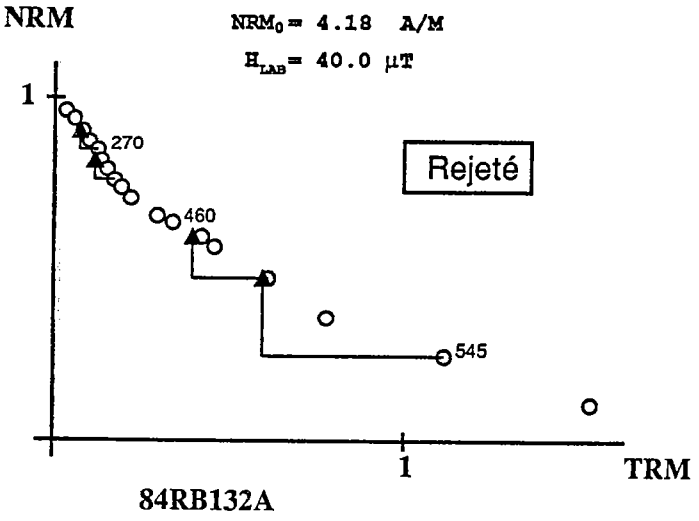

84RB132A

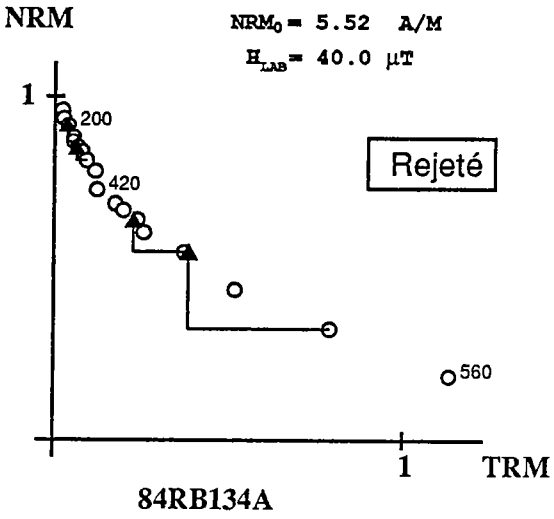

84RB134A

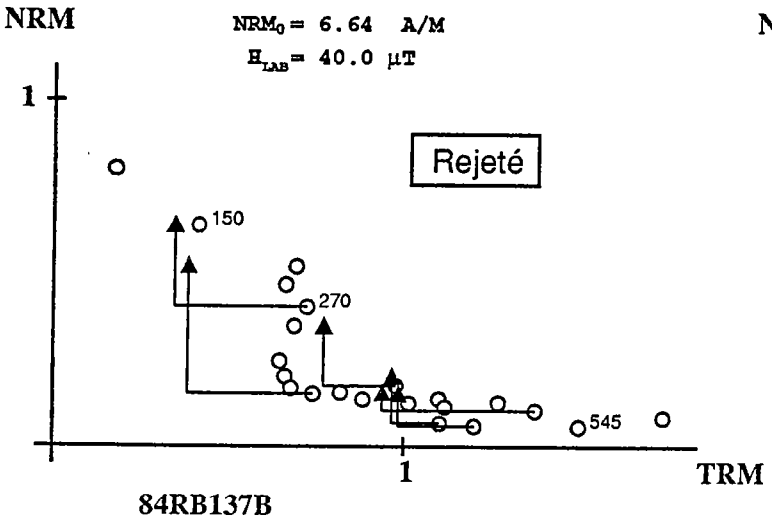

84RB137B

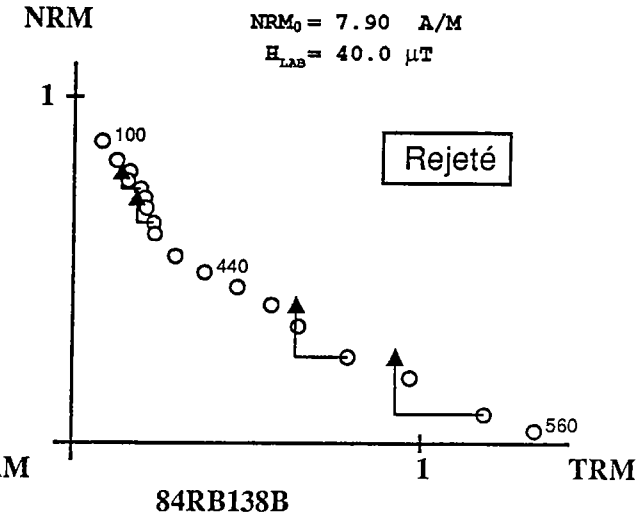

84RB138B

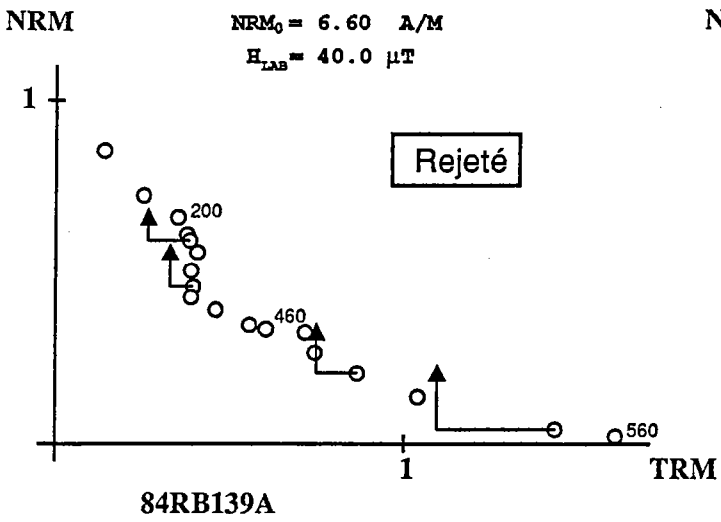

84RB139A

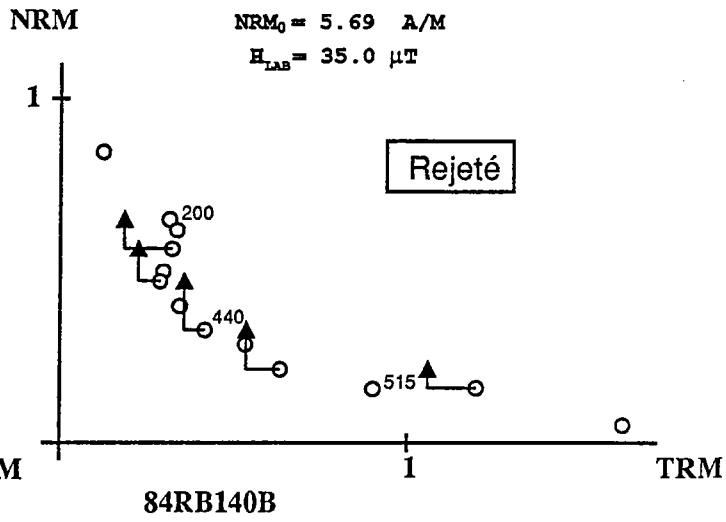

84RB140B

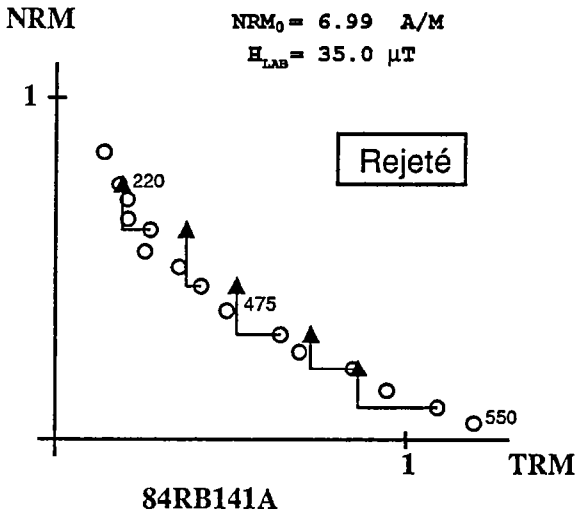

84RB141A

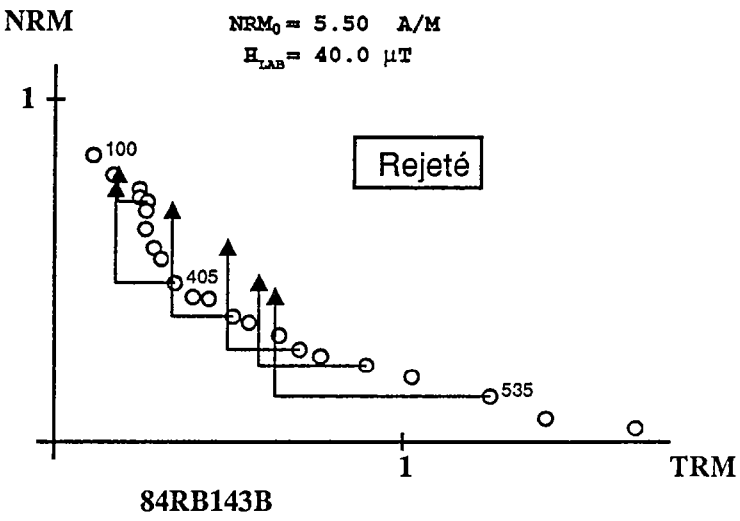

84RB143B

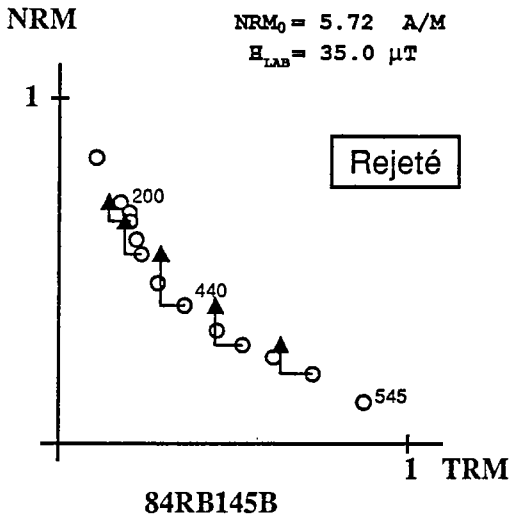

84RB145B

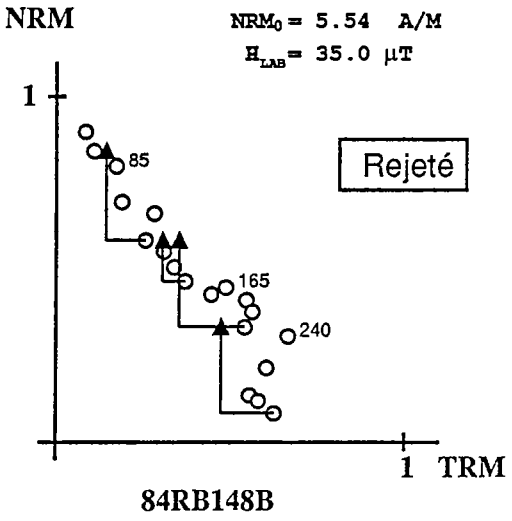

84RB148B

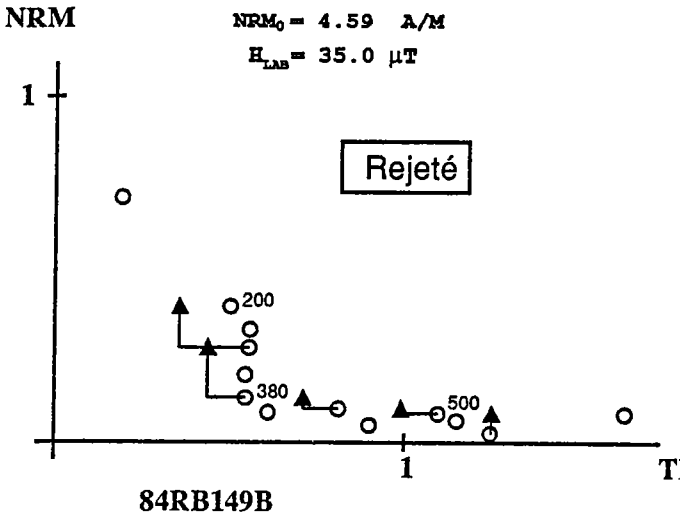

84RB149B

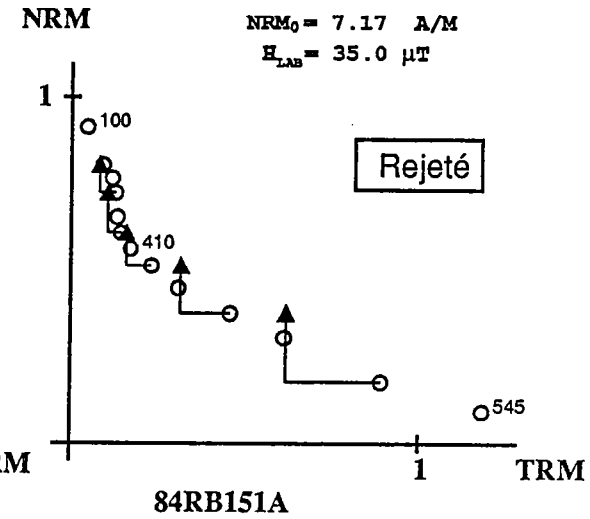

84RB151A

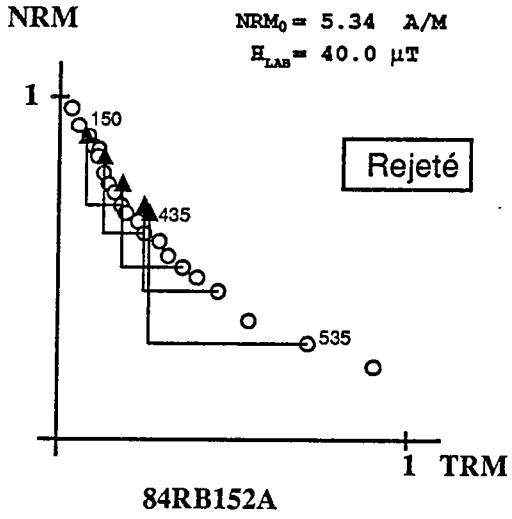

84RB152A

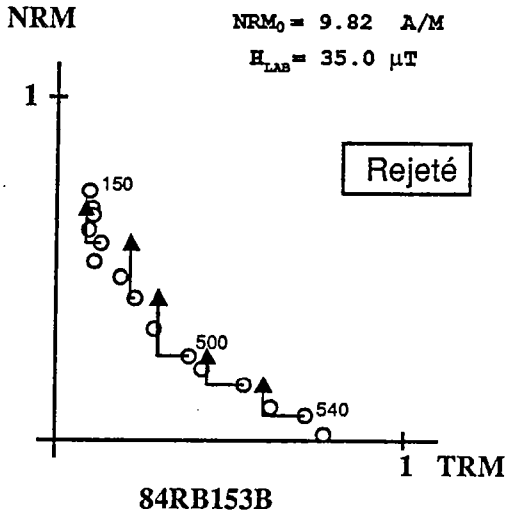

84RB153B

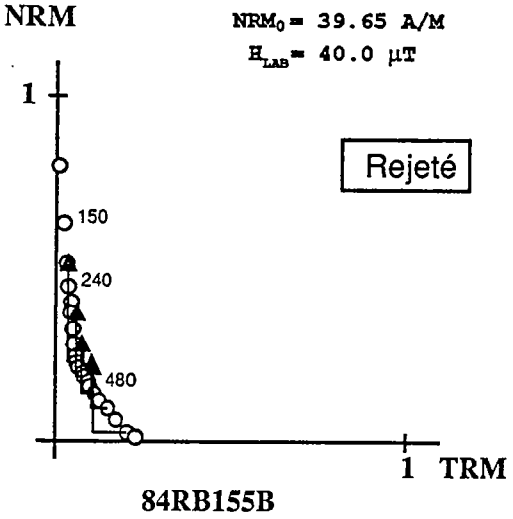

84RB155B

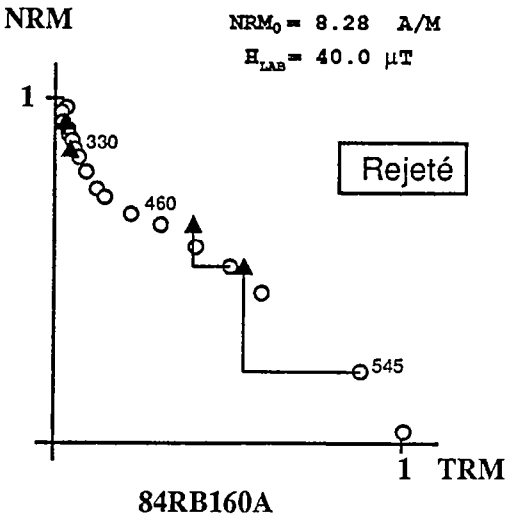

84RB160A

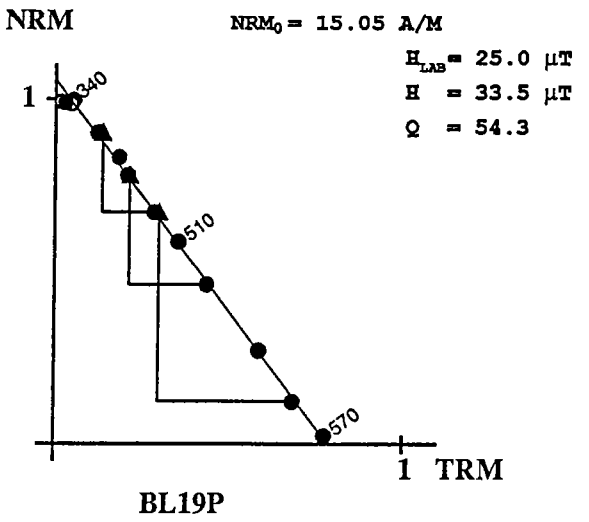

BL19P

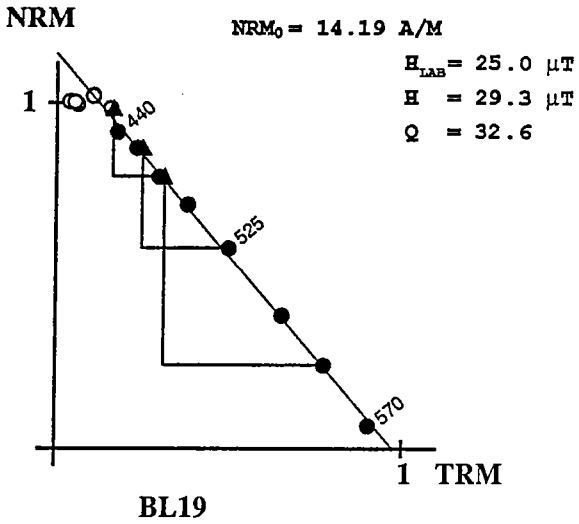

BL19

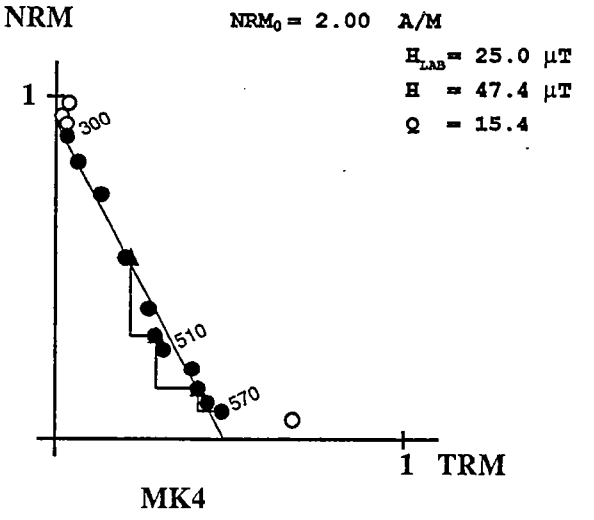

MK4

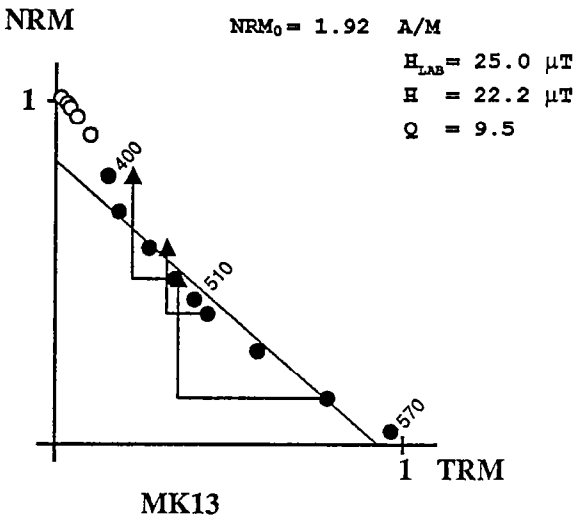

MK13

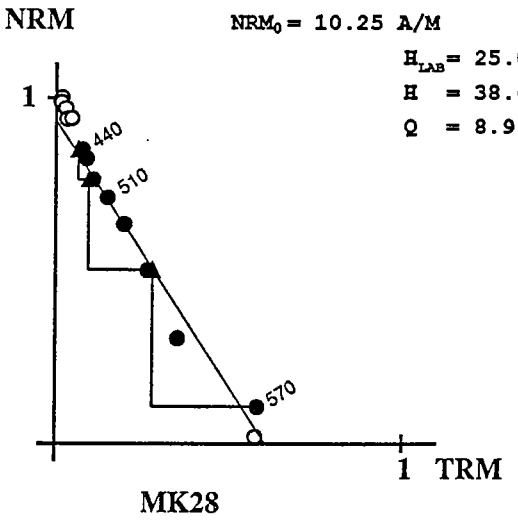

MK28

Echantillons d'Islande

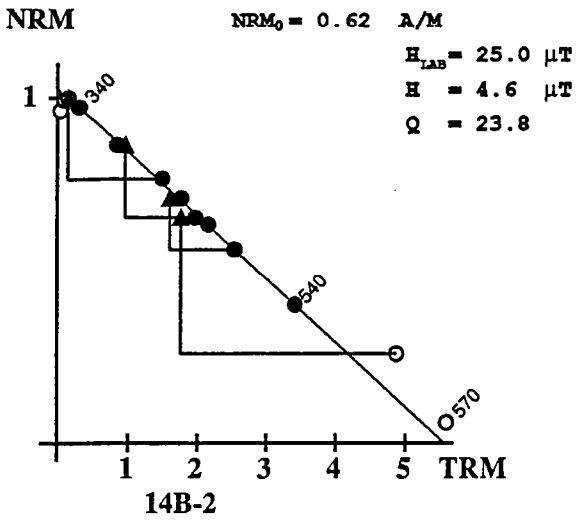
NRM
NRM$_0$ = 0.62 A/M
H$_{LAB}$ = 25.0 µT
H = 4.6 µT
Q = 23.8
1
340
540
570
1 2 3 4 5 TRM
14B-2

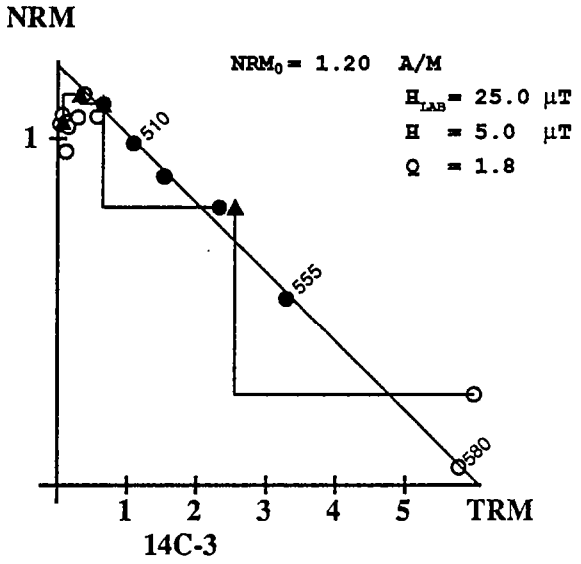
NRM
NRM$_0$ = 1.20 A/M
H$_{LAB}$ = 25.0 µT
H = 5.0 µT
Q = 1.8
1
510
555
580
1 2 3 4 5 TRM
14C-3

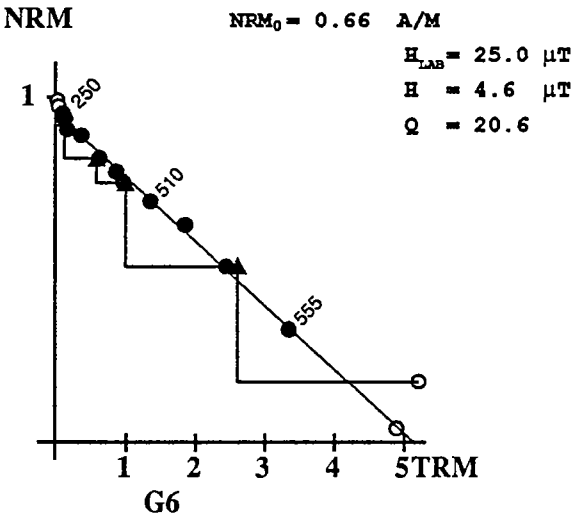
NRM
NRM$_0$ = 0.66 A/M
H$_{LAB}$ = 25.0 µT
H = 4.6 µT
Q = 20.6
1
250
510
555
1 2 3 4 5TRM
G6

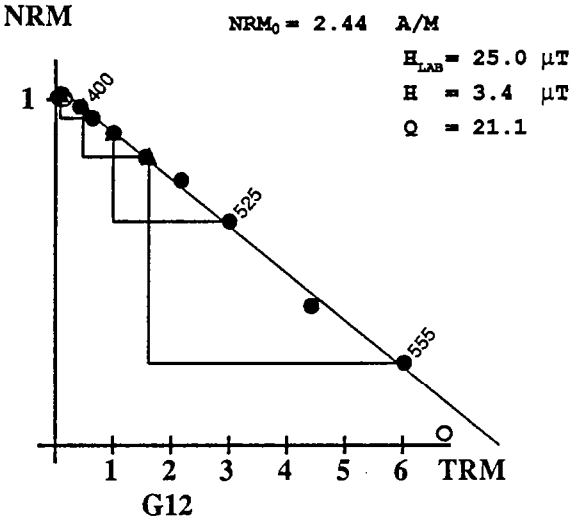
NRM
NRM$_0$ = 2.44 A/M
H$_{LAB}$ = 25.0 µT
H = 3.4 µT
Q = 21.1
1
400
525
555
1 2 3 4 5 6 TRM
G12

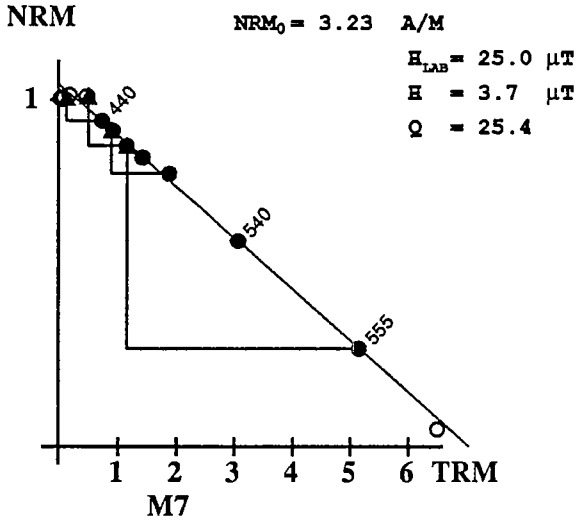
NRM
NRM$_0$ = 3.23 A/M
H$_{LAB}$ = 25.0 µT
H = 3.7 µT
Q = 25.4
1
440
540
555
1 2 3 4 5 6 TRM
M7

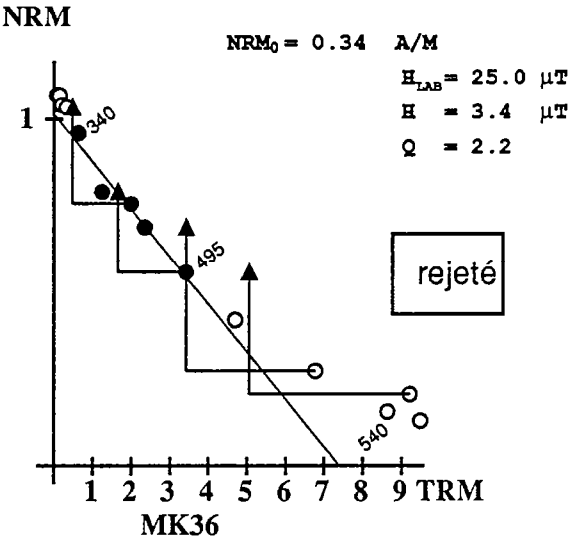
NRM
NRM$_0$ = 0.34 A/M
H$_{LAB}$ = 25.0 µT
H = 3.4 µT
Q = 2.2
1
340
495
540
rejeté
1 2 3 4 5 6 7 8 9 TRM
MK36

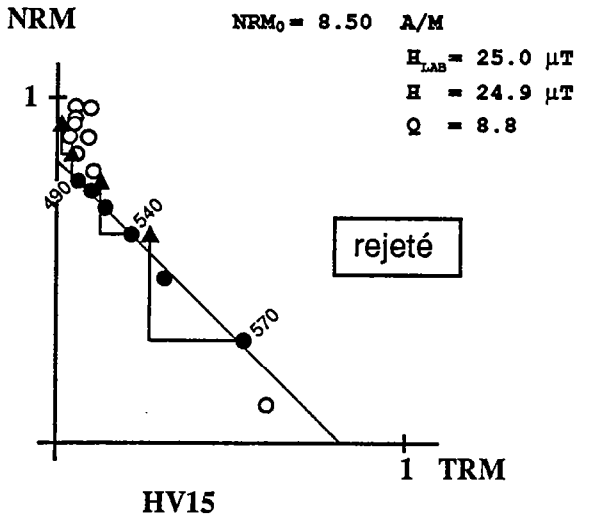

HV15

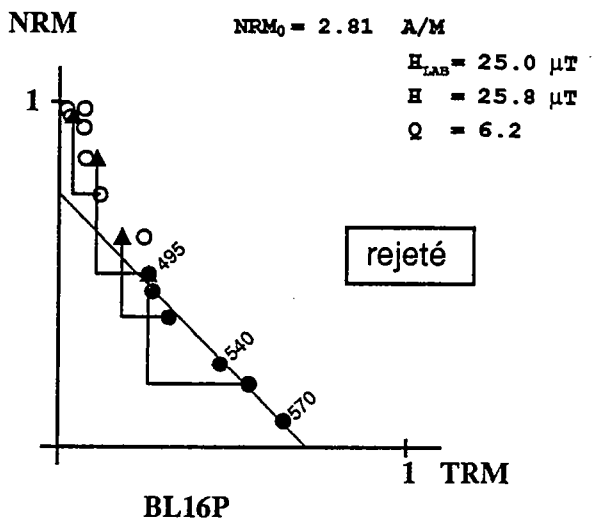

BL16P

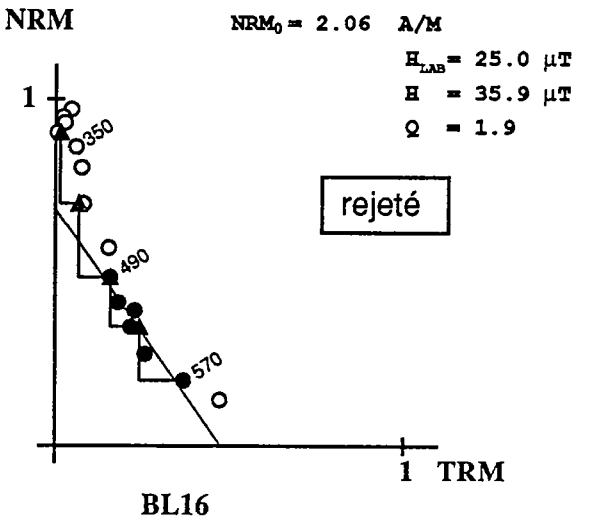

BL16

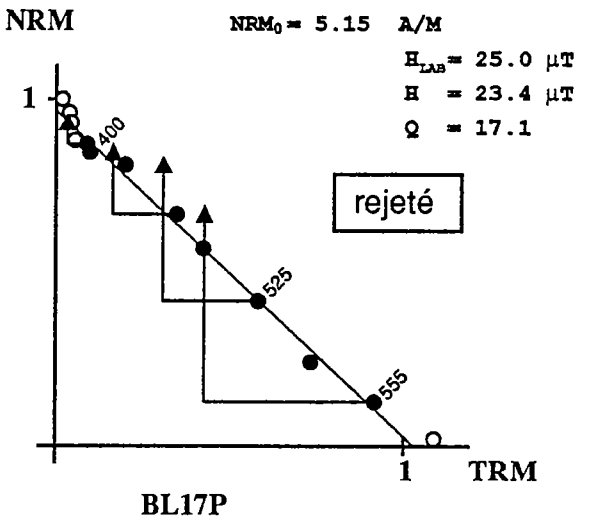

BL17P

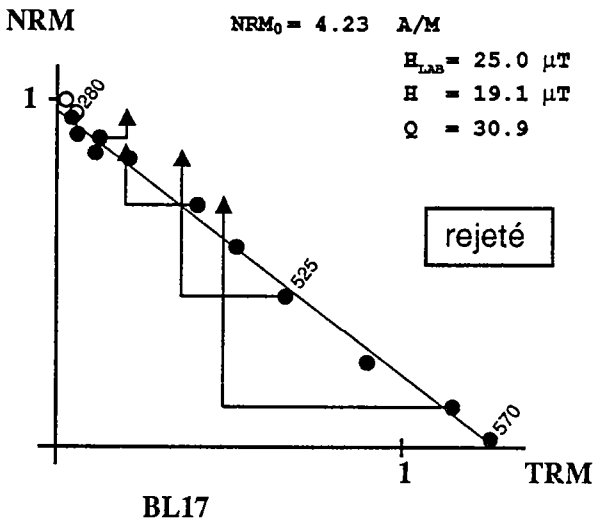

BL17

Echantillons de Louchadière

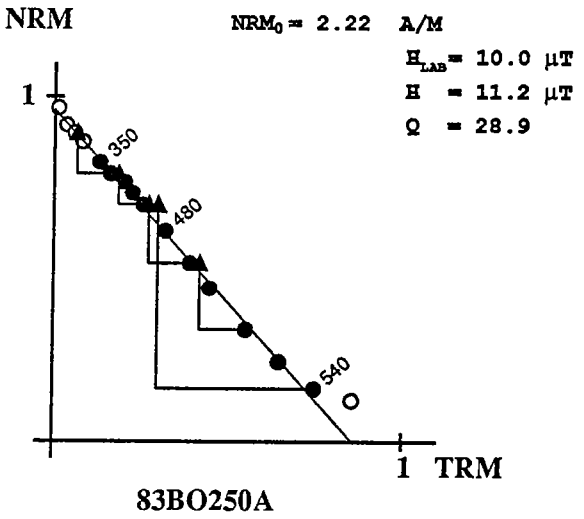

83BO250A

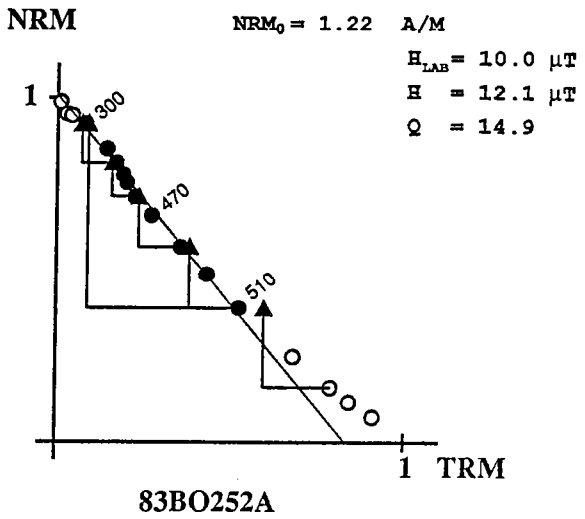

83BO252A

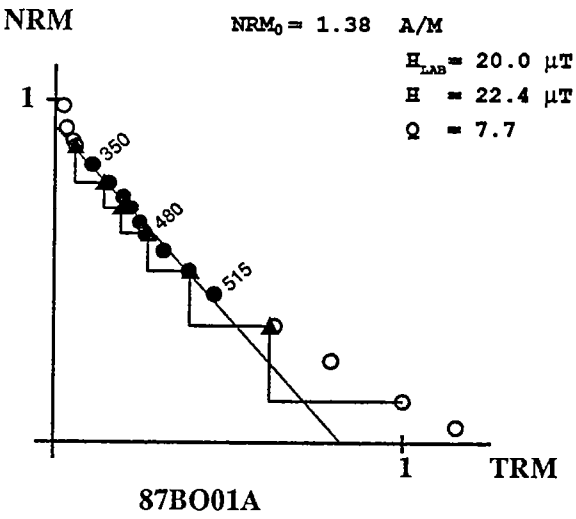

87BO01A

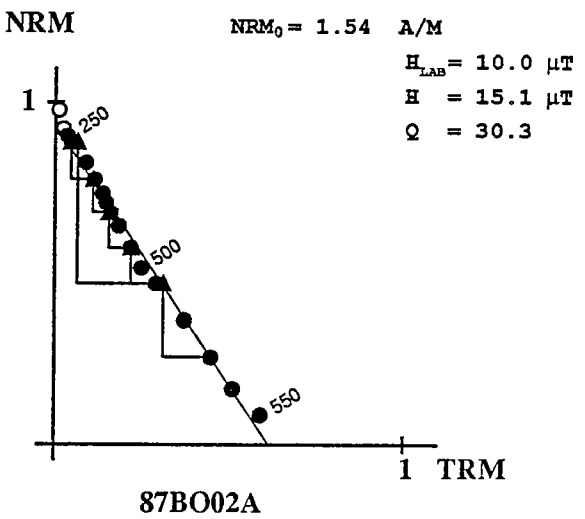

87BO02A

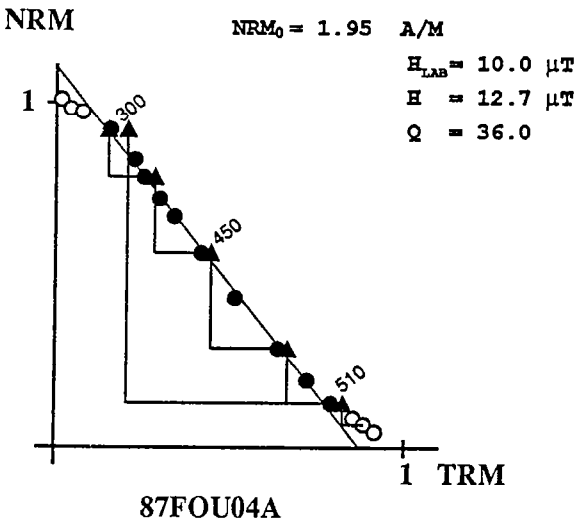

87FOU04A

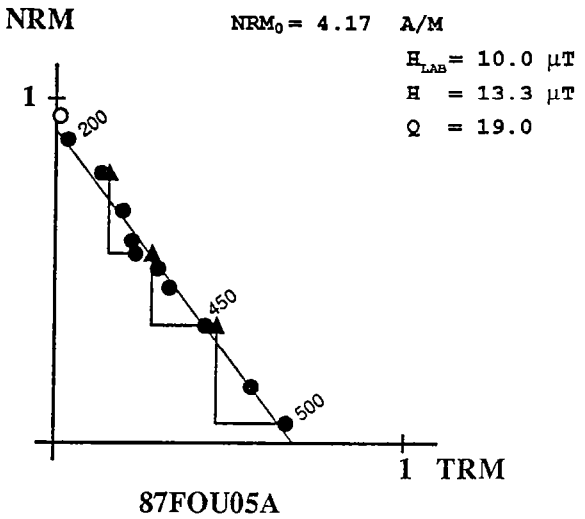

87FOU05A

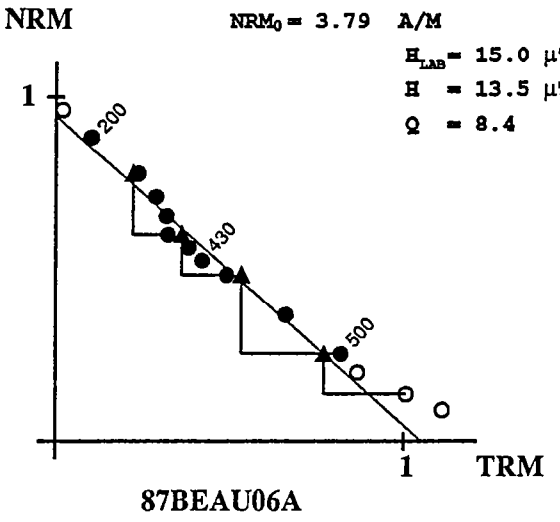

87BEAU06A

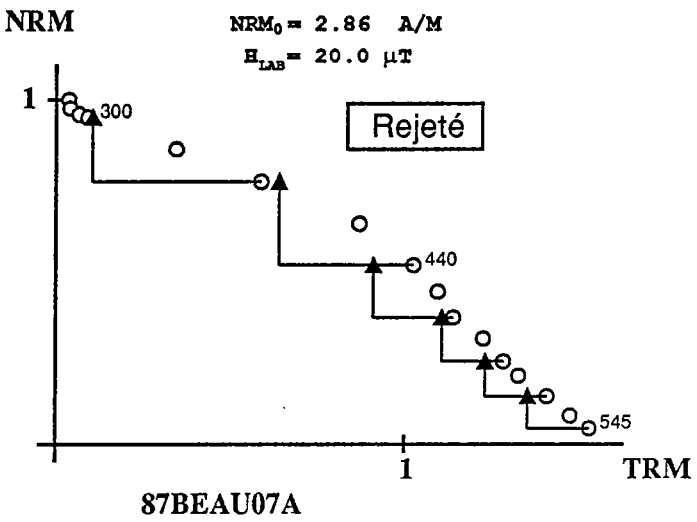

87BEAU07A

Echantillons de Tahiti

NRM

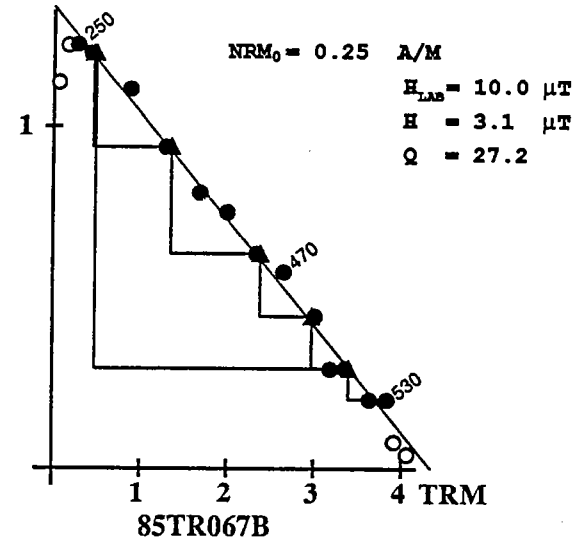

85TR067B

NRM

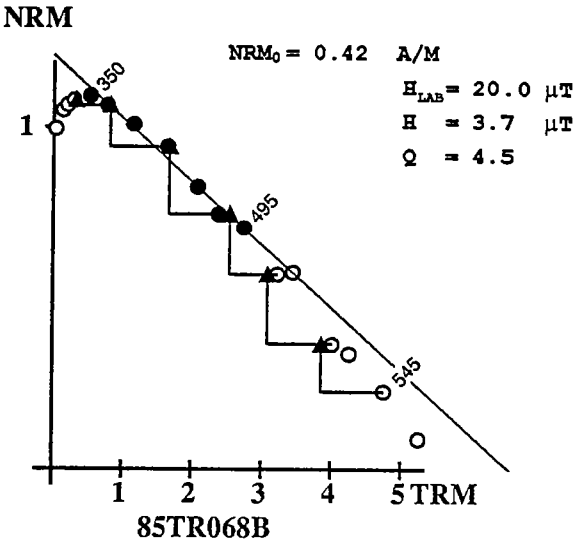

85TR068B

NRM

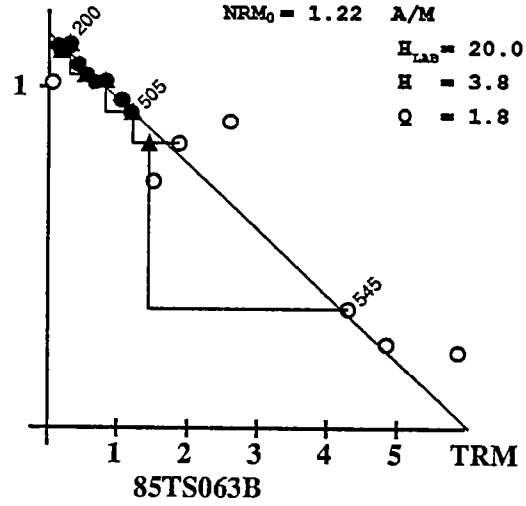

85TS063B

NRM

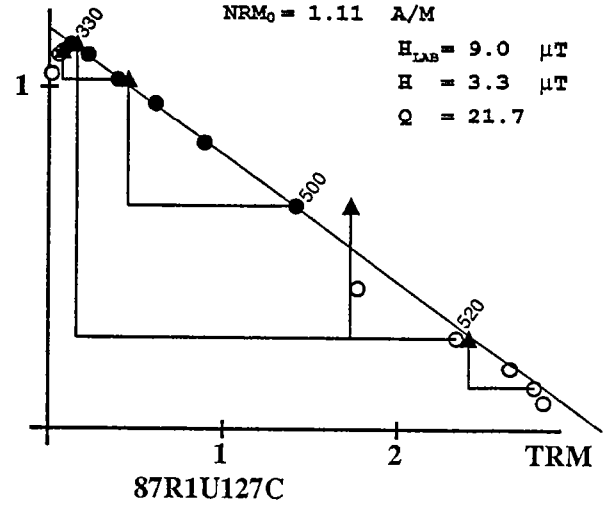

87R1U127C

NRM

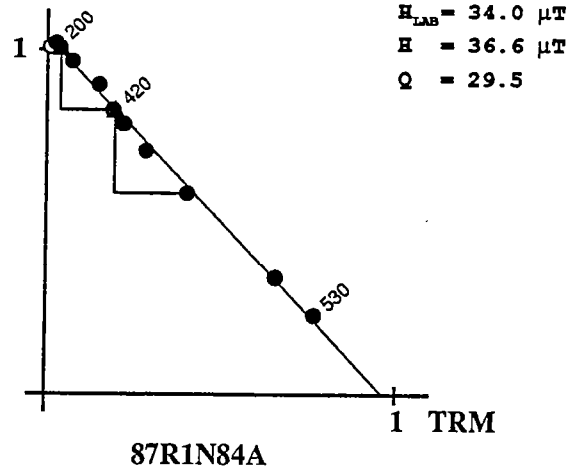

87R1N84A

NRM

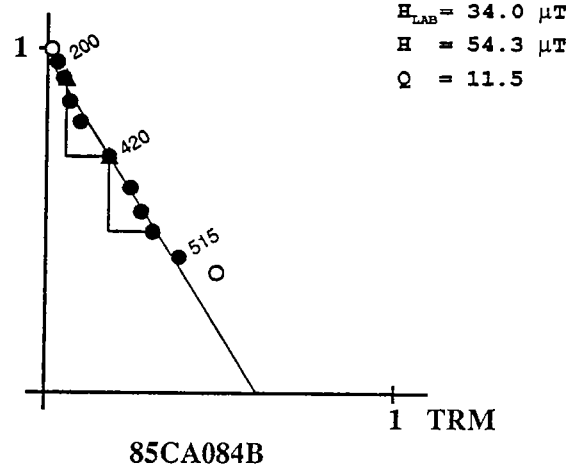

85CA084B

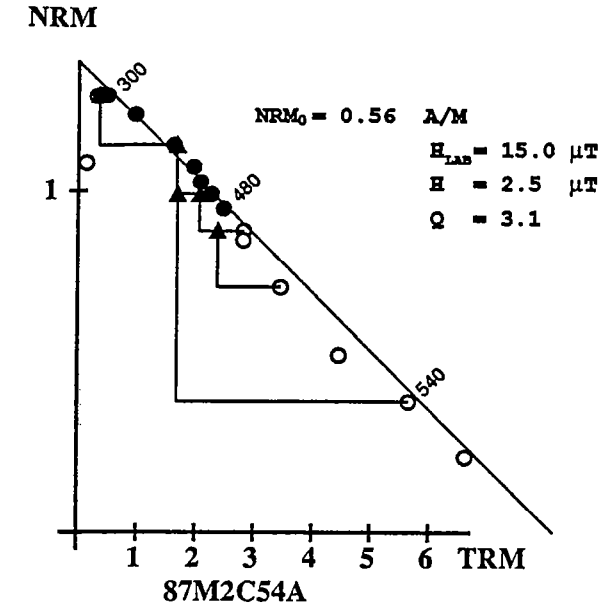
NRM
NRM$_0$ = 0.56 A/M
H$_{LAB}$ = 15.0 μT
H = 2.5 μT
Q = 3.1
300
480
540
1
1 2 3 4 5 6 TRM
87M2C54A

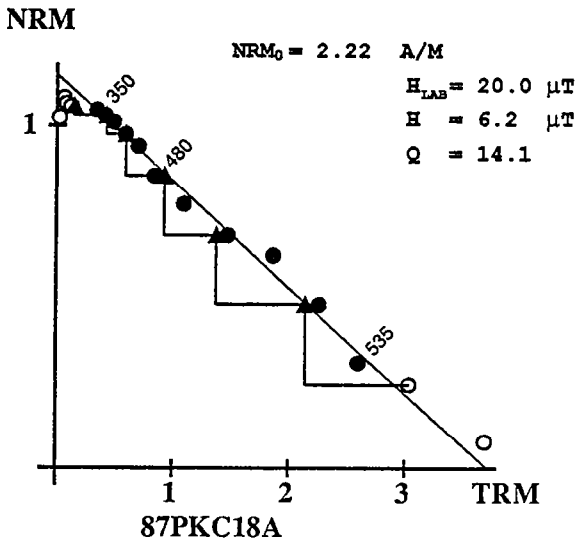
NRM
NRM$_0$ = 2.22 A/M
H$_{LAB}$ = 20.0 μT
H = 6.2 μT
Q = 14.1
350
480
535
1
1 2 3 TRM
87PKC18A

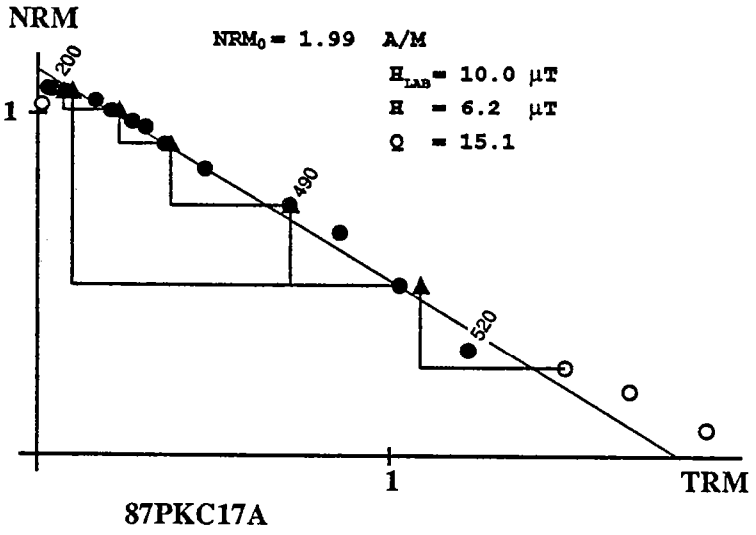
NRM
NRM$_0$ = 1.99 A/M
H$_{LAB}$ = 10.0 μT
H = 6.2 μT
Q = 15.1
200
490
520
1
1 TRM
87PKC17A

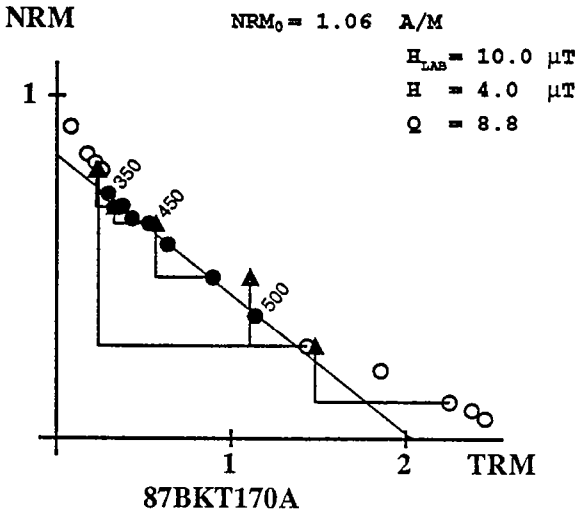
NRM
NRM$_0$ = 1.06 A/M
H$_{LAB}$ = 10.0 μT
H = 4.0 μT
Q = 8.8
350
450
500
1
1 2 TRM
87BKT170A

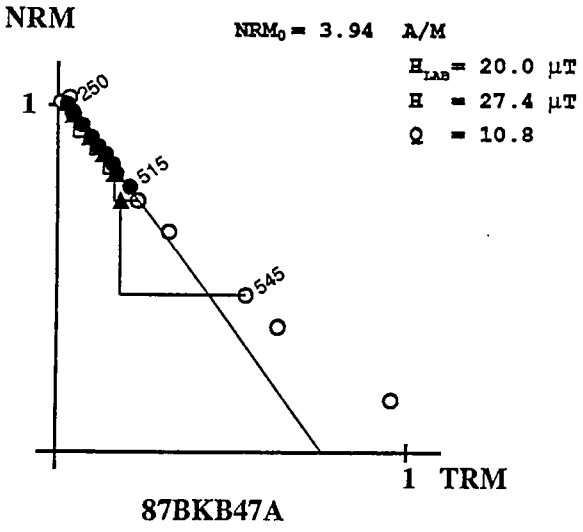
NRM
NRM$_0$ = 3.94 A/M
H$_{LAB}$ = 20.0 μT
H = 27.4 μT
Q = 10.8
250
515
545
1
1 TRM
87BKB47A

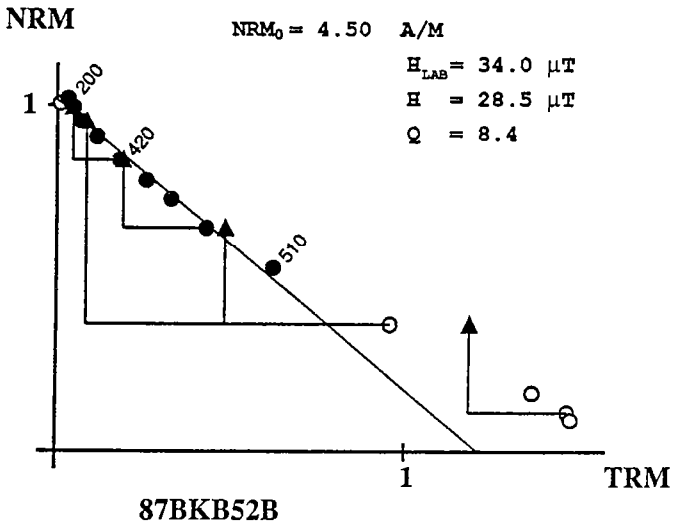
NRM
NRM$_0$ = 4.50 A/M
H$_{LAB}$ = 34.0 μT
H = 28.5 μT
Q = 8.4
200
420
510
1
1 TRM
87BKB52B

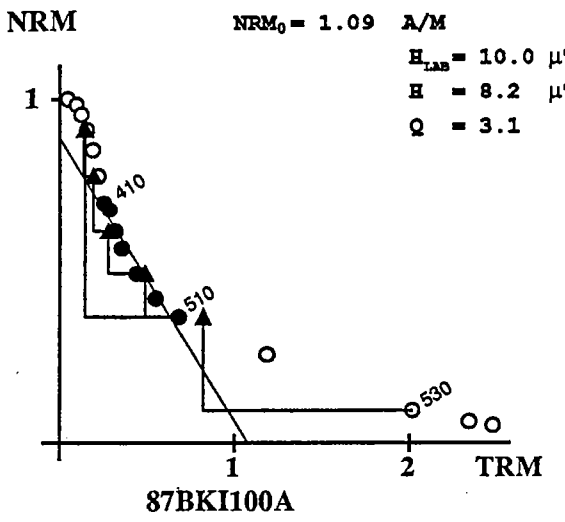

87BKI100A

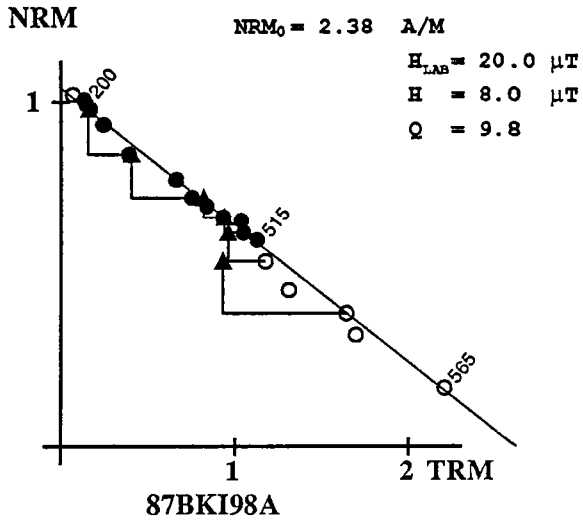

87BKI98A

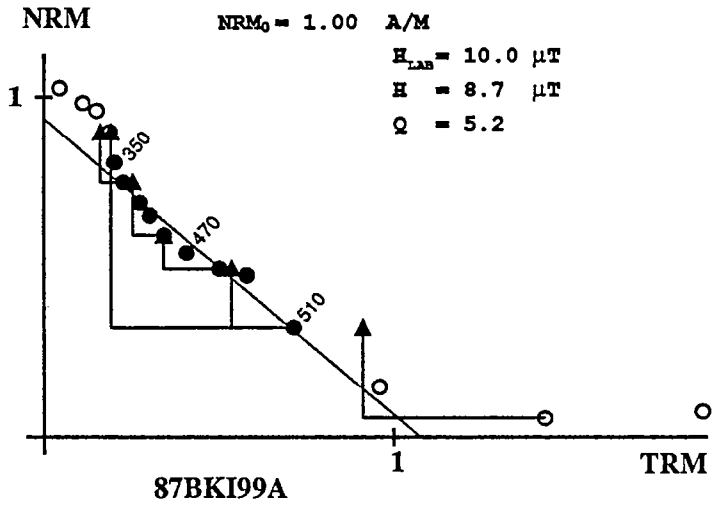

87BKI99A

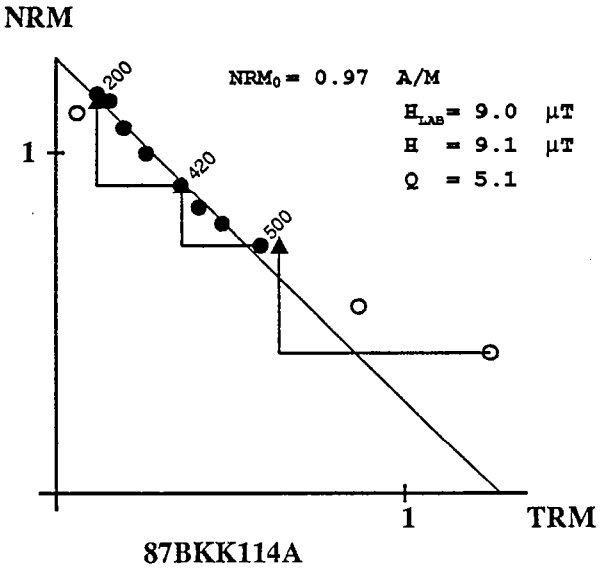

87BKK114A

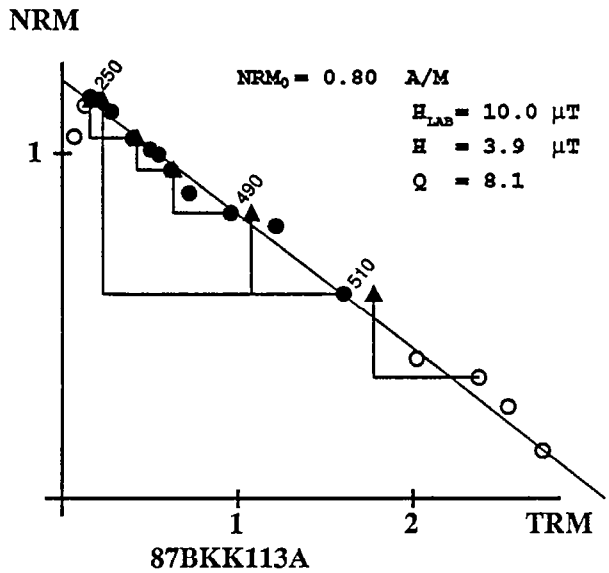

87BKK113A

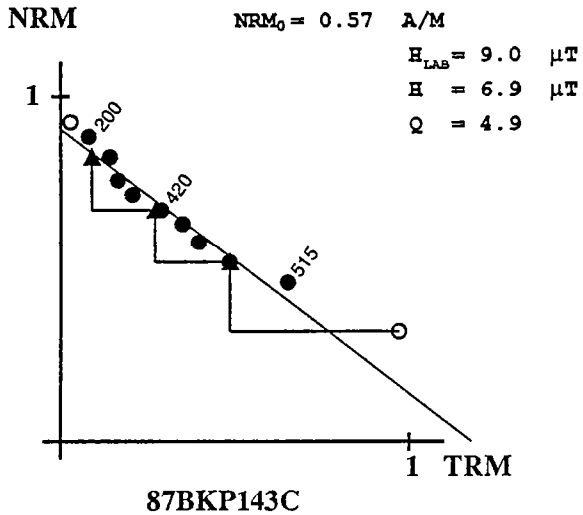

87BKP143C

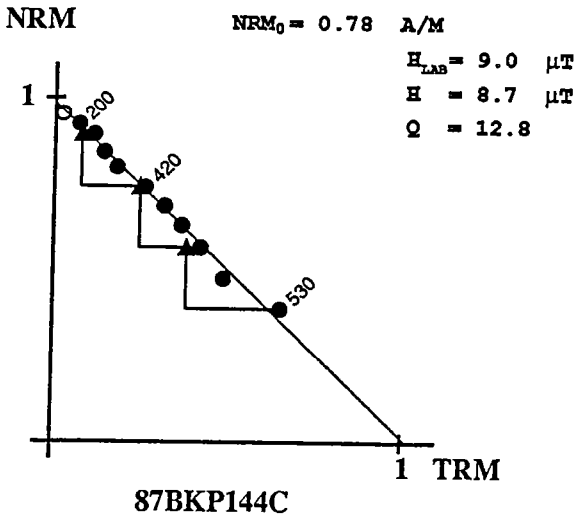

87BKP144C

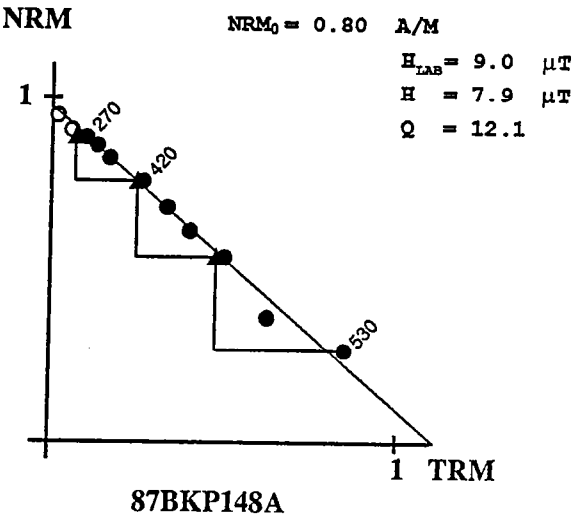

87BKP148A

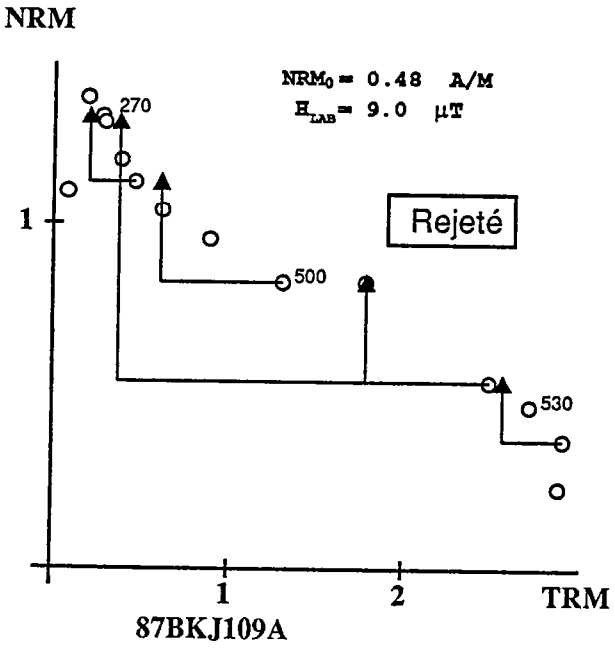

87BKJ109A

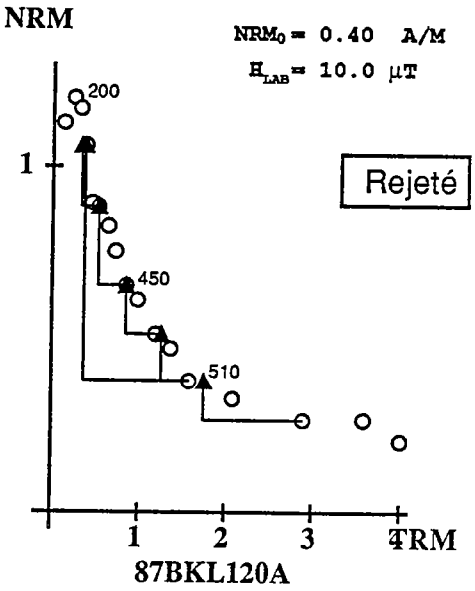

87BKL120A

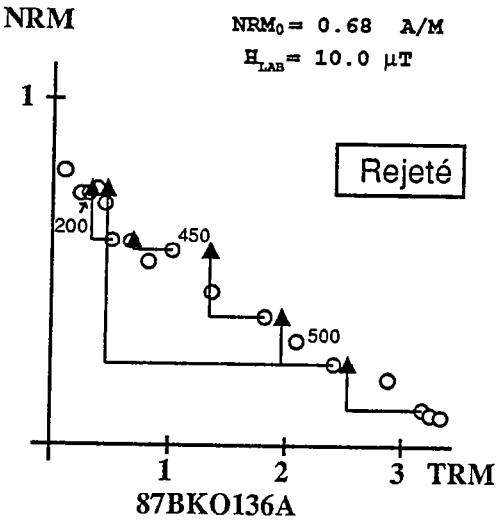

87BKO136A

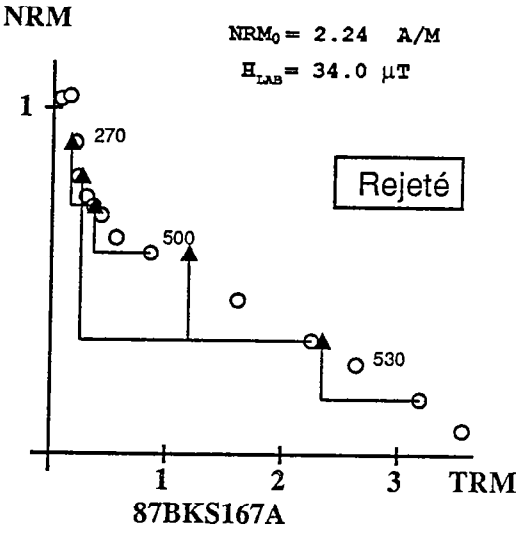

87BKS167A

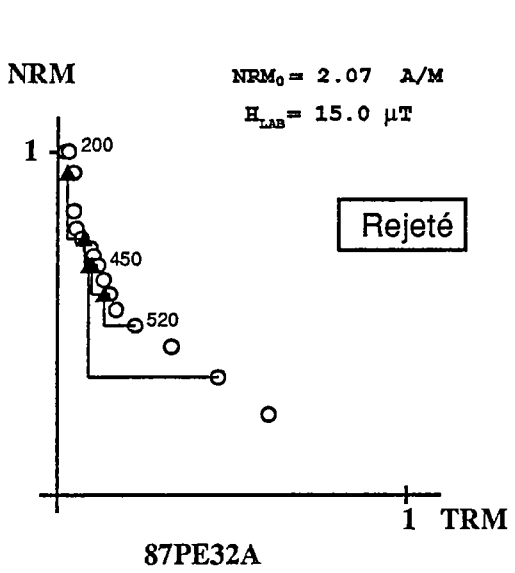

87PE32A

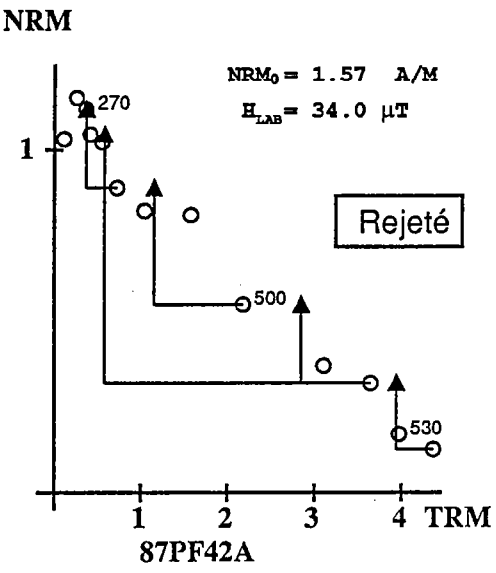

87PF42A

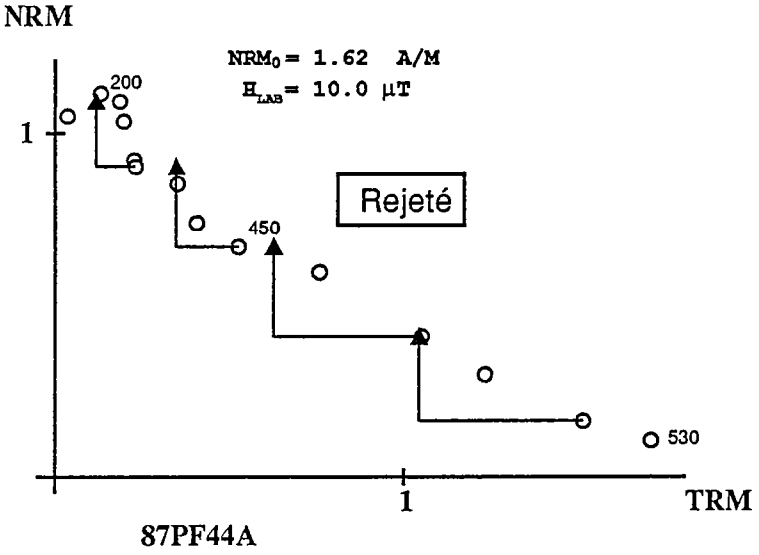

87PF44A

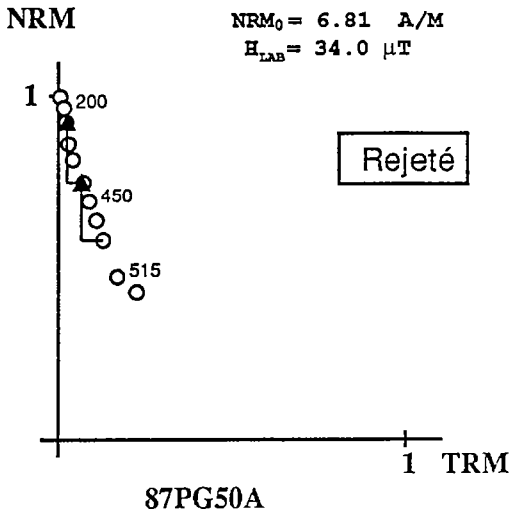

87PG50A

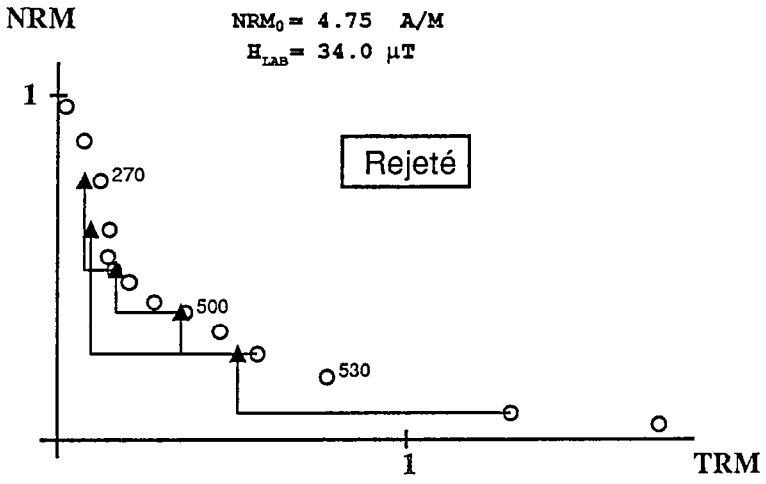

87PG49C

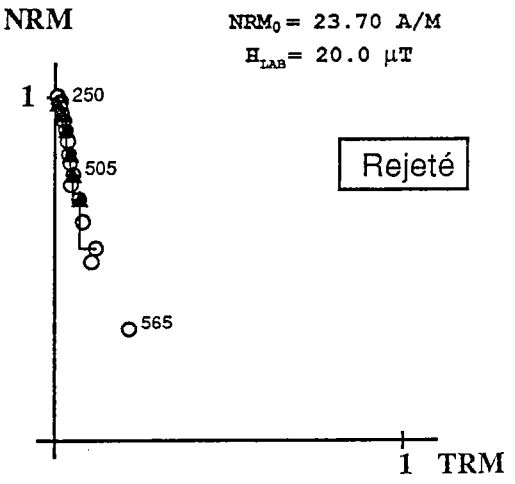

87PKE30A

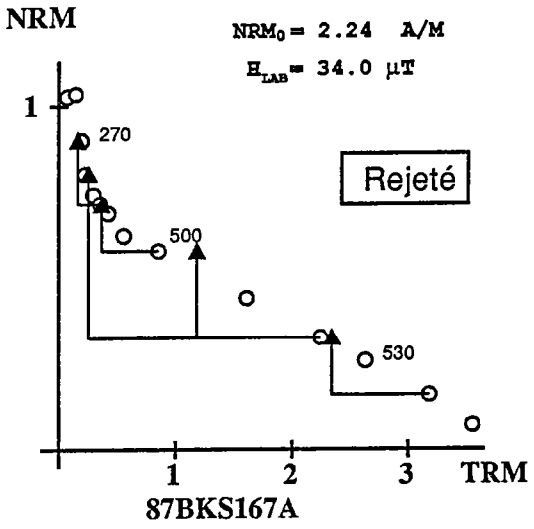
NRM
NRM0 = 2.24 A/M
HLAB = 34.0 µT
1
270
500
530
Rejeté
1 2 3 TRM
87BKS167A

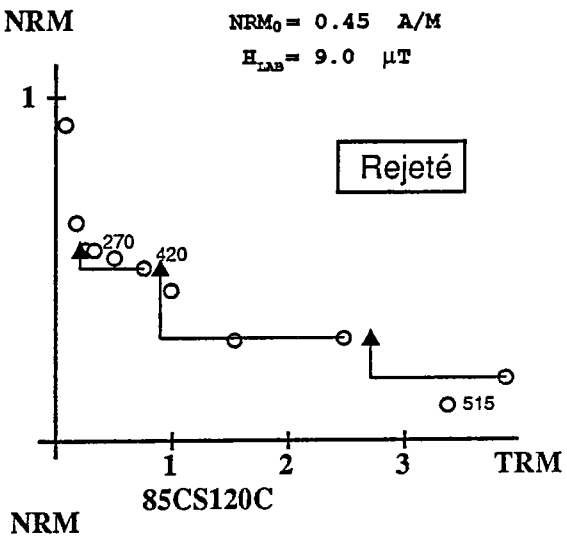
NRM
NRM0 = 0.45 A/M
HLAB = 9.0 µT
1
270
420
515
Rejeté
1 2 3 TRM
85CS120C

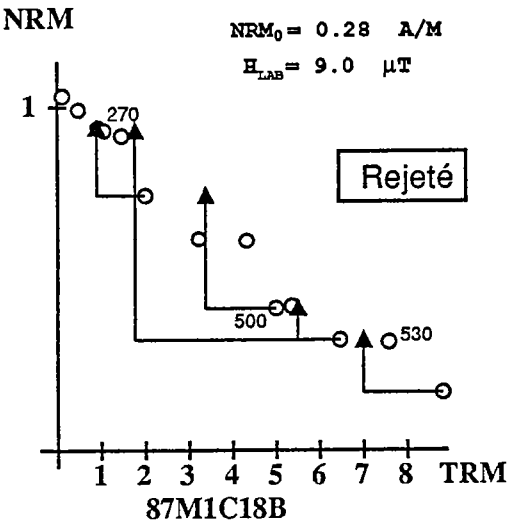
NRM
NRM0 = 0.28 A/M
HLAB = 9.0 µT
1
270
500
530
Rejeté
1 2 3 4 5 6 7 8 TRM
87M1C18B

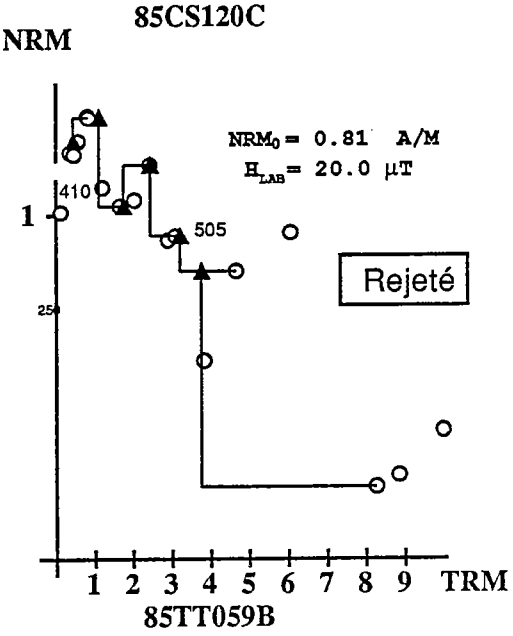
NRM
NRM0 = 0.81 A/M
HLAB = 20.0 µT
1
410
505
Rejeté
1 2 3 4 5 6 7 8 9 TRM
85TT059B

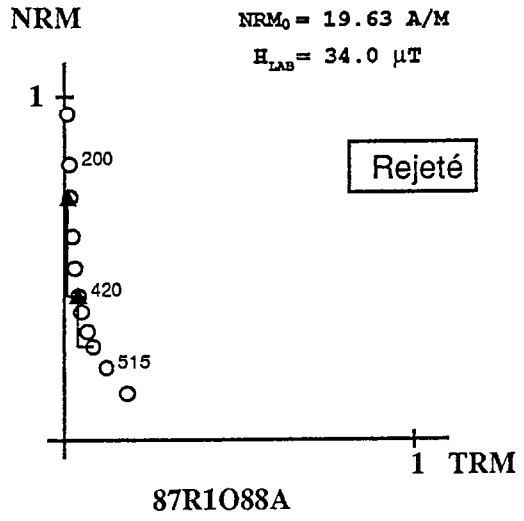
NRM
NRM0 = 19.63 A/M
HLAB = 34.0 µT
1
200
420
515
Rejeté
1 TRM
87R1O88A

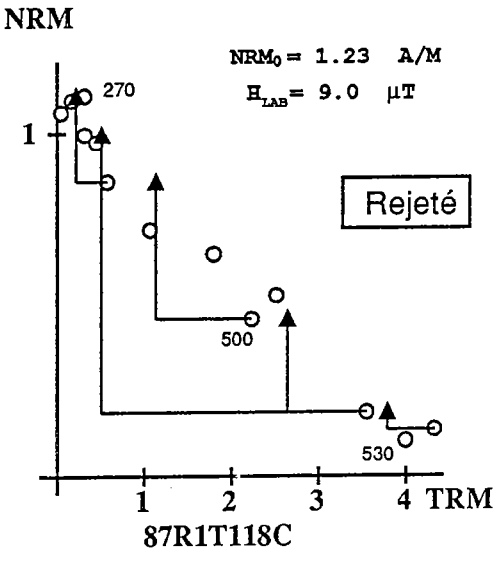
NRM
NRM0 = 1.23 A/M
HLAB = 9.0 µT
1
270
500
530
Rejeté
1 2 3 4 TRM
87R1T118C

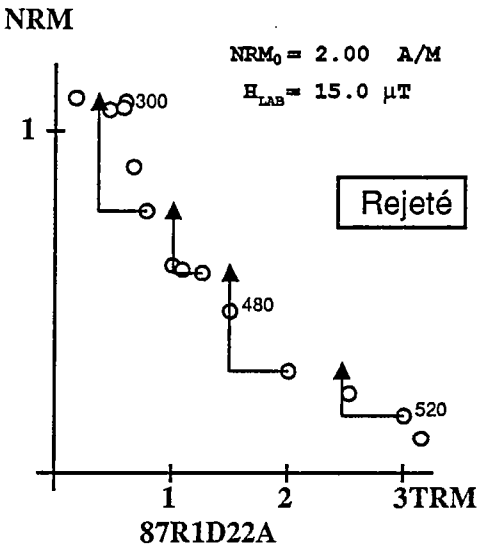
NRM
NRM0 = 2.00 A/M
HLAB = 15.0 µT
1
300
480
520
Rejeté
1
2
3TRM
87R1D22A

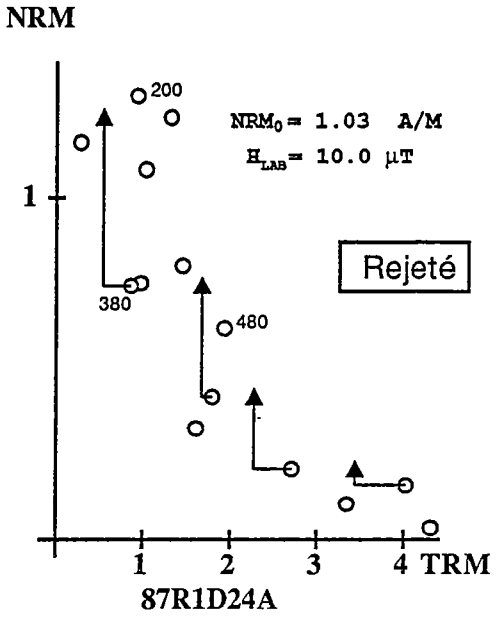
NRM
NRM0 = 1.03 A/M
HLAB = 10.0 µT
1
200
380
480
Rejeté
1
2
3
4 TRM
87R1D24A

Dans la même collection :

N°1 - H. MARTIN - Nature, origine et évolution d'un segment de croûte continentale archéenne : contraintes chimiques et isotopiques. Exemple de la Finlande orientale. **392 p., 183 fig., 51 tabl., 4 pl. (1985).** **140F.**

N°2 - G. QUERRE - Palingenèse de la croûte continentale à l' archéen : les granitoïdes tardifs (2,5-2,4 Ga) de Finlande Orientale. Pétrologie et géochimie. **226 p., 74 fig., 41 tabl., 3 pl.(1985).** **85F.**

N°3 - J. DURAND - Le Grès Armoricain. Sédimentologie. Traces fossiles. Milieux de dépôt. **150 p., 76 fig., 9 tabl., 19 pl. (1985).** **EPUISE**

N°4 - D. PRIOUR - Genèse des zones de cisaillement : Application de la méthode des éléments finis à la simulation numérique de la déformation des roches. **157 p., 106 fig., 7 tabl., (1985).** **55F.**

N°5 - V. NGAKO - Evolution métamorphique et structurale de la bordure sud-ouest de la "série de Poli". Segment camerounais de la chaîne panafricaine. **185 p., 76 fig., 16 tabl., 12 pl. (1986).** **70F.**

N°6 - J. DE POULPIQUET - Etude géophysique d'un marqueur magnétique situé sur la marge continentale sud-armoricaine. **159 p., 121 fig., 5 tabl. (1986).** **55F.**

N°7 - P. BARBEY - Signification géodynamique des domaines granulitiques. La ceinture des granulites de Laponie : une suture de collision continentale d'âge Protérozoïque inférieur (1.9-2.4 Ga). **324 p., 89 fig., 46 tabl., 11 pl. (1986).** **115F.**

N°8 - Ph. DAVY - Modélisation thermo-mécanique de la collision continentale. **233 p., 72 fig., 2 tabl. (1986). 95F.**

N°9 - Y. GEORGET - Nature et origine des granites peralumineux à cordiérite et des roches associées. Exemples des granitoïdes du Massif Armoricain (France) : Pétrologie et géochimie. **250 p., 140 fig., 67 tabl., (1986). 100F.**

N°10 - D. MARQUER - Transfert de matière et déformation progressive des granitoïdes. Exemple des massifs de l'Aar et du Gothard (Alpes centrales Suisses). **287 p., 134 fig., 52 tabl., 5 cartes hors-texte (1987). EPUISE**

N°11 - J.S. SALIS -Variation séculaire du champ magnétique terrestre. Direction et Paléointensité sur la période 7.000 - 70.000 BP dans la chaîne des Puys. **190 p., 73 fig., 28 tabl., 1 carte hors-texte (1987). 90F.**

N°12 - Y. GERARD - Etude expérimentale des interactions entre déformation et transformation de phase. Exemple de la transition calcite-aragonite. **126 p., 42 fig., 3 tabl., 10 pl. (1987). 75F.**

N°13 - H. TATTEVIN - Déformation et transformation de phases induites par ondes de choc dans les silicates. Caractérisation par la microscopie électronique en transmission. **150 p., 50 fig., 1 tabl., 13 pl. (1987). 95F.**

N°14 - J.L. PAQUETTE - Comportement des systèmes isotopiques U-Pb et Sm-Nd dans le métamorphisme éclogitique. Chaîne Hercynienne et chaîne Alpine. **190 p., 88 fig., 39 tab., 2 pl. (1987). 95F.**

N°15 - B. VENDEVILLE - Champs de failles et tectonique en extension : modélisation expérimentale. **392 p., 181 fig., 1 tabl., 82 pl. (1987). 265F.**

N°16 - E. TAILLEBOIS - Cadre géologique des indices sulfurés à Zn, Pb, Cu, Fe du secteur de Gouézec-St-Thois : Dévono-Carbonifère du flanc Sud du Bassin de Châteaulin (Finistère). **195 p., 64 fig., 41 tabl., 8 pl. photo., 8 pl. h.texte. (1987).** **110F.**

N°17 - J.P. COGNE - Contribution à l'étude paléomagnétique des roches déformées. **204 p., 86 fig., 17 tabl., (1987).** **90F.**

N°18 - E. DENIS - Les sédiments briovériens (Protérozoïque supérieur) de Bretagne septentrionale et occidentale : Nature, mise en place et évolution. **263 p., 148 fig., 26 tab., 8 pl. (1988).** **140F.**

N°19 - M. BALLEVRE - Collision continentale et chemins P-T : l'unité pennique du Grand Paradis (Alpes Occidentales). **340 p., 146 fig., 10 tabl., (1988).** **145F.**

N°20 - J.P. GRATTIER - L'équilibrage des coupes géologiques. Buts, méthodes et applications. Atelier du Groupe d'Etudes Tectoniques le 8 Avril 1987 à Rennes. **165 p., 82 fig., 2 tabl. (1988).** **85F.**

N°21 - R.P. MENOT - Magmatismes paléozoïques et structuration carbonifère du Massif de Belledonne (Alpes Françaises). Contraintes nouvelles pour les schémas d'évolution de la chaine varisque ouest-européenne. **465 p., 101 fig., 31 tab., 6 pl., (1988).** **200F.**

N°22 - S. BLAIS - Les ceintures de roches vertes archéennes de Finlande Orientale : Géologie, pétrologie, géochimie et évolution géodynamique. **312 p., 107 fig., 98 tab., 11 pl. photo, 1 pl. h.texte, (1989).** **160F.**

N°23 - A. CHAUVIN - Intensité du champ magnétique terrestre en période stable de transition, enregistrée par des séquences de coulées volcaniques du quaternaire. **217 p., 100 fig., 13 tab. (1989).** **100F.**

BON DE COMMANDE

A retourner à :

Centre Armoricain d'Etude Structurale des Socles
Mémoires et documents du CAESS
Université de Rennes I - Campus de Beaulieu
35042 - RENNES Cédex (France).

NOM .....

ORGANISME .....

ADRESSE .....

Veuillez me faire parvenir les ouvrages suivants :

N°	Auteur	Nb Exemplaires	Prix Unitaire	TOTAL

Frais d'envoi :
1 volume : 15,00 F.

Total	
Frais d'envoi	
Montant total	

Veuillez établir votre chèque au nom de l'Agent comptable de l'Université de Rennes I et le joindre au bon de commande.

Résumé

L'objectif de ce travail est l'étude du comportement du champ géomagnétique, en direction et en intensité, aux cours de périodes stables et de transition (excursions et inversions). Dans ce but, plusieurs études paléomagnétiques et de nombreuses déterminations de paléointensité par la méthode de Thellier ont été effectuées sur des coulés provenant de différentes provinces volcaniques.

Des paléointensités comprises entre 21 et 54 μT ont été obtenues sur des coulées de l'île de la Réunion, pour les périodes 5-11 Ka (mille ans) et 82-98 Ka. Ces données ainsi que la variation séculaire observée sur les directions, concordent avec des intensités du champ dipolaire et non-dipolaire comparables avec les valeurs actuelles.

Au contraire, de nouvelles données de paléointensité obtenues sur des laves volcaniques de directions intermédiaires, d'Islande et de la Chaîne des Puys, datées entre 40 et 50 Ka., confirment la baisse importante du champ durant l'excursion du Laschamp.

Une étude des inversions les plus récentes a été effectuée sur une séquence datée de 123 coulées de l'île de Tahiti (Polynésie française). Des enregistrements détaillés du champ de transition ont été obtenus pour le Jaramillo supérieur et le Cobb Mountain, alors que les transitions du Jaramillo inférieur et du Matuyama-Brunhes n'ont été enregistrées que par quelques coulées. Le Cobb Mountain apparait, dans cet enregistrement, comme une excursion inverse-transitionel-inverse. Les données acquises à Tahiti, combinées à d'autres déjà obtenues en Polynésie suggèrent une domination des termes zonaux au début des renversements.

L'intensité du champ de transition, à cette latitude, parait très faible, comme l'indiquent les paléointensités obtenues (3 à 8 μT). Cette observation combinée à une analyse de l'intensité d'aimantation des coulées, pourrait indiquer une variation de l'intensité moyenne du champ de transition avec la latitude.

MOTS-CLES

Champ Magnétique Terrestre, Paléomagnétisme, Paléointensité, Inversions, Excursion, Variation Séculaire.

Editions du C.A.E.S.S.
Université de Rennes I
F - 35042 - RENNES Cédex